

Drivers and processes of soil erosion in the cultivated steppe of Kazakhstan

Dissertation

zur Erlangung des

Doktorgrades der Naturwissenschaften (Dr. rer. nat.)

der

Naturwissenschaftlichen Fakultät III

Agrar- und Ernährungswissenschaften,

Geowissenschaften und Informatik

der Martin-Luther-Universität Halle-Wittenberg

vorgelegt von

Herrn Koza, Moritz

Gutachter:

Prof. Dr. Christopher Conrad

Prof. Dr. Georg Guggenberger

Datum der Verteidigung:

17.06.2024

Summary

One of the most urgent global challenges to achieving sustainable agriculture is the reduction of soil erosion. The semi-arid regions of Central Asia are expected to suffer even more from soil erosion than currently due to climate change and expanding agriculture. Empirical data from field observations are the foundation for evaluating the present erosion risks and projecting medium-term soil degradation hazards. The quantification of soil erosion rates in Central Asia is lacking, but it is necessary to assess the degradation potential under real soil conditions. Knowledge about wind erosion and its interactions with water erosion is particularly interesting, as they are less studied or even neglected scientifically. A systematic understanding of erosion drivers and processes is crucial for scientists, stakeholders, and farmers.

Therefore, a dataset from a series of sampling campaigns and field experiments on representative test sites under typical agricultural management practices and grassland vegetation across the Kazakh Steppe was established. The investigations focus mainly on three research gaps and are represented in detail in three scientific publications:

- (I) the variability of modeled soil losses caused by different pretreatments for particle size analyses and associated texture-based parameters (Koza et al., 2021),
- (II) the wind- and water erodibility of crop- and grassland derived from aggregate stability tests (Koza et al., 2022), and
- (III) the quantity and quality of soil loss by wind erosion under real soil conditions obtained from mobile wind tunnel experiments (Koza et al., 2024).

This dissertation takes a holistic approach to investigate the complex drivers and processes of soil erosion using various methods, including physical and chemical soil analyses, modeling, and field experiments.

The soil was chemically pretreated separately and successively with hydrochloric acid and hydrogen peroxide to dissolve common binding material before particle size analyses by laser diffraction were conducted. Measured values of clay, silt, sand, and fine sand contents were used as input data for the Single-event Wind Erosion Evaluation Program (SWEEP) to estimate soil loss variations. Crop- and grassland soils with a large range of physico-chemical soil properties were assessed for potential erodibility using several aggregate stability tests. An adjusted drop-shatter method was used to estimate the dry stability against weak mechanical forces, such as saltating particles striking the surface. Three wetting

treatments with distinguished conditions and energies were applied to simulate different disruptive effects of water caused by heavy rain, light rain or the impact of raindrops. In order to assess the wind erosion risk of the soil during the most erosive time of the year, field experiments were carried out with a mobile wind tunnel on typical arable surfaces present in spring (bare fallow, cultivated with barley, cultivated with maize). In addition, common disruptive forces soils experience during field cultivation (light cultivator, disc harrow, tractor tires) were considered to analyze the effects on soil losses.

- Laser diffraction analyses show that common pretreatments do not affect the texture classification of silt loams. The consequences for soil loss estimates from wind erosion modeling can be neglected when texture-based parameters, such as geometric mean diameter, are measured and not derived with a pedotransfer function.
- Results from extensive dry and wet aggregate stability tests prove that organic matter is the primary binding agent for typical steppe soils. However, the existing susceptibility of the soil to wind and water erosion is independent of its soil properties. Since the risk of erosion from heavy rain or snow melting is particularly high, it is recommended to consider the interacting processes of wind and water to mitigate further soil degradation.
- Mobile wind tunnel experiments on loamy sands revealed that mechanical stress from seedbed preparation determines soil susceptibility. However, the most severe soil losses were caused by tractor tires, which have to be considered a serious emission source in cultivated steppes. In addition, field experiments have shown that aeolian sediments are enriched in organic carbon after steppe conversion.

Overall, it is concluded that agriculture on steppe soils requires best-adapted measures for early erosion control and prevention.

With its sequential publications, findings, and considerations, this dissertation is an up-to-date and comprehensive study investigating soil erosion processes under anthropogenic pressure in northern Kazakhstan.

Zusammenfassung (Summary in German)

Eine der größten globalen Herausforderungen für eine nachhaltige Landwirtschaft ist die Reduzierung der Bodenerosion. Die semiariden Regionen Zentralasiens werden aufgrund des Klimawandels und der Ausweitung landwirtschaftlicher Nutzflächen in Zukunft voraussichtlich noch stärker von Bodenerosion betroffen sein als bisher. Empirische Daten aus Feldversuchen bilden die Grundlage für die Beurteilung der aktuellen Situation sowie für mittelfristige Prognosen. Die Quantifizierung der Bodenerosion in Zentralasien fehlt derzeit weitgehend, ist aber notwendig, um das Erosionspotential unter realen Bodenbedingungen zu bewerten. Von besonderem Interesse sind Kenntnisse über die Winderosion und ihre Wechselwirkungen mit der Wassererosion, da diese wissenschaftlich weniger untersucht oder sogar vernachlässigt werden. Ein systematisches Verständnis der Erosionsfaktoren und -prozesse ist für Wissenschaftler, Interessenvertreter und Landwirte gleichermaßen wichtig.

Zu diesem Zweck wurde ein Datensatz von Probenahmekampagnen und Feldversuchen auf repräsentativen Versuchsflächen in der kasachischen Steppe mit typischer landwirtschaftlicher Bewirtschaftung und Grünlandvegetation erstellt. Die Untersuchungen konzentrieren sich im Wesentlichen auf drei Forschungslücken und werden in drei wissenschaftlichen Veröffentlichungen ausführlich dargestellt:

- (I) die Variabilität der modellierten Bodenverluste aufgrund unterschiedlicher Vorbehandlungen für Korngrößenanalysen und zugehörige texturbasierte Parameter (Koza et al., 2021),
- (II) die Wind- und Wassererodierbarkeit von Acker- und Grünland anhand von Aggregatstabilitätstests (Koza et al., 2022), und
- (III) die Quantität und Qualität des Bodenabtrags durch Winderosion unter realen Bodenbedingungen mittels mobiler Windkanalversuche (Koza et al., 2024).

Die Dissertation verfolgt einen ganzheitlichen Ansatz zur Untersuchung der komplexen Treiber und Prozesse der Erosion unter Verwendung verschiedener methodischer Ansätze, einschließlich physikalischer und chemischer Bodenanalysen, Modellierung und Feldexperimenten.

Dafür wurde Boden chemisch separat und sukzessiv mit Salzsäure und Wasserstoffperoxid vorbehandelt, um gängige Bindematerialien aufzulösen. Im Anschluss wurde die Korngrößenverteilung mittels Laserbeugung analysiert und Gehalte von Ton, Schluff, Sand

und Feinsand für das Single-event Wind Erosion Evaluation Program (SWEEP) verwendet, um die Abweichungen beim modellierten Bodenabtrag abzuschätzen. Sowohl Acker- als auch Grünland, mit einem großen Spektrum an physikalisch-chemischen Bodeneigenschaften, wurden auf ihre Erodierbarkeit hin untersucht. Verschiedene Aggregatstabilitätstests wurden durchgeführt, um die Auswirkungen von Wind und Wasser zu simulieren, einschließlich Abrieb durch springende Bodenpartikel, Starkregen, leichten Regen und den Aufprall von Regentropfen. Mit einem mobilen Windkanal wurden Feldversuche durchgeführt, um das Winderosionspotential unter typischen Bedingungen während der erosivsten Jahreszeit zu beurteilen (Brache, Gerste, Mais). Darüber hinaus wurden häufig auftretende Bodenbearbeitungskräfte (leichter Grubber, Scheibenegge, Traktorreifen) berücksichtigt, um die Auswirkungen auf die Bodenabträge zu analysieren.

- Die Ergebnisse der Partikelgrößenanalysen zeigen, dass herkömmliche Vorbehandlungen keinen Einfluss auf die Klassifizierung der Texturklasse für schluffigen Lehm haben. Die Bodenverlustschätzungen aus der Winderosionsmodellierung können vernachlässigt werden, wenn texturbasierte Parameter wie der geometrische mittlere Durchmesser gemessen und nicht abgeleitet werden.
- Umfangreiche Aggregatstabilitätstests belegen, dass bei typischen Steppengebieten die bestehende Anfälligkeit des Bodens gegenüber Wind- und Wassererosion unabhängig von den Bodeneigenschaften ist. Da das Risiko von Erosion durch Starkregen oder Schneeschmelze besonders hoch ist, wird empfohlen, die Wechselwirkungen von Wind und Wasser zu berücksichtigen.
- Windkanalexperimente auf lehmigem Sand haben gezeigt, dass die Intensität der Feldbearbeitung die Erosionsanfälligkeit bestimmt. Insbesondere Fahrspuren führen zu außergewöhnlich hohen Bodenverlusten durch Wind und müssen als ernstzunehmende Erosionsquelle betrachtet werden. Die Anreicherung der äolischen Sedimente mit organischem Kohlenstoff ist eine Folge der Steppenumwandlung.

Nach aktuellem Kenntnisstand erfordern die landwirtschaftlich genutzten Steppengebiete Kasachstans optimal angepasste Maßnahmen zur frühzeitigen Erosionskontrolle und -vermeidung.

Die vorliegende Dissertation stellt mit ihren aufeinander aufbauenden Publikationen und Ergebnissen eine aktuelle und umfassende Studie zu Bodenerosionsprozessen unter anthropogenem Druck im Norden Kasachstans dar.

Резюме (Summary in Russian)

Одной из наиболее неотложных глобальных задач на пути достижения устойчивого сельского хозяйства является сокращение эрозии почвы. Ожидается, что полусухие регионы Центральной Азии пострадают от эрозии почвы больше, чем сейчас, из-за изменения климата и расширения сельского хозяйства. Эмпирические данные полевых наблюдений являются основой для оценки существующих рисков эрозии и прогнозирования среднесрочной опасности деградации почв. В Центральной Азии практически отсутствует количественная оценка скорости эрозии, хотя существует необходимость оценки потенциала эрозии в реальных почвенных условиях. Знания о ветровой эрозии и ее взаимодействии с водной эрозией представляют особый интерес, поскольку они менее изучены или даже игнорируются с научной точки зрения. Систематическое понимание движущих сил и процессов эрозии имеет решающее значение для ученых и фермеров.

Таким образом, был создан набор данных из серии кампаний по отбору проб и полевых экспериментов на репрезентативных испытательных участках с типичными методами управления сельским хозяйством, а также степной растительностью по всему северному Казахстану. Исследования сосредоточены в основном на трех пробелах в исследованиях и подробно представлены в трех научных публикациях:

- (I) изменчивость смоделированных потерь почвы, вызванных различными предварительными обработками для анализа размера частиц и параметров текстуры (Koza et al., 2021),
- (II) ветровая и водная эрозия луговых и пахотных земель, полученная в результате испытаний на совокупную устойчивость (Koza et al., 2022), и
- (III) количество и качество потерь почвы в результате ветровой эрозии в реальных почвенных условиях, полученных в ходе мобильных экспериментов в аэродинамической трубе (Koza et al., 2024).

В этой диссертации применяется целостный подход к исследованию сложных факторов и процессов эрозии с использованием ряда методологических подходов.

Перед проведением анализа размеров частиц методом лазерной дифракции почва была предварительно подвергнута химической обработке последовательно соляной кислотой и перекисью водорода для растворения общего связующего материала. Полученные содержания глины, ила, песка и мелкого песка использовались в качестве входных данных для программы оценки ветровой эрозии (Single-event Wind Erosion

Evaluation Program, SWEEP) для оценки изменений потерь почвы. Были проведены различные испытания на устойчивость заполнителя для имитации воздействия ветра и воды, включая абразивное воздействие отскакивающих частиц почвы, сильный дождь, легкий дождь и воздействие дождевых капель. Для оценки риска ветровой эрозии почвы в эрозионное время года были проведены полевые эксперименты с использованием передвижной аэродинамической трубы на типичных пахотных поверхностях, имеющих весной (чистый пар, возделываемый ячмень, возделываемый кукурузой). Дополнительно рассматривалось влияние на потери почвы обычных разрушительных сил, испытываемых почвой при обработке полей (легкий культиватор, дисковая борона, тракторные шины).

- Результаты анализа размера частиц показали, что обычная предварительная обработка не влияет на классификацию текстуры пылеватых суглинков. Оценками потерь почвы, полученными в результате моделирования ветровой эрозии, можно пренебречь, если параметры, основанные на текстуре, такие как средний геометрический диаметр, измеряются, а не выводятся.
- Результаты обширных испытаний устойчивости сухих и влажных агрегатов доказывают, что органическое вещество является основным связующим элементом для типичных степных почв. Однако существующая восприимчивость почвы к ветровой и водной эрозии не зависит от ее почвенных свойств. Поскольку риск эрозии в результате сильных дождей или таяния снега особенно высок. Рекомендуется учитывать взаимодействие ветра и воды для уменьшения дальнейшей деградации почвы.
- Эксперименты в аэродинамической трубе на суглинистых песках показали, что интенсивность обработки поля определяет подверженность эрозии. В частности, полосы движения сельхозтехники приводят к исключительно высокому уровню потери почвы из-за ветра. Обогащение эоловых отложений органическим углеродом является следствием культивирования степей.

Учитывая текущие результаты, сельское хозяйство с самого начала требует оптимально адаптированных мер для раннего контроля и предотвращения эрозии.

Данная диссертация, с ее последовательными публикациями и результатами, представляет собой комплексное и современное исследование процессов эрозии почв под антропогенным давлением на севере Казахстана.

Acknowledgments

This dissertation was made possible by the support and guidance of several people. I am very thankful to Prof. Dr. Christopher Conrad for supervising my dissertation. I would like to give deep gratitude to Dr. Gerd Schmidt for his constant support and encouragement, as well as his trust in my work. His expertise in Central Asia helped to overcome various challenges. I highly appreciate Dr. Julia Pöhlitz's steady help and cooperation on all publications.

Special thanks to Dr. Roger Funk for suggestions on the construction and application of the mobile wind tunnel. I would also like to thank Dorothee Kley for her logistical help and Michael von Hoff for supporting me with laboratory work. Additionally, I would like to acknowledge the Geocology research group for their helpful manner.

This dissertation was financed by the German Federal Ministry of Education and Research (BMBF) by funding the research project ReKKS (Innovative Solutions for Sustainable Agriculture and Climate Adaptation in the Dry Steppes of Kazakhstan and Southwestern Siberia). As part of a strong scientific consortium, I am thankful to Dr. Olga Shibistova for her efforts regarding the export of the mobile wind tunnel and the whole ReKKS team for their encouraging ideas, comments, and discussions. Collecting soil samples and conducting field experiments abroad depends on the expertise of local partners. Therefore, I especially thank Dr. Tobias Meinel and Kanat Akshalov for often making the seemingly impossible possible. I would also like to thank all agricultural holdings for their permission to sample and experiment on their fields.

Finally, I am especially grateful to my family and friends, who supported me during this journey.

Table of contents

	Page
Summary	I
Zusammenfassung (Summary in German)	III
Резюме (Summary in Russian)	V
Acknowledgments	VII
Table of contents	VIII
List of figures	IX
List of abbreviations	X
1. General introduction	1
2. State of soil erosion research	5
2.1 Fundamentals of soil erosion	5
2.2 Geography of erosion research	7
2.3 Scientific development and focus of erosion research.....	9
2.4 Factors influencing soil erosion.....	11
3. Research questions	13
4. Overview of material and methods	14
5. Publications	18
5.1 Koza et al. (2021): Consequences of chemical pretreatments in particle size analysis for modelling wind erosion.....	18
5.2 Koza et al. (2022): Potential erodibility of semi-arid steppe soils derived from aggregate stability tests.....	36
5.3 Koza et al. (2024): Wind erosion after steppe conversion in Kazakhstan.....	58
6. Discussion	75
7. Future research	79
8. Conclusion and synthesis	81
References	XI
Appendix	XX
Curriculum vitae	
Declaration on oath (Eidesstattliche Erklärung)	

List of figures

	Page
Fig. 2.1. Dependence of threshold friction velocity on particle size.....	5
Fig. 2.2. Main transport modes of particles during wind erosion events.....	6
Fig. 2.3. Typical wind erosion event during the Dust Bowl era	8
Fig. 2.4. Overview of factors influencing soil erosion.....	11
Fig. 4.1. Location of test sites in Kazakhstan and study area in Central Asia.....	14
Fig. 4.2. Typical situation in northern Kazakhstan: Cropland under cultivation.....	15
Fig. 4.3. Severe water and wind erosion events on a test site.....	15
Fig. 4.4. Mobile wind tunnel during field experiments on maize.....	17
Fig. A1. Typical signs of soil erosion observed in the study area.	XX
Fig. A2. Soil sampling and determination of soil type in the study area.....	XXI
Fig. A3. Fast and slow wetting tests to determine the resistance of the soil to rain	XXI
Fig. A4. The installation of the mobile wind tunnel	XXI

List of abbreviations

(The list also includes abbreviations used in the three publications.)

ASD	aggregate size distribution
EC	electrical conductivity
EF _p	potential erodible fraction
EF	erodible fraction
GMD	geometric mean diameter
H ₂ O ₂	hydrogen peroxide
HCl	hydrochloric acid
HCl _{sc}	hydrochloric acid soluble compounds
LDA	laser diffraction analysis
MWAC	Modified Wilson and Cook
MWD	mean weight diameter
PCA	principal component analysis
PSD	particle size distribution
SWEEP	Single-event Wind Erosion Evaluation Program
SOC	soil organic carbon
SUSTRA	Suspension Sediment Trap
TIC	total inorganic carbon
WEPS	Wind Erosion Prediction System

1. General introduction

The Earth's environment undergoes a profound human-induced transformation. Humans are changing the Earth's system by transforming the land, atmosphere, hydrological cycle, biodiversity, and altering essential elements within and between different components (e.g., carbon) (Steffen, 2005). Furthermore, most human-driven activities do not operate in separate, single cause-and-effect responses in the Earth's system. One of the most prominent examples is humans' combustion of fossil fuels, which increases non-reactive gases such as CO₂ in the atmosphere (Höök and Tang, 2013). The Earth's system responds with climate change to such an extent that tipping points are being triggered, causing impacts that are difficult to adapt to (Ritchie et al., 2021). Like burning fossil fuels, land conversion causes wide-ranging effects that induce feedback loops, which reinforce further changes (Steffen, 2005). Land use changes are responsible for up to 30% of anthropogenic greenhouse gas emissions and are major contributors to climate change (Tubiello et al., 2013).

Historically, land use conversion to agriculture has provided humans with a reliable food supply, allowing for permanent settlements and subsequent extensive population growth (Lev-Yadun et al., 2000). However, agricultural productivity has expanded tremendously due to the unprecedented demands of a growing population and consumption of food and energy. An estimated 40% of global land change is a consequence of agriculture (Turner et al., 2007). In detail, approximately 70% of the grasslands, 50% of savannas, 45% of the temperate deciduous forests, and 27% of the tropical forest biomes have been cleared or converted to support agriculture (Foley et al., 2011). Agriculture leaves the soil susceptible to soil erosion due to, e.g., removing plant cover and roots, destroying soil structure and aggregates, or soil compaction. These actions allow direct exposure of the soil to erosive forces, primarily from wind and precipitation (Gyssels et al., 2005; Morgan, 2005). While fertile topsoil is a finite source, up to 90% of global cropland experiences some degree of soil erosion (Pimentel and Kounang, 1998). During erosion, the soil gets detached, transported and deposited once the energy input ceases (Lal, 2017). Erosion processes cause environmental and economic damages both on- and off-site (Cerdà et al., 2009; Morgan, 2005). Agriculture is the primary source of aeolian and fluvial sediments (Wilkinson and McElroy, 2007). Data from global compilation surveys confirm that erosion rates from conventional agriculture exceed soil production rates (Montgomery, 2007). Soil erosion causes the loss not only of mineral particles but also organic components. Erosion processes can be selective, and in particular, wind erosion removes the

fine and silt-sized particles that contain disproportionately greater amounts of organic matter, causing several feedback effects. Locally, erosion reduces soil productivity (Gregorich et al., 1998; Lal, 2001), leading to food insecurity in exceptional situations. Globally, unknown soil organic carbon (SOC) loss rates from aeolian sediments cause uncertainty in the carbon cycle estimates (Chappell et al., 2013; Iturri and Buschiazzo, 2023).

Currently, about half of the global wheat production occurs on former grasslands. They are mainly located in the Great Plains of North America, the Pampas of South America, and the Eurasian Steppe Belt of Central Asia (Schultz, 2005). The cultivated steppes are often linked to semi-arid climate and steppe (or synonymously semi-arid) soils (Monger et al., 2005). In the Eurasian Steppe Belt Chernozems exist. They are the world's most fertile soils that score highest for food production due to their high organic matter storage. Average wheat yields are higher on Chernozems than on any other soil (Krasilnikov et al., 2018). More than 10% of the world's Chernozems are located in Kazakhstan. In the past and present, extensive steppe conversion has been carried out to tap into the potential of Chernozems and associated Kastanozems (Frühauf et al., 2020; Prishchepov et al., 2020). As a result, Kazakhstan's wheat exports contribute decisively to food security in Central Asia (FAO, 2012). However, of the total 84.5 million hectares of potential agricultural land, 25.5 million hectares are already affected by wind erosion and 1.0 million hectares by water erosion (Almaganbetov and Grigoruk, 2008).

The overall problem in the semi-arid regions of Central Asia is the serious threat of increasing soil erosion due to intensive agriculture causing soil erodibility (Robinson, 2016) and extreme climate conditions causing higher erosivity (Mirzabaev et al., 2016; Reyer et al., 2017). Soil erodibility describes the susceptibility of the soil to erode or, in reverse, to resist the erosive forces of wind velocity and precipitation (Funk and Reuter, 2006; Morgan, 2005). Semi-arid climates are characterized by annual precipitation between 250-500 mm, with hot, dry summers and cold, freezing winters. The risk of wind and water erosion will likely increase, particularly in Kazakhstan, because climate models indicate higher temperatures and changes in precipitation duration, magnitude, and intensity. Together, these will result in complex spatiotemporal patterns favoring the erosivity of wind and water (Duulatov et al., 2021; Li et al., 2020). In addition to increasing erosion rates, feedback loops could affect the global carbon cycle. While arid environments are major dust sources globally, the surrounding semi-arid regions could transform from former sinks into substantial sources by cultivation (Funk et al., 2014; Monger et al., 2005). Soils formed under semi-arid conditions, such as Chernozems, with

their high amounts of organic matter, can lead to significant emissions of greenhouse gases into the atmosphere and contribute to human-induced climate change if not properly managed (Cox et al., 2000; Lal, 2021).

In order to counteract these developments, it is necessary to identify corresponding processes in steppe ecosystems, quantify erosion risk associated with land use change, and derive adaptation measures. Understanding the impacts of land use intensification and extreme climate conditions requires an integrated perspective that includes wind and water erosion and their interactions (Field et al., 2009). Field studies comparing the absolute and relative magnitudes of wind and water erosion are limited (Breshears et al., 2003). Generally, wind erosion is much less studied than water erosion, and research on wind-water interactions is comparatively neglected (Bezak et al., 2021). Therefore, the interplay between aeolian and fluvial processes might be underestimated, which is a serious problem under semi-arid climate where erosion by wind and water often occur simultaneously (Visser et al., 2004) or successively at the same site. Especially when steppe soils are cultivated, and soils are exposed, wind and water erosion should be investigated together (Bullard and Livingstone, 2002; Field et al., 2009). However, comprehensive risk assessments of soil erosion in the cultivated steppes of Central Asia are lacking (Borrelli et al., 2021; Dou et al., 2022).

Reliable tools and methods are required to assess soil erosion and its processes. The number of studies focusing on soil erosion modeling is increasing (Bezak et al., 2021), and considerable progress has been achieved (Lal, 2001). In contrast, model calibration, validation, and evaluation have decreased proportionally and are needed for various soils and ecoregions of the world. Accordingly, empirical data sets derived from field measurements are particularly needed (Bezak et al., 2021; Lal, 2001). They cannot only support the implementation of sustainable management practices but also be used as benchmarks for erosion models (Webb et al., 2020). In-situ measurements and experiments provide in-depth knowledge of physical and chemical soil functions supporting agricultural adaptation and counter soil degradation within site-specific constraints (Horn et al., 2018).

Based on empirical data, this study provides detailed indications of the processes and drivers of soil erosion on arable steppe soils in northern Kazakhstan. Wind erosion is the most severe form of soil degradation in the study area (Almaganbetov and Grigoruk, 2008), but wind and water erosion processes can occur unnoticed. Therefore, this dissertation investigates wind and

water erosion from a holistic approach that investigates the drivers of soil erosion across different topics, ranging

- from single *to* various interacting key factors influencing erosion,
- from erodibility and erosivity *to* the combined effects determining erosion risk,
- from model estimates *to* field experiment measurements.

Research topics also take into account different spatial and temporal scales. Drivers and processes were studied locally to derive practical suggestions and on a regional scale by covering a wide range of physical and chemical soil characteristics from northern Kazakhstan. Considering current conditions and future predictions, the short- and long-term effects of erosive processes by wind and water on parent material and land use were investigated and discussed.

The extensive work resulted in a diverse dataset and the subsequent publication of three open-access papers. Together, they have contributed decisively to particle size analyses as key input data for wind *erosion modeling* (Koza et al., 2021), to the *erodibility of steppe soils* derived from aggregate stability test (Koza et al., 2022), and to the quantity and quality of *soil losses from wind erosion* after steppe conversion under real soil conditions (Koza et al., 2024). One corresponding published dataset (Koza et al., 2023) can be used in further research, e.g., as input data for modeling soil loss in semi-arid regions.

This dissertation aims to provide up-to-date information on the state and drivers of erosion under increasing anthropogenic pressure and changing climate. A better systematic understanding of the drivers of erosion in semi-arid regions is useful to scientists, stakeholders, and farmers in Central Asia and worldwide. The findings of this work could help to mitigate soil erosion and contribute to the Sustainable Development Goals (SDGs) by directly supporting the achievement of food security (SDG 2), the combat against climate change (SDG 13), and promoting sustainable use of terrestrial ecosystems (SDG 15). Furthermore, these studies are results of interdisciplinary work based on international collaborations that contributed to strengthening the means of implementation and revitalizing the global partnership for sustainable development (SDG 17) (United Nations, 2022).

2. State of soil erosion research

2.1 Fundamentals of soil erosion

The two main categories that determine soil erosion are the erodibility of the soil and the erosivity of the climate. Soil must have the potential to erode or, in reverse, the ability to resist the energy input. Once an erosive agent, such as wind or water, detaches and transports soil particles, soil erosion occurs. When sufficient energy is no longer available, the soil is deposited (Funk and Reuter, 2006).

Wind erosion occurs when the energy input from the wind is high enough to overcome the gravity force, aerodynamic drag, and particle rotation (Magnus force) to lift loose particles from an insufficiently protected susceptible surface. A certain wind or friction velocity has to be exceeded to set particles in motion. This benchmark is referred to as the threshold friction velocity. A close relationship exists between the threshold value and particle size for single grains. The lowest friction velocity occurs by particles of size between 80 μm and 100 μm . The threshold friction velocity increases with a greater diameter caused by weight or a smaller diameter by cohesive forces (Fig. 2.1). Natural soils consist of aggregated particles of different sizes and shapes. The average particles or aggregates in natural soils are larger than 0.84 μm and can be regarded as non-erodible since they are too heavy to be lifted by the wind force (Bagnold, 1941; Funk and Reuter, 2006; Shao, 2008).

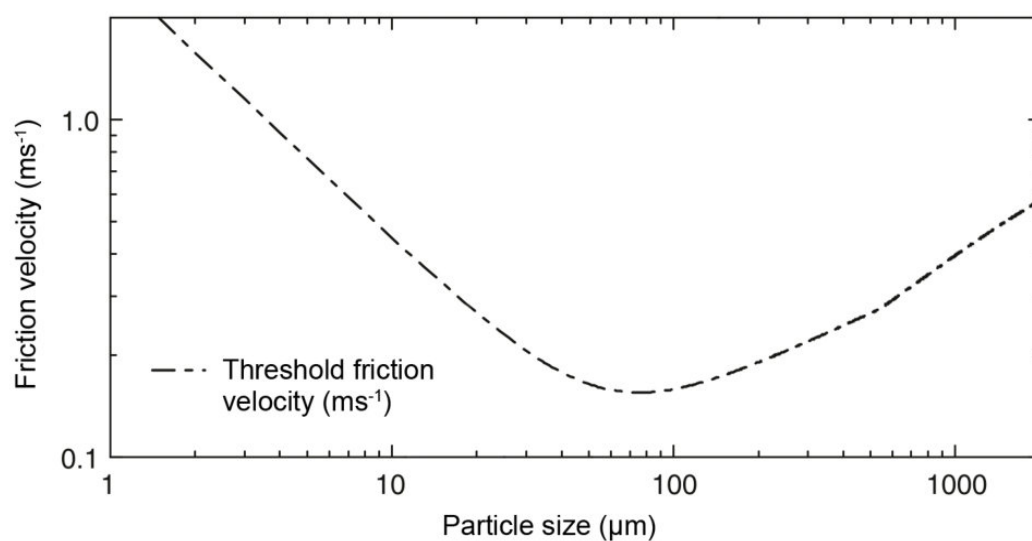


Fig. 2.1. Dependence of threshold friction velocity on particle size (modified from Shao, 2008).

Different particle sizes tend to move in different modes of motion when eroded by wind. Bagnold (1941) classified particle motions based on field and wind tunnel observations. The classification distinguishes mainly between creep, saltation, and suspension (Fig. 2.2). Particles larger than $500\ \mu\text{m}$ are too heavy to be lifted from the surface but can be pushed along the surface by wind or saltating particles, known as creep. Saltation is the movement of soil particles approximately $70\text{--}500\ \mu\text{m}$ in diameter that return to the ground after being lifted by dynamic force. On the ground, they rebound and continue their movement, either in further saltation or by striking other grains, causing the detachment of particles by abrasion. This leads to an increase in the downwind transport rate (avalanching). Therefore, saltation is a driving process of wind erosion. The wind's equilibrium or maximum transport capacity is reached after a certain distance. The capacity is independent of the soil type, but the distance from initiation to saturation varies with the soil's erodibility. Suspension refers to particles with a smaller terminal velocity than vertical upward-directed turbulent motions and entrainment into the atmosphere. Particles with diameters between $20\text{--}70\ \mu\text{m}$ can be suspended for a few hours (short-term suspension), while particles smaller than $20\ \mu\text{m}$ can be transported for days and several hundred kilometers (long-term suspension) (Bagnold, 1941; Funk and Reuter, 2006; Shao, 2008).

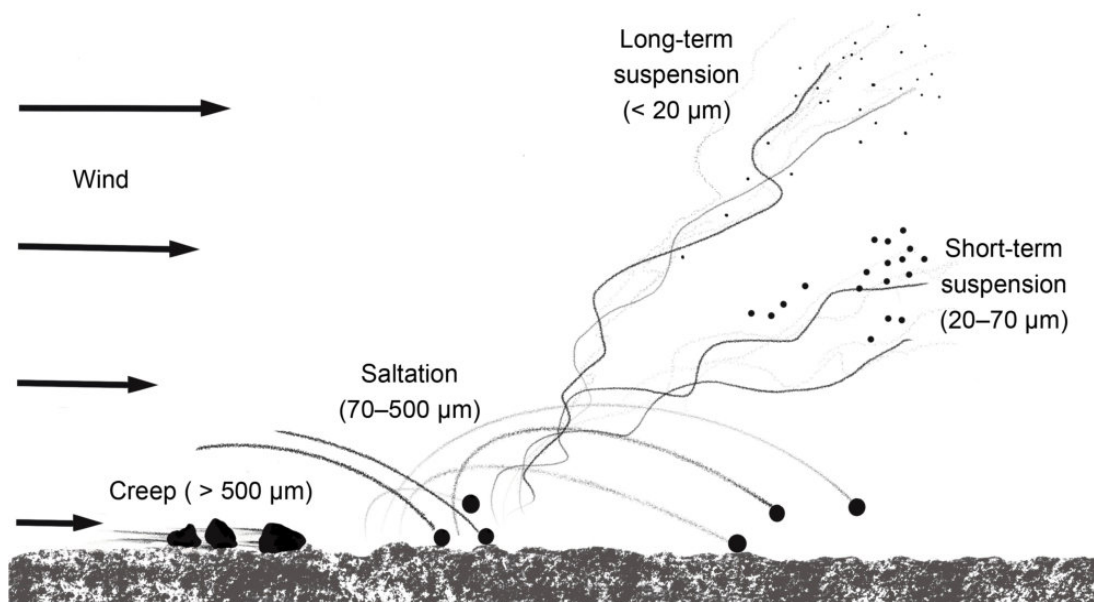


Fig. 2.2. Main transport modes of particles during wind erosion events (own illustration after Funk and Reuter, 2006).

The most important detaching agent for water erosion is water from rainfall or running water. Depending on the soil's reaction to water by its moisture level, structural state (aggregate stability), and magnitude, many different types of water erosion exist (e.g., splash, sheet, inter-rill, rill, gully, etc.) (Morgan, 2005). The energy is available from the difference in height of the raindrop to the soil structural unit. Hence, mass, height, and gravity form the potential energy, which is then converted into the energy of motion related to the eroding agent's mass and velocity. However, energy input can also be caused by mechanical stress internally. Inter-rill erosion on cultivated soils occurs mainly from the breakdown of aggregates by precipitation. Aggregate breakdown is caused by air compression (slaking) when the soil is dry and wetting occurs rapidly during heavy rainfall. In case aggregates are initially partially wetted or the rainfall intensity is low, the disintegration occurs due to disproportional swelling of materials (Le Bissonnais, 1996; Morgan, 2005).

Based on the fundamentals of soil erosion, various practices can be applied to control erosion. The most effective strategy is covering the soil with standing residues because it creates a surface that is more resistant to erosive forces. A surface that can resist wind and water can also be created by tillage that produces clods and increases surface roughness. Shelterbelts and bushes can be used to break the airflow. Strip-till systems disturb the soil only in the row where the seed is planted, leaving crop residues in between to trap particles in saltation. Morgan (2005) provides more detailed about the effects of different conservation practices on soil erosion.

2.2 Geography of erosion research

Historically, the influence of erosion on agriculture has already been noticed by Plato and Aristotle (Montgomery, 2007) before Anno Domini. By the 4th century, civilizations all around the world used methods to control erosions (Brevik and Hartemink, 2010). During the last century, soil erosion's mechanisms, processes, rates, and control have been studied scientifically. Still, substantial improvements were archived after the 1960s by considering the impacts and interrelationships of these factors (Cerdà et al., 2009). Research shows that erosion processes are being studied worldwide and in-depth information about the hotspots of soil erosion can be found in the literature review of Zhuang et al. (2015). Important occasions and events focusing on wind and associated water erosion from Europe, the USA, and the study area are described in the following. In general, research was intensified, not exclusively, but especially where land conversion caused severe, large-scale soil degradation.

Soil erosion research has been predominantly concentrated in Europe and the USA throughout the last century, and recently, it has experienced an increasing interest in China and Australia (Zhuang et al., 2015). In Germany, one of the first publications dealing with wind erosion as an agricultural problem dates back to the 18th century (Gleditsch, 1767). However, until today, the USA has been the largest contributor to global soil erosion research (Zhuang et al., 2015). A first book dedicated to "The movement of soil material by wind" was published by E. E. Free (1911). In the 1920s–1930s, H. H. Bennet started a soil conservation movement to address soil erosion and protection (Morgan, 2005). Subsequent initial steps for developing separate wind and water erosion models were taken to evaluate different soil conservation practices (Morgan and Quinton, 2001). However, serious attention was drawn to wind erosion as a soil degradation process after catastrophic soil losses by overgrazing and cultivation were triggered during dry periods in the Great Plains (Fig. 2.3), known as the Dust Bowl era (1935–1938). Subsequently, the causes and effects of wind erosion became a serious research focus (Tatarko et al., 2013).



Fig. 2.3. Typical wind erosion event during the Dust Bowl era (Tatarko et al., 2013).

In Russia, V. V. Dokuchaev initiated 1876 the investigation of the causes of agricultural degradation in Chernozems. Increasing large-scale soil degradation affected agricultural productivity following the Virgin Lands Campaign (1954–1963), the largest global ecosystem conversion of the 20th century, in which approximately 420,000 km² of native grassland was converted to cropland for grain production. New land management practices were addressed (Frühauf et al., 2020), and erosion prevention methods have been studied, for example, at the

Barayev Research and Production Center for Grain Farming. In the Soviet Union, afforestation became an agricultural policy to protect soil from erosion by 1950–1960s (Chendev et al., 2015). Unfortunately, knowledge and research documentation about soil erosion processes and their mitigation in the semi-arid regions have been partly lost after the collapse in 1991.

After the 1970s, Western Europe recognized even more that erosion also causes problems in arable lowlands. In particular, wind erosion has been ignored as a land degradation process in the past but is now receiving attention as a source of air pollution in addition to sneaking soil fertility loss (Funk and Reuter, 2006).

2.3 Scientific development and focus of erosion research

Research to predict or evaluate soil erosion must be based on experimental results (Mutchler et al., 2017). An important role in developing methods to control erosion is the interplay between field experiments and modeling. In this subchapter, the main achievements are described.

Since the early 1900s, it has been known that environmental variables, such as wind and water, soil fauna, microorganisms, roots, and inorganic binding agents, influence aggregate formation and stabilization (Six et al., 2004). Before the 1950s, there was a deficiency in quantifying single influences and feedback mechanisms. The hierarchical concept that primary particles and binding agents, such as organic matter, are bound together into stable microaggregates, which are in turn bound together into macroaggregates by temporary and transient binding agents, was proposed in 1982 (Tisdall and Oades, 1982). Aggregates and their stability not only physically protect soil organic matter (Six et al., 2004) but also reduce erosion (Barthès and Roose, 2002; Le Bissonnais, 1996). Le Bissonnais (1996) made a major effort to develop a standard method for measuring the disintegration of aggregates under the influence of rain to assess the soil's erodibility.

Until today, our understanding of wind erosion has been largely derived from tunnel-based investigations that link laboratory to field experiments. The seminal work was mainly done in a stationary wind tunnel by R. Bagnold (1941), who first moved the study of wind erosion from a descriptive to a process-oriented research topic (Tsoar, 1994). A wind tunnel allows to study aeolian processes under controlled conditions, such as wind speed and surface parameters. Mobile wind tunnels are particularly suitable for assessing the natural soil surface for erodibility (Van Pelt et al., 2010). The first major paper about the requirements was published in 1951

based on the experiences of Zingg and Chepil (Zingg, 1951). Early on, wind tunnel experiments were conducted to understand why some soils are more susceptible to erosion than others (Chepil, 1950a). Since then, mobile wind tunnel experiments have been used on numerous soil types worldwide (Larionov, 1993; Van Pelt et al., 2010). Groundbreaking series based on wind tunnel experiments ("Dynamics of wind erosion", "Properties of soil which influence wind erosion" and "Factors that influence clod structure and erodibility of soil by wind") was published by W. S. Chepil. The relationship between the percentage of sand, silt, and clay to the soil erodibility and the proportion of erodible fraction as the most susceptible fraction of dry aggregates were noticed (Chepil, 1952) and wind force, soil moisture, organic matter, mechanical stress by agricultural activities, vegetation cover and field size as controlling factors recognized (Chepil and Woodruff, 1963). At the Barayev Research and Production Center for Grain Farming, a mobile wind tunnel was likely used for experiments in the 1960s. Extensive research was undertaken, but no further information about the material, methods, or results could be disclosed. Worldwide, mobile wind tunnels are rare because the expenses are high, and applications are difficult to conduct. Latest mobile wind tunnel experiments were carried out in Hungary (Farsang et al., 2022), Morocco (Marzen et al., 2020), Iran (Sirjani et al., 2019), Israel (Tanner et al., 2016) and China (Zhang et al., 2014). Overall, mobile wind tunnel experiments can be very effective and are of great potential because field experiments under real soil conditions provide valuable data for understanding erosion processes or calibrating wind erosion models. During real wind erosion events, wind erosion can also be quantified by sampling detached particles. The most common traps are the Modified Wilson and Cook (MWAC) sediment trap, the Suspension Sediment Trap (SUSTR), or the Big Spring Number Eight (BSNE) sampler. Collected sediments can then be used for quantity measurements and quality analyses. A properly designed, calibrated, constructed, and operated wind tunnel can obtain useful information in a relatively short period (Van Pelt and Zobeck, 2013). In contrast, the independent samplers rely on the occurrence of natural events. Besides wind tunnel experiments and independent samplers, optical or acoustic sensors can detect particles' intensity and movement. Another method is to measure the height difference of the topsoil layer before and after erosion or deposition with an altimeter or ruler. Fallout environmental radionuclides can also be used as tracers and chronometers for soil erosion (Funk, 2016).

Based on controlling factors derived from field experiments, the first Wind Erosion Equation was developed in the 1960s after thirty years of research (Morgan and Quinton, 2001). On the contrary, the first attempts for an equation that derives soil loss by water erosion were already

published in 1940, leading to physically based models such as the Universal Soil Loss Equation (USLE) (Morgan, 2005). The simple Wind Erosion Equation expressed soil loss as a function of aggregate size distribution (ASD), surface roughness length, and surface residue (Woodruff and Siddoway, 1965). The limitations of the Wind Erosion Equation were recognized, and in 1985, the official genesis of a new Wind Erosion Prediction System (WEPS) occurred. The documentation for a more process-based, modular structured model was published ten years later. After various milestone events, WEPS was installed in 2010 on 15,000 computers (Wagner, 2013). The WEPS model provides easy access to inputs and outputs, has been extensively validated worldwide, and is a state-of-the-art research and decision-support system (Tatarko et al., 2019, 2016).

Overall, great effort has been made globally to determine soil loss estimations under different environmental conditions and agricultural practices, leading to the development of various adaptation measures to prevent erosion practically and erosion models to evaluate different soil conservation practices. Although models differ in complexity and specific capabilities, such as the range of spatial and temporal scales, they are all based on an ongoing improving understanding of factors influencing erosion and their processes.

2.4 Factors influencing soil erosion

The state of the art for each specific research gap is described in detail in the corresponding publication. This section briefly outlines the factors influencing soil erosion (Fig. 2.4).

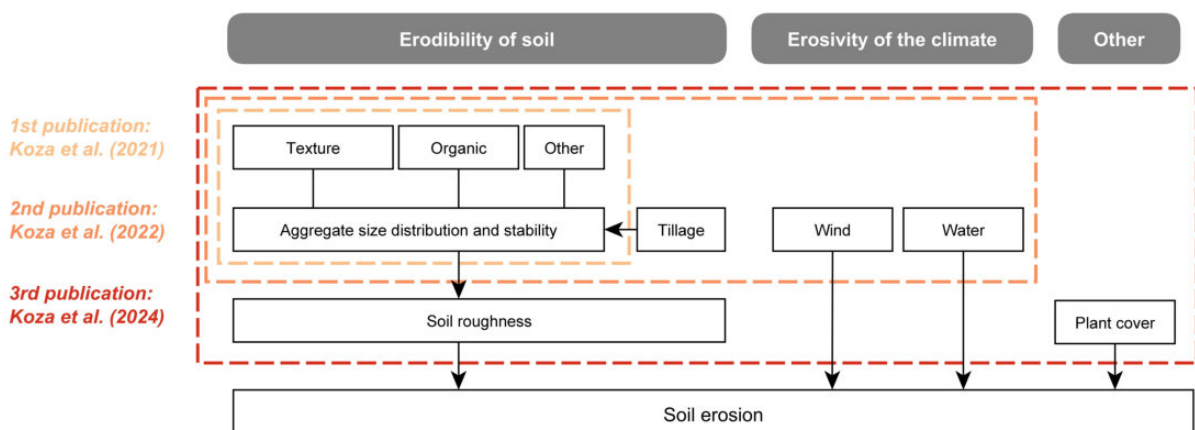


Fig. 2.4. Overview of categories determining (gray boxes) and factors (white boxes) influencing soil erosion. The three sequential publications' development process and contribution to this dissertation are shown inside the dashed boxes.

The soil's erodibility mainly depends on soil texture derived from particle size distribution (PSD) and binding material, which influence the formation of aggregates and crusts as well as water-holding capacity (Chepil, 1952; Scheffer et al., 2016). Primary soil properties are a key component of any data set used for implementing sustainable agricultural practices. The PSD is an important input data for wind erosion models such as SWEEP (Jarrah et al., 2020) or indirectly used by the K-factor in water erosion models (Alewell et al., 2019). Besides the traditional and standardized sieving/sedimentation method, the common laser diffraction analysis (LDA) is proposed as a standard method for particle size analysis in soil science (Bittelli et al., 2019). It is also used for input data for modeling (Pi and Sharratt, 2017). Hence, the impact of different pretreatments on soil texture and the consequences for erosion modeling and soil loss estimates were explored (Koza et al., 2021).

Primary particles exist mainly as structural units under natural conditions. Hence, aggregate size and stability are the main factors that influence soil erodibility (Chepil, 1950b) but are related to cultivation, erosive forces, and soil wetting (Kemper and Rosenau, 2018). In reverse, the stability of aggregates is directly linked to the soil's erodibility by its resistance against disruptive forces. Mechanical stress can occur externally (e.g., by tillage, saltation of particles, raindrop impact, etc.) or internally (e.g., slaking, swelling, etc) (Diaz-Zorita et al., 2002). Due to the existing climatic conditions, steppe soils are susceptible to various erosive and disruptive forces. During dry summers, heavy and light rain events are common. Still, most of the annual precipitation occurs as snowfall, causing extreme snowmelt in spring. The stability of soil aggregates against the mechanical forces of wind and water on crop- and grassland has been investigated side-by-side in the dry steppe of Kazakhstan (Koza et al., 2022).

In order to assess soil loss under natural conditions, soil erodibility, and climate erosivity must be considered in interaction with additional factors (e.g., plant cover). Together, they cause a high temporal and spatial variability of erosion potential at a particular site. The highest climatic erosivity is usually during spring and coincides with seedbed preparation (Funk and Reuter, 2006). Further, the effect of plants on wind erosion depends on the surface or silhouette of the crop that covers the soil or breaks the airflow. While a permanent vegetation cover is the best protection against wind erosion, temporal variations occur depending on the crop type or the plant growth according to the season on arable land (Funk, 2016). Consequently, erosion-controlling factors such as vegetation, aggregate, and mechanical stress during field cultivation were tested with field experiments on steppe soils (Koza et al., 2024).

3. Research questions

The overall research question unifying the three publications is:

What are the main drivers of erosion under the influence of parent material, land use, and climate in the cultivated steppe of Kazakhstan?

In order to derive recommendations for sustainable land use management of semi-arid soils under cultivation, various knowledge gaps were filled. In specific, this dissertation investigates and answers the following research questions in more detail:

Koza et al., 2021:

- *Which chemical pretreatment efficiently removes the binding agents to successfully measure PSD by laser diffraction?*
- *What are the effects of different pretreatments for measuring particle sizes with laser diffraction for modeling soil loss estimates?*

Koza et al., 2022:

- *Which physical and chemical soil properties of the topsoil enhance aggregation and counteract erosion in dry steppe soils?*
- *How does land use affect aggregate stability and how erodible are steppe soils by wind and water?*

Koza et al., 2024:

- *What are the short-term effects of various agricultural management practices on surface characteristics and soil loss rates by wind erosion?*
- *What particle and aggregate sizes are detached and deposited during aeolian processes?*
- *How much organic carbon is lost by wind erosion?*

4. Overview of materials and methods

The study area connects the central with the east-central part of the Eurasian Steppe and is located in the northeastern part of Kazakhstan (latitude: 51–54°N; longitude 69–79°E). In the dry steppe, various types of Chernozem and Kastanozem soils with silty and sandy textures form a heterogeneous pattern (Koza et al., 2022; Uspanov et al., 1975). While Chernozems are present north of Astana, Kastanozems dominate from Astana to the international border with Russia in the east. The climate is continental, with hot and dry summers (FAO, 2012). Test sites are characterized by comparable annual mean temperatures (2.7–3.9°C) and precipitation (297–347 mm) based on weighted interpolation 1991–2020 (Harris et al., 2020; Zepner et al., 2021) (Fig. 4.1). Most of the annual precipitation occurs as snowfall and severe thunderstorms in the summer can cause flash floodings. The study area is characterized by strong winds with gusts over 40 m s⁻¹ (FAO, 2012).

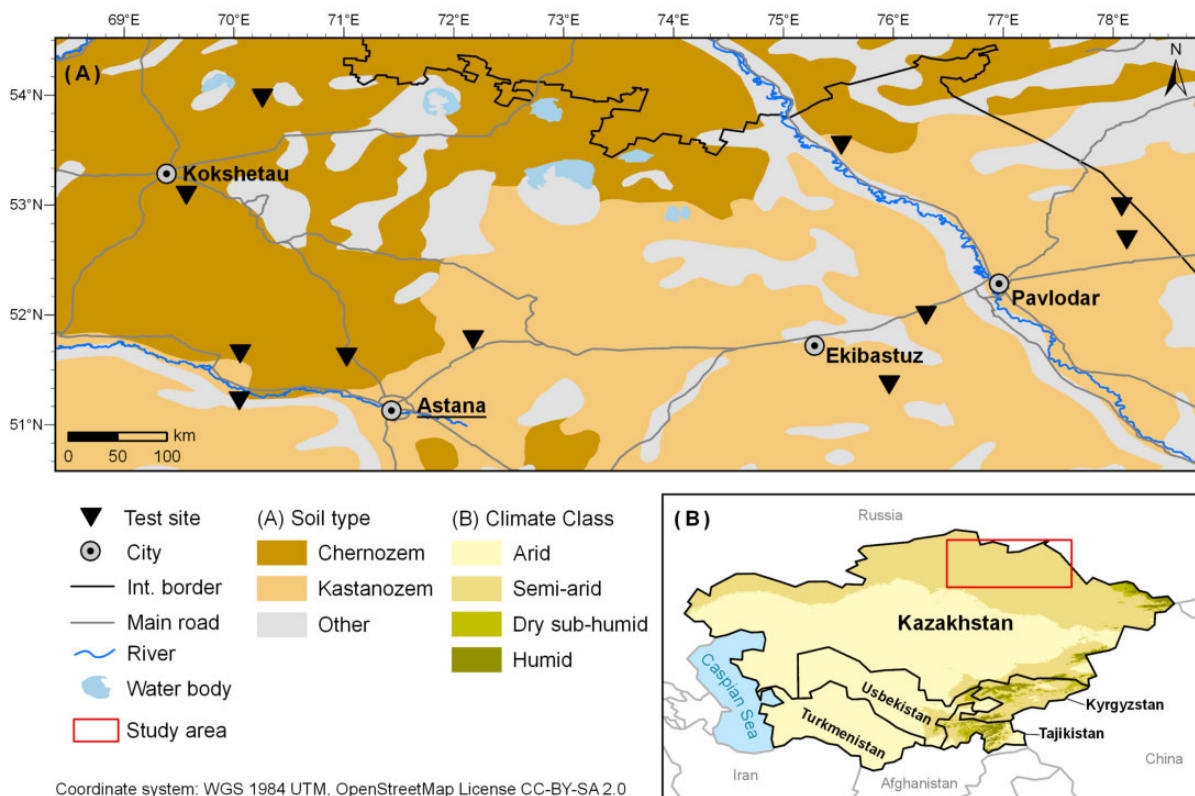


Fig. 4.1. Location of eleven test sites with dominant soil types in Kazakhstan (A) (FAO/UNESCO, 2007) and the study area with climate classes in Central Asia (B) (Zomer et al., 2022).

The study area has been under agricultural management since the Virgin Lands Campaign in the 1950s. Even though large areas of arable land were abandoned after the collapse of the

4. Overview of materials and methods

Soviet Union more than 20 years ago, most areas have been reploughed by today (Frühauf et al., 2020; Prishchepov et al., 2020). Currently, northern Kazakhstan comprises the most extensive area of arable land (Fig. 4.2). Despite cropland, native steppes or pastures exist. Overall, the study area's parent material, land use, and climate are predestined for soil erosion (Fig. 4.3, Appendix Fig. A1).



Fig. 4.2. Typical situation in northern Kazakhstan: Cropland under cultivation.

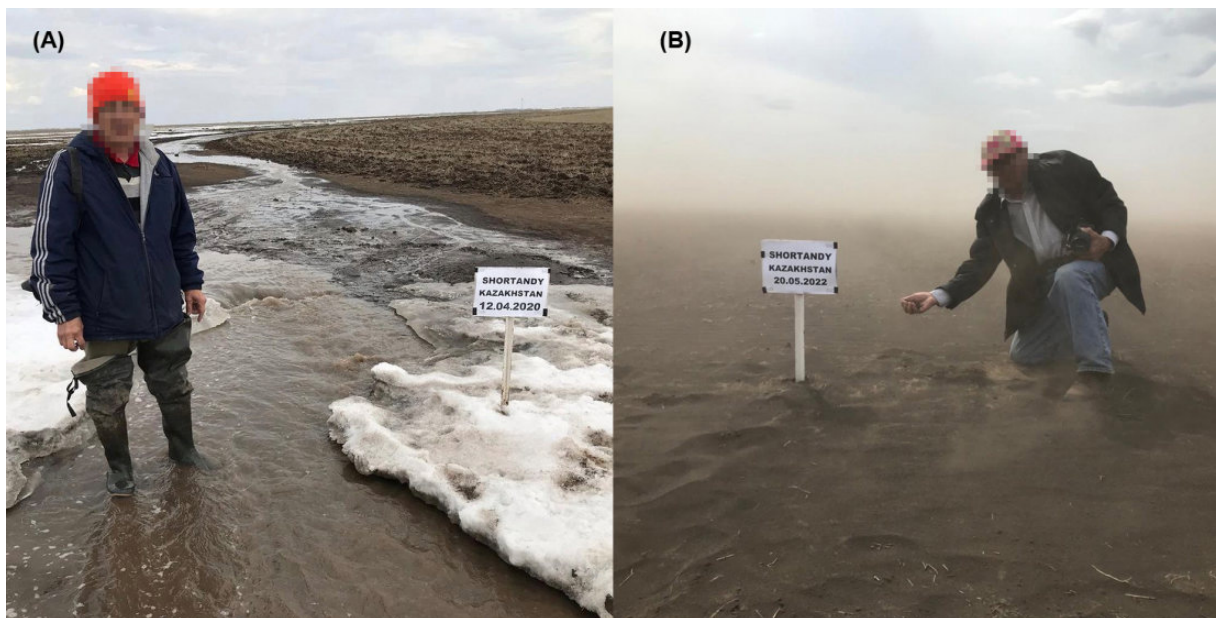


Fig. 4.3. Severe water (A) and wind (B) erosion events in 2020 and 2022 on a test site (with friendly permission of Kanat Akshalov).

The publications contributing to this cumulative dissertation are based on soil sampling campaigns and field experiments conducted in northern Kazakhstan between April 2018 and June 2022 (including postponed activities due to the global COVID-19 pandemic). Various test sites throughout the study area were located and investigated, depending on the specific research focus and external circumstances. Each publication contains a map of the study area in focus. In a total of six field trips over 500 soil samples (Appendix Fig. A2) from eleven test sites (Fig. 4.1) were collected. Soils were analyzed at laboratories of the Barayev Research and Production Center for Grain Farming Kazakhstan and Martin Luther University Halle-Wittenberg. Additional datasets were collected or processed in-situ.

Soil samples from various plots were analyzed for their physical and chemical soil parameters. Overall comprehensive data from the topsoil was collected, including pH values, electrical conductivity (EC), soil texture derived from sieving/sedimentation as well as LDA (further information in Koza et al., 2021), soil carbon content (SOC), total inorganic carbon (TIC), nitrogen content, aggregate stability and size distribution (Appendix Fig. A3) including the erodible fraction (EF) (further information about the applied forces and used indices in Koza et al., 2022) as well as the geometric mean diameter (GMD). Aeolian sediments were also analyzed with laser diffraction to measure the dry ASD. Additional surface parameters were measured, such as the soil water content, and the aerodynamic roughness length (Koza et al., 2024).

Soil loss estimates were modeled with the process-based computer model SWEEP (Single-event Wind Erosion Evaluation Program, Version 1.5.52, USDA-ARS, Manhattan/Kansas, USA). This sub-model of WEPS, estimates soil loss for single-day storm events under the influence of site-specific input data and physical fundamentals of soil erosion. The SWEEP computes soil loss in response to surface conditions (biomass, soil layer, surface condition) and weather (wind speed and direction) on a sub-hourly basis. After determining the threshold friction velocity based on different input parameters (full list of used parameters and values are shown on page 35, in Koza et al., 2022, Table 1) at which erosion begins, it then calculates when the aerodynamic forces overcome the retaining forces. Once wind speed exceeds the threshold, it calculates soil losses over a series of individual grid cells representing the field. The model's outcome is total soil loss in kg m^{-2} , which is divided into the loss by saltation, creep, and suspension (Tatarko, 2008).

A meteorological station was installed at a test site in August 2018 to monitor weather conditions in the study area, including temperature, solar radiation, wind speed, and direction, precipitation, and soil moisture (further description in Koza et al., 2022). The following equipment was constructed and/or set up (Appendix Fig. A4) to explore and investigate soil loss by wind erosion under real soil conditions between 2018 and 2022 (Fig. 4.4):

- A mobile wind tunnel to simulate wind erosion events with a velocity of up to 15 m s^{-1} under real conditions on various surfaces and test sites.
- Various MWAC samplers to collect aeolian sediments detached from the ground at different heights during wind tunnel experiments.
- Modified SUSTRA to collect higher amounts of aeolian sediments in one height for quality analyses.

A more comprehensive explanation about the equipment used to quantify wind erosion is published by Koza et al. (2024). Additional sediment traps, such as Bottle Sediment Traps (BOSTRA) (Funk et al., 2004) and a Sand trap (Rotnicka, 2013) were also built and used to explore their potential for collecting aeolian sediments during experiments or natural events.

Statistical analyses and graphs were performed with Rstudio (Version 4.1.2, Rstudio Team, Vienna, Austria). Maps were prepared with ArcGIS (Desktop Release 10.6, ESRI, Redlands, USA) and ArcGIS Pro (Version 2.4.1, ESRI, Redlands, USA).



Fig. 4.4. *The mobile wind tunnel with MWAC samplers and SUSTRA for collecting aeolian sediments during field experiments on maize.*

5. Publications

5.1 Koza et al. (2021): Consequences of chemical pretreatments in particle size analysis for modelling wind erosion

Full bibliographic citation:

Koza, M., Schmidt, G., Bondarovich, A., Akshalov, K., Conrad, C., Pöhlitz, J., 2021.

Consequences of chemical pretreatments in particle size analysis for modelling wind erosion. *Geoderma* 396, 115073.

<https://doi.org/10.1016/j.geoderma.2021.115073>

Scientific presentation and discussion of this study:

Koza, M., Schmidt, G., Bondarovich, A., Akshalov, K., Conrad, C., Pöhlitz, J., 2022. How does chemical pretreatment in particle size analysis affect modeling wind erosion? *Jahrestagung der Deutschen Bodenkundlichen Gesellschaft*. Tier, Germany.

Koza, M., Prays, A., Bondarovich, A., Ashalov, K., Conrad, C., Schmidt, G., 2020. How does pretreatment of dry steppe soils affect particle size analysis by laser diffraction? *EGU General Assembly 2020*, EGU2020-9415. Online.

<https://doi.org/10.5194/egusphere-egu2020-9415>

Preface:

Soil texture is one of the primary soil properties affecting the susceptibility to water and wind erosion. It is, therefore, a key to any data set used for implementing sustainable practices. Various methods exist to measure PSD. The laser diffraction method is increasingly applied in soil science because of its methodological advantages against traditional sedimentation methods (Bittelli et al., 2019). Still, the impacts of different pretreatments prior to LDA to remove binding agents have not been tested. It is unclear to what extent common pretreatments for the determination of soil texture cause a change in soil loss estimations.

Summary:

This publication investigates the influence of various pretreatments to remove binding agents on the PSD measured by LDA. Considering the importance of soil texture and binding agents regarding soil erodibility, this study evaluates the consequences of these pretreatments for wind erosion modeling as an applied approach. Overall, this first publication (Koza et al., 2021) provides fundamental recommendations for LDA, wind erosion modeling under semi-arid conditions, and first insights into wind erosion processes of the study area.

Highlights:

- Chemical pretreatment with HCl resulted in incomplete dispersion or aggregation.
- Oxidisation of organic binding material with H₂O₂ caused complete sample dispersion.
- Pretreatments for PSD did not affect texture class.
- Pedotransfer functions based on PSD by laser diffraction need further investigation.
- Soil loss estimates showed no variation based on obtained PSD data.



Contents lists available at ScienceDirect

Geoderma

journal homepage: www.elsevier.com/locate/geoderma

Consequences of chemical pretreatments in particle size analysis for modelling wind erosion

Moritz Koza^{a,*}, Gerd Schmidt^a, Andrej Bondarovich^b, Kanat Akshalov^c, Christopher Conrad^a, Julia Pöhlitz^a

^a Department of Geoecology, Institute of Geosciences and Geography, Martin Luther University Halle-Wittenberg, 06120 Halle (Saale), Germany

^b Department of Economic Geography and Cartography, Institute of Geography, Altai State University, 656049 Barnaul, Russia

^c Department of Soil and Crop Management, Barayev Research and Production Center for Grain Farming, 474010 Shortandy, Kazakhstan

ARTICLE INFO

Handling Editor: Morgan Cristine L.S.

Keywords:

Soil texture
Laser diffraction
Hydrochloric acid
Hydrogen peroxide
Wind erosion prediction system
SWEEP
Derivation of soil characteristics

ABSTRACT

The particle size distribution (PSD) of soil plays a vital role in wind erosion prediction. However, the impact of different pretreatments to remove binding agents for PSD and consequences for wind erosion modelling have not been tested. We collected 90 topsoil samples of Chernozems and Kastanozems from different test sites in Kazakhstan. Soil samples covered typical land-use types and farming methods with calcium carbonate contents reaching from 2.2 to 117.3 g kg⁻¹ and soil organic carbon content from 11.2 to 48.7 g kg⁻¹. Prior to particle size analysis by laser diffraction, samples were chemically pretreated separately and successively with 10% hydrochloric acid (HCl), to dissolve carbonates and 30% hydrogen peroxide (H₂O₂), to oxidise organic binding material. The HCl pretreatment resulted in incomplete dispersion or even aggregation due to calcium ions released by the dissolution of carbonates, while removing organic matter with H₂O₂ caused complete sample dispersion. The associated changes in PSD were overall minor, and only a few of our samples were assigned to a different texture class. Obtained PSD data was used to calculate texture-based properties, such as the geometric mean diameter (GMD), with a pedotransfer function. Calculated and measured input data were applied to the Single-event Wind Erosion Evaluation Program (SWEEP) to estimate potential soil losses. As a result, SWEEP's simulations showed substantial variations if the GMD is calculated based on PSD under the influence of different pretreatments. At the same time, there was no variation if the GMD was independently measured. We suggest that for standard particle size analysis of calcareous soils, pretreatment with HCl should be avoided because it might cause misleading results. Considering the variation induced by PSD analysis and resulting potential soil losses, pretreatments for laser diffraction analysis can be omitted for the investigated, silt-dominated Chernozems and Kastanozems if additional texture-based parameters are measured.

1. Introduction

Adapting agriculture to climate change is currently one of the most urgent challenges worldwide (Keesstra et al., 2016; UN, 2019; WEF, 2020). The semi-arid steppe regions of Asia suffer from extreme climate conditions and land-use management. This enhances wind and water erosion which causes a loss in soil productivity (Abbas et al., 2020; FAO, 2017; Li et al., 2020; Reyer et al., 2017).

Kazakhstan is one of the world's largest grain exporters (FAO, 2017). It showed its yield potential in 2009 with 2.5% of the world's total wheat

(*Triticum* L.) production (FAO, 2012; Sommer et al., 2013). As the largest country in Central Asia, it is the most important grain exporter with potentially up to 84.5 Mio hectares of agricultural land (Almaganbetov and Grigoruk, 2008). However, Kazakhstan is likely a major hotspot of heat stress for wheat in the future climate change scenario A1B (2071–2100) predicted from the baseline climate (1971–2000) (Teixeira et al., 2013). Water scarcity (FAO, 2012) and wind erosion affect agricultural productivity already on about 25.5 Mio hectares (Almaganbetov and Grigoruk, 2008). Counteracting these developments require reliable tools and methods to quantitatively assess soil erosion risk under

Abbreviations: GMD, geometric mean diameter; H₂O₂, hydrogen peroxide; HCl, hydrochloric acid; HCl_{SC}, hydrochloric acid soluble compounds; LDA, laser diffraction analysis; PSD, particle size distribution; SWEEP, Single-event Wind Erosion Evaluation Program.

* Corresponding author.

E-mail address: moritz.koza@geo.uni-halle.de (M. Koza).

<https://doi.org/10.1016/j.geoderma.2021.115073>

Received 16 December 2020; Received in revised form 22 February 2021; Accepted 1 March 2021

Available online 4 May 2021

0016-7061/© 2021 The Authors. Published by Elsevier B.V. This is an open access article under the CC BY license (<http://creativecommons.org/licenses/by/4.0/>).

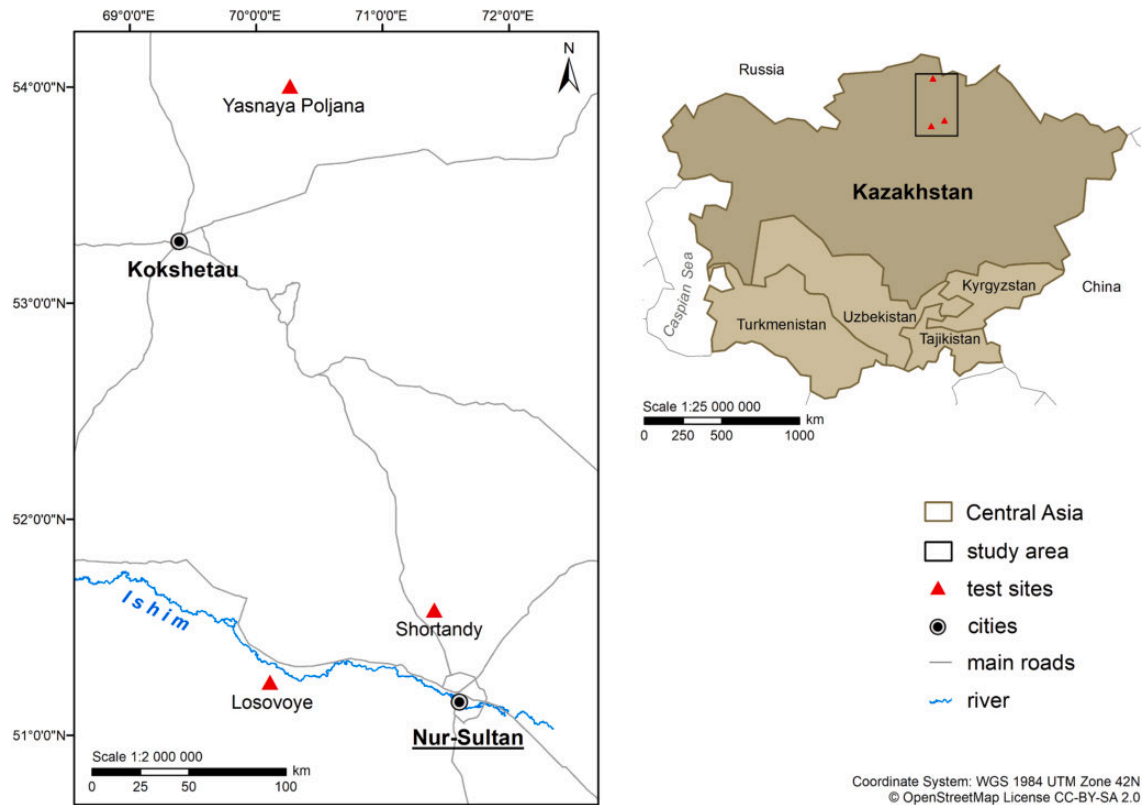


Fig. 1. Geographical location of the study area in Central Asia, including the three test sites in Kazakhstan. The test field for soil loss estimations and the meteorological station are located in Losovoye.

current and future climatic conditions.

Soil texture is a key component of any data set used for implementing sustainable agricultural practices (Kettler et al., 2001). It is one of the primary soil properties affecting the soil's susceptibility to water and wind erosion (Bowker et al., 2008; Zobeck and Van Pelt, 2015). Estimating the loss of soil by water erosion with the Revised Universal Soil Loss Equation (RUSL) requires both information on soil texture and organic matter content to derive the soil erodibility factor (K-factor). In wind erosion models, the percentages of silt, sand, and clay are critical components independent of the models' complexity or capabilities (Jarrah et al., 2020). They are necessary in order to estimate soil loss with the Wind Erosion Prediction System (WEPS) or needed to compute the erodible fraction to apply the Revised Wind Erosion Equation (RWEQ).

Particle size analysis to assign texture classes requires the dispersion of soil aggregates and the removal of binding agents: iron oxide, carbonates, and organic matter (Gee and Or, 2002). Iron oxide coatings are usually not discussed for the topsoil layer in dry steppe biomes. They are just slightly weathered and do not indicate acidity of less than a pH value of six. Carbonates can be removed using hydrochloric acid (HCl). However, decalcification is not a standardized procedure, and this time-consuming pretreatment is often omitted in PSD (ISO 11277, 2002; Schulte et al., 2016). To remove organic matter, hydrogen peroxide (H_2O_2) has been recommended as a standard oxidant for most soils (Gee and Or, 2002; Kroetsch and Wang, 2007). However, all chemical pretreatments could lead to unpredictable effects on particle size distribution (PSD). For instance, HCl does not only remove carbonates but also small amounts of organic matter (Bisutti et al., 2004) and might dissolve

poorly ordered metal oxides, too (Carroll and Starkey, 1971). A treatment with H_2O_2 might lead to a disintegration of layered silicates and, when applied to calcareous soils, result in precipitation of calcium oxalate (Mikutta et al., 2005). Currently, there is uncertainty about the consequences of different soil pretreatments on PSD analysis and the subsequent variation in soil erosion estimates.

Therefore, we compared PSD data from non-pretreated soil, soil after two different HCl pretreatments, after H_2O_2 pretreatment, and after sequential H_2O_2 and HCl pretreatment. After each pretreatment, PSD was measured by laser diffraction analysis (LDA). This method has become widely used and accepted in soil science. Laser diffraction is in good agreement with independent optical methods (Bittelli et al., 2019) and has been applied to wind erosion modelling in the past (Pi et al., 2016).

For our experiment, we relied on Chernozem and Kastanozem soils from the dry steppe biome of Kazakhstan. They contain high amounts of organic matter and secondary carbonates (Eckmeier et al., 2007) as binding agents and are also favourable for agriculture. However, their parent material consists of aeolian sediments and is most vulnerable to wind erosion in drylands (Schmidt et al., 2020).

Based on different texture data, we modelled potential soil losses by wind erosion for an arable field in Kazakhstan's dry steppe with the Single-event Wind Erosion Evaluation Program (SWEEP). This sub-model of the Wind Erosion Prediction System, the state-of-the-art research and decision-support system to predict wind erosion worldwide, estimates soil losses for a single day storm event under the influence of site-specific input data (Hagen, 1991; Tatarko et al., 2019). Besides texture, texture-based properties, such as the geometric mean

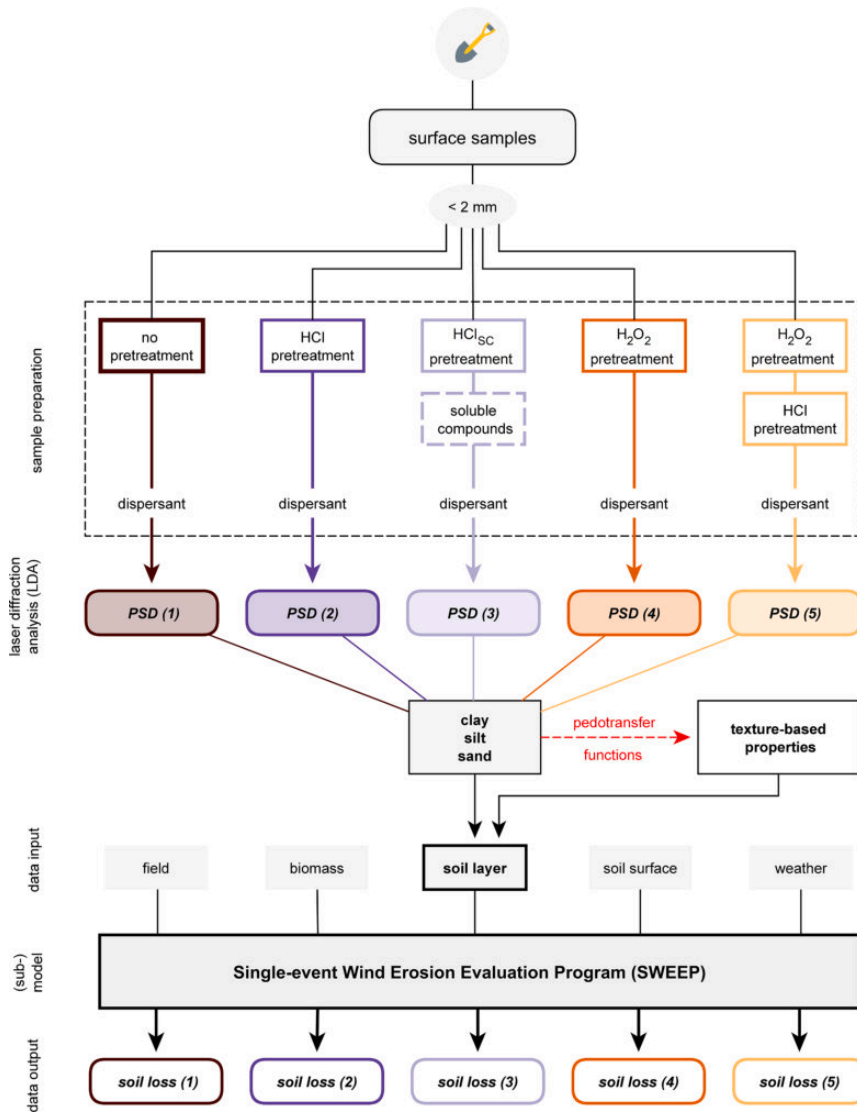


Fig. 2. Hierarchical data structure defining the study design. Sample preparation for measuring particle size distribution (PSD) by laser diffraction included no pretreatment and four different pretreatments, such as hydrochloric acid (HCl) pretreatment, HCl soluble compounds (HCl_{SC}) pretreatment, hydrogen peroxide (H₂O₂) pretreatment and the sequential hydrogen peroxide and hydrochloric acid (H₂O₂ + HCl) pretreatment. Results of PSD were used as data input for the Single-event Wind Erosion Evaluation Program (SWEEP) to estimate soil losses by wind erosion and to calculate texture-based properties with pedotransfer functions from the SWEEP user manual (Tatarko, 2008).

diameter (GMD) and other, are important input data for SWEEP. In case only a minimum of measured parameters are available, these texture-based properties can be derived from PSD with pedotransfer functions.

The main objectives of this study are (i) to compare the effects of different chemical pretreatments on PSD by LDA, (ii) to test the efficiency of pretreatments to remove binding agents, and (iii) to compare modelling estimates of soil loss based on PSD with either calculated or measured GMD.

2. Material and methods

2.1. Study area

The study area is located in the north-eastern part of Kazakhstan, which is mostly flat. The area of interest connects the central and the east-central part of the Eurasian steppe belt. Test sites (Fig. 1) are north of Kokshetau in Yasnaya Poljana (Ясная Поляна: 54°01'11.8"N, 70°15'00.2"E), north of Kazakh's capital Nur-Sultan in Shortandy (Шортанды: 51°34'35.2"N, 71°16'04.3"E) and west at the Ishim River in Losovoye (Лозовое: 51°11'58.9"N, 70°02'06.2"E). All test sites belong administratively to North Kazakhstan and Akmola. Both are provided with water by the Ishim river basin, which has the lowest groundwater reserves in Kazakhstan (FAO, 2012). The study area covers a transect of 300 km with a dry continental climate, following a weak climatic gradient in precipitation and temperature from north to south. The annual precipitation height and mean annual temperature in Yasnaya Poljana are 352.0 mm and 2.8 °C, in Shortandy 327.0 mm and 3.3 °C, and Losovoye 297.8 mm and 3.7 °C (1989–2019) based on weighted interpolation (Harris et al., 2020; Zepner et al., 2020). One-third of the annual precipitation occurs as snowfall. Overall, different types of Chernozem and Kastanozem soils form a heterogeneous pattern in the study area (FAO/UNESCO, 2007; Uspanov et al., 1975). Haplic Chernozems are dominant at the north end of the study area close to Yasnaya Poljana. In Shortandy, Calcic Chernozems and around Losovoye, primarily Calcic Kastanozems exist (Uspanov et al., 1975).

Kazakhstan experienced the most considerable anthropogenic land cover change in the twentieth century. During the 'Virgin Lands Campaign', about 420 000 km² of temperate grassland, mainly in northern Kazakhstan and in the Altai region of Russia, were converted into arable land for grain production (Frühauf et al., 2020; Prishchepov et al., 2020). Large areas of arable land were abandoned after the collapse of the Soviet Union in 1991. However, most areas have been reploughed by now. North Kazakhstan and Akmola together with Kostanay comprise the most extensive areas of arable land in Kazakhstan. Grain crops are mainly cultivated, and spring wheat (*Triticum aestivum* L.) is the most common crop. Despite agriculture, there are pastures and native steppes with *Stipa* (*Stipa capillata* L.), Volga fescue (*Festuca valesiaca* Schleich. ex Gaudin) and shrubs (*Artemisia* spp.) typical (Rachkovskaya and Bragina, 2012).

2.2. Soil sampling

In late May of 2018, we took 90 undisturbed topsoil samples from twelve fields using 250 cm³ soil sample rings (diameter = 80 mm, height = 50 mm; Eijkelkamp, Giesbeek, Netherlands). A wide range of different land-use types (native steppe, pasture and arable fields) and farming methods were covered, including standard tillage practices such as fallow, deep tillage (with chisel plough), no-till (without tillage), reduced tillage (shallow tillage with a cultivator or disc harrow), diverse tillage (with new farming procedures or machines). Irrigation was not present. Each of the three fields in Yasnaya Poljana were sampled with six topsoil samples. In Shortandy, two fields, and Losovoye, seven fields were sampled with eight topsoil samples each ($n = (3 \times 6) + (9 \times 8) = 90$). Samples on arable fields were taken before they were being sowed. Each field was sampled randomly according to the general agricultural sampling procedure up to 30 cm representing

the topsoil layer (Conklin and Meinholz, 2004). All samples were taken within the A horizon and the depth to where tillage practices extend.

2.3. Physical-chemical soil analysis

Soil samples from field sampling were transferred to plastic bags, air-dried, gently crushed, and dry sieved with a 2-mm sieve. Loose organic material was separated by electrostatics. Each sample (<2 mm) was then adequately split into subsamples (ISO 14488, 2007) for physical-chemical soil analysis.

Soil pH was determined potentiometrically using a glass electrode in a 1:5 suspension of soil in distilled water (ISO 10390, 2005). Electric conductivity was measured at a soil-to-water ratio of 1:2.5 (Sonmez et al., 2008). The calcium carbonate (CaCO₃) content was calculated by analysing the carbonate content using a Scheibler calcimeter (Carl Hamm, Essen, Germany). Therefore, the volume of carbon dioxide released after adding 4 M HCl (ISO 10693, 1995) was determined. Total carbon and total nitrogen were determined after high-temperature combustion of 1 g soil by 950 °C using an elemental analyser (vario Max Cube, Elementar, Langensfeld, Germany). Soil organic carbon was calculated from total carbon and calcium carbonate (organic carbon = total carbon – 0.12 × calcium carbonate). Organic matter was estimated from organic carbon by the factor 1.72 (FAO, 2006).

2.4. Particle size analysis

2.4.1. Sample preparation

For particle size analysis, subsamples were exposed to the following pretreatments (Fig. 2):

no pretreatment: 2 ml of 0.05 M sodium pyrophosphate (Na₄P₂O₇ × 10 H₂O) solution was added as the dispersion medium to 10-g soil. The soil turned to a 'paste-like' consistency as required for LDA (ISO 13320, 2009).

HCl pretreatment: 25 ml of deionised water was added to 10-g soil. For each percentage of carbonate, 1 ml of 10% HCl was added dropwise until pH decreased between 4.0 and 4.5, resulting in a maximal volume of 70 ml. Afterwards, the suspension was kept on a heating plate at 50 °C until the reaction ceased completely. After removing the clear supernatant, the dispersion medium was added as described above.

HCl soluble compounds (HCl_{SC}) pretreatment: 10-g soil was pretreated as mentioned before. Following the HCl treatment, the recovered soil was resuspended in deionised water between 500 and 3000 ml until the electric conductivity in the clear supernatant turned < 500 µS/cm. After removing the supernatant, the dispersion medium was added.

H₂O₂ pretreatment: 10-g soil was pretreated with 30% H₂O₂. Each time, 15 ml H₂O₂ was added to avoid excessive foam production, and no more than 100 ml H₂O₂ was applied. After the initial reaction ceased, the suspension was kept for one hour on a heating plate at 50 °C. Afterwards, the suspension was allowed to settle and the clear supernatant removed with a pipette. The dispersion medium was added.

H₂O₂ + HCl pretreatment: 10-g soil was sequentially pretreated with H₂O₂ and HCl as described above but without washing out soluble compounds. The dispersion medium was added.

2.4.2. Laser diffraction analysis

The PSD was measured with a laser diffraction analyser (Helos/KR, Sympatec GmbH, Clausthal-Zellerfeld, Germany) equipped with a 60 W sonotrode and a fully automated wet dispersion unit of 1000 ml water (Quixel, Sympatec GmbH, Clausthal-Zellerfeld, Germany). A second replicate was measured to ensure the first measurement. The diffraction system uses a helium-neon laser light source (wavelength = 632.8 nm) with fibre optical cable and a fixed beam expansion unit (Sympatec, 2012). It has an accuracy of ± 1%, a precision of < 0.04%, and comparability from one system to another of < 1% (Sympatec, 2019). It does not merge laser diffraction and light scattering and determines 49 physical particle size classes ranging from 0.5 to 3500 µm.

Table 1
Single-event Wind Erosion Evaluation Program (SWEEP) input parameters and values for modelling wind erosion on the 29th of April 2019 on a fallow arable test field in Losovoye. Values were measured, assumed, estimated or calculated following the SWEEP user manual (Tatarako, 2008).

SWEEP	parameter	source	value
Field	x length, y length [m]	estimated	2000.00
	angle from north [°]	assumed	0.00
	wind barriers	estimated	none
Biomass	residue average height [m]	assumed	0.00
	residue stem area index [m ² m ⁻²]	assumed	0.00
	residue leaf area index [m ² m ⁻²]	assumed	0.00
	residue flat cover [m ² m ⁻²]	estimated	0.30
	growing crop average height [m]	assumed	0.00
	growing crop stem area index [m ² m ⁻²]	assumed	0.00
	growing crop leaf area index [m ² m ⁻²]	assumed	0.00
	row spacing [m]	assumed	0.00
	seed placement	estimated	furrow
	number of layers	measured	1.00
Soil layer	thickness [mm]	measured	300.00
	sand fraction [kg kg ⁻¹]	measured *	0.08–0.14
	very fine sand fraction [kg kg ⁻¹]	measured *	0.06–0.11
	silt fraction [kg kg ⁻¹]	measured *	0.69–0.79
	clay fraction (<2 μm) [kg kg ⁻¹]	measured *	0.07–0.19
	rock volume fraction [m ³ m ⁻³]	assumed	0.00
	dry bulk density [kg m ⁻³]	measured	1.09
	average aggregate density [kg m ⁻³]	calculated	1.46
	average dry aggregate stability [ln(J kg ⁻¹)]	calculated	1.80–2.98
	geometric mean diameter [mm]	calculated **	4.15–5.30
	geometric standard deviation [mm mm ⁻¹]	calculated	15.47–15.96
	minimum aggregate size [mm]	estimated	0.01
	maximum aggregate size [mm]	estimated	14.84–18.86
	soil wilting point water content [kg kg ⁻¹]	measured	0.15
	surface crust fraction [m ² m ⁻²]	assumed	0.00
	surface crust thickness [m m ⁻¹]	assumed	0.00
	loose material on crust [m ² m ⁻²]	assumed	0.00
	loose mass on crust [kg m ⁻²]	assumed	0.00
	crust density [kg m ⁻³]	calculated	1.46
	crust stability [ln(J kg ⁻¹)]	calculated	1.80–2.98
allmaras random roughness [mm]	estimated	10.00	
ridge height [mm]	assumed	0.00	
ridge spacing [mm]	estimated	300.00	
ridge width [mm]	estimated	100.00	
ridge orientation from north [°]	assumed	0.00	
dike spacing [mm]	assumed	0.00	
snow depth [mm]	assumed	0.00	
hourly surface water content [kg kg ⁻¹]	assumed	0.00	
Weather	air density [kg m ⁻³]	calculated	1.18
	wind direction from north [°]	measured	250.8
	anemometer height [m]	measured	2.00
	wind speed (max) [m s ⁻¹]	measured	Fig. 3

* data input varies depending on pretreatment of particle size analysis by LDA (Table 2 and Table 3).

** data input first derived from soil texture and calculated (Table 2), then measured (Table 3).

In laser diffraction, particles scatter light with different intensities according to their size in the near forward direction. The diffraction of light by a single particle is described mathematically by the Fraunhofer theory because it applies to mixtures of different materials. No optical properties, such as each particle's refractive index, are required (Green and Perry, 2007; ISO 13320, 2009). Particle size analysis was applied to 2–3 g of soil for 20 sec after 1 min of 60 W sonicating. During laser diffraction, the extent of obscuration was always between 20 and 30%. Based on the United States Department of Agriculture (USDA), eight particle size subclasses were used to present PSD data between 0.5 and 2000 μm (Soil Science Division Staff, 2017). The used 2–50–2000 μm particle size classification system is currently most common in wind erosion and land-surface modelling (Shao, 2008).

Table 2

The data input of clay [kg kg⁻¹], silt [kg kg⁻¹], sand [kg kg⁻¹] and very fine sand [kg kg⁻¹] were measured by laser diffraction analysis. The geometric mean diameter of aggregate sizes [mm], average dry aggregate stability [ln(J kg⁻¹)], geometric standard deviation of aggregate sizes [mm] and maximum aggregate size [mm] derived from results of laser diffraction analysis following the SWEEP user manual (Tatarako, 2008). Estimates of soil losses for a fallow arable test field in Losovoye are shown as data output. Total soil loss [kg m⁻²] consists of saltation and creep loss [kg m⁻²] and suspension loss [kg m⁻²]. The fine particulate matter of 10 μm or less in diameter (PM₁₀) [kg m⁻²] is part of the suspension loss.

	data input SWEEP measured (laser diffraction analysis)				data input SWEEP estimated (derived values by pedotransfer functions)				data output SWEEP simulated			
	clay [kg kg ⁻¹]	silt [kg kg ⁻¹]	sand [kg kg ⁻¹]	very fine sand [kg kg ⁻¹]	geometric mean diameter of aggregate sizes [mm]	average dry aggregate stability* [ln(J kg ⁻¹)]	geometric standard deviation of aggregate sizes [mm mm ⁻¹]	max. aggregate size [mm]	total soil loss [kg m ⁻²]	saltation/creep loss [kg m ⁻²]	suspension loss [kg m ⁻²]	PM ₁₀ loss [kg m ⁻²]
no pretreatment	0.16	0.72	0.12	0.09	4.84	2.71	15.80	17.15	5.717	0.887	4.830	0.175
HCl pretreatment	0.07	0.79	0.14	0.11	4.15	1.80	15.47	14.84	12.858	0.885	11.973	0.643
HCl/sc pretreatment	0.13	0.74	0.13	0.09	4.60	2.48	15.70	16.35	7.904	0.995	6.908	0.255
H ₂ O ₂ pretreatment	0.19	0.74	0.08	0.06	5.30	2.94	15.96	18.68	3.753	0.730	3.022	0.112
H ₂ O ₂ + HCl pretreatment	0.19	0.69	0.11	0.08	5.11	2.98	15.90	18.04	3.595	0.732	2.863	0.106

* average dry aggregate stability is also used as an estimate for crust stability (Tatarako, 2008).

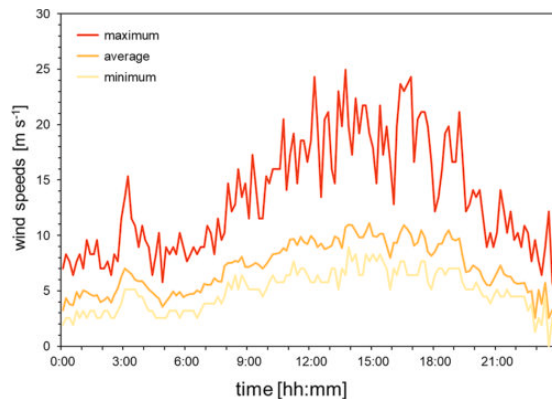


Fig. 3. Wind speeds [m s^{-1}] on the 29th of April 2019 from the meteorological station in Losovoye. The data consists of 10-min wind speed averages, minima and maxima. Wind speed maxima were used for modelling wind erosion following the SWEEP user manual (Tatarko, 2008).

2.5. Wind erosion modelling

2.5.1. Test site for wind erosion modelling

The wind erosion model was set up for 24 h on the 29th of April 2019 for a test field in Losovoye ($51^{\circ}11'11.2''\text{N}$, $70^{\circ}04'13.3''\text{E}$), which has been cultivated with a deep tillage chisel plough (<300 mm) since 2010. This area's prevalent soil type was identified as a dark chestnut calcareous soil (Uspanov et al., 1975), which corresponds to a Calcic Kastanozem (Stolbovoi, 2000). The field size is about 2000×2000 m, a standard field size for the study area. There was no wind barrier to protect the test field. The test field was to be sowed on the 20th of May and fallow that day.

A meteorological station of about 6 km from the test site measured weather data ($51^{\circ}14'12.3''\text{N}$, $70^{\circ}04'09.8''\text{E}$) and provided 10-min averages. The day's average wind speed was 7.06 m s^{-1} . The highest measured wind speed ($v_{\text{max}} = 24.96 \text{ m s}^{-1}$) in 2019, while topsoil was not frozen, was recorded that day. The day's average temperature was 15.4°C , and there was no precipitation measured.

Overall soil physics, agricultural implementations as well as weather parameters were predestined for a wind erosion event.

2.5.2. Single-event wind erosion evaluation program (SWEEP)

The process-based computer model SWEEP (Version 1.5.52, USDA-ARS, Manhattan/Kansas, USA) was used to simulate soil loss by wind erosion on the test site. The open-source model provides easy access to in- and outputs for a single-day storm event (Jarrah et al., 2020) and has been extensively validated worldwide (Tatarko et al., 2016). The SWEEP computes soil loss and deposition of a specific test site with particular field size and orientation in response to wind speed, wind direction, and surface conditions on a sub-hourly basis. The model determines first the threshold friction velocity at which erosion begins. Then, it calculates when the aerodynamic forces (aerodynamic drag and the aerodynamic lift) overcome the retarding forces of the surface particles (gravity force and the inter-particle cohesive force). In the final step, it simulates multiple physical erosion processes for each surface condition (Shao, 2008; Tatarko, 2008). The threshold is calculated based on different input parameters regarding biomass, soil layer, soil surface, and weather. Once wind speed exceeds the threshold, it calculates soil losses over a series of individual grid cells representing the field. To evaluate off-site impacts, the model's outcome of total soil loss in kg m^{-2} is divided in saltation plus creep and suspension loss. Fine particulate matter of $10 \mu\text{m}$ or less in diameter (PM_{10}) is also identified as part of suspension (Tatarko, 2008).

The Wind Erosion Prediction System has been developed initially

for soils with organic matter content of less than 0.03 kg kg^{-1} (Tatarko, 2020). The test field with an average organic matter content of 0.025 kg kg^{-1} could be applied to SWEEP. All input parameters of the test field are shown in Table 1.

Field: Because of the extensive field size, the number of grids was increased manually to 400×400 cells. The discretisation of SWEEP depends on the erosion activity in each grid cell, which should be downsized by increasing soil surface processes. However, it should generally be at least 7×7 m.

Biomass: Input parameters regarding biomass could be mostly omitted because the test site was fallow. Residue flat cover, described as the flat biomass cover [$\text{m}^2 \text{ m}^{-2}$], was minimal and could be estimated with photo examples from the SWEEP user manual (Tatarko, 2008).

Soil layer: Quantities of clay ($<2 \mu\text{m}$ [kg kg^{-1}]), silt ($2\text{--}50 \mu\text{m}$ [kg kg^{-1}]), sand ($50\text{--}2000 \mu\text{m}$ [kg kg^{-1}]) and of the subclass very fine sand ($50\text{--}100 \mu\text{m}$ [kg kg^{-1}]) from LDA were used. The test sites average was used as input data and varied depending on PSD pretreatment (see * Table 1 and Table 2). To reduce the uncertainty of missing data, assumptions were made carefully by considering all available information. Estimates were used from the SWEEP user manual (Tatarko, 2008), including all equations to derive texture-based properties. In-depth descriptions of the used functions are explained in the Technical Documentation (Tatarko, 2020).

The average aggregate density is the oven-dry weight of soil aggregates (<2 mm) per unit volume of dry soil aggregates [kg m^{-3}]. It was calculated using the method of Rawls (1983) from the SWEEP user manual (Eq. (1)).

$$\text{aggregate density} = 2.01 \times (0.72 + 0.00092 \times \text{layer depth}) \quad (1)$$

with,

layer depth is described as the bottom depth of the layer [mm].

The average aggregate stability is described as the mean of the natural logarithm of aggregates crushing energy [$\ln(\text{J kg}^{-1})$] (Eq. (2)).

$$\text{aggregate stability} = 0.83 + 15.7 \times \text{clay} - 23.8 \times \text{clay}^2 \quad (2)$$

The GMD was calculated directly from PSD and test fields average content of organic matter (0.025 kg kg^{-1}) and calcium carbonate (0.074 kg kg^{-1}) (Eq. (3)).with,

$$\begin{aligned} \text{GMD} = & \exp(1.343 - 2.235 \times \text{sand} - 1.226 \times \text{silt} - 0.0238 \\ & \times \text{sand/clay} + 33.6 \times \text{organic matter} + 6.85 \times \text{calcium carbonate}) \\ & \times (1 + 0.006 \times \text{surface layer depth}) \end{aligned} \quad (3)$$

surface layer depth is 10 mm, and the sand, silt and clay fractions

were measured under the influence of different pretreatments (Table 2).

The averaged GMD was utilised to calculate the geometric standard deviation (Eq. (4)) and the maximum aggregate size (Eq. (5)).

$$\text{Geometric standard deviation} = 1 / (0.0203 + 0.00193 \times \text{GMD} + 0.074 / \text{GMD}^{0.5}) \quad (4)$$

$$\text{Max. aggregate size} = \text{geometric standard deviation}^p \times \text{GMD} + 0.84 \quad (5)$$

with, $p = 1.52 \times \text{geometric standard deviation}^{-0.449}$

Soil surface: Event-based input data such as crust density and crust stability were estimated by applying aggregate density and aggregate stability values. Allmaras random roughness was estimated following the pin-type profile meter (Allmaras et al., 1966) via photo examples from the user manual. Surface water content could be omitted based on meteorological data.

Weather: One hundred and forty-four measured values of wind speed were applied. Following SWEEP's advice, the maximum wind speed for each 10-min period (Fig. 3) and the mean wind direction (250.8°) was used as data input. Aerodynamic roughness was automatically ignored by SWEEP because wind speeds were measured at anemometer site under field conditions. Air density was estimated by SWEEP itself based on elevation (335 m) and the day's average temperature.

2.5.3. Geometric mean diameter

To improve modelling results, the GMD (Table 1), was determined by fitting the measured mass percentage of different aggregate sizes to a log-normal function (Gardner, 1956; Larney, 2007). Therefore, a horizontal sieve apparatus (Analysette 3, Fritsch GmbH, Idar-Oberstein, Germany) with eight different sieves (8 mm, 5 mm, 3 mm, 2 mm, 0.85 mm, 0.5 mm, 0.25 mm, and 0.05 mm) was applied for 1 min with an amplitude of 1 mm to four samples from the test field. The GMD was then utilised to derive the geometric standard deviation and the maximum aggregate size with pedotransfer functions (Eqs. (4) and (5)) and used for modelling erosion losses (Table 3).

2.6. Statistical analysis

The open-source software 'RStudio' (Version 1.2.5019, RStudio Team, Boston, USA) as an integrated development environment for 'R' was used to perform statistical analysis and graphical illustrations of LDA results (R Core Team, 2020; RStudio Team, 2020). Texture classes and texture triangles were computed and illustrated with the 'soiltex' package (Moeys, 2018).

Statistical analyses were carried out for each field and each test site. In Yasnaya Poljana each test site is represented by the average of six measured values, and the average mean of test sites in Shortandy and Losovoye consisted of eight values. All parameters, including LDA results of different parameters, were tested for normal distribution (Shapiro-Wilk test) and variance homogeneity (Levene's test) followed by variance analyses (one-way ANOVA). Tukey's range test was used to identify mean group values that are significantly different ($p \leq 0.05$) and are presented in Appendixes Table A1 and Table B1.

3. Results

3.1. Effect of pretreatments on texture class

The results of LDA showed that samples from the study area were predominantly assigned to the texture class silt loam (Soil Science Division Staff, 2017). Pretreatments for PSD did not influence the assigned texture class (Fig. 4). Silt loam consists of more than 50% silt and between 12 and 27% clay or between 50 and 80% silt and less than 12% clay.

Nevertheless, exceptions were assigned to adjacent texture classes

depending on the pretreatment used. All samples with no pretreatment were assigned to silt loam (Fig. 4(1)). In comparison, one-third of HCl pretreated samples (Fig. 4(2)) showed a low amount of clay content (between 5 and 9%) and a high amount of silt content (>80%) and were therefore assigned to silt. Results of HCl_{SC} pretreatment (Fig. 4(3)) assigned three out of 90 samples as silt (>80% silt content). The H₂O₂ pretreatment (Fig. 4(4)) assigned one sample as loam because of its low silt content (49%) and one as silty clay loam as a result of high clay content (30%). Following the results of H₂O₂ + HCl pretreatment (Fig. 4(5)), only one sample was assigned as silty clay loam (28% clay content).

Even though silt loam is the dominant texture class for all pretreatments, the distribution of results within one class varies for each method. The HCl pretreatment results (Fig. 4(2)) show a low scatter, while pretreatments including H₂O₂ (Fig. 4(4) and 4(5)) result in a higher scattering. Data of averaged clay, silt, and sand fractions for each test field are shown in Appendix Table A1.

3.2. Effect of pretreatments on particle size distribution

The averaged cumulative distribution curves of the different pretreatments are shown in Fig. 5. Each curve represents one pretreatment and consists of 40 physically measured classes. Values shown are the averages of all samples. The curves order was mainly the same on all three test sites and under all typical land-use types. Pretreating samples with H₂O₂ generated the highest dispersion (Fig. 5(4)) while pretreating additionally with HCl afterwards did not cause further dispersion for most fields. Only two fields in Yasnaya Poljana (pasture and arable land) showed further breakdown into smaller particles with H₂O₂ + HCl pretreatment. On average, samples with no pretreatment were slightly better dispersed than samples pretreated with HCl_{SC}. Contrary, HCl pretreatment had the opposite effect, and PSD shifted into coarser sizes (Fig. 5(2)).

The scatterplots in Fig. 6 show the effects of pretreatment on PSD for all samples. Comparing the two different HCl pretreatments with no pretreatment showed that percentages of clay, silt, and sand were similar between no pretreatment and HCl_{SC} pretreatment (Fig. 6A). In contrast to HCl pretreatment (Fig. 6B), the amount of silt increases and clay drastically decreases. Samples with no pretreatment showed between 8 and 20% of clay but only between 5 and 9% after pretreating with HCl. Comparing H₂O₂ pretreatment and H₂O₂ + HCl pretreatment revealed no drastic shift between particle classes (Fig. 6C). Measured values are close to the 1:1 line for both methods. Primary dispersion is already seen in samples pretreated with only H₂O₂ in comparison to samples with no pretreatment. The H₂O₂ pretreatment increases the amount of clay and decreases the sand and silt fraction (Fig. 6D).

3.3. Influence of calcium carbonate content on HCl pretreatment

The calcium carbonate content in the study area spanned for the single measured samples from 2.2 to 117.3 g kg⁻¹ with an average of 32.5 g kg⁻¹ for all Chernozem and 52.6 g kg⁻¹ for all Kastanozem samples. Overall, arable fields had a higher content of calcium carbonate on average (56.5 g kg⁻¹) than uncultivated fields (27.9 g kg⁻¹) (Appendix Table B1).

The content of calcium carbonate affected PSD if pretreated with HCl and had no effect if pretreated with HCl_{SC} (data not shown). The HCl pretreatment mainly changed the relative amount of coarse and fine silt minimal. Samples pretreated with HCl tended to increase the coarse silt fraction while the fine silt and coarse clay fraction decreased. The difference between HCl pretreatment and no pretreatment for samples with high calcium carbonate content was not as distinct as the difference between no pretreatment and H₂O₂ pretreatment for samples with high organic carbon content.

Table 3

Measured data input of clay [kg kg^{-1}], silt [kg kg^{-1}], sand [kg kg^{-1}], very fine sand [kg kg^{-1}], and geometric mean diameter of aggregate sizes [mm]. Average dry aggregate stability [$\text{ln}(\text{J kg}^{-1})$] was derived from clay content. Geometric standard deviation of aggregate sizes [mm] and maximum aggregate size [mm] were derived from the SWEEP user manual (Tatarko, 2008). Estimates of soil losses for a fallow arable test field in Losovoye are shown as data output. Total soil loss [kg m^{-2}] consists of saltation and creep loss [kg m^{-2}] and suspension loss [kg m^{-2}]. The fine particulate matter of 10 μm or less in diameter (PM_{10}) [kg m^{-2}] is part of the suspension loss.

	data input SWEEP measured (laser diffraction analysis)					measured (dry sieving)			estimated (derived values by pedotransfer functions)			data output SWEEP simulated					
	clay	silt	sand	very fine sand	geometric mean diameter of aggregate sizes	geometric mean diameter of aggregate sizes	average dry aggregate stability*	geometric standard deviation of aggregate sizes	max. aggregate size	total soil loss	saltation/creep loss	suspension loss	PM_{10} loss	total soil loss	saltation/creep loss	suspension loss	PM_{10} loss
	[kg kg^{-1}]	[kg kg^{-1}]	[kg kg^{-1}]	[kg kg^{-1}]	[mm]	[mm]	[$\text{ln}(\text{J kg}^{-1})$]*	[mm mm^{-1}]	[mm]	[kg m^{-2}]	[kg m^{-2}]	[kg m^{-2}]	[kg m^{-2}]	[kg m^{-2}]	[kg m^{-2}]	[kg m^{-2}]	[kg m^{-2}]
no pretreatment	0.16	0.72	0.12	0.09	1.18	1.18	2.58	11.03	4.93	10.125	1.114	9.011	0.317	10.125	1.114	9.011	0.317
HCl pretreatment	0.07	0.79	0.14	0.11	1.18	1.18	2.58	11.03	4.93	9.561	1.020	8.541	0.442	9.561	1.020	8.541	0.442
HCl _{sc} pretreatment	0.13	0.74	0.13	0.09	1.18	1.18	2.58	11.03	4.93	10.243	1.139	9.104	0.325	10.243	1.139	9.104	0.325
H_2O_2 pretreatment	0.19	0.74	0.08	0.06	1.18	1.18	2.58	11.03	4.93	9.852	1.064	8.788	0.316	9.852	1.064	8.788	0.316
H_2O_2 + HCl pretreatment	0.19	0.69	0.11	0.08	1.18	1.18	2.58	11.03	4.93	9.927	1.080	8.847	0.318	9.927	1.080	8.847	0.318

* average dry aggregate stability is also used as an estimate for crust stability (Tatarko, 2008).

3.4. Influence of organic carbon content on H_2O_2 pretreatment

The organic carbon content in the study area reached for the single measured samples from 11.2 to 48.7 g kg^{-1} with an average of 29.5 g kg^{-1} for all Chernozem and 16.3 g kg^{-1} for all Kastanozem samples. Overall, arable fields had a lower content of organic carbon on average (17.7 g kg^{-1}) than uncultivated fields (26.6 g kg^{-1}) (Appendix Table B1).

The effect of H_2O_2 pretreatment depends on organic carbon content and affects texture subclasses differently (Fig. 7).

In comparison to HCl pretreatment effects (see 3.3), results of H_2O_2 pretreatment showed the opposite effect. There was no difference between no pretreatment and H_2O_2 pretreatment for particle sizes above 100 μm (data not shown). However, H_2O_2 pretreatment decreased particles of very fine sand (50–100 μm) and coarse silt (20–50 μm) (Fig. 7A and B) in comparison to no pretreatment. The H_2O_2 pretreatment causes an increase of particles in the fine silt (2–20 μm) and coarse clay (0.2–2 μm) subclasses (Fig. 7C and D). Additionally, differences within subclasses between no pretreatment and H_2O_2 pretreatment rely upon the amount of organic carbon. While the sample with the lowest organic carbon content led to a small difference in the coarse silt fraction between no pretreatment (22%) and H_2O_2 pretreatment (14%), the sample with the highest organic carbon content caused a considerable difference between no pretreatment (26%) and H_2O_2 pretreatment (8%). This behaviour applies contrary to the fine silt fraction.

The mentioned effects of organic carbon on H_2O_2 pretreatment were similar to H_2O_2 + HCl pretreatment (data not shown).

3.5. Simulated soil loss using SWEEP

3.5.1. Impact of PSD pretreatments on derived properties

The PSD (Table 2) of different pretreatments from the test field in Losovoye ranged for clay from 0.07 to 0.19 kg kg^{-1} , silt from 0.69 to 0.79 kg kg^{-1} , and sand from 0.08 to 0.14 kg kg^{-1} . The very fine sand subclass ranged from 0.06 to 0.11 kg kg^{-1} . Pretreatments with H_2O_2 led to the highest amount of clay (0.19 kg kg^{-1}) and the lowest amount of very fine sand (0.06 kg kg^{-1}). In comparison, HCl pretreatment led to the highest amount of very fine sand (0.11 kg kg^{-1}) and the lowest amount of clay (0.07 kg kg^{-1}).

Calculated values of aggregate stability reached from 1.80 to 2.98 $\text{ln}(\text{J kg}^{-1})$, the GMD from 4.15 to 5.30 mm, the geometric standard deviation from 15.47 to 15.96 mm mm^{-1} , and the maximum aggregate size from 14.84 to 18.68 mm (Table 2). Modelling results were diverse if PSD under the impact of different pretreatments was used to estimate texture-based properties to model wind erosion.

SWEEP simulated a total soil loss between 3.595 kg m^{-2} for H_2O_2 + HCl pretreatment and 12.858 kg m^{-2} for HCl pretreatment. It further simulated the lowest soil losses for H_2O_2 pretreatment, regardless of whether HCl was used or not. If PSD with no pretreatment was used to calculate derived properties, SWEEP simulated a total soil loss of 5.717 kg m^{-2} . Overall, the largest part of total soil loss was due to suspension. The no pretreatment and HCl pretreatment estimates were similar for the saltation/creep loss (0.887 and 0.885 kg m^{-2}). However, they differed for soil loss by suspension (4.830 and 11.973 kg m^{-2}).

Because H_2O_2 pretreatment removed particle binding agents most efficiently, the potential total soil loss estimate simulated by SWEEP (3.753 kg m^{-2}) is shown for the test field in Fig. 8A. All texture-based properties were calculated from PSD data (including H_2O_2 pretreatment). The simulation of soil loss due to saltation and creep movement (0.730 kg m^{-2}) is visualised in Fig. 8B.

3.5.2. Impact of PSD pretreatment on potential soil loss

For the case that PSD and GMD were independently measured, and additional texture-based properties were used as steady estimates, SWEEP simulated a possible total soil loss between 9.561 and 10.243 kg m^{-2} , depending on pretreatments used for LDA

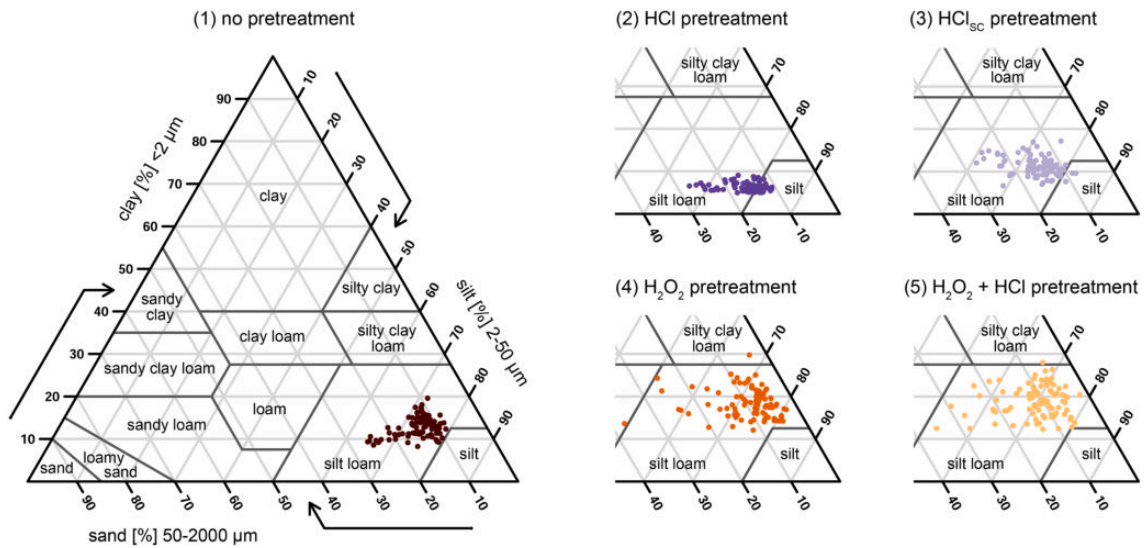


Fig. 4. Soil texture triangles (Soil Science Division Staff, 2017) defining texture classes for all samples ($n = 90$) depending on different pretreatments: (1) no pretreatment, (2) hydrochloric acid (HCl) pretreatment, (3) hydrochloric acid soluble compounds (HCl_{sc}) pretreatment, (4) hydrogen peroxide (H_2O_2) pretreatment, (5) sequential hydrogen peroxide and hydrochloric acid ($\text{H}_2\text{O}_2 + \text{HCl}$) pretreatment. Texture classes were assigned from clay, silt and sand fractions measured by laser diffraction analysis (LDA).

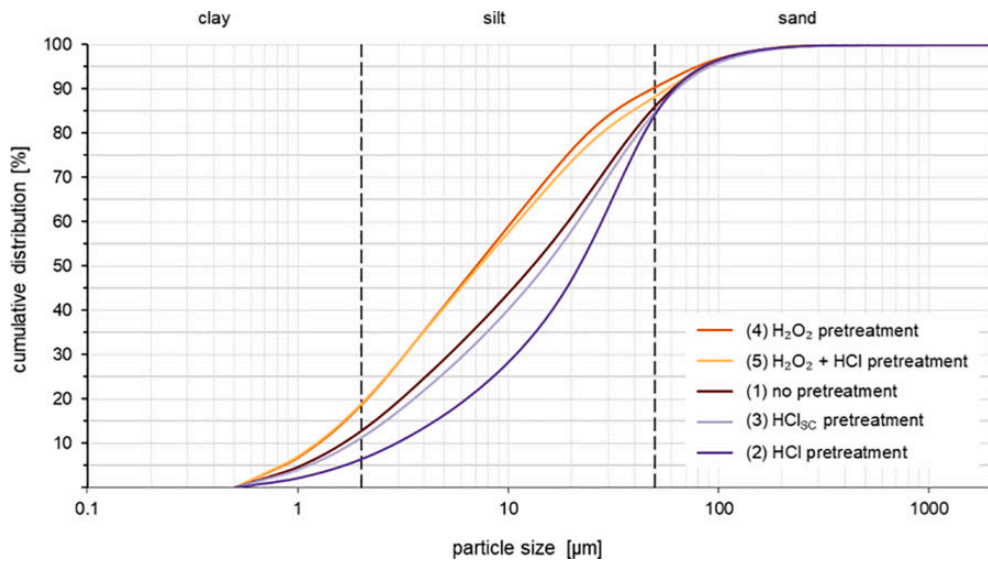


Fig. 5. Cumulative distribution of particle size analysis by laser diffraction (logarithmic scale) depending on pretreatment: (1) no pretreatment, (2) hydrochloric acid (HCl) pretreatment, (3) hydrochloric acid soluble compounds (HCl_{sc}) pretreatment, (4) hydrogen peroxide (H_2O_2) pretreatment, (5) sequential hydrogen peroxide and hydrochloric acid ($\text{H}_2\text{O}_2 + \text{HCl}$) pretreatment. Data shown represent averages of all samples ($n = 90$). The laser diffraction analyser measured 40 physical classes up to 100% cumulative distribution.

(Table 3). Pretreatments of particle size analysis did not affect SWEEP's output severely. From the total soil loss, only $1.020\text{--}1.139 \text{ kg m}^{-2}$ of soil were lost through saltation and creep movement, while most soil was lost due to suspension ($8.847\text{--}9.104 \text{ kg m}^{-2}$).

Comparison between calculated and measured GMD for modelling results are shown in Fig. 8. Measured PSD (including H_2O_2 pretreatment) and measured GMD was used to simulate potential soil losses with SWEEP. Visualisations of the total soil loss (9.852 kg m^{-2} , Fig. 8C) and

saltation and creep loss (1.064 kg m^{-2} , Fig. 8D) are shown.

4. Discussion

4.1. Efficiency of pretreatments to remove carbonates

The dominant occurrence of silt loam in the study area results from the same parent material loess, which is an aeolian and reworked

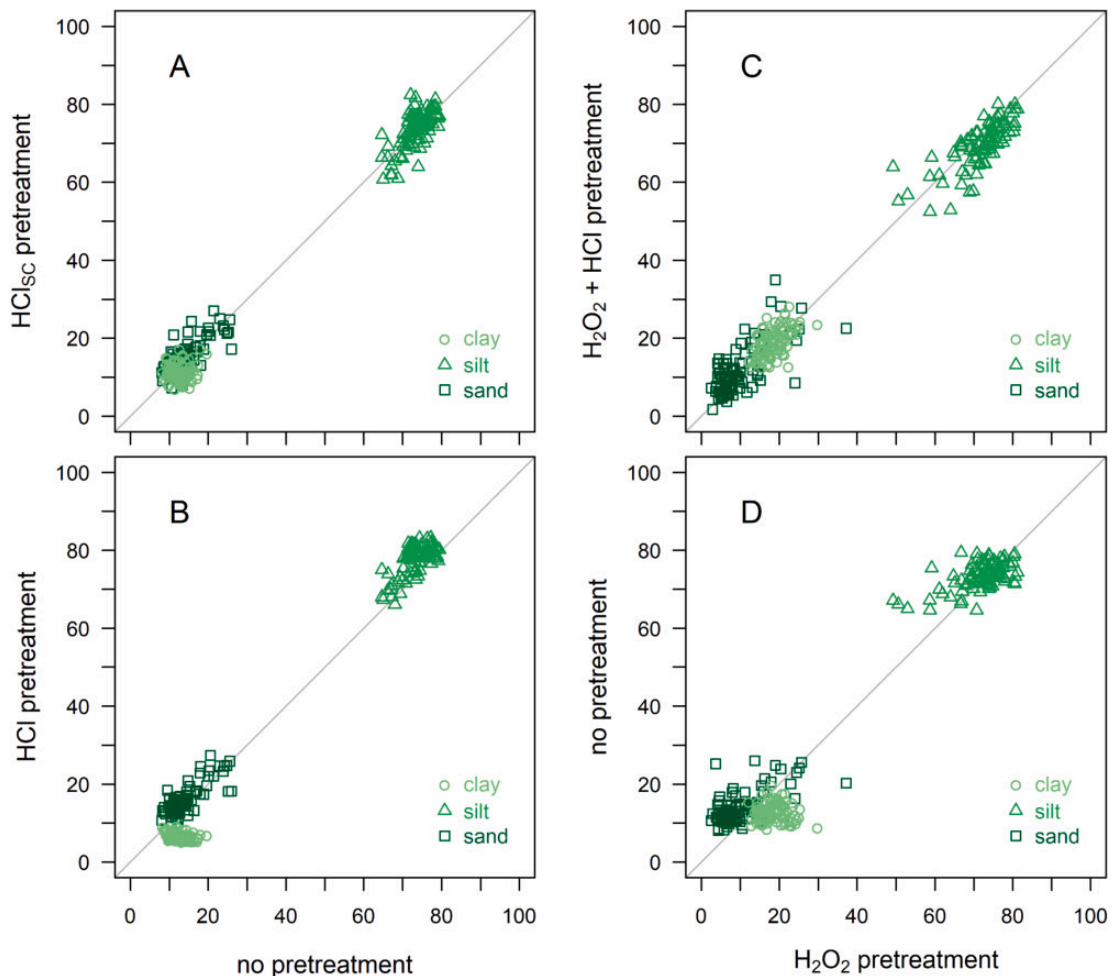


Fig. 6. Scatter plots of cumulative particle size [%] comparing the clay (○), silt (△) and sand (□) fractions between different pretreatments. On the left side, results of (A) hydrochloric acid soluble compounds (HCl_{SC}) pretreatment and (B) hydrochloric acid (HCl) pretreatment are compared to no pretreatment. On the right side, differences between (C) the sequential hydrogen peroxide and the hydrochloric acid (H₂O₂ + HCl) pretreatment and (D) no pretreatment are compared to the hydrogen peroxide pretreatment (H₂O₂). The grey line corresponds to the 1:1 line.

aeolian carbonaceous sediment. Chernozems and Kastanozems of the study area are located within the Russian loess belt (Muhs et al., 2014) and experience similar soil pedogenesis. The high concentration of secondary carbonates usually starts in Chernozem soils within 50 cm, at the lower limit of the A horizon (Eckmeier et al., 2007).

In our study, HCl pretreatments caused incomplete dispersion. Schulte et al. (2016) observed that HCl pretreatment is particularly selective and inscrutable. Adding plain HCl to samples dissociates carbonates and may cause a cationic bridging effect of the calcium ions (Ca²⁺). In that case, carbonates act as an abundant source of calcium ions due to HCl pretreatment. Calcium ions favour inter-molecular interactions between clay and organic matter to form a covalent bond (Rowley et al., 2018; Six et al., 2004; Virto et al., 2011; Wuddivira and Camps-Roach, 2007). The mechanism behind this stabilisation is the

flocculation of negatively charged separates by outer-sphere interactions. If samples are already pretreated with H₂O₂, and organic matter is oxidised, the described effect does not occur for Kastanozem soils. Only Chernozem soils of Yasnaya Poljana, with the high organic carbon content and the low carbonate content, showed a slight increase in smaller particles if pretreated with H₂O₂ + HCl. Reasons could be HCl's selective character during pretreatment, or that HCl is already affecting mineral compounds. In case the soil is pretreated with HCl and soluble compounds are washed out, particles remain similar in size. Pretreatments with HCl did not dissolve aggregates, had no considerable effect or even caused aggregation. Carbonates are not the primary binding agent between particles in our study. We would advise avoiding decalcification of Chernozems and Kastanozems because it might lead to unpredictable effects.

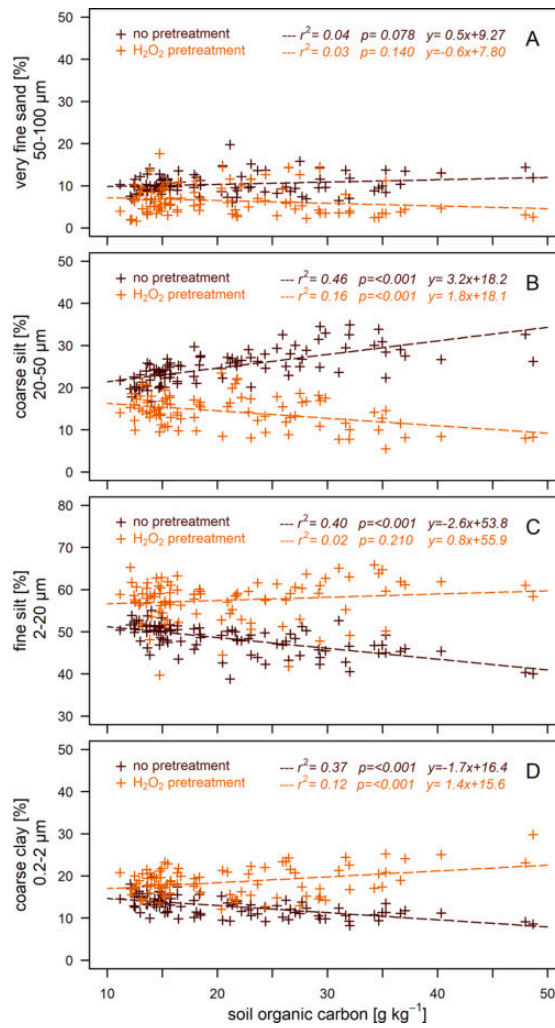


Fig. 7. Influence of soil organic carbon content [g kg⁻¹] on H₂O₂ pretreatment (+, dark brown) was compared with no pretreatment (+, light orange) for the texture subclasses (A) very fine sand (50–100 μm), (B) coarse silt (20–50 μm), (C) fine silt (2–20 μm) and (D) coarse clay (0.2–2 μm) in %. Trendline (---) and statistics for each pretreatment and texture subclasses are shown.

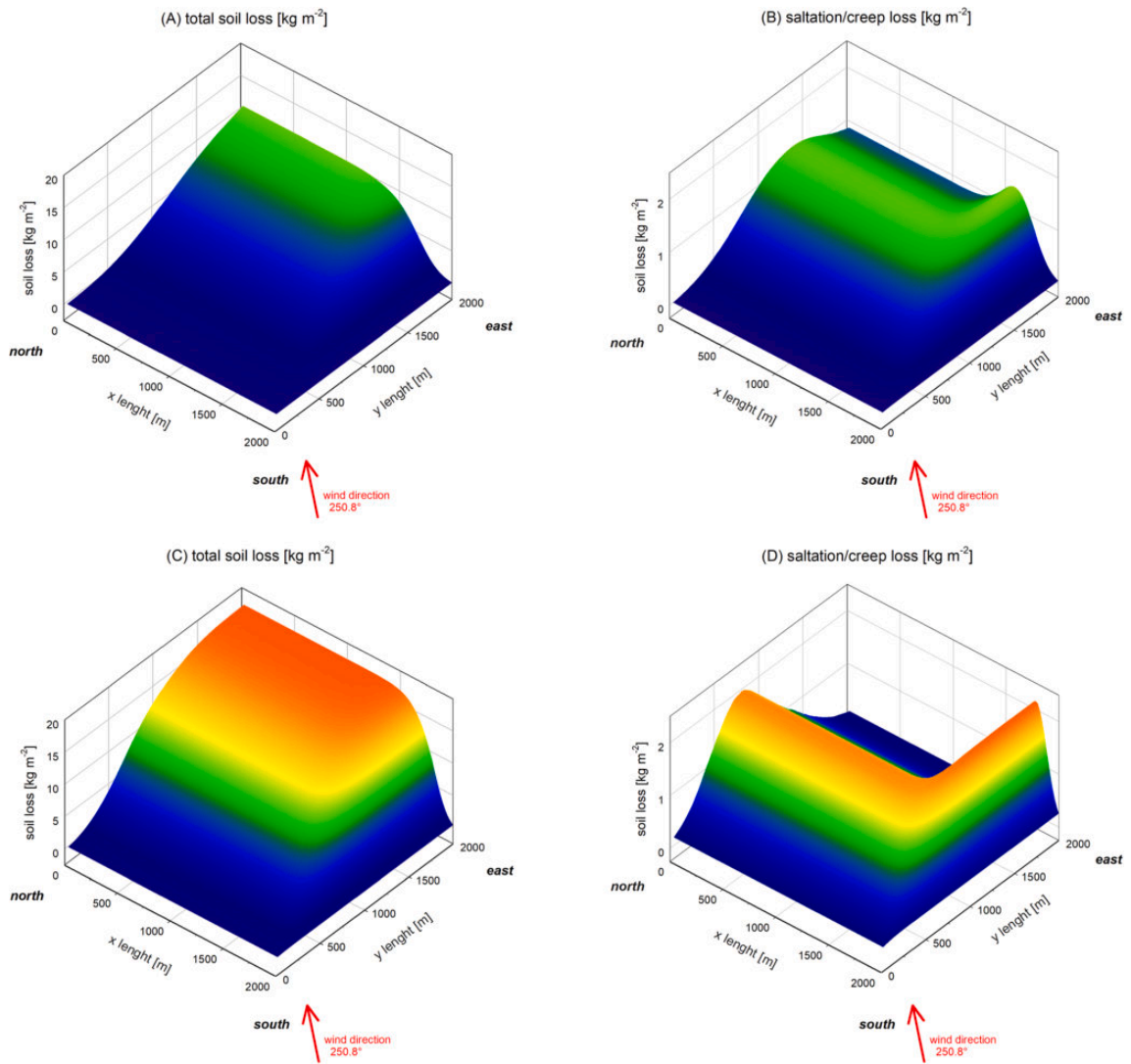


Fig. 8. Graphical visualisation of total soil loss [kg m^{-2}] (A and C) and saltation/creep soil loss [kg m^{-2}] (B and D) for the test field simulated by SWEEP. A and B show soil loss simulations based on laser diffraction analysis, including a hydrogen peroxide pretreatment (Table 1 and Table 2) if the geometric mean diameter is calculated with a pedotransfer function from the SWEEP user manual. C and D show soil loss simulations based on laser diffraction analysis, including a hydrogen peroxide pretreatment and independently measured GMD (Table 1 and Table 3).

4.2. Efficiency of pretreatments to remove organic matter

The distribution of Chernozems and Kastanozems from north to south reflects a declining humus gradient similar to the western Siberian steppe (Bischoff et al., 2018). Our results also agree with the organic carbon loss study in the Russian dry steppe caused by land-use changes from native ecosystems to arable fields (Illiger et al., 2019).

Mineral components, especially the silt and clay fraction, are strongly associated with organic matter. All samples pretreated with H₂O₂ showed dispersion of soil aggregates and an increasing amount of finer particles. Our results agree with the study of Di Stefano et al. (2010). They also measured a shift towards finer particles in PSD by LDA with H₂O₂ pretreatment, especially in the silt fraction.

Fisher et al. (2017) pretreated samples with sodium hypochlorite solution (NaClO) to remove organic matter and subsequently with HCl to remove carbonates. Using sodium hypochlorite differs from international standard methodologies but is suitable for their local Australian soils. They expected that the difference of the effect by NaClO + HCl pretreatment depends on the amount of organic carbon content. However, their results did not show a significant correlation between pretreatment and organic carbon content but showed a significant effect due to the soil type and therefore expected differences between no pretreatment and chemical pretreatment for different soil types. This supports our results of Chernozems and Kastanozems. The difference between no pretreatment and H₂O₂ pretreatment correlated with the organic carbon content and indicates that organic matter is likely the primary binding agent. Our results show that H₂O₂ pretreatment offers a complete dispersion for measuring PSD.

4.3. Pretreatments for laser diffraction analysis

Results of LDA assigned overall the same texture class in our study. Chemical pretreatment, soil type or land-use did not have an impact. On our test sites, chemical pretreatments for particle size analysis can be omitted if only the texture class is of interest. Even though sample preparation did affect particles within the silt fraction between 2 and 50 µm most severely, particles of the coarse and fine silt fractions are subjected to compensating effects. Changes in subclasses are hidden if they are not explicitly observed.

We agree with Fisher et al. (2017) that the advantages and disadvantages of using pretreatments for LDA for a broader range of soil types are warranted. In their study, the purpose of adapting a pretreatment for removing carbon seemed only of little purpose. Different effects were observed from pretreatment, but sample preparation generally decreased rather than increased the concordance correlation coefficient. Our results show similarities because only H₂O₂ pretreatment was efficient but did not change PSD severely. Additional pretreatments seem questionable despite the time-consuming preparation and potentially misleading results.

Laser diffraction has been increasingly applied for analysing PSD (Yang et al., 2019). It measures a 3-dimensional shape with a 1-dimensional parameter (Fisher et al., 2017) differently than the sieve and sedimentation method. Overall, LDA dismisses methodological disadvantages of the traditional sedimentation methods (Bittelli et al., 2019). It is questionable if the complete dispersion for particle size analysis is always necessary if measured by laser diffraction. Even though little is known about the possible effects of different

pretreatments (Fisher et al., 2017), our results showed only minimal differences. For most soil types with a low and medium amount of organic binding material, a pretreatment seems nonessential if PSD is measured by laser diffraction.

4.4. Modelling effect of LDA pretreatments on wind erosion

The Wind Erosion Prediction System is a promising tool, and SWEEP can be used to estimate soil loss easily for single wind events in the dry steppe of Kazakhstan. Wind barriers were not present at the test site, even though Russia systematically introduced wind agroforestry to protect soils from erosion in the late nineteenth century (Chendev et al., 2015). Since 1991, the afforestation of agricultural land in Kazakhstan has usually been decreased because of political and economic change. In Losovoye, shelterbelts were partly cleared in the past because the trapped amount of snow caused gully erosion after melting.

Soil texture is a critical parameter for estimating wind erosion processes. However, particles without structure and binding agents do not occur under field conditions in the dry steppe's topsoil layer. Properties derived from particle sizes, such as dry aggregate size distribution and aggregate stability, have a considerable impact on wind erosion modelling results which can be changed by mechanical breakdown. Parameters regarding the actual size and distribution of aggregates in the field have a higher impact on SWEEP's output than soil texture parameters from LDA under the influence of different pretreatments. Suppose the texture-based parameters were derived and used as input, soil loss estimates were very diverse and ranged between 3.3 and 11.8 mm of topsoil depth. All estimates would be noticeable under field conditions. Chepil (1960) associated quantities of annual soil loss of around 37 t ha⁻¹ to be distinctly visible.

Regarding particle size, the very fine sand fraction is the determining factor in wind erosion because of its lowest threshold (Shao, 2008). Our results of LDA showed low amounts of sand, including low amounts of very fine sand in general, and SWEEP predicted low salination loss. Pretreatment of samples did not lead to a shift in soil texture class. Silt loam with a generally low amount of fine sand is not that susceptible to wind erosion from the perspective of size.

In our study, the consequences of chemical pretreatments for particle size analysis by LDA for modelling wind erosion did not differ, if the additional parameter GMD was independently measured. The SWEEP simulations from our test field are representative for our study area because averaged PSD data estimated similar soil losses. At the test field, topsoil loss was estimated less than 10 mm during the potentially strong wind event independent of LDA pretreatment. These potential soil losses are certainly overestimations, based on the maximum wind speeds as input data. However, with quantities of about 100 t ha⁻¹, they would cause considerable on- and off-site damage (Funk and Reuter, 2006).

Modelling results indicate that parameters derived from soil texture are more influential for wind erosion modelling than the texture itself. Therefore, deriving GMD from texture and binding agents with a pedotransfer function or a regression equation from the erodible fraction needs further validation (Fryrear et al., 1994; López et al., 2007; Rakkar et al., 2019). This is especially important for different dry steppe soil types, with a high aggregation potential at the microscale. New pedotransfer functions are required to derive soil parameters based on PSD with no pretreatment (Zimmermann and Horn, 2020) and for PSD data obtained by laser diffraction.

5. Conclusions

For particle size analysis of Chernozem and Kastanozem soils, an HCl pretreatment to dissolve carbonates should be avoided because it leads to incomplete dispersion or even an aggregation. An H₂O₂ pretreatment to remove organic binding material is sufficient. However, chemical pretreatments to remove binding agents for LDA did not significantly affect PSD in our study. Consequences for wind erosion modelling are major if texture-based parameters are derived by pedotransfer functions based on PSD and used as input data. In case independently measured GMD is available the consequences are minimal. Altogether, we conclude that derived properties from PSD by LDA require further investigation for dry steppe soils. A validation of the soil loss under field conditions with an in-situ experiment will be the next step.

Declaration of Competing Interest

The authors declare that they have no known competing financial interests or personal relationships that could have appeared to influence the work reported in this paper.

Acknowledgements

We highly appreciate the constructive comments from three anonymous reviewers and the editor regarding this manuscript. We thank the whole ReKKS Team and the Department of Geocology and the Department of Soil Sciences and Soil Protection from the Martin Luther University Halle-Wittenberg (MLU). We are particularly grateful to Dorothee Kley (MLU), Olga Shibistova (Leibniz University, Hannover), and Tobias Meinel (Amazone, Nur-Sultan) for logistical assistance. Patrick Illiger (MLU) and Aleksey Prays (MLU), we thank for supporting fieldwork. We appreciate TOO Taynsha Astyk, TOO Fermer 2002, and the Barayev Center for their permission to take soil samples. We thank Michael von Hoff (MLU) for operating the laser diffraction analyser and Alexander Kaestner (Sympatec, Clausthal-Zellerfeld) for technical assistance. Thanks to Lisa Haselow (UFZ, Halle) for meteorological data. Last but not least, we especially acknowledge Klaus Kaiser (MLU) and Robert Mikutta (MLU), as well as Roger Funk (ZALF, MÜNCHENBERG), John Tatarko (USDA-ARS, Fort Collins), Markus Koch (Leibniz University, Hannover), Thomas Thienelt (MLU) and Muhammad Usman (MLU) for ideas, comments, and discussion.

Funding source

This study was conducted within the research project [ReKKS \(Innovative Solutions for Sustainable Agriculture and Climate Adaptation in the Dry Steppes of Kazakhstan and Southwestern Siberia\)](#) and funded by the [German Federal Ministry of Education and Research \(BMBF\)](#) - grant number: FKZ 01LZ1704B.

Appendix A

Table A1 Cumulated clay, silt and sand fractions under different pretreatments: (1) no pretreatment, (2) hydrochloric acid (HCl) pretreatment, (3) hydrochloric acid soluble compounds (HCl_{sc}) pretreatment, (4) hydrogen peroxide (H₂O₂) pretreatment, (5) sequential hydrogen peroxide and hydrochloric acid (H₂O₂ + HCl) pretreatment from a variety of land-use types at three test sites. Statistical significance ($p \leq 0.05$) between pretreatments for each test site is indicated by lower case letters.

test site	land-use type	clay [%] 0-2 µm					silt [%] 2-50 µm					sand [%] 50-2000 µm				
		(1)	(2)	(3)	(4)	(5)	(1)	(2)	(3)	(4)	(5)	(1)	(2)	(3)	(4)	(5)
		Yasnaya Poljana	steppe	11.27 ^b	7.14 ^b	9.20 ^b	19.61 ^a	20.25 ^a	73.15 ^a	74.74 ^a	77.73 ^a	74.98 ^a	73.37 ^a	15.58 ^b	5.65 ^a	15.14 ^b
	pasture	10.45 ^c	6.72 ^b	9.97 ^c	16.10 ^a	20.55 ^d	78.11 ^a	78.29 ^a	80.01 ^a	77.61 ^{ab}	74.35 ^b	11.44 ^b	5.62 ^a	13.27 ^b	12.43 ^b	5.10 ^a
	diverse tillage	11.56 ^b	7.41 ^b	11.41 ^b	19.20 ^a	22.58 ^a	76.05 ^{ab}	70.37 ^a	78.27 ^b	75.07 ^{ab}	70.03 ^a	12.39 ^{ab}	10.43 ^{ab}	14.32 ^a	13.52 ^{ab}	7.39 ^b
Shortandy	steppe	12.70 ^c	6.91 ^b	10.66 ^{bc}	19.97 ^a	19.60 ^a	73.73 ^{ab}	70.69 ^a	76.50 ^b	73.98 ^{ab}	71.74 ^{ab}	13.57 ^b	9.34 ^a	16.60 ^b	15.35 ^b	8.67 ^a
	reduced tillage	12.65 ^c	6.04 ^b	9.83 ^c	20.76 ^a	19.35 ^a	77.74 ^c	72.85 ^a	81.09 ^b	78.81 ^{bc}	73.56 ^a	10.80 ^c	6.61 ^a	12.46 ^b	12.22 ^{bc}	6.510 ^a
	steppe	10.68 ^d	6.56 ^b	13.87 ^{cd}	18.29 ^a	16.22 ^{ac}	66.80 ^b	58.51 ^a	68.61 ^b	64.66 ^b	58.10 ^a	22.53 ^a	23.20 ^a	24.83 ^a	21.47 ^a	25.68 ^a
Losovoye	pasture	12.14 ^c	6.52 ^b	11.97 ^c	16.18 ^a	17.27 ^a	71.74 ^{ab}	74.03 ^{ab}	76.73 ^a	71.97 ^{ab}	69.86 ^b	16.11 ^b	9.78 ^a	16.75 ^b	16.07 ^b	12.87 ^{ab}
	diverse tillage	14.00 ^d	5.86 ^b	8.83 ^c	19.40 ^a	16.79 ^{ad}	72.69 ^{ab}	73.20 ^b	79.62 ^b	76.67 ^{ab}	69.19 ^{ab}	13.31 ^b	7.40 ^a	14.52 ^b	14.50 ^b	14.02 ^b
	deep tillage	15.76 ^{ac}	6.91 ^b	13.17 ^c	18.83 ^a	19.34 ^a	72.30 ^b	73.64 ^a	79.44 ^b	73.58 ^a	69.32 ^a	11.94 ^{ab}	7.53 ^a	13.66 ^b	13.26 ^b	11.34 ^{ab}
	no-tillage	15.56 ^d	5.54 ^b	11.85 ^c	19.34 ^a	18.66 ^a	72.17 ^a	72.84 ^a	79.82 ^b	72.90 ^a	68.58 ^a	12.27 ^b	7.81 ^a	14.64 ^b	15.25 ^b	12.71 ^{ab}
	reduced tillage	11.61 ^c	5.70 ^b	11.68 ^c	17.02 ^a	17.62 ^a	72.78 ^{ab}	70.50 ^{ab}	75.72 ^b	69.38 ^{ab}	67.18 ^b	15.61 ^{ab}	12.4 ^{ab}	18.59 ^{ab}	18.94 ^b	15.26 ^{ab}
	fallow	13.67 ^c	6.19 ^b	11.20 ^c	17.91 ^a	19.76 ^a	74.84 ^a	74.20 ^a	79.92 ^b	75.39 ^a	70.33 ^c	11.48 ^c	7.89 ^a	13.89 ^b	13.42 ^b	9.91 ^c

Appendix B

Table B1

Parameters of physical–chemical analysis including particle size analysis with different pretreatments from two test sites and different land-use-types: (I) steppe, (II) pasture, (III) diverse tillage, (IV) deep tillage, (V) no-tillage, (VI) reduced tillage and (VII) fallow. Statistical significance ($p \leq 0.05$) between land-use-types is indicated by lower case letters. The Single-event Wind Erosion Evaluation Program (SWEEP) was applied to the deep tillage test site (IV).

Parameter	Yasnaya Poljana			Losovoye						
	(I)	(II)	(III)	(I)	(II)	(III)	(IV)	(V)	(VI)	(VII)
bulk density [g cm ⁻³]	1.02 ^a	1.06 ^a	0.98 ^a	1.17 ^a	1.12 ^a	1.12 ^a	1.09 ^a	1.11 ^a	1.06 ^a	1.08 ^a
total carbon [g kg ⁻¹]	39.6 ^a	34.5 ^{ab}	31.8 ^b	21.5 ^{ab}	24.3 ^a	23.2 ^a	23.4 ^a	24.2 ^a	19.1 ^b	22.3 ^{ab}
total nitrogen [g kg ⁻¹]	3.39 ^a	2.73 ^{ab}	2.57 ^b	1.88 ^{ab}	1.96 ^a	1.52 ^b	1.56 ^b	1.53 ^b	1.61 ^{ab}	1.73 ^{ab}
soil organic carbon [g kg ⁻¹]	35.3 ^a	30.9 ^a	29.5 ^a	21.1 ^b	19.4 ^{ab}	13.7 ^c	14.5 ^c	13.7 ^c	15.2 ^{ac}	16.2 ^{ac}
calcium carbonate [g kg ⁻¹]	36.5 ^a	30.0 ^a	19.3 ^a	2.8 ^c	41.2 ^a	78.7 ^b	74.2 ^b	88.0 ^b	32.7 ^a	50.9 ^a
particle size and sample preparation										
clay [%]										
(1) no pretreatment	11.27 ^a	10.45 ^a	11.56 ^a	10.68 ^b	12.14 ^{ab}	14.00 ^{ac}	15.76 ^c	15.56 ^c	11.61 ^{ab}	13.68 ^{ac}
(2) HCl pretreatment	7.14 ^a	6.72 ^a	7.41 ^a	6.56 ^{ab}	6.52 ^{ab}	5.86 ^{bc}	6.91 ^a	5.54 ^c	5.70 ^{bc}	6.19 ^{abc}
(3) HCl _{SC} pretreatment	9.20 ^a	9.97 ^a	11.41 ^a	13.87 ^a	11.97 ^a	8.83 ^b	13.17 ^a	11.85 ^a	11.68 ^{ab}	11.20 ^{ab}
(4) H ₂ O ₂ pretreatment	19.61 ^a	16.10 ^a	19.20 ^a	18.29 ^a	16.18 ^a	19.40 ^a	18.83 ^a	19.34 ^a	17.02 ^a	17.91 ^a
(5) H ₂ O ₂ + HCl pretreatment	20.23 ^a	20.55 ^a	22.58 ^a	16.22 ^a	17.27 ^a	16.79 ^a	19.34 ^a	18.66 ^a	17.62 ^a	19.76 ^a
silt [%]										
(1) no pretreatment	73.15 ^b	78.11 ^a	76.05 ^{ab}	66.80 ^b	71.74 ^a	72.69 ^a	72.30 ^a	72.17 ^a	72.78 ^a	74.84 ^a
(2) HCl pretreatment	77.73 ^a	80.01 ^a	78.27 ^a	68.61 ^d	76.73 ^{ab}	79.62 ^{ac}	79.44 ^{ac}	79.82 ^{ac}	75.72 ^b	79.92 ^c
(3) HCl _{SC} pretreatment	74.98 ^a	77.60 ^a	75.07 ^a	64.66 ^c	71.97 ^{ab}	76.67 ^b	73.58 ^{ab}	72.90 ^{ab}	69.38 ^{ac}	75.39 ^b
(4) H ₂ O ₂ pretreatment	74.74 ^a	78.29 ^a	70.37 ^a	58.51 ^b	74.03 ^a	73.20 ^a	73.64 ^a	72.84 ^a	70.50 ^a	74.20 ^a
(5) H ₂ O ₂ + HCl pretreatment	73.37 ^a	74.35 ^a	70.03 ^a	58.10 ^b	69.86 ^a	69.19 ^a	69.32 ^a	68.58 ^a	67.18 ^a	70.33 ^a
sand [%]										
(1) no pretreatment	15.58 ^a	11.44 ^a	12.39 ^a	22.53 ^c	16.11 ^a	13.31 ^{ab}	11.94 ^{ab}	12.27 ^{ab}	15.61 ^{ab}	11.48 ^b
(2) HCl pretreatment	15.14 ^a	13.27 ^a	14.32 ^a	24.83 ^d	16.75 ^{ab}	14.52 ^{ac}	13.66 ^c	14.64 ^{ac}	18.59 ^b	13.89 ^{ac}
(3) HCl _{SC} pretreatment	15.82 ^a	12.43 ^a	13.52 ^a	21.47 ^c	16.07 ^{abc}	14.50 ^{ab}	13.26 ^b	15.25 ^{ab}	18.94 ^{ac}	13.42 ^{ab}
(4) H ₂ O ₂ pretreatment	5.65 ^a	5.62 ^a	10.43 ^a	23.20 ^b	9.78 ^a	7.40 ^a	7.53 ^a	7.81 ^a	12.49 ^a	7.89 ^a
(5) H ₂ O ₂ + HCl pretreatment	6.40 ^{ab}	5.10 ^a	7.39 ^b	25.68 ^b	12.87 ^a	14.02 ^a	11.34 ^a	12.76 ^a	15.21 ^a	9.91 ^a

References

- Abbas, F., Hammad, H.M., Ishaq, W., Farooque, A.A., Bakhat, H.F., Zia, Z., Fahad, S., Farhad, W., Cerda, A., 2020. A review of soil carbon dynamics resulting from agricultural practices. *J. Environ. Manage.* 268, 110319 <https://doi.org/10.1016/j.jenvman.2020.110319>.
- Allmaras, R.R., Burwell, R.E., Larson, W.E., Holt, R.F., 1966. Total Porosity and Random Roughness of the Intertow Zone as Influenced by Tillage.
- Almagambetov, N., Grigoruk, V., 2008. Degradation of Soil in Kazakhstan: Problems and Challenges. In: Simeonov, L., Sargsyan, V. (Eds.), *Soil Chemical Pollution, Risk Assessment, Remediation and Security*. Springer, Netherlands, Dordrecht, pp. 309–320. https://doi.org/10.1007/978-1-4020-8257-3_27.
- Bischoff, N., Mikutta, R., Shubitova, O., Dohrmann, R., Herdtle, D., Gerhard, L., Fritzsche, F., Puzanov, A., Silanteva, M., Grebennikova, A., Guggenberger, G., 2018. Organic matter dynamics along a salinity gradient in Siberian steppe soils. *Biogeosciences* 15, 13–29. <https://doi.org/10.5194/bg-15-13-2018>.
- Bisutti, I., Hille, I., Raessler, M., 2004. Determination of total organic carbon – an overview of current methods. *TRAC, Trends Anal. Chem.* 23, 716–726. <https://doi.org/10.1016/j.trac.2004.09.003>.
- Bittelli, M., Andrenelli, M.C., Simonetti, G., Pellegrini, S., Artioli, G., Piccoli, I., Morari, F., 2019. Shall we abandon sedimentation methods for particle size analysis in soils? *Soil Tillage Res.* 185, 36–46. <https://doi.org/10.1016/j.still.2018.08.018>.
- Bowker, M.A., Belnap, J., Bala Chaudhary, V., Johnson, N.C., 2008. Revisiting classic water erosion models in drylands: The strong impact of biological soil crusts. *Soil Biol. Biochem.* 40, 2309–2316. <https://doi.org/10.1016/j.soilbio.2008.05.008>.
- Carroll, D., Starkey, H.C., 1971. Reactivity of Clay Minerals with Acids and Alkalies. *Clays Clay Miner.* 19, 321–333. <https://doi.org/10.1346/CCMN.1971.0190508>.
- Chende, Y., Sauer, T., Ramirez, G., Burras, C., 2015. History of East European Chernozem Soil Degradation; Protection and Restoration by Tree Windbreaks in the Russian Steppe. *Sustainability* 7, 705–724. <https://doi.org/10.3390/su7010705>.
- Chepil, W.S., 1960. Conversion of Relative Field Erodibility to Annual Soil Loss by Wind. *Soil Science Society of America Proceedings* 143–145. <https://doi.org/10.2136/sssaj1960.03615995002400020022x>.
- Conklin, A.R., Meinhardt, R., 2004. *Field sampling: principles and practices in environmental analysis*. Books in soils, plants, and the environment. Marcel Dekker, New York.
- Di Stefano, C., Ferro, V., Mirabile, S., 2010. Comparison between grain-size analyses using laser diffraction and sedimentation methods. *Biosyst. Eng.* 106, 205–215. <https://doi.org/10.1016/j.biosystemseng.2010.03.013>.
- Eckmeier, E., Gerlach, R., Gehrt, E., Schmidt, M.W.I., 2007. Pedogenesis of Chernozems in Central Europe – A review. *Geoderma* 139, 288–299. <https://doi.org/10.1016/j.geoderma.2007.01.009>.
- FAO, 2006. *Guidelines for soil description*, 4th ed. ed. Food and Agriculture Organization of the United Nations (FAO), Rome. Available from: <http://www.fao.org/3/a-a0541e.pdf>.
- FAO/UNESCO, 2007. *The Digital Soil Map of the World, 1:5,000,000; Version 3.6*. Food and Agriculture Organization of the United Nations, Rome, United Nations Educational, Scientific and Cultural Organization, Paris. Available from: <http://www.fao.org/geonetwork/srv/en/metadata.show%3Fid=14116>.
- FAO, 2012. *AQUASTAT Country profile - Kazakhstan*. Food and Agriculture Organization of the United Nations (FAO), Rome. Available from: <http://www.fao.org/3/ca0366en/CA0366EN.pdf>.
- FAO, 2017. *Kazakhstan - Country fact sheet on food and agriculture policy trends - Kazakhstan*. Food and Agriculture Organization of the United Nations (FAO), Rome. Available from: <http://www.fao.org/3/a-i7676e.pdf>.
- Fisher, P., Aumann, C., Chia, K., O'Halloran, N., Chandra, S., 2017. Adequacy of laser diffraction for soil particle size analysis. *PLoS ONE* 12, e0176510. <https://doi.org/10.1371/journal.pone.0176510>.
- Frühau, M., Meinel, T., Schmidt, G., 2020. The Virgin Lands Campaign (1954–1963) Until the Breakdown of the Former Soviet Union (FSU): With Special Focus on Western Siberia. In: Frühau, M., Guggenberger, G., Meinel, T., Theesfeld, I., Lentz, S. (Eds.), *KULUNDA: Climate Smart Agriculture, Innovations in Landscape Research*. Springer International Publishing, Cham, pp. 101–118. https://doi.org/10.1007/978-3-030-15927-6_8.
- Fryrear, D.W., Krammes, C.A., Williamson, D.L., Zobeck, T.M., 1994. Computing the wind erodible fraction of soils.
- Funk, R., Reuter, H.I., 2006. Wind Erosion. In: Boardman, J., Poesen, J. (Eds.), *Soil Erosion in Europe*. John Wiley & Sons, Ltd, Chichester, UK, pp. 563–582. <https://doi.org/10.1002/0470859202.ch41>.
- Gardner, W.R., 1956. Representation of Soil Aggregate-Size Distribution by a Logarithmic-Normal Distribution. *Soil Sci. Soc. Am. J.* 20, 151–153. <https://doi.org/10.2136/sssaj1956.0361599500200003x>.
- Gee, G.W., Or, D., 2002. *2.4 Particle-Size Analysis*. In: Dane, J.H., Topp, C.G. (Eds.), *SSSA Book Series*. Soil Science Society of America. <https://doi.org/10.2136/sssabookser5.4.c12>.
- Green, D.W., Perry, R.H., 2007. *Perry's Chemical Engineers' Handbook, Eighth ed.* McGraw-Hill Professional Publishing, Blacklick, USA.
- Hagen, L.J., 1991. A wind erosion prediction system to meet user needs. *J. Soil Water Conserv.* 46, 106–111.
- Harris, I.C., Jones, P.D., Osborn, T., 2020. CRU TS4.04: Climatic Research Unit (CRU) Time-Series (TS) version 4.04 of high-resolution gridded data of month-by-month variation in climate (Jan. 1901–Dec. 2019). Available from: <https://catalogue.ceda.ac.uk/uuid/89e1e34ec3554dc98594a5732622bce9>.
- Illiger, P., Schmidt, G., Walde, I., Hese, S., Kudrjavzev, A.E., Kurepina, N., Mizgirev, A., Stephan, E., Bondarovich, A., Frühau, M., 2019. Estimation of regional soil organic carbon stocks merging classified land-use information with detailed soil data. *Sci. Total Environ.* 695, 133755 <https://doi.org/10.1016/j.scitotenv.2019.133755>.
- ISO 10390, 2005. *Soil quality - Determination of pH*. International Organization for Standardization (ISO), Geneva.
- ISO 10693, 1995. *Soil quality - Determination of carbonate content - Volumetric method*. International Organization for Standardization (ISO), Geneva.
- ISO 11277, 2002. *Soil quality - Determination of particle size distribution in mineral soil and material - Method by sieving and sedimentation*. International Organization for Standardization (ISO), Geneva.

- ISO 13320, 2009. Particle Size Analysis - Laser diffraction methods. International Organization for Standardization (ISO), Geneva.
- ISO 14488, 2007. Particulate materials - Sampling and sample splitting for the determination of particulate properties. International Organization for Standardization (ISO), Geneva.
- Jarrah, M., Mayel, S., Tataro, J., Funk, R., Kuka, K., 2020. A review of wind erosion models: Data requirements, processes, and validity. *CATENA* 187, 104388. <https://doi.org/10.1016/j.catena.2019.104388>.
- Keesstra, S.D., Bouma, J., Wallinga, J., Titttonell, P., Smith, P., Cerda, A., Montanarella, L., Quinton, J.N., Pachepsky, Y., van der Putten, W.H., Bardgett, R.D., Moolenaar, S., Mol, G., Jansen, B., Fresco, L.O., 2016. The significance of soils and soil science towards realisation of the United Nations Sustainable Development Goals. *SOIL* 2, 111–128. <https://doi.org/10.5194/soil-2-111-2016>.
- Kettler, T.A., Doran, J.W., Gilbert, T.L., 2001. Simplified Method for Soil Particle-Size Determination to Accompany Soil-Quality Analyses. *Soil Sci. Soc. Am. J.* 65, 849. <https://doi.org/10.2136/sssaj2001.653849x>.
- Kroetsch, D., Wang, C., 2007. Particle Size Distribution. In: Carter, M., Gregorich, E. (Eds.), *Soil Sampling and Methods of Analysis*. Second Edition. CRC Press. <https://doi.org/10.1201/9781420005271>.
- Larney, F., 2007. Dry-Aggregate Size Distribution. In: Carter, M., Gregorich, E. (Eds.), *Soil Sampling and Methods of Analysis*. Second Edition. CRC Press. <https://doi.org/10.1201/9781420005271>.
- Li, J., Ma, X., Zhang, C., 2020. Predicting the spatiotemporal variation in soil wind erosion across Central Asia in response to climate change in the 21st century. *Sci. Total Environ.* 709. <https://doi.org/10.1016/j.scitotenv.2019.136060>.
- López, M.V., de Dios Herrero, J.M., Hevia, G.G., Gracia, R., Buschiazzi, D.E., 2007. Determination of the wind-erodible fraction of soils using different methodologies. *Geoderma* 139, 407–411. <https://doi.org/10.1016/j.geoderma.2007.03.006>.
- Mikutta, R., Kleber, M., Kaiser, K., Jahn, R., 2005. Review: Organic matter removal from soils using hydrogen peroxide, sodium hypochlorite, and disodium peroxodisulfate. *Soil Sci. Soc. Am. J.* 69, 120. <https://doi.org/10.2136/sssaj2005.0120>.
- Moeys, J., 2018. The soil texture wizard: R functions for plotting, classifying, transforming and exploring soil texture data 104. Available from: https://cran.r-project.org/web/packages/soiltexture/vignettes/soiltexture_vignette.pdf.
- Muhs, D.R., Prins, M., Machalet, B., 2014. Loess as a Quaternary paleoenvironmental indicator. *PAGES Mag* 22, 84–85. <https://doi.org/10.22498/pages.22.2.84>.
- Pi, H., Sharratt, B., Feng, G., Lei, J., Li, X., Zheng, Z., 2016. Validation of SWEEP for creep, saltation, and suspension in a desert-oasis ecotone. *Aeolian Res.* 20, 157–168. <https://doi.org/10.1016/j.aeolia.2016.01.006>.
- Prishchepov, A.V., Schierhorn, F., Dronin, N., Ponkina, E.V., Müller, D., 2020. 800 Years of Agricultural Land-use Change in Asian (Eastern) Russia. In: Frühauf, M., Guggenberger, G., Meinel, T., Theesfeld, I., Lentz, S. (Eds.), *KULUNDA: Climate Smart Agriculture, Innovations in Landscape Research*. Springer International Publishing, Cham, pp. 67–87. https://doi.org/10.1007/978-3-030-15927-6_6.
- R Core Team, 2020. R: A language and environment for statistical computing. R Foundation for Statistical Computing, Vienna. Available from: <https://www.r-project.org/>.
- RStudio Team, 2020. R: Integrated Development for R. RStudio, Boston. Available from: <https://rstudio.com/products/rstudio/>.
- Rachkovskaya, E.I., Bragina, T.M., 2012. Steppes of Kazakhstan: Diversity and Present State. In: Wergler, M.J.A., van Staaldin, M.A. (Eds.), *Eurasian Steppes. Ecological Problems and Livelihoods in a Changing World*. Plant and Vegetation. Springer, Netherlands, Dordrecht, pp. 103–148. https://doi.org/10.1007/978-94-007-3886-7_3.
- Rakkar, M.K., Blanco-Canqui, H., Tataro, J., 2019. Predicting soil wind erosion potential under different corn residue management scenarios in the central Great Plains. *Geoderma* 353, 25–34. <https://doi.org/10.1016/j.geoderma.2019.05.040>.
- Rawls, W.J., 1983. Estimating Soil Bulk Density from Particle Size Analysis and organic matter content. *Soil Sci.* 135, 123–125. <https://doi.org/10.1097/00010694-198302000-00007>.
- Reyer, C.P.O., Otto, I.M., Adams, S., Albrecht, T., Baarsch, F., Carlsburg, M., Coumou, D., Eden, A., Ludi, E., Marcus, R., Mengel, M., Mosello, B., Robinson, A., Schleussner, C.-F., Serdeczny, O., Stagl, J., 2017. Climate change impacts in Central Asia and their implications for development. *Reg Environ Change* 17, 1639–1650. <https://doi.org/10.1007/s10113-015-0893-z>.
- Rowley, M.C., Grand, S., Verrecchia, E.P., 2018. Calcium-mediated stabilisation of soil organic carbon. *Biogeochemistry* 137, 27–49. <https://doi.org/10.1007/s10533-017-0410-1>.
- Schmidt, G., Illiger, P., Kudryavtsev, A.E., Bischoff, N., Bondarovich, A.A., Koshanov, N. A., Rudev, N.V., 2020. Physical Soil Properties and Erosion. In: Frühauf, M., Guggenberger, G., Meinel, T., Theesfeld, I., Lentz, S. (Eds.), *KULUNDA: Climate Smart Agriculture*. Springer International Publishing, Cham, pp. 155–166. https://doi.org/10.1007/978-3-030-15927-6_11.
- Schulte, P., Lehmkuhl, F., Steininger, F., Loibl, D., Lockot, G., Protze, J., Fischer, P., Stauch, G., 2016. Influence of HCl pretreatment and organo-mineral complexes on laser diffraction measurement of loess-paleosol-sequences. *CATENA* 137, 392–405. <https://doi.org/10.1016/j.catena.2015.10.015>.
- Shao, Y., 2008. Physics and modelling of wind erosion, 2. rev. & exp. In: *Atmospheric and oceanographic sciences library*, ed. ed Springer, S.I. <https://doi.org/10.1007/978-1-4020-8895-7>.
- Six, J., Bossuyt, H., Degryze, S., Deneff, K., 2004. A history of research on the link between (micro)aggregates, soil biota, and soil organic matter dynamics. *Soil Tillage Res.* 79, 7–31. <https://doi.org/10.1016/j.still.2004.03.008>.
- Soil Science Division Staff, 2017. Soil survey manual, USDA Handbook 18., edited by C. Ditzler, K. Scheffe, and H. C. Monger. United States Department of Agriculture, Government Printing Office, Washington, D.C. Available from: https://www.nrcs.usda.gov/wps/portal/nrcs/detail/soils/ref/?cid=nrsc142p2_054262.
- Sommer, R., Glazirina, M., Yuldashev, T., Otarov, A., Ibraeva, M., Martynova, L., Bekenov, M., Kholov, B., Ibragimov, N., Kobilov, R., Karaev, S., Sultonov, M., Khasanova, F., Esanbekov, M., Mavlyanov, D., Isaev, S., Abdurahimov, S., Kramov, R., Shezdyukova, L., de Pauw, E., 2013. Impact of climate change on wheat productivity in Central Asia. *Agric. Ecosyst. Environ.* 178, 78–99. <https://doi.org/10.1016/j.agee.2013.06.011>.
- Sonmez, S., Buyuktas, D., Okturen, F., Citak, S., 2008. Assessment of different soil to water ratios (1:1, 1:2.5, 1:5) in soil salinity studies. *Geoderma* 144, 361–369. <https://doi.org/10.1016/j.geoderma.2007.12.005>.
- Stolbovoi, V., 2000. Soils of Russia: Correlated with the Revised Legend of the FAO Soil Map of the World and World Reference Base for Soil Resources, International Institute for Applied Systems Analysis, Laxenburg, Austria. Available from: <http://pure.iiasa.ac.at/id/eprint/6111/1/RR-00-013.pdf>.
- Sympatec, 2019. Sympatec-Helos: Technische Spezifikationen. Sympatec GmbH, Clausthal-Zellerfeld.
- Sympatec, 2012. HELOS/R: Central Unit - Operating Instructions. Sympatec GmbH, Clausthal-Zellerfeld.
- Tataro, J. (Ed.), 2008. Single-event Wind Erosion Evaluation program: SWEEP user manual draft (updated 6 October 2020). United States Department of Agriculture, Agricultural Research Service, Manhattan, KA, USA.
- Tataro, J., van Donk, S.J., Ascough, J.C., Walker, D.G., 2016. Application of the WEPS and SWEEP models to non-agricultural disturbed lands. *Heliyon* 2, e00215. <https://doi.org/10.1016/j.heliyon.2016.e00215>.
- Tataro, J., Wagner, L., Fox, F., 2019. The Wind Erosion Prediction System and its Use in Conservation Planning. In: Wendroth, O., Lascano, R.J., Ma, L. (Eds.), *Advances in Agricultural Systems Modeling*. American Society of Agronomy and Soil Science Society of America, Madison, WI, USA, pp. 71–101. <https://doi.org/10.2134/advagricsystmodel8.2017.0021>.
- Teixeira, E.I., Fischer, G., van Velthuisen, H., Walter, C., Ewert, F., 2013. Global hot-spots of heat stress on agricultural crops due to climate change. *Agric. For. Meteorol.* 170, 206–215. <https://doi.org/10.1016/j.agrformet.2011.09.002>.
- Tataro, J. (Ed.), 2020. The Wind Erosion Prediction System (WEPS): Technical Documentation, USDA Agriculture Handbook 727. United States Department of Agriculture, Agricultural Research Service, Beltsville, MD, USA. Available from: <https://www.ars.usda.gov/research/software/download/?softwareid=415>.
- UN, 2019. Sustainable development goals report 2019. United Nations (UN) publication issued by the Department of Economic and Social Affairs, New York. Available from: <https://unstats.un.org/sdgs/report/2019>.
- Uspanov, U.U., Yevstifeyev, U.G., Storozhenko, D.M., Lobova, E.V., 1975. Soil Map of the Kazakh SSR 1:2,500,000.
- Virto, I., Gartzia-Bengoetxea, N., Fernández-Ugalde, O., 2011. Role of Organic Matter and Carbonates in Soil Aggregation Estimated Using Laser Diffractometry. *Pedosphere* 21, 566–572. [https://doi.org/10.1016/S1002-0160\(11\)60158-6](https://doi.org/10.1016/S1002-0160(11)60158-6).
- WEF, 2020. The Global Risks Report 2020. World Economic Forum, Cologny. Available from: http://www3.weforum.org/docs/WEF_Global_Risk_Report_2020.pdf.
- Wuddivira, M.N., Camps-Roach, G., 2007. Effects of organic matter and calcium on soil structural stability. *Eur. J. Soil Sci.* 58, 722–727. <https://doi.org/10.1111/j.1365-2389.2006.00861.x>.
- Yang, Y., Wang, L., Wendroth, O., Liu, B., Cheng, C., Huang, T., Shi, Y., 2019. Is the Laser Diffraction Method Reliable for Soil Particle Size Distribution Analysis? *Soil Sci. Soc. Am. J.* 83, 276. <https://doi.org/10.2136/sssaj2018.07.0252>.
- Zepner, L., Karrasch, P., Wiemann, F., Bernard, L., 2020. ClimateCharts.net – an interactive climate analysis web platform. *Int. J. Digital Earth* 1–19. <https://doi.org/10.1080/17538947.2020.1829112>.
- Zimmermann, I., Horn, R., 2020. Impact of sample pretreatment on the results of texture analysis in different soils. *Geoderma* 371, 114379. <https://doi.org/10.1016/j.geoderma.2020.114379>.
- Zobeck, T.M., Van Pelt, R.S., 2015. Wind Erosion. In: Hatfield, J.L., Sauer, T.J. (Eds.), *Soil Management: Building a Stable Base for Agriculture*. Soil Science Society of America, Madison, WI, USA, pp. 209–227. <https://doi.org/10.2136/2011.soilmanagement.c14>.

5.2 Koza et al. (2022): Potential erodibility of semi-arid steppe soils derived from aggregate stability tests

Full bibliographic citation:

Koza, M., Pöhlitz, J., Prays, A., Kaiser, K., Mikutta, R., Conrad, C., Vogel, C., Meinel, T., Akshalov, K., Schmidt, G., 2022. Potential erodibility of semi-arid steppe soils derived from aggregate stability tests. *European Journal of Soil Science* 73, e13304. <https://doi.org/10.1111/ejss.13304>

Scientific presentations and discussions of this study:

Koza, M., Pöhlitz, J., Prays, A., Kaiser, K., Mikutta, R., Conrad, C., Vogel, C., Meinel, T., Akshalov, K., Schmidt, G., 2022. Aggregate stability and potential erodibility of dry steppe soils. *EGU General Assembly 2022*. EGU22-2803. Vienna, Austria. <https://doi.org/10.5194/egusphere-egu22-2803>

Koza, M. 2021. Natural limitations influence the effect of tillage on aggregation in dry steppe soils. *1st EU Soil Observatory Stakeholders Forum – Young Soil Researchers Forum*. Online.

Koza, M. 2020. Effects of land-use transformation on wind erosion in the dry steppes. *1st International IALE-Russia conference*. Online

Preface:

The results of the first publication (Koza et al., 2021) showed that small differences in PSD do not affect soil loss estimations when texture-based properties such as the GMD are measured and not derived by pedotransfer function. Hence, the importance of aggregate stability and size distribution based on field samples for estimating erosion risk was concluded (Diaz-Zorita et al., 2002; Le Bissonnais, 1996; Skidmore et al., 1994) and addressed in the second publication.








Summary:

Soil aggregates composed of primary particles and binding agents were evaluated for their erodibility against tillage, wind, and water. This publication examines the structural resistance of soil against the disruptive forces steppe soils experience under field conditions. For conceptual and practical reasons an indirect method was used to estimate the potential erodibility. Aggregate stabilities of crop- and grassland were compared to investigate the effects of tillage. The EF was used as the important parameter to investigate the susceptibility to wind, and three different wetting treatments were used to simulate the disruptive effects of water. Koza et al. (2022) is the first study in northern Kazakhstan that examines aggregate resistances against different mechanical stresses and discusses the interrelated potential erodibility by wind and water.

Highlights:

- Organic matter is the important binding agent enhancing aggregation in steppe topsoils.
- Tillage always declines aggregate stability even without SOC changes.
- All cropland soils are prone to wind or water erosion independent of their soil properties.
- Despite the semi-arid conditions, erosion risk by water seems higher than by wind.

Potential erodibility of semi-arid steppe soils derived from aggregate stability tests

Moritz Koza¹  | Julia Pöhlitz¹ | Aleksey Prays² | Klaus Kaiser²  |
Robert Mikutta²  | Christopher Conrad¹  | Cordula Vogel³  |
Tobias Meinel⁴ | Kanat Akshalov⁵  | Gerd Schmidt¹ 

¹Department of Geocology, Institute of Geosciences and Geography, Martin Luther University Halle-Wittenberg, Halle (Saale), Germany

²Soil Science and Soil Protection, Institute of Agricultural and Nutritional Sciences, Martin Luther University Halle-Wittenberg, Halle (Saale), Germany

³Institute of Soil Science and Site Ecology, Technische Universität Dresden, Tharandt, Germany

⁴TОО Amazone Kazakhstan, Amazonen-Werke H. Dreyer SE & Co. KG, Hasbergen, Germany

⁵Soil and Crop Management, Barayev Research and Production Center for Grain Farming, Shortandy, Kazakhstan

Correspondence

Moritz Koza, Institute of Geosciences and Geography, Martin Luther University Halle-Wittenberg, Von-Seckendorff-Platz 4, 06120 Halle (Saale), Germany.
Email: moritz.koza@geo.uni-halle.de

Funding information

Bundesministerium für Bildung und Forschung

Abstract

Erosion is a severe threat to the sustainable use of agricultural soils. However, the structural resistance of soil against the disruptive forces steppe soils experience under field conditions has not been investigated. Therefore, 132 topsoils under grass- and cropland covering a large range of physico-chemical soil properties (sand: 2–76%, silt: 18–80%, clay: 6–30%, organic carbon: 7.3–64.2 g kg⁻¹, inorganic carbon: 0.0–8.5 g kg⁻¹, pH: 4.8–9.5, electrical conductivity: 32–946 µS cm⁻¹) from northern Kazakhstan were assessed for their potential erodibility using several tests. An adjusted drop-shatter method (low energy input of 60 Joule on a 250-cm³ soil block) was used to estimate the stability of dry soil against weak mechanical forces, such as saltating particles striking the surface causing wind erosion. Three wetting treatments with various conditions and energies (fast wetting, slow wetting, and wet shaking) were applied to simulate different disruptive effects of water. Results indicate that aggregate stability was higher for grassland than cropland soils and declined with decreasing soil organic carbon content. The results of the drop-shatter test suggested that 29% of the soils under cropland were at risk of wind erosion, but only 6% were at high risk (i.e. erodible fraction >60%). In contrast, the fast wetting treatment revealed that 54% of the samples were prone to become “very unstable” and 44% “unstable” during heavy rain or snowmelt events. Even under conditions comparable to light rain events or raindrop impact, 53–59% of the samples were “unstable.” Overall, cropland soils under semi-arid conditions seem much more susceptible to water than wind erosion. Considering future projections of increasing precipitation in Kazakhstan, we conclude that the risk of water erosion is potentially underestimated and needs to be taken into account when developing sustainable land use strategies.

In memory of Yves Le Bissonnais and his efforts in establishing a standardised method to determine aggregate stability.

This is an open access article under the terms of the [Creative Commons Attribution](https://creativecommons.org/licenses/by/4.0/) License, which permits use, distribution and reproduction in any medium, provided the original work is properly cited.

© 2022 The Authors. *European Journal of Soil Science* published by John Wiley & Sons Ltd on behalf of British Society of Soil Science.

Highlights

- Organic matter is the important binding agent enhancing aggregation in steppe topsoils.
- Tillage always declines aggregate stability even without soil organic carbon changes.
- All croplands soil are prone to wind or water erosion independent of their soil properties.
- Despite the semi-arid conditions, erosion risk by water seems higher than by wind.

KEYWORDS

climate change, land use, soil organic carbon, soil texture, water erosion, wind erosion

1 | INTRODUCTION

Drylands cover 41% of the Earth's land surface and are particularly vulnerable to human activities and climate change (Reynolds et al., 2007). Large areas in the semi-arid steppe regions of Central Asia are currently under severe threat of increasing soil erosion due to intense agriculture and increasingly extreme climate conditions (Mirzabaev et al., 2016; Reyer et al., 2017; Robinson, 2016). Central Asia's most important grain producer is Kazakhstan, with 84.5 Mio hectares of potential agricultural land (FAO, 2012). However, 25.5 Mio hectares are already affected by wind erosion and 1 Mio hectare by water erosion due to missing vegetation cover and unsustainable land use (Almagambetov & Grigoruk, 2008; Cerdà et al., 2009). In northern Kazakhstan, approximately, 23 Mio hectares of native grassland were converted into cropland during the largest global ecosystem conversion in the twentieth century ("Virgin Lands Campaign") (Frühauf et al., 2020; Prishchepov et al., 2020). Strong wind gusts over 40 m s^{-1} favour wind erosion, and extreme snowmelts during spring or heavy rain events during summer cause erosion by water (FAO, 2012; Muñoz Sabater, 2019; Wang et al., 2020; WHO, 2012). Under the dry continental climate, 66% of the annual precipitation occurs as snowfall and severe thunderstorms in the summer are often linked to flash floodings (FAO, 2012; Harris et al., 2020; Zepner et al., 2021). Climate models indicate that the risk of soil erosion will increase in northern Kazakhstan in future (Li et al., 2020; Teixeira et al., 2013). Extreme temperature episodes enhance draughts (Teixeira et al., 2013; Wang et al., 2020; WHO, 2012), and in response to increasing rainfall duration, magnitude, and intensity, the risk of water erosion (Duulatov et al., 2021).

The susceptibility of soil to erosion depends mainly on the stability of its structure against mechanical stress, which is directly linked to the stability of aggregates (Diaz-Zorita et al., 2002; Le Bissonnais, 2016, 1996b). In turn, the

formation of aggregates is linked to soil properties that promote interactions among primary particles, such as rearrangement, flocculation, and cementation (Amézketa, 1999; Bronick & Lal, 2005; Diaz-Zorita et al., 2002; Six et al., 2004). For example, higher soil clay content typically increases aggregate stability, although swelling of clay during wetting (Bronick & Lal, 2005) can promote the breakdown of aggregates. Especially in semi-arid regions, soluble salts can contribute to the aggregation and disaggregation of primary particles (Amézketa, 1999; Fernández-Ugalde et al., 2011; Virto et al., 2011). Besides inorganic constituents, organic matter is an important binding agent (Jarvis et al., 2012; Tisdall & Oades, 1982) but its effect on aggregate stability varies considerably depending on soil type and external factors such as climate and land use (Six et al., 2004). For instance, tillage is the agricultural land use practice that most deteriorates aggregate stability (Amézketa, 1999; Bronick & Lal, 2005; Diaz-Zorita et al., 2002; Six et al., 2004). However, the mutual effects of agriculture and soil properties on aggregate stability and potential erodibility on steppe soils have not been comprehensively addressed.

Methods for determining aggregate stability often vary in the mechanical stress used and complicate the comparability between studies and field conditions (Almajmaie et al., 2017; Amézketa, 1999; Diaz-Zorita et al., 2002). As there is no single standardised procedure available to rank the soils' structural resistance against the disruptive forces of wind and water, it is necessary to combine different methods to assess erosion susceptibility (Kemper & Rosenau, 2018). The adjusted drop-shatter method with a low energy input of 60 Joule can be applied to estimate the stability of dry soil against weak mechanical forces, such as saltating particles striking the surface, causing the suspension of soil particles during a wind erosion event (Diaz-Zorita et al., 2002; Hadas & Wolf, 1984; Larney, 2007; López et al., 2007; Shao, 2008). The three wetting tests proposed by Le Bissonnais (2016,

1996b) are usually applied to estimate aggregate stability in terms of water erosion under various wetting conditions and energies: the fast wetting treatment assesses the breakdown during heavy rain or snowmelt, the slow wetting treatment is used to simulate the effect of light rain, and the wet shaking treatment addresses mechanical breakdown by raindrop impact (Le Bissonnais, 2016, 1996b). This uniform framework is considered the best approach to assess aggregate stability over a wide range of potentially erosive conditions and has been applied successfully worldwide (Bartoli et al., 2016).

In this study, we applied the four aggregate stability tests described above to explore the resistance of aggregates of steppe soils against different mechanical stresses to assess the potential erodibility by wind and water. We assessed the extent and relevant factors of aggregation by studying soils with a wide range of physico-chemical properties sampled at seven sites across northern Kazakhstan. Additionally, we compared soils from cropland with grassland at each site to single out the effect of tillage on aggregate stability under given soil conditions. Ultimately, our objectives were (i) to determine the main soil properties enhancing aggregation, (ii) to explore the effect of tillage (grassland vs. cropland), and (iii) to assess the potential erodibility of cropland by investigating the consequences of mechanical stress on aggregate stability similar to disruptive forces by wind and water.

2 | MATERIALS AND METHODS

2.1 | Study area

The study area is located in the north of Kazakhstan and connects the central with the east-central part of the

Eurasian steppe (Figure 1). The dry continental climate at the seven test sites is characterised by comparable annual mean temperatures (2.5–3.8°C) and precipitation (299–352 mm) based on weighted interpolation (1989–2018) (Harris et al., 2020; Zepner et al., 2021). Sites 1 and 2 are located close to Kokshetau, Sites 3, 4, and 5 close to Astana, Site 6 is located south of Ekibastuz, and Site 7 east of the Irtysh close to the border of Russia and the Kulunda steppe (Figure 1). Soils at Sites 1 and 2 are Haplic Chernozems, those at Site 5 are Calcic Kastanozems, and at Sites 3, 4, 6, and 7 are Haplic Kastanozems (FAO, 2014). Kastanozems correspond in the national classification system to Dark Chestnut Soils (Stolbovoi, 2000; Uspanov et al., 1975). A meteorological station (ecoTech GmbH, Bonn, Germany) with a multi-sensor (WXT536, Vaisala GmbH, Hamburg, Germany) at a two-meter height was installed on Site 1 to monitor real weather conditions in the study area, including temperature, wind speed, and precipitation.

2.2 | Soil sampling

Soil samples were collected in May and June 2019. Each site was represented by one native grassland and up to six cropland plots. Native grassland plots were used for occasional grazing but had never been cultivated. The typical vegetation on grassland was dominated by *Stipa capillata* L., Volga fescue (*Festuca valesiaca* Schleich. ex Gaudin), and shrubs (*Artemisia* spp.). Grassland plots were conscientiously selected for representing an initial situation to reference the effect of tillage at each site. All croplands were under reduced tillage, which is the most common practice in the study area. Croplands were managed for spring wheat, the most common crop.

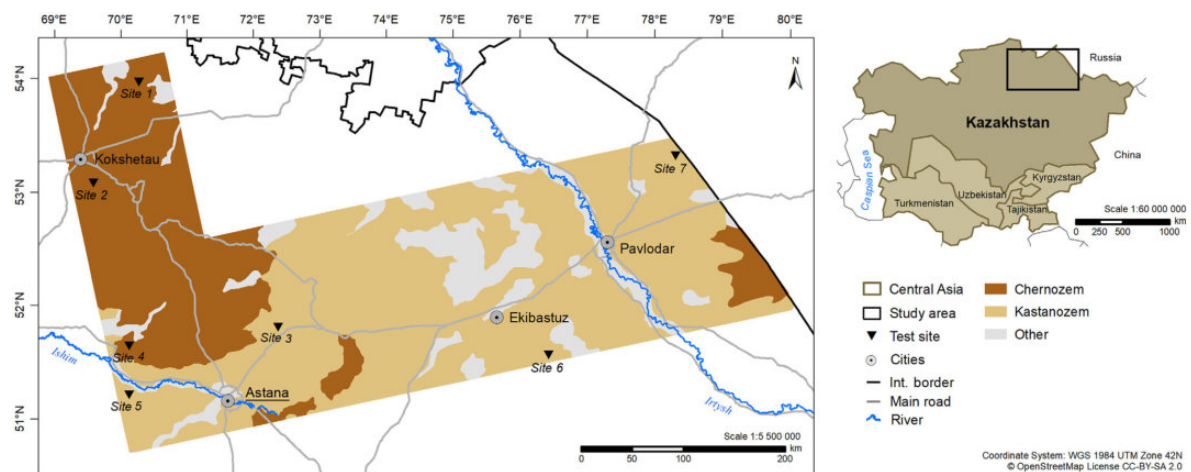


FIGURE 1 Location of the study area with seven test sites and dominant soil types in northern Kazakhstan (Uspanov et al., 1975)

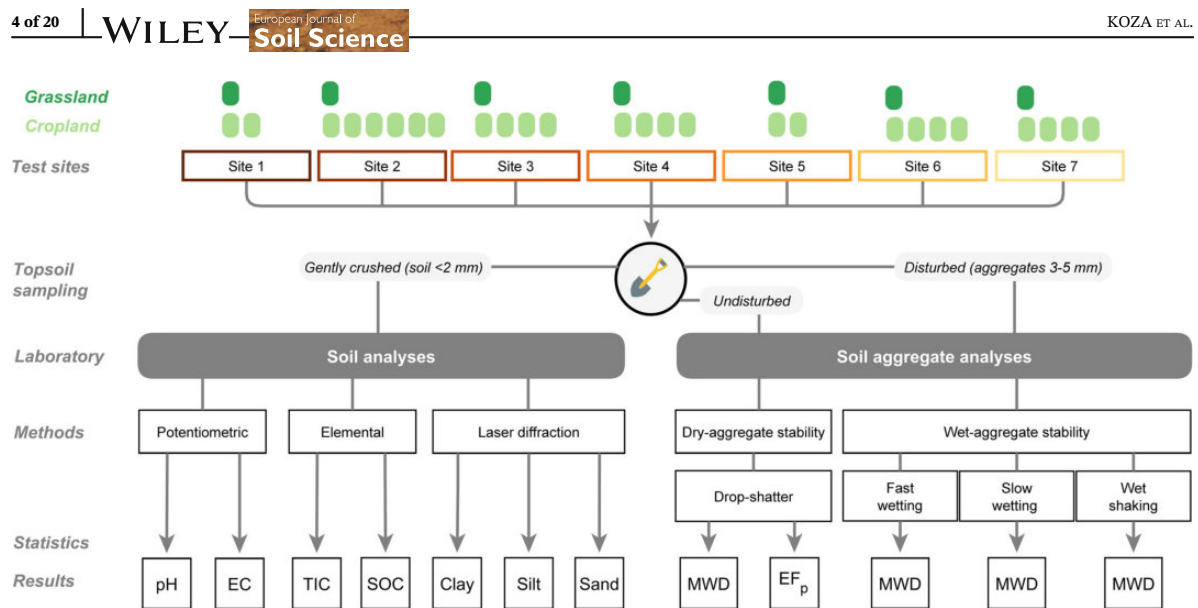


FIGURE 2 Study design with applied materials and methods. Abbreviations: EC, electrical conductivity; TIC, total inorganic carbon; SOC, soil organic carbon; MWD, mean weight diameter; and EF_p, potential erodible fraction

In total, seven native grassland and 26 continuous cropland plots were sampled. Despite being managed similarly, cropland plots differed slightly in terms of management practices, machinery used, and field characteristics, such as different ages after conversion and crop history (Table A1). Topsoil samples were collected from 0–5 cm depth, most susceptible to erosion (Zachar, 1982). Each plot was sampled at four randomly selected spots ($n = 33 \text{ plots} \times 4 \text{ spots} = 132$) (Figure 2). Soil cores of 250 cm³ (diameter = 80 mm, height = 50 mm) were taken and transferred into plastic bags for transportation. Before conducting soil analyses, they were air-dried at 40°C for 24 h, gently crushed, and dry-sieved to <2-mm with loose organic material removed. For analysing dry-aggregate stability, 132 undisturbed soil blocks of 250 cm³ (width = 50 mm, length = 100 mm, height = 55 mm) and for wet-aggregate stability, 132 boxes (width = 50 mm, length = 100 mm, height = 55 mm) with soil aggregates broken apart by hand from clods were collected ($n = 132 \text{ spots} \times 3 \text{ sample types} = 396$).

2.3 | Soil analyses

The pH and electrical conductivity (EC) were measured in distilled water at a 1-to-2.5 soil-to-solution (weight-to-volume) ratio. Total carbon and total nitrogen were analysed by dry combustion at 950°C (varioMax Cube, Elementar Analysensysteme GmbH, Langensfeld, Germany). Total inorganic carbon (TIC) was analysed by

dispersing 2 g of ground sample material in 50 ml 2 M HCl at 50°C and subsequent detection of the released CO₂ (soliTIC modul interfaced to the varioMax Cube, Elementar Analysensysteme GmbH, Langensfeld, Germany). The soil organic carbon (SOC) content was calculated by subtracting TIC from total carbon. Soil texture was evaluated by a laser diffraction analyser (Helos/KR, Sympatec GmbH, Clausthal Zellerfeld, Germany) equipped with a 60 W sonotrode for wet dispersion (Quixel, Sympatec GmbH, Clausthal Zellerfeld, Germany). Before texture analyses, soil was pre-treated with 30% hydrogen peroxide (H₂O₂) (Koza et al., 2021) and 0.05 M sodium pyrophosphate (Na₄P₂O₇ · 10 H₂O) to remove organic matter and support dispersion (ISO 13320, 2009). Analyses were carried out in duplicates with 2–3 g soil for 20 s (20–30% obscuration rate). Single-particles were described mathematically by the Fraunhofer theory (Green & Perry, 2007; ISO 13320, 2009). Particle size classes of >2, 2–50, and 50–2000 μm were used for assigning soil texture (Soil Science Division Staff, 2017).

2.4 | Soil aggregate analyses

2.4.1 | Dry-aggregate stability

Drop-shatter

An adjusted drop-shatter method (Hadas & Wolf, 1984; Marshall & Quirk, 1950) was used to estimate the stability of dry soil against weak mechanical forces during

saltation bombardment. The energy applied onto the undisturbed soil blocks of 250 cm³ was 60 J derived from Equation 1:

$$E^* = m \times g \times h \times n \quad (1)$$

where E^* is the cumulative energy J imparted on the soil sample, and m the mass defined by a 6-kg metal plate dropped onto the sample once (n) from a height (h) of 0.1 m with the gravitation acceleration (g) of 9.81 m s⁻².

Fragment size distribution: The dry-aggregate size distribution after mechanical impact was obtained by dry sieving. Therefore, a horizontal sieving apparatus (Analysette 3, Fritsch GmbH, Idar-Oberstein, Germany) with eight different sieves (8, 5, 3, 2, 0.85, 0.5, 0.25, and 0.05 mm) was used for 60 s and an amplitude of 1 mm. Sieving time was restricted to prevent fragmentation due to abrasion (Cole, 1939). The dry-aggregate size distribution after drop-shatter was described by the mean weight diameter (MWD), which is commonly used as a stability index (Nimmo & Perkins, 2002), as calculated based on Equation 2:

$$\text{MWD} = \sum_{i=1}^n \bar{x}_i w_i \quad (2)$$

where x_i is the mean diameter of the size fraction [mm], and w_i is the proportion of the total sample retained on the sieve. The upper limit was estimated by doubling the size of the largest sieve (Larney, 2007). The derived midpoint (12 mm) was used as an MWD for samples that did not disintegrate under the impact of 60 J.

The erodible fraction, a simple index for potential wind erosion (Larney, 2007), can be calculated as the weight percent of aggregates <0.84 mm after separating fragments (Chepil, 1953). Sieving can be obtained with a rotary (Chepil, 1962) or a comparable horizontal sieve (López et al., 2007). A European standard sieve size of 0.85 mm can also be used (Leys et al., 1996). The potential erodible fraction (EF_p) was calculated after drop-shatter and dry sieving with an 0.85 mm horizontal sieve using Equation 3:

$$EF_p = \frac{W < 0.85}{TW} \times 100\% \quad (3)$$

where $W < 0.85$ is the weight [g] of <0.85-mm aggregates, and TW is the initial weight [g] of the total sample. In general, soils with an $EF > 60\%$ are considered critical (Anderson & Wenhardt, 1966) and indicate a high risk of wind erosion (Larney, 2007). In contrast, an $EF < 40\%$ indicates a negligible risk of wind erosion. (Leys

et al., 1996). However, according to the erodibility classification by Shiyaty (1965), as cited by Zachar (1982) and López et al. (2007), an $EF > 50\%$ already indicates a high risk of wind erosion. Still, they consider $EF < 40\%$ to indicate substantial resistance to wind erosion.

2.4.2 | Wet-aggregate stability

A unified framework with three treatments was used to analyse aggregate stability against water disruption. The treatments were conducted on 3–5 mm aggregates collected previously by dry sieving. If gravel was visually present within the 3–5 mm aggregate fraction, samples were omitted to avoid misleading results. Immediately before each test, aggregates were oven-dried at 40°C for 24 h and cooled in a desiccator (ISO 10930, 2011).

Fast wetting

The fast wetting treatment, also called “slaking”, corresponds to a heavy rain event and is recommended for comparing soils containing high amounts of organic carbon (Le Bissonnais, 2016, 1996b), such as the Chernozems in the study area. As the first step, 4 g of aggregates were gently immersed in a 250-ml beaker filled with 50 ml deionised water. After 10 min, the supernatant was decanted, and aggregates were carefully transferred to a 0.05-mm sieve immersed in ethanol to determine fragment size distribution.

Slow wetting

The slow wetting treatment corresponds to a light rain event on soil aggregates. A fine-pored cellulose sponge (height 3.7 cm) was placed in a flat vessel for pre-wetting. Distilled water was added to a height of 3 cm. A filter paper (DP 5893125, Hanemühle Fine Art GmbH, Dassel, Germany) was placed on the sponge and saturated. Then, 4 g aggregates were arranged on the filter paper. Thus, capillary flow slowly wetted aggregates for 30 min before being transferred to a 0.05-mm sieve immersed in ethanol to determine fragment size distribution.

Wet shaking

The mechanical breakdown by shaking after pre-wetting treatment corresponds to the breakdown by raindrop impact. Aggregates were pre-wetted with 95% ethanol to remove air from aggregates. Then, 4 g of aggregates were gently immersed in a 250-ml beaker filled with 50 ml 95% ethanol. After 10 min, the ethanol was removed with a pipette. The soil aggregates were then carefully transferred to a 250-ml Erlenmeyer flask filled with 200 ml deionised water. Then, the flask was shaken for 1 min at 20 rounds per minute using an overhead shaker (GFL

3040, Gesellschaft für Labortechnik mbH, Burgwedel, Germany). After letting the soil fragments settle for 30 min, the water was removed. The aggregates were carefully transferred to a 0.05-mm sieve immersed in ethanol to determine fragment size distribution.

Fragment size distribution

Two successive steps were completed to measure fragment size distribution after each treatment. First, aggregates transferred to a 0.05-mm sieve immersed in ethanol (95%) were moved five times in circles by hand to separate fragments >0.05 mm from fragments <0.05 mm. Ethanol (95%) was used to reduce further breakdown and was recycled by filtering. Second, fragments >0.05 mm were dried at 40°C for 48 h and then sieved. A horizontal sieving apparatus with six different sieves (2, 1, 0.5, 0.2, 0.1, and 0.05 mm) was used to separate fragments. Dry sieving was carried out for 60 s with an amplitude of 0.5 mm. The measured mass percentage of each size fraction was used to calculate the MWD (Equation 2) for each breakdown mechanism. A gravel correction is necessary to avoid misinterpretation of results if gravel content is between 10% and 40% (ISO 10930, 2011). Since samples with gravel were avoided initially, the content was always less than 10%. Still, if gravel was retained on the 2 mm sieve, it was weighted additionally, and the MWD was calculated without gravel.

According to Le Bissonnais (2016, 1996b), the stability of aggregates can be classified based on the following MWD values: >2 mm “very stable” aggregates, 1.3–2.0 mm “stable” aggregates, 0.8–1.3 mm “medium” stable aggregates, 0.4–0.8 mm “unstable” aggregates, and <0.4 mm as “very unstable” aggregates. “Very unstable” aggregates indicate a “high permanent risk,” “unstable” aggregates indicate “frequent” risk, and “medium” stable aggregates suggest “variable” risk depending on climatic parameters. The risk of water erosion is “limited” for “stable” aggregates and “very low” for “very stable” aggregates (ISO 10930, 2011).

2.5 | Statistical analyses

RStudio (Version 4.1.2, RStudio Team) was used for statistical analyses and graphs (R Core Team, 2020). All measured properties from each plot were tested for normal distribution (Shapiro-Wilk test) and variance homogeneity (Levene’s test), followed by variance analyses (one-way ANOVA). Tukey’s HSD (honestly significant difference) test was performed to identify mean group values that are significantly different (Table A1). For all soils, texture triangles (Figure 3) were illustrated with the “soiltexture” package (Moeyss, 2018) and the principal component analysis (PCA) (Figure 4) with “factoextra” (Kassambara &

Mundt, 2020). Pearson’s correlation was performed between aggregate stability indicators and all measured soil properties for all samples and individual sites (Table A2). Significances of correlations are indicated at a level of $p < 0.05$. Subsequently, a correlation matrix was generated with “corrplot” (Taiyun & Simko, 2021) for all soils (Figure 5). The aggregate stability indicators from grassland and cropland were tested for normal distribution (Shapiro-Wilk test) and variance homogeneity (Levene’s test). Afterward, Welch’s *t*-test (unequal variance *t*-test) was applied for each site due to unequal sample groups (Figure 6).

All soils and cropland soils from each site were tested for variance homogeneity (Levene’s test), followed by the rank-based Kruskal-Wallis test to compare sites and to assess erosion risk across the study area. The Dunn’s test was used as post hoc for the non-parametric pairwise multiple comparisons (Figure 7). Further, variance analyses (one-way ANOVA) and Tukey’s HSD test were conducted for comparing the three different wet-aggregate stability indicators on all sites (not shown).

3 | RESULTS

3.1 | Soil properties and aggregate stabilities in the study area

The pH of all soil samples was 7.3 ± 0.8 (mean \pm SD), the EC $261.9 \pm 158.3 \mu\text{S cm}^{-1}$, the C:N ratio 11.6 ± 1.2 , the TIC content $1.7 \pm 2.3 \text{ g kg}^{-1}$, and the SOC content $23.9 \pm 10.9 \text{ g kg}^{-1}$. In the study area, more than half of the samples had a silt loam texture ($n = 87$); the remaining soils were classified as either loam ($n = 26$), sandy loam ($n = 14$), silty clay loam ($n = 8$), or loamy sand ($n = 1$). Overall, the samples of the seven sites covered a wide range of sand (2–76%), silt (18–80%), and clay contents (6–30%). A textural gradient occurred from Sites 1–3 with low sand content to Sites 6–7 with high ones (Figure 3a). The SOC contents decreased with declining clay and silt contents (Figure 3b). The average MWD of aggregates determined by drop-shatter was $6.6 \pm 3.0 \text{ mm}$ and EF_p accounted for $34.2 \pm 15.3\%$. Indicators of wet-aggregate stability showed an MWD after fast wetting of $0.6 \pm 0.5 \text{ mm}$, after slow wetting of $1.0 \pm 0.6 \text{ mm}$, and after wet shaking of $1.0 \pm 0.5 \text{ mm}$ (Table A1). Aggregate stability was highest in soils from Site 1 and lowest in soils from Site 7, independent of the mechanical stress applied.

3.2 | Relationship between soil properties and aggregate stability

The two main principal components of the PCA describe 69.5% of the data variability. The PCA shows a strong

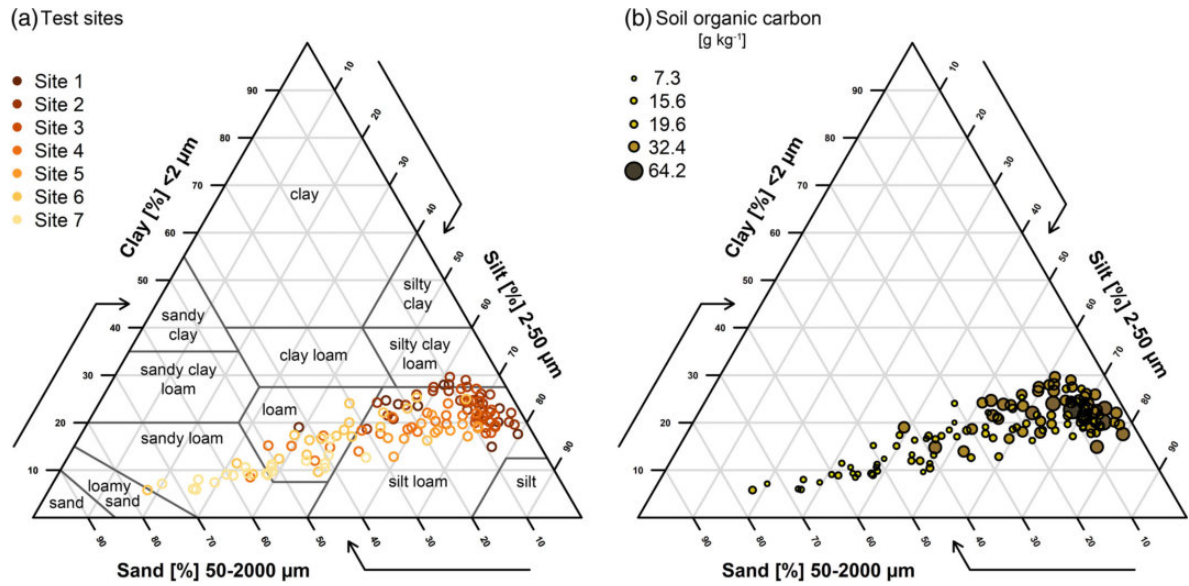


FIGURE 3 Soil texture triangles define textural classes (a) (Soil Science Division Staff, 2017) of all sites and soil organic carbon contents in combination with clay, silt, and sand contents (b). It shows the decrease of SOC content with increasing sand content. The legend is classified according to minima, first quartile, median, third quartile, and maxima of soil organic carbon contents

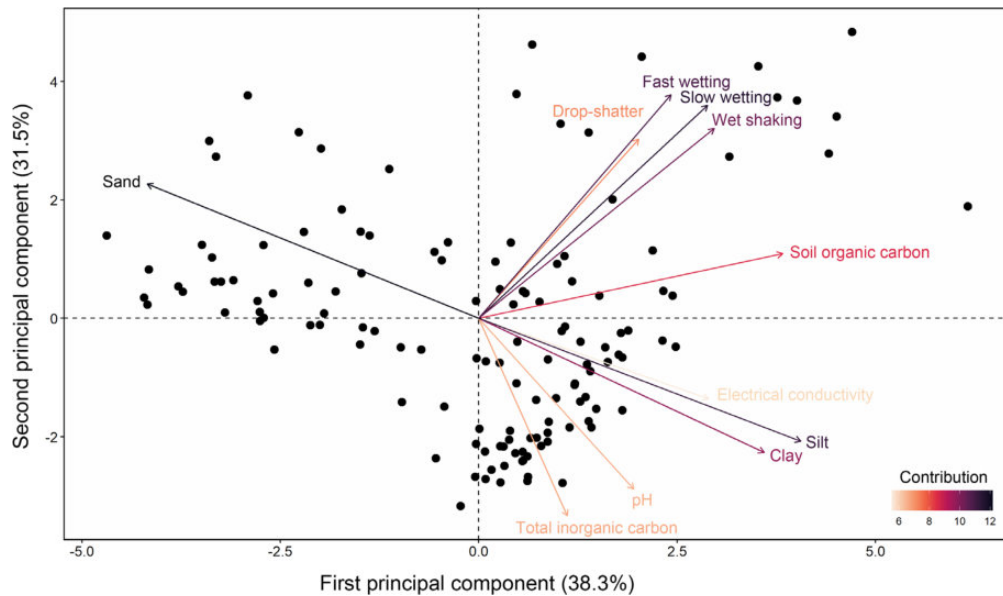


FIGURE 4 Biplot of the principal component analysis (PCA) indicates a strong relationship between different aggregate stability indicators due to eigenvectors close to each other. The closest relationship between all stability indicators and soil organic carbon can also be observed. Texture, soil organic carbon, and aggregate stability indicators strongly contribute to the principal components indicated by arrow length

positive correlation between the different aggregate stability indicators. The eigenvectors of drop-shatter, fast wetting, slow wetting, and wet shaking form a small

angle (Figure 4), indicating a similar relationship between the various aggregate stability indicators and soil properties. However, the correlation among the three

wet-aggregate stability indicators ($r = 0.87\text{--}0.92$) was higher than those with the stability indicator determined by drop-shatter ($r = 0.50\text{--}0.59$) (Figure 5). The PCA eigenvector of SOC suggests a positive relationship to the aggregate stability indicators, showing a strong relationship (Figure 4), which is in line with correlation analysis (Figure 5). A moderate correlation was observed between aggregate stability determined by drop-shatter and SOC ($r = 0.51$). The correlation coefficients were similar for SOC and aggregate stability determined by fast wetting ($r = 0.42$), slow wetting ($r = 0.49$), and wet shaking ($r = 0.43$). In addition, a negative and very weak correlation was observed between TIC and all aggregate stability indicators (Figure 5). Both PCA and bivariate correlation analysis showed that other soil properties had only a minor impact on soil aggregate stability.

Noteworthy, the relationships between soil properties and aggregate stability indicators varied strongly between sites (Table A2). While the correlation between SOC and aggregate stability is strong at Site 1, 3, and 5, and moderate at Site 2, correlations were nonsignificant at Sites 4, 6, and 7. The SOC contents on Site 6 ($13.3 \pm 3.2 \text{ g kg}^{-1}$) and 7 ($14.1 \pm 2.9 \text{ g kg}^{-1}$) were the lowest in the study area (Table A3), but this does not apply to Site 4 ($25.3 \pm 10.3 \text{ g kg}^{-1}$), where SOC contents were similar to those at Site 3 ($21.2 \pm 4.1 \text{ g kg}^{-1}$) and 5 ($19.8 \pm 5.4 \text{ g kg}^{-1}$). Additionally, the silt content at Site 1 ($64.3 \pm 11.5\%$) affected all four aggregate stability indicators ($r = 0.67\text{--}0.78$). However, at Site 2, the silt content was similar ($65.4 \pm 7.6\%$) to that at Site 1 but only a weak, nonsignificant correlation with aggregate stability could be observed. Further, TIC had a moderate negative impact on aggregate stability at Site 3 and a strong negative at Site 5, with both sites being well above the average TIC content of all sites (Site 3: $4.7 \pm 0.9 \text{ g kg}^{-1}$, Site 5: $5.0 \pm 3.6 \text{ g kg}^{-1}$; all sites: $1.7 \pm 2.3 \text{ g kg}^{-1}$; Table A3). The correlation between TIC and the wet-aggregate stability was higher than for the dry-aggregate stability determined by drop-shatter (Table A2).

3.3 | Comparison of aggregate stability and soil properties on grassland and cropland

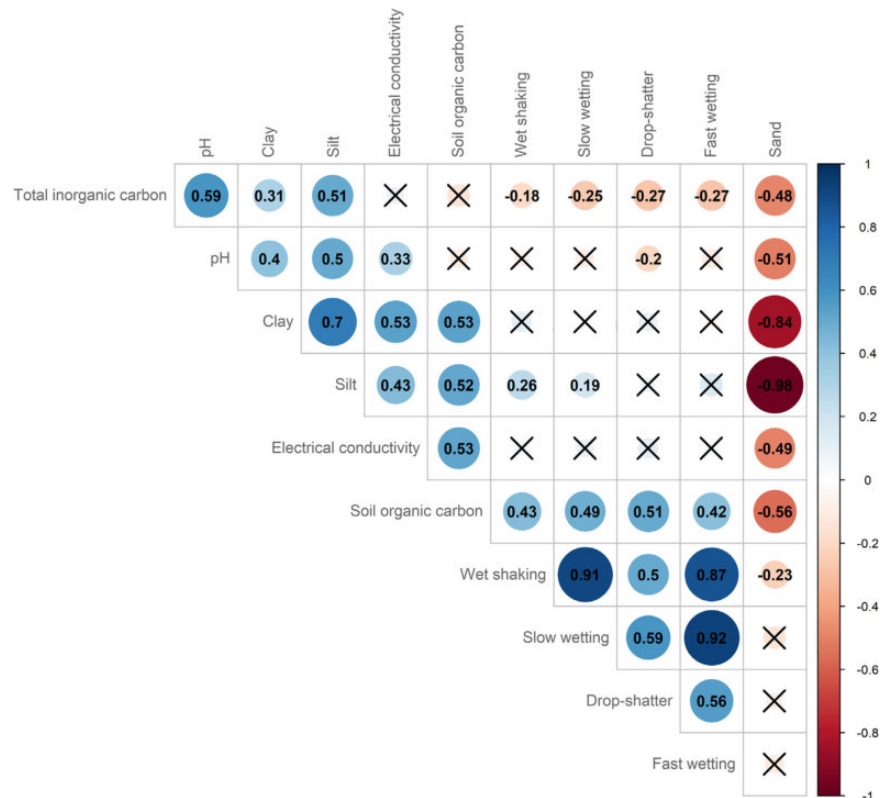
Mean values of aggregate stability indicators were higher for grassland than cropland at all sites (Table A3), showing a decline in aggregate stability from grassland to cropland. The decline was 14–62% for the drop-shatter, 65–77% for the fast wetting treatment, 39–69% for the slow wetting, and 38–70% for the wet shaking, respectively (Figure 6). Overall, mean values of SOC were

higher for grassland than for cropland (Table 2). Comparing grass- with cropland, SOC decreased between 1–30% (Figure 6) due to tillage. A significant decrease could only be observed at Sites 1 and 3 (Figure 6; Table A1). The TIC and clay content were generally higher on cropland than on grassland (Table A3).

3.4 | Comparison of erosion risk on cropland under different mechanical stresses

Mechanical stress applied to cropland soils with drop-shatter revealed a mean MWD of $5.8 \pm 2.4 \text{ mm}$ and an average EF_p of $33.9 \pm 15.7\%$, suggesting that all croplands are prone to wind erosion. Mean values obtained by drop-shatter for Sites 3–7 with lower SOC contents showed significantly higher EF_p than Sites 1–2, indicating a higher susceptibility to wind erosion (Figure 7). About 71% of the soils showed EF_p of <40% (negligible risk of wind erosion), while the remaining 29% of soils had values above and are, therefore, at risk of wind erosion. However, only about 6% of the study soils, all located at Sites 3–6, showed very high EF_p values of >60%, indicating a “high” risk of wind erosion (Anderson & Wenhardt, 1966). Results obtained for all sites indicate that fast wetting was significantly more disruptive than the other wet-aggregate stability treatments (Figure 8a–c). Comparing the different wet-aggregate stability treatments revealed that the decline MWD values increased with increasing overall stability (Figure 8a,b). In general, the fast wetting treatment caused lower average MWD values ($0.4 \pm 0.2 \text{ mm}$) than slow wetting ($0.8 \pm 0.3 \text{ mm}$) and wet shaking ($0.8 \pm 0.3 \text{ mm}$) (Table A3). This means 98% of the soils of the study area were at a “frequent” (44%) or “permanently high” (54%) risk of water erosion upon heavy rain or snowmelt events. Especially, Sites 3, 5, and 7 showed significantly lower MWD values than other sites, indicating a “permanently high” risk of water erosion. As simulated by the slow wetting treatment, even a light rain event revealed “frequent” erosion risk for 59% of the samples. Especially, Sites 3–7, where SOC is below 30 g kg^{-1} , seem prone to water erosion at relatively moderate disruption by wetting. The wet shaking treatment showed similar results (“frequent” risk on 53% of the samples) as the slow wetting treatment (Figure 7; Figure 8a,b). Gentle rain and raindrop impact caused the highest risk of water erosion on Site 7, similar to the fast wetting treatment. Hence, the overall soil erodibility by water, independent of wetting energy applied, is the highest on Site 7, where the lowest SOC and clay content were measured in the study area.

FIGURE 5 Correlation matrix reveals significant linear correlations ($p < 0.05$) between soil organic carbon, texture, and the four aggregate stability indicators determined by the drop-shatter, fast wetting, slow wetting, and wet shaking test. The positive correlation between aggregate stability indicators and soil organic carbon indicates that organic is the most important binding agent, enhancing aggregation



4 | DISCUSSION

4.1 | Soil properties promoting aggregation in steppe soils

A significant positive relationship was observed between SOC and aggregate stability in the study area, indicating organic matter as an important binding agent. This result aligns with a previous study (Koza et al., 2021), and underlines the importance of organic matter, which contributes decisively to aggregate stability in the semi-arid steppe, similar to other climatic zones (e.g., Eynard et al., 2005; Malobane et al., 2021; Rahmati et al., 2020; Xue et al., 2019). Overall, aggregate stability increased with increasing SOC content, independent of the disruptive force applied. However, no strong relationship between aggregate stability and SOC could be detected on Site 4, even though SOC did not differ from Sites 3 and 5. This reflects the possibility of additional factors that influence aggregate stability, such as biotic factors (e.g., plant species, roots, microbial activity, termites) or soil management (e.g. fertiliser, crop history) (Amézketa, 1999; Bronick & Lal, 2005). The lack of relationships between measured soil properties and aggregate stabilities on Sites 6 and 7 suggests that these soils did not contain enough

binding agents (e.g., SOC and clay) to effectively support aggregate formation (Bronick & Lal, 2005). While it is generally accepted that inorganic carbon favours soil aggregation (Bronick & Lal, 2005; Six et al., 2004), the effect may depend on clay content and the particle size of calcium carbonates (Dimoyiannis et al., 1998; Le Bissonnais, 1996a). Our results revealed a negative correlation between TIC and aggregate stability. Surprisingly, inorganic carbon seemed less relevant as a binding agent in northern Kazakhstan, even in soils with high TIC content. However, this agrees with a previous study from that region, where dissolving carbonates for texture analysis did not cause dispersion of aggregates (Koza et al., 2021). Dimoyiannis et al. (1998) observed that silt-sized carbonates negatively influenced wet-aggregate stability in Greek agricultural soils. One reason might be that soils low in clay content and with silt-sized calcium carbonates feature the typical instability of silty soils (Le Bissonnais, 1996a).

4.2 | Effect of tillage on aggregate stability and soil properties

Our results are consistent with previous studies, showing that aggregate stability was lower for cropland than

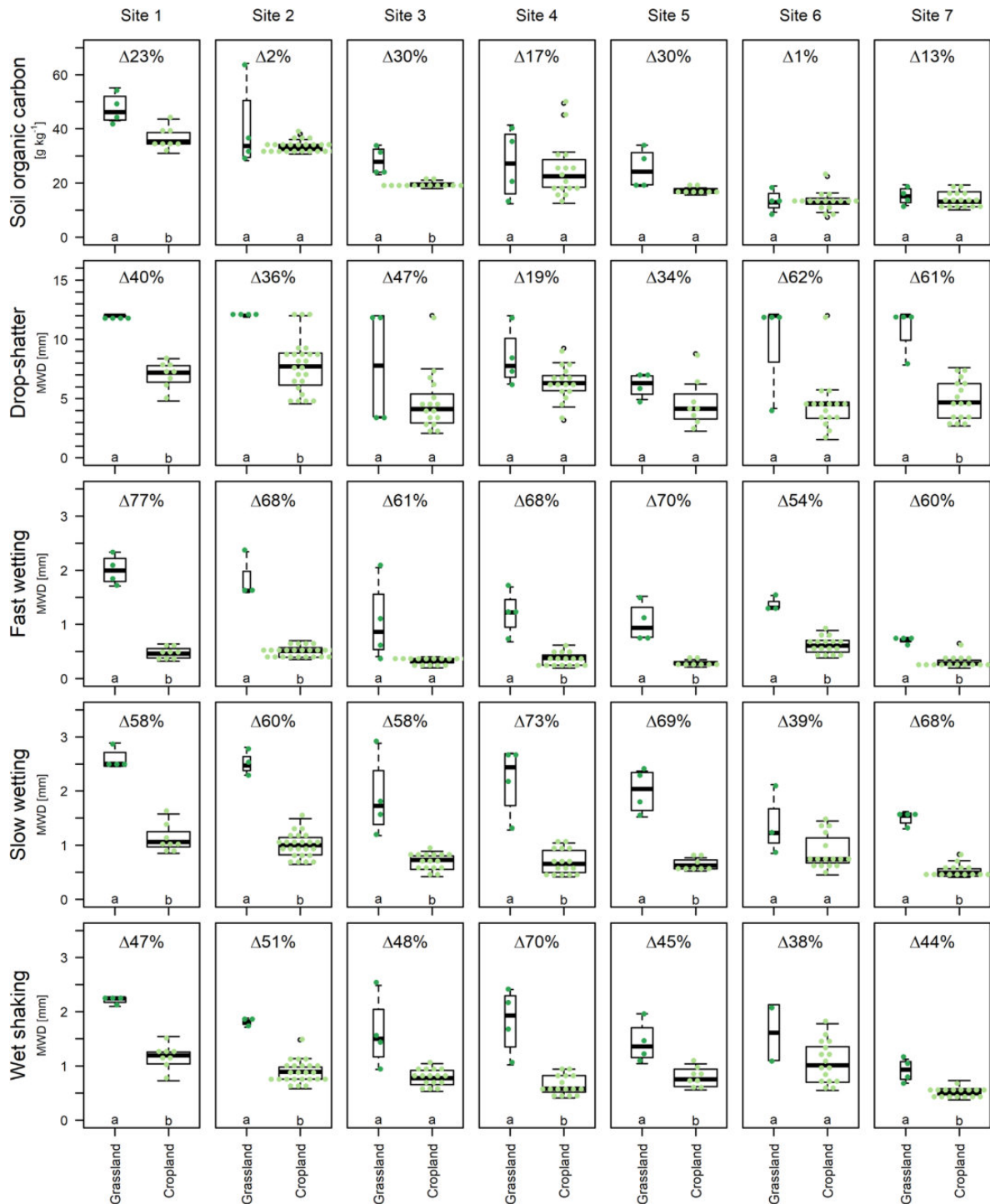


FIGURE 6 Boxplots for all sites show the soil organic carbon content for grassland (dark green dots) and cropland soils (light green dots) and the lower mean weight diameters (MWD) for all aggregate stability indicators. Every dot represents the measurement of one individual soil sample. The number of samples defines the width of each boxplot, and numbers above the boxplot indicate the relative decline from grassland to cropland. Different lower case letters indicate significant differences ($p < 0.05$) between the two dominant land use types

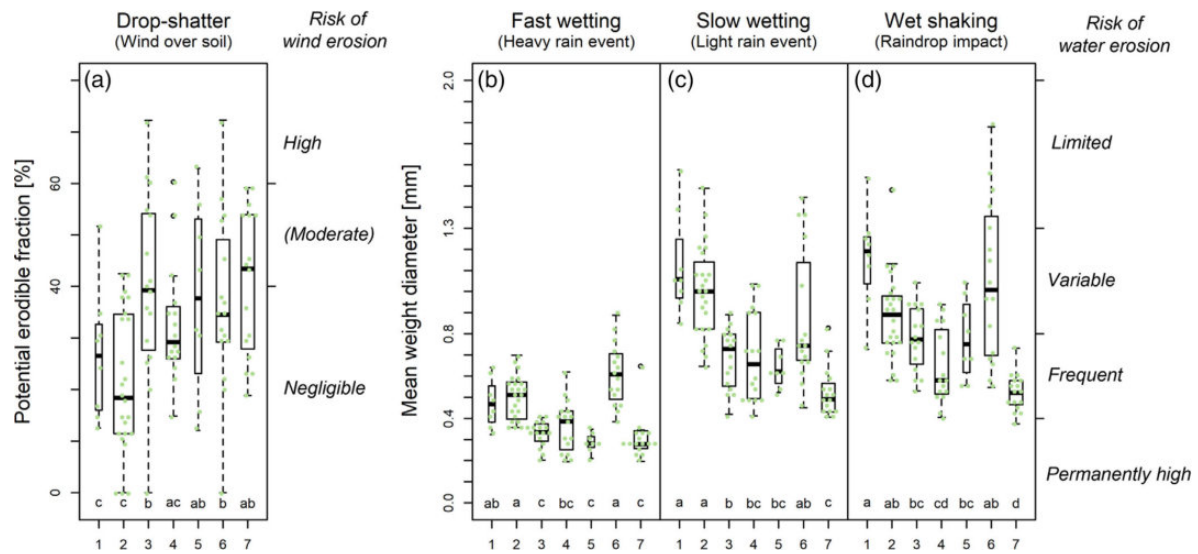


FIGURE 7 Erosion risk as determined from four aggregate stability tests similar to disruptive forces soils experiences under field conditions. Boxplots show that cropland is more vulnerable to the disruptive forces of water than wind. Especially, the severe breakdown of aggregates during heavy rain or snowmelt events causes a high risk of water erosion. The number of samples defines the width of each boxplot. Different lower case letters show significant differences ($p < 0.05$) between sites for each stability indicator

grassland (e.g. Six et al., 1998). The breakdown of soil structure by tillage is due to mechanical stress repeatedly applied to soil (Amézqueta, 1999). Six et al. (1998) showed that frequently disrupted soils contain less intra-aggregate particular organic matter and less stable micro-aggregates within macroaggregates. Additionally, cropland soils rewet much faster than grassland soils because of their lower organic matter content (Caron et al., 1996; Six et al., 2004). Higher organic matter contents typically increase the water drop penetration time (Chenu et al., 2000), thus reducing overall soil wettability (Woche et al., 2017). Therefore, the disruptive force by wetting during wet-dry cycles outweighs the stabilising effect of drying, particularly for cropland soils, causing an overall decrease in aggregation (Six et al., 2004). In addition, the studied grassland soils had extensive visible roots, similar to observations in the prairies of North America (Beniston et al., 2014). Roots physically stabilise the soil structure and thus, account for the higher aggregate stability of grassland soils as determined by the drop-shatter method (Tisdall & Oades, 1982).

Similar patterns in aggregate stability of cropland vs grassland soils have been observed in the Kulunda steppe of southern Russia (Bischoff et al., 2016; Illiger et al., 2019; Schmidt et al., 2020). Bischoff et al. (2016) also noted a decrease in SOC contents and aggregate stability, determined by wet-sieving, from grassland to cropland across different steppe types (forest, typical, dry). Mikhailova et al. (2000) compared Chernozems from the

Kursk region of Russia under native grassland with a continuously cropped plot and observed a relative decline in SOC content of 38% (grassland = $55.3 \pm 2.7 \text{ g kg}^{-1}$; cropland = $34.5 \pm 1.5 \text{ g kg}^{-1}$). This result is similar to the substantial SOC loss due to tillage at Sites 1 and 3 but disagrees with findings at Site 2 with similar SOC content. In summary, aggregation decreases with decreasing SOC content, but tillage further worsens the structural stability of soils. Our study suggests to use agricultural practices that support soil organic matter accumulation and minimising the disruptive impact of tillage (e.g., by direct seeding, mulching, or catch crops) because they provide the highest potential for reducing the vulnerability of steppe soils against erosion.

Apart from soil degradation due to declining aggregate stability and mostly decreasing SOC contents, cropping also affected TIC and clay contents of the studied soils. The higher TIC contents in cropland than in grassland soils can be explained by tillage-induced erosion of topsoil layers. Typically, topsoils are more depleted in TC than the less weathered deeper horizons. Removal of surface soil exposes deeper material and thus, results in apparent increases in topsoil TIC contents (Suarez, 2017). The higher clay content in the cropland soils suggests depletion of particles $>2 \mu\text{m}$, likely by wind erosion. Even though tillage does not directly influence soil texture, previous studies have shown that wind redistributes particles in semi-arid grasslands (Larney, 2007; Li et al., 2009), especially in the absence of vegetation

(Gyssels et al., 2005). Since clay has a higher threshold against aerodynamic forces due to more efficient cohesion of particles (Shao, 2008), wind erosion causes preferential removal of coarser particles and subsequent clay enrichment in topsoils of croplands.

4.3 | Assessment of potential erodibility on cropland by mechanical stress

Measuring aggregate stability with different methods revealed that all cropland soils in the study area are principally prone to erosion by wind and water. This supports the view of erosion as the major factor in soil degradation of croplands in Central Asia (Hamidov et al., 2016; Mirzabaev et al., 2016). The aggregate size distribution of dry soil is a major factor influencing wind erosion (Skidmore et al., 1994). Applying mechanical stress with the drop-shatter method on dry soil to assess the erodibility by wind showed that almost all soils are potentially erodible. Results of EF_p from Kazakhstan are well in line with measurements from semi-arid Argentinean Pampas ($EF = 39.5\%$) using a rotary sieve on similar soils (Colazo & Buschiazzo, 2010). The risk of wind erosion in northern Kazakhstan is moderate, as 29% of the soils are prone, and 71% are expected to resist wind erosion. Still, soils low in SOC exhibit a higher EF_p , suggesting an increased risk of wind erosion in the study area, particularly once SOC is further lost by less sustainable agricultural practices. Yet, wind erosion depends on additional environmental factors such as micro-topographic (microrelief, vegetation cover, etc.), macro-topographic conditions (windbreaks, etc.), and especially climate (wind abundance and speed, temperature, rainfall, etc.) (Shao, 2008). In Central Asia, the wind erosion rate is mostly related to wind speed ($r^2 = 0.31-0.72$), followed by temperature ($r^2 = 0.06-0.66$), and precipitation ($r^2 = 0.16-0.56$). Due to the strong correlations between erosion rate and climate factors, northern Kazakhstan will likely be highly sensitive to climate change (Li et al., 2020).

In our study area, wind occurred predominantly (98.5%) at wind speeds of $3.4 \pm 2.1 \text{ m s}^{-1}$ in the year after soil sampling (observed period: 07/01/2019–06/30/2020), with wind gusts reaching up to 21.5 m s^{-1} at 2 m height. However, assuming that the aerodynamic drag and lift overcome the retarding forces of the surface particles at speeds of $4-6 \text{ m s}^{-1}$ in 30 cm above the soil surface (Scheffer et al., 2016), potential wind erosion events are rather rare. Considering the logarithmic wind profile (Shao, 2008) and estimated surface roughness of 0.005 m for fallow with negligible vegetation (Wieringa, 1992), wind speeds must exceed 5.9 m s^{-1} at 2 m height. Based

on measured 15 min time intervals, wind speeds high enough to potentially start erosion on bare fallow occurred at 13% during the observed period. This indicates limited wind speed events for potential wind erosion on bare fallow in the study area. In Central Asia, the wind speed increased significantly ($+0.6 \text{ m s}^{-1} \text{ decade}^{-1}$, $p < 0.001$) from 2011 to 2019, and moderate and heterogeneous changes are expected in future (Li et al., 2020; Wang et al., 2020). However, projections for northern Kazakhstan include particularly strong warmings and increasing precipitation that will also affect wind erosion severely, leading to complex spatiotemporal patterns (Li et al., 2020).

The disruptive force of water is another major factor causing the breakdown of aggregates, thus triggering soil erosion on cropland (Li & Fang, 2016). Applying three different wetting treatments simulating different field-relevant events of water-induced disruptions showed that all studied soils are at risk of water erosion. Depending on the applied wetting treatment, the erosion risk varies among soils, indicating that aggregate stability is ultimately controlled by the properties of the soil and the amount of energy applied (Le Bissonnais, 2016, 1996b). The fast wetting treatment indicated a severe breakdown of aggregates for all cropland soils. This aligns with Le Bissonnais (2016, 1996b), who showed that fast wetting during heavy rain or snowmelt is highly disruptive because of the slaking effect, that is, the compression of air trapped inside aggregates upon wetting (Le Bissonnais, 2016, 1996b; Yoder, 1936). In contrast, the disruption by slow wetting, as during sustained light rainfall, is assumed to result from disproportional swelling of materials, while wet shaking treatment decreases the mechanical cohesion upon raindrop impact (Le Bissonnais, 2016, 1996b).

According to the World Meteorological Organisation (WMO, 2018), precipitation $<2.5 \text{ mm h}^{-1}$ is defined as light rain, $2.5-10 \text{ mm h}^{-1}$ as moderate rain, and $10-50 \text{ mm h}^{-1}$ as heavy rain. In the study area, precipitation was measured on 154 days (observed period: 07/01/2019–06/30/2020), accounting for a total of 245.4 mm. Overall, rain occurred predominantly as light rain (96.6%), and it seems that differential swelling could be an important mechanism for the breakdown of aggregates in the study area. Thus, during light rain events or as a consequence of raindrop impact, there is a “frequent” risk in all situations or a “variable” risk of water erosion depending on topographic and climatic conditions (ISO 10930, 2011). Especially soils on Site 3–7 with SOC contents $<30 \text{ g kg}^{-1}$ are prone to water erosion during rainfall. Besides repetitive snowmelt in spring, heavy rain events were recorded in September 2019 (10.0 mm h^{-1}) and February 2020 (10.5 mm h^{-1}), assuming an intense aggregate

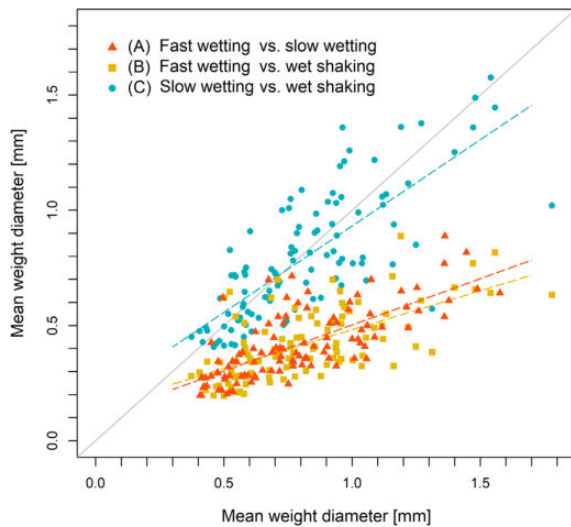


FIGURE 8 Scatterplot compares the three different wet-aggregate stability treatments with each other. The fast wetting treatment is the most disruptive test. In contrast, the MWDs obtained by slow wetting and wet shaking treatment are comparable. The positions of the dots to the 1:1 line indicate that the decline of aggregate stability between fast wetting and the other treatments increases with increasing MWD

breakdown and subsequent erosion by water runoff independent of the soil properties. However, the disruptive force of slaking during the heavy rain event under field conditions in September could be influenced by plant residues after harvesting (Six et al., 2004). In February, the soil temperature was still below the water freezing point and disruptive forces by water possibly interfered with structural changes induced by frost (Six et al., 2004).

Future model projections indicate a change in precipitation duration, magnitude, and intensity, causing an increase in rainfall erosivity in northern Kazakhstan (Duulatov et al., 2021). Based on an intermediate combined approach valuing duration and magnitude equally, Pruski and Nearing (2002) reported that every 1% of precipitation change could cause a 1.7% change in erosion. While currently all cropland soils in northern Kazakhstan are prone to disruptive forces by water, erosion might increase under higher precipitation rates in future, leaving the strongest negative impact on SOC-poor soils.

5 | CONCLUSIONS

Soil organic matter is the most important binding agent that supports aggregate stability in topsoils under grass- and cropland in semi-arid steppe regions. Tillage was not consistently accompanied by decreasing SOC content but

always declined aggregate stability. We showed that soil properties, such as organic matter content and texture, determine the aggregate stability in a given soil. At the same time, tillage serves as an additional modifier enhancing the overall risk of wind and water erosion on all croplands. Nevertheless, erosion risk is generally higher for soils with low SOC content. Our results suggest that the aggregate stability of cropland soils in northern Kazakhstan is more vulnerable to the disruptive forces caused by water than by wind. The soil erodibility by wind is moderate, and wind speed conditions imply limited risk. In contrast, the breakdown of aggregates during wetting reveals a serious threat of water erosion. Even though the region is semi-arid, recurring heavy rain and snowmelt events imply a severe risk. Furthermore, disrupting aggregates by water may also promote subsequent soil loss by wind erosion. In particular, slaking during snowmelt potentially paves the way for extensive wind erosion in spring. The semi-arid steppe soils of Central Asia might face an even higher risk of combined water and wind erosion in future since predicted rainfall conditions might cause an increase in topsoil slaking. Therefore, sustainable land use strategies need to consider the potential risk of water erosion to mitigate further soil degradation.

ACKNOWLEDGEMENTS

We are particularly grateful to Dorothee Kley and Olga Shibistova for logistical assistance. Thanks to all agricultural holdings for their permission and support to take soil samples. We thank Michael von Hoff, Merle Schrader, and Christine Krenkewitz for assisting laboratory work. We especially acknowledge Norbert Bischoff for his expertise from the Kulunda steppe, as well as Markus Koch and Muhammad Usman for their advice regarding Rstudio. Finally, we thank the editor and two anonymous reviewers for their constructive comments on this manuscript.

This study was supported by the German Federal Ministry of Education and Research (BMBF) by funding the research project: Innovative Solutions for Sustainable Agricultural and Climate Adaptation in the Dry Steppes of Kazakhstan and Southwestern Siberia (ReKKS). Grant/Award Number: 01LZ1704. Open Access funding enabled and organized by Projekt DEAL.








CONFLICT OF INTEREST

The authors declare no conflicts of interest.

DATA AVAILABILITY STATEMENT

The data that support the findings of this study are available from the corresponding author upon reasonable request.

ORCID

Moritz Koza  <https://orcid.org/0000-0002-7487-6668>
 Klaus Kaiser  <https://orcid.org/0000-0001-7376-443X>
 Robert Mikutta  <https://orcid.org/0000-0002-7186-6528>
 Christopher Conrad  <https://orcid.org/0000-0002-0807-7059>
 Cordula Vogel  <https://orcid.org/0000-0002-6525-2634>
 Kanat Akshalov  <https://orcid.org/0000-0003-2586-9944>
 Gerd Schmidt  <https://orcid.org/0000-0003-1557-5627>

REFERENCES

- Almaganbetov, N., & Grigoruk, V. (2008). Degradation of soil in Kazakhstan: Problems and challenges. In L. Simeonov & V. Sargsyan (Eds.), *Soil chemical pollution, risk assessment, remediation and security* (pp. 309–320). Springer. https://doi.org/10.1007/978-1-4020-8257-3_27
- Almajmaie, A., Hardie, M., Acuna, T., & Birch, C. (2017). Evaluation of methods for determining soil aggregate stability. *Soil and Tillage Research*, *167*, 39–45. <https://doi.org/10.1016/j.still.2016.11.003>
- Amézqueta, E. (1999). Soil aggregate stability: A review. *Journal of Sustainable Agriculture*, *14*, 83–151. https://doi.org/10.1300/J064v14n02_08
- Anderson, C. H., & Wenhardt, A. (1966). Soil erodibility, fall and spring. *Canadian Journal of Soil Science*, *46*, 255–259. <https://doi.org/10.4141/cjss66-040>
- Robinson, S. (2016). Land degradation in Central Asia: Evidence, perception and policy. In: R. Behnke & M. Mortimore (Eds.), *The end of desertification?* (pp. 451–490). Springer. https://doi.org/10.1007/978-3-642-16014-1_17
- Mirzabaev, A., Goedecke, J., Dubovyk, O., Djanibekov, U., Le, Q.B., Aw-Hassan, A. (2016). Economics of land degradation in Central Asia. In: E. Nkonya, A. Mirzabaev, & J. von Braun (Eds.), *Economics of land degradation and improvement—A global assessment for sustainable development* (eds. Nkonya, E., Mirzabaev, A. & von Braun, J.), pp. 261–290. Springer International Publishing. https://doi.org/10.1007/978-3-319-19168-3_10
- Bartoli, F., Hallett, P. D., & Cerdan, O. (2016). Le Bissonnais, Y. 1996. Aggregate stability and assessment of crustability and erodibility: 1. Theory and methodology. *European Journal of Soil Science*, *47*, 425–437. *European Journal of Soil Science*, *6*. https://doi.org/10.1111/ejss.3_12311
- Beniston, J. W., DuPont, S. T., Glover, J. D., Lal, R., & Dungait, J. A. J. (2014). Soil organic carbon dynamics 75 years after land-use change in perennial grassland and annual wheat agricultural systems. *Biogeochemistry*, *120*, 37–49. <https://doi.org/10.1007/s10533-014-9980-3>
- Bischoff, N., Mikutta, R., Shibistova, O., Puzanov, A., Reichert, E., Silanteva, M., Grebennikova, A., Schaarschmidt, F., Heinicke, S., & Guggenberger, G. (2016). Land-use change under different climatic conditions: Consequences for organic matter and microbial communities in Siberian steppe soils. *Agriculture, Ecosystems & Environment*, *235*, 253–264. <https://doi.org/10.1016/j.agee.2016.10.022>
- Bronick, C. J., & Lal, R. (2005). Soil structure and management: A review. *Geoderma*, *124*, 3–22. <https://doi.org/10.1016/j.geoderma.2004.03.005>
- Caron, J., Espindola, C. R., & Angers, D. A. (1996). Soil structural stability during rapid wetting: Influence of land use on some aggregate properties. *Soil Science Society of America Journal*, *60*, 901–908. <https://doi.org/10.2136/sssaj1996.0361599500600030032x>
- Cerdà, A., Flanagan, D. C., le Bissonnais, Y., & Boardman, J. (2009). Soil erosion and agriculture. *Soil and Tillage Research*, *106*, 107–108. <https://doi.org/10.1016/j.still.2009.10.006>
- Chenu, C., Bissonnais, Y. L., & Arrouays, D. (2000). Organic matter influence on clay wettability and soil aggregate stability. *Soil Science Society of America Journal*, *64*, 1479–1486. <https://doi.org/10.2136/sssaj2000.6441479x>
- Chepil, W. S. (1953). Field structure of cultivated soils with special reference to erodibility by wind. *Soil Science Society of America Proceedings*, *17*, 185–190.
- Chepil, W. S. (1962). A compact rotary sieve and importance of dry sieving in physical soil analysis. *Soil Science Society of America Journal*, *26*, 4–6. <https://doi.org/10.2136/sssaj1962.03615995002600010002x>
- Colazo, J. C., & Buschiazzi, D. E. (2010). Soil dry aggregate stability and wind erodible fraction in a semiarid environment of Argentina. *Geoderma*, *159*, 228–236. <https://doi.org/10.1016/j.geoderma.2010.07.016>
- Cole, R. C. (1939). Soil macrostructure as affected by cultural treatment. *Hilgardia*, *12*, 427–472. <https://doi.org/10.3733/hilg.v12n06p427>
- Diaz-Zorita, M., Perfect, E., & Grove, J. H. (2002). Disruptive methods for assessing soil structure. *Soil and Tillage Research*, *64*, 3–22. [https://doi.org/10.1016/S0167-1987\(01\)00254-9](https://doi.org/10.1016/S0167-1987(01)00254-9)
- Dimoyiannis, D. G., Tsadilas, C. D., & Valmis, S. (1998). Factors affecting aggregate instability of Greek agricultural soils. *Communications in Soil Science and Plant Analysis*, *29*, 1239–1251. <https://doi.org/10.1080/00103629809370023>
- Duulatov, E., Chen, X., Issanova, G., Orozbaev, R., Mukanov, Y., & Amanambu, A. C. (2021). *Current and Future Trends of Rainfall Erosivity and Soil Erosion in Central Asia*. Springer International Publishing. <https://doi.org/10.1007/978-3-030-63509-1>
- Eynard, A., Schumacher, T., Lindstrom, M., & Malo, D. (2005). Effects of agricultural management systems on soil organic carbon in aggregates of Ustolls and Usterts. *Soil and Tillage Research*, *81*, 253–263. <https://doi.org/10.1016/j.still.2004.09.012>
- FAO. (2012). *Aquastat: Kazakhstan*. Food and Agriculture Organization of the United Nations (FAO).
- FAO. (2014). *World reference base for soil resources 2014: International soil classification system for naming soils and creating legends for soil maps*. Food and Agriculture Organization of the United Nations (FAO).
- Fernández-Ugalde, O., Virto, I., Barré, P., Gartzia-Bengoetxea, N., Enrique, A., Imaz, M. J., & Bescansa, P. (2011). Effect of carbonates on the hierarchical model of aggregation in calcareous semi-arid Mediterranean soils. *Geoderma*, *164*, 203–214. <https://doi.org/10.1016/j.geoderma.2011.06.008>
- Frühau, M., Meinel, T., & Schmidt, G. (2020). The virgin lands campaign (1954–1963) until the breakdown of the former Soviet Union (FSU): With special focus on western Siberia. In M. Frühau, G. Guggenberger, T. Meinel, I. Theesfeld, & S. Lentz (Eds.), *KULUNDA: Climate smart agriculture* (pp. 101–118). Springer International Publishing. https://doi.org/10.1007/978-3-030-15927-6_8

- Green, D. W., & Perry, R. H. (2007). *Perry's chemical engineers' handbook* (8th ed.). McGraw-Hill Professional Publishing.
- Gyssels, G., Poesen, J., Bochet, E., & Li, Y. (2005). Impact of plant roots on the resistance of soils to erosion by water: A review. *Progress in Physical Geography: Earth and Environment*, 29, 189–217. <https://doi.org/10.1191/0309133305pp443ra>
- Hadas, A., & Wolf, D. (1984). Refinement and re-evaluation of the drop-shatter soil fragmentation method. *Soil and Tillage Research*, 4, 237–249. [https://doi.org/10.1016/0167-1987\(84\)90023-0](https://doi.org/10.1016/0167-1987(84)90023-0)
- Hamidov, A., Helming, K., & Balla, D. (2016). Impact of agricultural land use in Central Asia: A review. *Agronomy for Sustainable Development*, 36, 6. <https://doi.org/10.1007/s13593-015-0337-7>
- Harris, I. C., Jones, P. D., & Osborn, T. (2020). CRU TS4.04: Climatic research unit (CRU) time-Series (TS) version 4.04 of high-resolution gridded data of month-by-month variation in climate (Jan. 1901–Dec. 2019). *Scientific Data*, 7, 109.
- Illiger, P., Schmidt, G., Walde, I., Hese, S., Kudrjavzev, A. E., Kurepina, N., Mizgirev, A., Stephan, E., Bondarovich, A., & Frühauf, M. (2019). Estimation of regional soil organic carbon stocks merging classified land-use information with detailed soil data. *Science of the Total Environment*, 695, 133755. <https://doi.org/10.1016/j.scitotenv.2019.133755>
- ISO 10930. (2011). *Soil quality—Measurement of the stability of soil aggregates subjected to the action of water*. International Organization for Standardization (ISO).
- ISO 13320. (2009). *Particle size analysis—Laser diffraction methods*. International Organization for Standardization (ISO).
- Jarvis, S., Tisdall, J., Oades, M., Six, J., Gregorich, E., & Kögel-Knabner, I. (2012). Landmark papers. *European Journal of Soil Science*, 63, 1–21. <https://doi.org/10.1111/j.1365-2389.2011.01408.x>
- Kassambara, A., Mundt, F. (2020). R package “factoextra”: Extract and visualise the results of multivariate data analyses (version 1.0.7).
- Kemper, W. D., & Rosenau, R. C. (2018). Aggregate stability and size distribution. In A. Klute (Ed.), *SSSA Book Series* (pp. 425–442). Soil Science Society of America, American Society of Agronomy. <https://doi.org/10.2136/sssabookser5.1.2ed.c17>
- Koza, M., Schmidt, G., Bondarovich, A., Akshalov, K., Conrad, C., & Pöhlitz, J. (2021). Consequences of chemical pretreatments in particle size analysis for modelling wind erosion. *Geoderma*, 396, 115073. <https://doi.org/10.1016/j.geoderma.2021.115073>
- Larney, F. (2007). Dry-aggregate size distribution. In M. Carter & E. Gregorich (Eds.), *Soil sampling and methods of analysis* (2nd ed., pp. 821–831). CRC Press. <https://doi.org/10.1201/9781420005271.ch63>
- Le Bissonnais, Y. (1996a). Soil characteristics and aggregate stability. In M. Agassi (Ed.), *Soil erosion, conservation, and rehabilitation* (pp. 41–60). CRC Press.
- Le Bissonnais, Y. (1996b). Aggregate stability and assessment of soil crustability and erodibility: I. Theory and methodology. *European Journal of Soil Science*, 47, 425–437. <https://doi.org/10.1111/j.1365-2389.1996.tb01843.x>
- Le Bissonnais, Y. (2016). Aggregate stability and assessment of soil crustability and erodibility: I. Theory and methodology. *European Journal of Soil Science*, 67, 11–21. https://doi.org/10.1111/ejss.4_12311
- Leys, J., Koen, T., & McTainsh, G. (1996). The effect of dry aggregation and percentage clay on sediment flux as measured by a portable field wind tunnel. *Soil Research*, 34, 849. <https://doi.org/10.1071/SR9960849>
- Li, J., Ma, X., & Zhang, C. (2020). Predicting the spatiotemporal variation in soil wind erosion across Central Asia in response to climate change in the 21st century. *Science of the Total Environment*, 709, 136060. <https://doi.org/10.1016/j.scitotenv.2019.136060>
- Li, J., Okin, G. S., & Epstein, H. E. (2009). Effects of enhanced wind erosion on surface soil texture and characteristics of windblown sediments: Wind erosion and soil characteristics. *Journal of Geophysical Research: Biogeosciences*, 114, G02003. <https://doi.org/10.1029/2008JG000903>
- Li, Z., & Fang, H. (2016). Impacts of climate change on water erosion: A review. *Earth-Science Reviews*, 163, 94–117. <https://doi.org/10.1016/j.earscirev.2016.10.004>
- López, M. V., de Dios Herrero, J. M., Hevia, G. G., Gracia, R., & Buschiazzi, D. E. (2007). Determination of the wind-erodible fraction of soils using different methodologies. *Geoderma*, 139, 407–411. <https://doi.org/10.1016/j.geoderma.2007.03.006>
- Malobane, M. E., Nciizah, A. D., Bam, L. C., Mudau, F. N., & Wakindiki, I. I. C. (2021). Soil microstructure as affected by tillage, rotation and residue management in a sweet sorghum-based cropping system in soils with low organic carbon content in South Africa. *Soil and Tillage Research*, 209, 104972. <https://doi.org/10.1016/j.still.2021.104972>
- Marshall, T., & Quirk, J. (1950). Stability of structural aggregates of dry soil. *Australian Journal of Agricultural Research*, 1, 266. <https://doi.org/10.1071/AR9500266>
- Mikhailova, E. A., Bryant, R. B., Vassenev, I. I., Schwager, S. J., & Post, C. J. (2000). Cultivation effects on soil carbon and nitrogen contents at depth in the russian Chernozem. *Soil Science Society of America Journal*, 64, 738–745. <https://doi.org/10.2136/sssaj2000.642738x>
- Moeyns, J. (2018). *The soil texture wizard: R functions for plotting, classifying, transforming and exploring soil texture data*. Retrieved from https://cran.r-project.org/web/packages/soiltexture/vignettes/soiltexture_vignette.pdf.
- Muñoz Sabater, J. (2019). *ERA5-land monthly averaged data from 1981 to present*. Copernicus Climate Change Service (C3S) Climate Data Store (CDS). <https://doi.org/10.24381/CDS.68D2BB30>
- Nimmo, J. R., & Perkins, K. S. (2002). 2.6 Aggregate stability and size distribution. In J. H. Dane & G. Clarke Topp (Eds.), *SSSA book series* (pp. 317–328). Soil Science Society of America. <https://doi.org/10.2136/sssabookser5.4.c14>
- Prishchepov, A. V., Schierhorn, F., Dronin, N., Ponkina, E. V., & Müller, D. (2020). 800 years of agricultural land-use change in asian (eastern) Russia. In M. Frühauf, G. Guggenberger, T. Meinel, I. Theesfeld, & S. Lentz (Eds.), *KULUNDA: Climate smart agriculture* (pp. 67–87). Springer International Publishing. https://doi.org/10.1007/978-3-030-15927-6_6
- Pruski, F. F., & Nearing, M. A. (2002). Runoff and soil-loss responses to changes in precipitation: A computer simulation study. *Journal of Soil and Water Conservation*, 57, 7–16.
- R Core Team. (2020). *A language and environment for statistical computing*. R Foundation of Statistical Computing.
- Rahmati, M., Eskandari, I., Kouselou, M., Feiziasl, V., Mahdavinia, G. R., Aliasgharzad, N., & McKenzie, B. M. (2020). Changes in soil organic carbon fractions and residence time

- five years after implementing conventional and conservation tillage practices. *Soil and Tillage Research*, 200, 104632. <https://doi.org/10.1016/j.still.2020.104632>
- Reyer, C. P. O., Otto, I. M., Adams, S., Albrecht, T., Baarsch, F., Carlsburg, M., Coumou, D., Eden, A., Ludi, E., Marcus, R., Mengel, M., Mosello, B., Robinson, A., Schleussner, C.-F., Serdeczny, O., & Stagl, J. (2017). Climate change impacts in Central Asia and their implications for development. *Regional Environmental Change*, 17, 1639–1650. <https://doi.org/10.1007/s10113-015-0893-z>
- Reynolds, J. F., Smith, D. M. S., Lambin, E. F., Turner, B. L., Mortimore, M., Batterbury, S. P. J., Downing, T. E., Dowlatabadi, H., Fernández, R. J., Herrick, J. E., Huber-Sannwald, E., Jiang, H., Leemans, R., Lynam, T., Maestre, F. T., Ayarza, M., & Walker, B. (2007). Global desertification: Building a science for dryland development. *Science*, 316, 847–851. <https://doi.org/10.1126/science.1131634>
- Scheffer, F., Schachtschabel, P., & Blume, H.-P. (2016). *Soil science* (1st ed.). Springer.
- Schmidt, G., Illiger, P., Kudryavtsev, A. E., Bischoff, N., Bondarovich, A. A., Koshanov, N. A., & Rudev, N. V. (2020). Physical soil properties and erosion. In M. Frühauf, G. Guggenberger, T. Meinel, I. Theesfeld, & S. Lentz (Eds.), *KULUNDA: Climate smart agriculture* (pp. 155–166). Springer International Publishing. https://doi.org/10.1007/978-3-030-15927-6_11
- Shao, Y. (2008). *Physics and modelling of wind erosion*. Springer, Cambridge. <https://doi.org/10.1007/978-1-4020-8895-7>
- Shiyatyi, E. I. (1965). Wind structure and velocity over a rugged soil surface. *Bulletin of Agriculture*, 10 (in Russian) Cited by Zachar, D. (1982). Erosion factors and conditions governing soil erosion and erosion processes. In *Soil erosion* (pp. 205–387). Elsevier.
- Six, J., Bossuyt, H., Degryze, S., & Deneff, K. (2004). A history of research on the link between (micro)aggregates, soil biota, and soil organic matter dynamics. *Soil and Tillage Research*, 79, 7–31. <https://doi.org/10.1016/j.still.2004.03.008>
- Six, J., Elliott, E. T., Paustian, K., & Doran, J. W. (1998). Aggregation and soil organic matter accumulation in cultivated and native grassland soils. *Soil Science Society of America Journal*, 62, 1367–1377. <https://doi.org/10.2136/sssaj1998.03615995006200050032x>
- Skidmore, E. L., Hagen, L. J., Armbrust, D. V., Durar, A. A., Fryrear, D. W., Potter, K. N., Wagner, L. E., & Zobeck, T. M. (1994). In R. Lal (Ed.), *Soil erosion, research methods* (2nd ed., pp. 295–330). St. Lucie Press.
- Soil Science Division Staff (2017). Soil survey manual. In C. Ditzler, K. Scheffe, & H. C. Monger (Eds.), *Handbook 18*. Government Printing Office Retrieved from https://www.nrcs.usda.gov/wps/portal/nrcs/detailfull/soils/ref/?cid=nrcs142p2_054262
- Stolbovoi, V. (2000). *Soils of Russia: Correlated with the revised legend of the FAO soil map of the world and world Reference Base for soil resources*. International Institute for Applied Systems Analysis.
- Suarez, D. L. (2017). Inorganic carbon: Land use impacts. In R. Lal (Ed.), *Encyclopedia of soil science* (3rd ed., p. 1210). CRC Press. <https://doi.org/10.1081/E-ESS3-120001765>
- Taiyun, W., Simko, V. (2021). R package “corrplot”: Visualisation of a correlation matrix (version 0.92).
- Teixeira, E. I., Fischer, G., van Velthuizen, H., Walter, C., & Ewert, F. (2013). Global hot-spots of heat stress on agricultural crops due to climate change. *Agricultural and Forest Meteorology*, 170, 206–215. <https://doi.org/10.1016/j.agrformet.2011.09.002>
- Tisdall, J. M., & Oades, J. M. (1982). Organic matter and water-stable aggregates in soils. *European Journal of Soil Science*, 33, 141–163. <https://doi.org/10.1111/j.1365-2389.1982.tb01755.x>
- Uspanov, U.U., Yevstifeyev, U.G., Storozhenko, D.M., Lobova, E.V. (1975). Soil map of the kazakh SSR 1:2.500.000.
- Virto, I., Gartzia-Bengoetxea, N., & Fernández-Ugalde, O. (2011). Role of organic matter and carbonates in soil aggregation estimated using laser diffractometry. *Pedosphere*, 21, 566–572. [https://doi.org/10.1016/S1002-0160\(11\)60158-6](https://doi.org/10.1016/S1002-0160(11)60158-6)
- Wang, W., Samat, A., Ge, Y., Ma, L., Tuheti, A., Zou, S., & Abuduwaili, J. (2020). Quantitative soil wind erosion potential mapping for Central Asia using the Google earth engine platform. *Remote Sensing*, 12, 3430. <https://doi.org/10.3390/rs12203430>
- WHO. (2012). *Capacity of the health system in Kazakhstan for crisis management: Kazakhstan, 2010*. World Health Organization, Regional Office for Europe.
- Wieringa, J. (1992). Updating the Davenport roughness classification. *Journal of Wind Engineering and Industrial Aerodynamics*, 41, 357–368. [https://doi.org/10.1016/0167-6105\(92\)90434-C](https://doi.org/10.1016/0167-6105(92)90434-C)
- WMO. (2018). *Guide to meteorological instruments and methods of observation*. World Meteorological Organization.
- Woche, S. K., Goebel, M.-O., Mikutta, R., Schurig, C., Kaestner, M., Guggenberger, G., & Bachmann, J. (2017). Soil wettability can be explained by the chemical composition of particle interfaces—An XPS study. *Scientific Reports*, 7, 42877. <https://doi.org/10.1038/srep42877>
- Xue, B., Huang, L., Huang, Y., Zhou, F., Li, F., Kubar, K. A., Li, X., Lu, J., & Zhu, J. (2019). Roles of soil organic carbon and iron oxides on aggregate formation and stability in two paddy soils. *Soil and Tillage Research*, 187, 161–171. <https://doi.org/10.1016/j.still.2018.12.010>
- Yoder, R. E. (1936). A direct method of aggregate analysis of soils and a study of the physical nature of erosion losses. *Agronomy Journal*, 28, 337–351. <https://doi.org/10.2134/agronj1936.00021962002800050001x>
- Zachar, D. (1982). Erosion factors and conditions governing soil erosion and erosion processes. In *Soil erosion* (pp. 205–387). Elsevier. [https://doi.org/10.1016/S0166-2481\(08\)70647-0](https://doi.org/10.1016/S0166-2481(08)70647-0)
- Zepner, L., Karrasch, P., Wiemann, F., & Bernard, L. (2021). *ClimateCharts.net*—An interactive climate analysis web platform. *International Journal of Digital Earth*, 14(3), 338–356. <https://doi.org/10.1080/17538947.2020.1829112>

How to cite this article: Koza, M., Pöhlitz, J., Prays, A., Kaiser, K., Mikutta, R., Conrad, C., Vogel, C., Meinel, T., Akshalov, K., & Schmidt, G. (2022). Potential erodibility of semi-arid steppe soils derived from aggregate stability tests. *European Journal of Soil Science*, 73(5), e13304. <https://doi.org/10.1111/ejss.13304>

APPENDIX A

TABLE A1 Mean values of soil properties for all plots from each site under both land use types (grassland, grass; cropland, crop). Lower case letters indicate statistical significances ($p < 0.05$); MWD refers to the mean weight diameter

Site(s)	Land-use type	n	pH [-]	Electrical conductivity [$\mu\text{S cm}^{-1}$]	Total inorganic carbon [g kg^{-1}]	Soil organic carbon [g kg^{-1}]	Clay [%]	Silt [%]	Sand [%]	Drop-shatter MWD [mm]	Fast wetting MWD [mm]	Slow wetting MWD [mm]	Wet shaking MWD [mm]
1	Grass	1	6.7 ^b	167.0 ^b	0.1 ^{ab}	47.6 ^a	18.9 ^a	76.0 ^a	5.1 ^b	12.0 ^a	2.0 ^a	2.6 ^a	2.2 ^a
	Crop	4	6.5 ^b	306.0 ^{ab}	0.4 ^a	36.6 ^b	22.1 ^a	50.7 ^b	27.2 ^a	6.1 ^b	0.5 ^b	1.2 ^b	1.2 ^b
	Crop	4	7.6 ^a	481.0 ^a	0.1 ^b	36.0 ^b	25.1 ^a	65.9 ^a	9.0 ^b	7.5 ^b	0.4 ^b	1.1 ^b	1.2 ^b
2	Grass	4	8.3 ^a	564.0 ^a	0.9 ^{bc}	40.0 ^a	21.1 ^b	74.7 ^a	4.2 ^b	12.0 ^a	1.8 ^a	2.5 ^a	1.8 ^a
	Crop	4	7.1 ^b	336.5 ^a	0.1 ^c	34.9 ^a	24.6 ^{ab}	63.4 ^{bed}	12.0 ^{ab}	9.9 ^{ab}	0.6 ^b	1.1 ^{bc}	0.9 ^{bc}
	Crop	4	7.4 ^{ab}	412.8 ^a	0.4 ^c	33.7 ^a	22.7 ^{ab}	55.6 ^d	21.8 ^a	9.5 ^{ab}	0.6 ^b	1.1 ^{bc}	1.0 ^{bc}
	Crop	4	7.7 ^{ab}	419.5 ^a	2.9 ^{ac}	32.8 ^a	27.8 ^a	60.5 ^{cd}	11.7 ^{ab}	8.3 ^{bc}	0.6 ^b	1.0 ^{bc}	0.9 ^{bc}
	Crop	4	7.7 ^{ab}	396.8 ^a	2.6 ^{ab}	32.9 ^a	23.8 ^{ab}	69.2 ^{abc}	7.0 ^b	5.1 ^c	0.4 ^b	0.9 ^{bc}	0.7 ^{bc}
	Crop	4	7.4 ^{ab}	364.3 ^a	0.1 ^c	34.3 ^a	21.3 ^b	72.2 ^{ab}	6.5 ^b	6.0 ^c	0.5 ^b	1.2 ^b	1.1 ^b
	Crop	4	7.7 ^{ab}	423.8 ^a	1.9 ^{abc}	32.1 ^a	25.5 ^{ab}	62.6 ^{bed}	12.0 ^{ab}	7.8 ^{bc}	0.4 ^b	0.7 ^c	0.7 ^c
3	Grass	4	7.9 ^a	196.3 ^b	3.5 ^c	28.2 ^a	20.5 ^a	71.9 ^a	7.6 ^a	7.7 ^a	1.0 ^a	1.9 ^a	1.6 ^a
	Crop	4	7.9 ^a	242.5 ^b	5.2 ^{ab}	19.8 ^b	21.1 ^a	71.7 ^a	7.2 ^a	4.8 ^a	0.4 ^{ab}	0.8 ^b	0.9 ^a
	Crop	4	7.9 ^a	375.3 ^a	5.4 ^a	19.2 ^b	21.8 ^a	72.5 ^a	5.7 ^a	3.5 ^a	0.4 ^{ab}	0.7 ^b	0.8 ^b
	Crop	4	8.0 ^a	213.0 ^b	5.2 ^{ab}	19.7 ^b	24.3 ^a	68.1 ^a	7.6 ^a	5.0 ^a	0.3 ^{ab}	0.6 ^b	0.7 ^b
	Crop	4	7.9 ^a	174.3 ^b	4.1 ^{bc}	19.1 ^b	21.6 ^a	70.3 ^a	8.1 ^a	5.3 ^a	0.3 ^b	0.7 ^b	0.7 ^b
4	Grass	4	6.3 ^b	384.0 ^a	0.1 ^b	27.0 ^a	12.3 ^b	45.0 ^b	42.7 ^a	8.4 ^a	1.2 ^a	2.2 ^a	1.8 ^a
	Crop	4	7.0 ^{ab}	392.3 ^a	0.2 ^b	27.5 ^a	19.1 ^a	55.8 ^{ab}	25.1 ^{ab}	6.8 ^{ab}	0.4 ^b	0.8 ^b	0.8 ^b
	Crop	4	8.3 ^a	353.3 ^a	4.4 ^a	23.4 ^a	21.2 ^a	66.9 ^a	11.9 ^b	4.9 ^b	0.4 ^b	0.7 ^b	0.6 ^b
	Crop	4	6.3 ^b	310.3 ^a	0.1 ^b	21.0 ^a	18.6 ^a	51.1 ^{ab}	30.3 ^{ab}	6.6 ^{ab}	0.2 ^b	0.5 ^b	0.5 ^b
	Crop	4	6.7 ^{ab}	311.3 ^a	0.6 ^b	27.6 ^a	19.0 ^a	54.8 ^{ab}	26.3 ^{ab}	7.0 ^{ab}	0.5 ^b	0.7 ^b	0.7 ^b
5	Grass	4	7.1 ^b	147.8 ^b	0.1 ^b	25.3 ^a	16.0 ^a	59.9 ^b	24.1 ^a	6.2 ^a	1.0 ^a	2.0 ^a	1.4 ^a
	Crop	4	7.9 ^a	266.3 ^a	7.4 ^a	16.5 ^b	19.0 ^a	69.1 ^a	11.9 ^{ab}	4.6 ^a	0.3 ^b	0.7 ^b	0.9 ^b
	Crop	4	8.2 ^a	231.0 ^{ab}	7.5 ^a	17.5 ^{ab}	19.2 ^a	65.1 ^{ab}	15.7 ^{ab}	4.6 ^a	0.3 ^b	0.6 ^b	0.7 ^b
6	Grass	4	6.7 ^a	64.8 ^a	0.1 ^a	13.5 ^a	10.2 ^a	35.7 ^a	54.1 ^a	10.0 ^a	1.4 ^a	1.4 ^a	1.6 ^a
	Crop	4	7.2 ^a	355.5 ^a	0.2 ^a	11.5 ^a	17.8 ^a	50.8 ^a	31.4 ^a	2.5 ^b	0.5 ^b	0.7 ^a	0.7 ^a
	Crop	4	7.4 ^a	160.0 ^a	0.2 ^a	12.9 ^a	19.9 ^a	49.0 ^a	31.1 ^a	4.1 ^b	0.7 ^b	1.2 ^a	1.4 ^a

(Continues)

TABLE A1 (Continued)

Site(s)	Land-use type	n	pH [-]	Electrical conductivity [$\mu\text{S cm}^{-1}$]	Total inorganic carbon [g kg^{-1}]	Soil organic carbon [g kg^{-1}]	Clay [%]	Silt [%]	Sand [%]	Drop-shatter MWD [mm]	Fast wetting MWD [mm]	Slow wetting MWD [mm]	Wet shaking MWD [mm]
7	Crop	4	7.3 ^a	170.5 ^a	0.2 ^a	14.2 ^a	17.2 ^a	44.9 ^a	37.9 ^a	4.7 ^b	0.6 ^b	0.8 ^a	1.0 ^a
	Crop	4	7.2 ^a	108.5 ^a	0.1 ^a	14.5 ^a	19.6 ^a	51.5 ^a	28.8 ^a	6.8 ^{ab}	0.6 ^b	0.8 ^a	1.1 ^a
	Grass	4	6.5 ^b	49.0 ^b	0.1 ^a	15.3 ^a	7.8 ^a	34.8 ^a	57.3 ^a	11.0 ^a	0.7 ^a	1.5 ^a	0.9 ^a
	Crop	4	7.3 ^a	134.5 ^{ab}	0.3 ^a	16.2 ^a	9.5 ^a	35.0 ^a	55.5 ^a	3.6 ^c	0.4 ^b	0.6 ^b	0.5 ^b
	Crop	4	6.4 ^b	138.8 ^a	0.1 ^a	11.6 ^a	9.3 ^a	32.5 ^a	57.8 ^a	6.7 ^b	0.3 ^b	0.5 ^b	0.5 ^b
	Crop	4	6.5 ^b	70.8 ^{ab}	0.1 ^a	13.1 ^a	10.9 ^b	36.1 ^a	53.0 ^a	3.4 ^c	0.3 ^b	0.5 ^b	0.5 ^b
	Crop	4	6.7 ^b	61.5 ^{ab}	0.1 ^a	14.2 ^a	11.6 ^a	45.9 ^a	42.5 ^a	5.7 ^{bc}	0.3 ^b	0.5 ^b	0.6 ^b

TABLE A2 Correlation coefficients (r) between aggregate stabilities and soil properties with statistical significances levels ($p < 0.001 = ***$, $p < 0.01 = **$, $p < 0.05 = *$) for all sites

Site(s)	Aggregate stability indicators	pH r^p	Electrical conductivity r^p	Total inorganic carbon r^p	Soil organic carbon r^p	Clay r^p	Silt r^p	Sand r^p
All	Drop-shatter	-0.20 *	0.12	-0.27 **	0.51 ***	0.10	0.06	-0.08
	Fast wetting	-0.11	0.05	-0.27 **	0.42 ***	-0.04	0.15	-0.10
	Slow wetting	-0.09	0.09	-0.25 **	0.49 ***	0.00	0.19 *	-0.14
	Wet shaking	-0.07	0.06	-0.18 *	0.43 ***	0.12	0.26 **	-0.23 **
1	Drop-shatter	-0.16	-0.55	-0.17	0.76 **	-0.53	0.78 **	-0.65 *
	Fast wetting	-0.37	-0.69 *	-0.24	0.81 **	-0.63 *	0.68 *	-0.50
	Slow wetting	-0.33	-0.74 **	-0.22	0.77 **	-0.51	0.67 *	-0.53
	Wet shaking	-0.21	-0.65 *	-0.19	0.77 **	-0.56	0.74 **	-0.59 *
2	Drop-shatter	0.01	0.17	-0.27	0.30	-0.04	-0.27	0.29
	Fast wetting	0.57 **	0.52 **	-0.12	0.22 *	-0.28	0.36	-0.25
	Slow wetting	0.45 *	0.44 *	-0.21	0.38 **	-0.36	0.38	-0.24
	Wet shaking	0.31	0.34	-0.28	0.40 **	-0.32	0.40 *	-0.27
3	Drop-shatter	0.21	-0.33	-0.43 **	0.35 ***	0.13	-0.18	0.15
	Fast wetting	-0.20	-0.05	-0.64 **	0.77 ***	-0.09	0.19	-0.25
	Slow wetting	-0.10	-0.19	-0.67 **	0.83 ***	-0.21	0.23	-0.10
	Wet shaking	-0.16	-0.07	-0.59 **	0.77 ***	-0.12	0.18	-0.17
4	Drop-shatter	-0.61 **	0.20	-0.38	0.48 *	-0.28	-0.43	0.40
	Fast wetting	-0.37	0.20	-0.21	0.25	-0.55	-0.31 *	0.39
	Slow wetting	-0.32	0.37	-0.23	0.24	-0.60	-0.34 **	0.42
	Wet shaking	-0.34	0.32	-0.22	0.21	-0.59	-0.36 **	0.43
5	Drop-shatter	-0.62 *	-0.09	-0.38	0.52	0.15	-0.55	0.40
	Fast wetting	-0.85 ***	-0.60 *	-0.86 ***	0.85 ***	-0.53	-0.52	0.61 *
	Slow wetting	-0.89 ***	-0.57	-0.92 ***	0.87 ***	-0.59 *	-0.54	0.64 *
	Wet shaking	-0.78 **	-0.50	-0.73 **	0.75 **	-0.51	-0.35	0.47
6	Drop-shatter	-0.02	-0.27	-0.12	0.38	-0.02	-0.05	0.04
	Fast wetting	-0.01	-0.22	-0.16	0.05	-0.21 *	-0.40 **	0.36 **
	Slow wetting	0.12	-0.20	-0.09	0.12	0.01	-0.25	0.18
	Wet shaking	-0.02	-0.41	-0.30	0.41	0.26	0.04	-0.12
7	Drop-shatter	-0.42	-0.32	-0.22	0.07	-0.27	0.01	0.05
	Fast wetting	0.03	-0.20	-0.16	0.16	-0.53 *	-0.27	0.35
	Slow wetting	-0.05	-0.33	-0.19	0.26	-0.41	-0.11	0.19
	Wet shaking	-0.18	-0.17	-0.28	0.43	-0.13	0.24	-0.16

TABLE A3 Soil properties of all sites and both land use types (grassland, grass; cropland, crop)

Site(s)	Land-use type(s)	n	pH	Electrical conductivity [$\mu\text{S cm}^{-1}$]	Total inorganic carbon [g kg^{-1}]	Soil organic carbon [g kg^{-1}]	Clay [%]	Silt [%]	Sand [%]	Drop-shatter MWD [mm]	Fast wetting MWD [mm]	Slow wetting MWD [mm]	Wet shaking MWD [mm]
All	Both	132	7.3±0.8	261.9±158.3	1.7±2.3	23.9±10.9	18.8±5.7	57.3±14.4	23.9±18.9	6.6±3.0	0.6±0.5	1.0±0.6	1.0±0.5
	Grass	28	7.1±0.8	198.6±162.5	0.7±1.2	28.1±13.9	15.3±5.4	56.9±18.0	29.9±23.0	9.6±3.1	1.3±0.6	2.0±0.6	1.6±0.5
	Crop	104	7.3±0.8	277.8±144.3	2.5±1.2	22.8±9.6	19.8±5.4	57.4±13.3	17.5±1.3	5.8±2.4	0.4±0.2	0.8±0.3	0.8±0.3
1	Both	12	6.9±0.5	322.2±157.0	0.2±0.2	40.2±6.7	22.2±3.8	64.3±11.5	13.4±10.8	8.7±2.5	1.0±0.7	1.6±0.7	1.5±0.5
	Grass	4	6.7±0.3	167.0±58.1	0.1±0.1	47.6±4.9	18.9±3.0	76.0±2.3	5.1±2.4	12.0±0.0	2.0±0.2	2.6±0.1	2.2±0.1
	Crop	8	7.0±0.6	399.8±131.3	0.2±0.2	36.4±3.6	23.9±2.9	58.5±9.6	17.6±10.9	7.0±1.1	0.5±0.1	1.1±0.2	1.2±0.2
2	Both	32	7.6±0.5	405.5±126.0	1.3±1.3	34.4±6.1	23.8±3.0	65.4±7.6	10.7±7.4	8.4±2.5	0.6±0.5	1.2±0.5	1.0±0.3
	Grass	4	8.3±0.8	564.0±382.0	0.9±0.6	40.0±14.3	21.1±1.3	74.7±4.0	4.2±3.1	12.0±0.0	1.8±0.3	2.5±0.2	1.8±0.1
	Crop	28	7.5±0.3	392.3±52.6	1.3±1.4	33.5±1.9	24.3±2.9	63.9±6.9	11.8±7.4	7.7±2.2	0.5±0.1	1.0±0.2	0.9±0.2
3	Both	20	7.9±0.1	240.3±79.2	4.7±0.9	21.2±4.1	21.9±2.7	70.9±3.0	7.2±1.3	5.3±3.1	0.5±0.4	0.9±0.6	0.9±0.4
	Grass	4	7.9±0.1	196.3±27.0	3.5±0.8	28.2±4.4	20.5±1.8	71.9±1.3	7.6±1.5	7.7±4.3	1.0±0.6	1.9±0.6	1.6±0.6
	Crop	16	7.9±0.1	251.3±83.9	5.0±0.6	19.5±0.8	22.2±2.8	70.7±3.3	7.1±1.2	4.7±2.4	0.3±0.1	0.7±0.1	0.8±0.1
4	Both	20	6.9±1.1	350.2±94.5	1.1±1.9	25.3±10.3	18.0±3.8	54.7±10.3	27.3±13.6	6.7±1.8	0.5±0.4	1.0±0.7	0.9±0.6
	Grass	4	6.3±0.7	384.0±115.3	0.1±0.0	27.0±11.6	12.3±2.4	45.0±6.1	42.7±8.4	8.4±2.2	1.2±0.4	2.2±0.6	1.8±0.5
	Crop	16	7.1±1.1	341.8±86.5	1.3±2.0	24.9±9.9	19.5±2.4	57.1±9.7	23.4±11.8	6.3±1.4	0.4±0.1	0.7±0.2	0.6±0.2
5	Both	12	7.7±0.5	215.0±66.1	5.0±3.6	19.8±5.4	18.1±2.1	64.7±5.0	17.2±6.1	5.1±1.8	0.5±0.4	1.1±0.7	1.0±0.4
	Grass	4	7.1±0.2	147.8±65.2	0.1±0.0	25.3±6.3	16.0±1.9	59.9±2.9	24.1±3.9	6.2±0.8	1.0±0.3	2.0±0.4	1.4±0.3
	Crop	8	8.0±0.3	248.6±32.1	7.4±0.9	17.0±1.0	19.1±1.2	67.1±4.0	13.8±3.4	4.6±1.9	0.3±0.0	0.6±0.1	0.8±0.2
6	Both	20	7.2±0.9	171.9±176.3	0.2±0.2	13.3±3.2	17.0±5.3	46.4±10.8	36.6±15.3	5.6±3.3	0.7±0.3	1.0±0.4	1.1±0.4
	Grass	4	6.7±0.5	64.8±28.5	0.1±0.1	13.5±3.5	10.2±3.8	35.7±11.0	54.1±13.9	10.0±3.4	1.4±0.1	1.4±0.5	1.6±0.5
	Crop	16	7.3±0.9	198.6±187.2	0.2±0.2	13.3±3.2	18.7±4.2	49.0±9.0	32.3±12.2	4.5±2.2	0.6±0.1	0.9±0.3	1.1±0.4
7	Both	20	6.7±0.4	90.9±51.9	0.1±0.2	14.1±2.9	9.8±2.6	36.9±8.8	53.2±10.9	6.1±2.9	0.4±0.2	0.7±0.4	0.6±0.2
	Grass	4	6.5±0.1	49.0±20.0	0.1±0.0	15.3±2.9	7.8±1.9	34.8±9.0	57.3±10.9	11.0±1.8	0.7±0.0	1.5±0.1	0.9±0.2
	Crop	16	6.7±0.4	101.4±52.1	0.1±0.2	13.8±2.8	10.3±2.5	37.4±8.7	52.2±10.6	4.8±1.6	0.3±0.1	0.5±0.1	0.5±0.1

Note: Values are shown as arithmetic means ± SD; MWD refers to the mean weight diameter.

5.3 Koza et al. (2024): Wind erosion after steppe conversion in Kazakhstan

Full bibliographic citation:

Koza, M., Funk, R., Pöhlitz, J., Conrad, C., Shibistova, O., Meinel, T., Akshalov, K., Schmidt, G., 2024. Wind erosion after steppe conversion in Kazakhstan. *Soil and Tillage Research* 236, 105941. <https://doi.org/10.1016/j.still.2023.105941>

Full bibliographic citation of the peer-reviewed dataset (Koza et al., 2023):

Koza, M., Funk, R., Schmidt, G., 2023. Wind erosion after steppe conversion in Kazakhstan: Data from mobile wind tunnel experiments [Dataset]. *Leibniz centre for Agricultural Landscape Research (ZALF)*. <https://doi.org/10.4228/zalf-qq16-t967>

Scientific presentation and discussion of this study:

Koza, M., Pöhlitz, J., Funk, R., Meinel, T., Akshalov, K., Schmidt, G., 2023. In-situ quantification of wind erosion on arable soils in the dry steppe of Kazakhstan. *Jahrestagung der Deutschen Bodenkundlichen Gesellschaft*. Halle (Saale), Germany

Preface:

After evaluating the overall resistance of aggregates to disruptive forces and discussing the results (Koza et al., 2022), it was concluded that steppe soils are prone to wind and water erosion. However, quantifying soil loss by wind under real soil conditions is lacking for Central Asia but crucial for a comprehensive approach.

Summary:

This publication assesses soil losses by wind velocity of 15 m s^{-1} (at 0.5 m height) under real soil conditions using a mobile wind tunnel. Wind erosion was quantified on fallow that was recently converted from grassland and arable plots cultivated with common crops. Additionally, soil loss rates were quantified after mechanical stress was applied, similar to common agricultural practices. The PSD and ASD, as well as SOC contents of topsoil, aeolian sediments, and depositions, were investigated. This third publication (Koza et al., 2024) is the first up-to-date study that provides recommendations for wind erosion prevention based on field experiments conducted under real soil conditions.

Highlights:

- First wind erosion study with a mobile wind tunnel in Kazakhstan.
- Vegetation, aggregation, and tillage as erosion-controlling factors were tested.
- Mechanical stress from seedbed preparation determines soil susceptibility to wind erosion.
- Tractor tire tracks must be considered a serious emission source.
- Steppe conversion requires best-adapted measures of erosion prevention early on.



Contents lists available at ScienceDirect

Soil & Tillage Research

journal homepage: www.elsevier.com/locate/still

Wind erosion after steppe conversion in Kazakhstan

Moritz Koza^{a,*}, Roger Funk^b, Julia Pöhlitz^a, Christopher Conrad^a, Olga Shibistova^c, Tobias Meinel^d, Kanat Akshalov^e, Gerd Schmidt^a

^a Department of Geocology, Institute of Geosciences and Geography, Martin Luther University Halle-Wittenberg, 06120 Halle (Saale), Germany

^b Landscape Pedology, Leibniz Centre for Agricultural Landscape Research (ZALF), 15374 Müncheberg, Germany

^c Institute of Soil Science, Leibniz University Hanover, 30419 Hanover, Germany

^d Amazonen-Werke H. Dreyer SE & Co. KG, 49205 Hasbergen, Germany

^e Soil and Crop Management, Barayev Research and Production Center for Grain Farming, 474010 Shortandy, Kazakhstan

ARTICLE INFO

Keywords:

Wind tunnel
On-farm experimentation
Soil management
Soil loss
Particle size distribution
Soil organic carbon

ABSTRACT

Semi-arid regions of Central Asia suffer from wind erosion due to expanding steppe conversion and unsustainable farming practices. Empirical data from field observations are needed to support the implementation of adapted management. In this study, a mobile wind tunnel was used for the first time in Kazakhstan to assess the soil's erodibility under real conditions. Field experiments were conducted on loamy sands with different initial conditions that are typical for the most erosive time of the year: a bare surface with a cloddy structure after recent steppe conversion, a weak crust on a plot with barley (*Hordeum vulgare* L.), and a plot with loose material in the rows of maize plants (*Zea mays* L.). Subsequently, different levels of mechanical stress (low, moderate, high) were considered to analyze the effect of disruptive forces soils experience during field cultivation (light cultivator, disc harrow, tractor tires) on possible soil losses. The results of wind tunnel experiments showed already great differences under initial conditions. The cloddy structure of the recent steppe conservation had the lowest susceptibility against wind erosion due to a good aggregation and a large roughness, resulting in soil loss of 12 g m⁻². The plot grown with barley was less affected by wind erosion due to the weak crust, smaller distances between plants, and leaves close to the ground (soil loss of 34 g m⁻²). Maize was also the most problematic crop in the study area because wind can blow below the plant canopy without considerable resistance during the early growth stages. Additionally, existing deposits in the maize rows from previous erosion events led to the highest soil loss of 1609 g m⁻². Mechanical stress by seedbed preparation generally increased the erodible fraction, resulting in higher soil losses (light cultivator: 198 ± 129 g m⁻², disc harrow: 388 ± 258 g m⁻²). The most severe disruption of soil structure occurred on tractor tire tracks, causing a loss of 2767 ± 1810 g m⁻². Consequently, the pulverizing effect of tractor tires on dry soil must be considered a serious emission source. Comparing the soil organic carbon content of topsoil and eroded material showed that organic carbon was enriched only in the aeolian sediments of the recently converted plot (+69%). We conclude that soils after steppe conversion need to be treated with particular care from the very beginning so that severe events from the past are not repeated.

1. Introduction

Soil degradation is an ongoing problem worldwide (Keesstra et al., 2016; Lal, 2001). Particular agriculture is often under the pressure of soil erosion, causing the redistribution of valuable topsoil, nutrients, and organic carbon (Cerdà et al., 2009; Montgomery, 2007). Aeolian processes usually occur without being noticed (Chepil, 1960; Funk et al.,

2014) but data from global compilation surveys confirm that erosion rates from conventional agriculture are up to two times higher than soil production rates (Montgomery, 2007).

In the past, an extreme example has shown that soil cultivation can contribute to wind erosion, triggering a socio-ecological crisis (Peters et al., 2008). Known as the Dust Bowl Syndrome in the Great Plains of the USA during the 1930s, multiple natural and anthropogenic factors,

Abbreviations: ASD, aggregate size distribution; EF, erodible fraction; MWAC, Modified Wilson and Cook; PSD, particle size distribution; SOC, soil organic carbon; SUSTRA, Suspension Sediment Trap.

* Corresponding author.

E-mail address: moritz.koza@geo.uni-halle.de (M. Koza).

<https://doi.org/10.1016/j.still.2023.105941>

Received 27 April 2023; Received in revised form 24 October 2023; Accepted 31 October 2023

Available online 21 November 2023

0167-1987/© 2023 The Authors. Published by Elsevier B.V. This is an open access article under the CC BY license (<http://creativecommons.org/licenses/by/4.0/>).

including extensive steppe conversion, unsustainable farming practices and severe drought, caused devastating soil erosion on 20–40 million hectares (Hornbeck, 2012; McLeman et al., 2014; Zobeck et al., 2013). The Dust Bowl initially started on individual fields and turned into erosion among areas until it expanded to broad-scale events with land-atmosphere interactions (Peters et al., 2008), exceeding soil loss rates that have ever been recorded. Dust storms are still occurring in the Great Plains, but their current extent is far less concerning due to the adaptation of conservation tillage and no-till farming practices (Lal et al., 2007; Lee and Gill, 2015). Still, in many parts of the world, soil cultivation causes a considerable increase in wind erosion events (Shao, 2008).

The semi-arid steppe regions of Central Asia are challenged by soil erosion due to intense agriculture and extreme climate conditions (Reyer et al., 2017; Robinson, 2016). This is reinforced as climate models indicate an increase in the natural factors that promote wind erosion, such as higher temperatures and a change in precipitation patterns (Duulatov et al., 2021; Li et al., 2020b). Kazakhstan, in particular, faces an increasing risk of soil degradation due to wind erosion (Li et al., 2020b). Historically, northern Kazakhstan was part of the largest steppe conversion of the twentieth century (Virgin Lands Campaign, 1954–1963), where extensive grasslands were converted to arable land for grain production. Moldboard plowing was commonly used for steppe conversion and cultivation in order to increase spring wheat production, but it caused severe wind erosion and soil degradation (Meinel and Akshalov, 2015). Large areas of cropland were abandoned during the collapse of the Soviet Union (1991), but recent steppe conversion is expanding arable land again (Frühhauf et al., 2020; Kraemer et al., 2015; Prishchepov et al., 2020). As a result, cascading effects may be possible as more land is exposed to wind erosion (Peters et al., 2008). Severe soil degradation in Kazakhstan could also threaten food security in Central Asia because of its important role as a grain exporter (FAO, 2012). Hence, soil erosion mitigation is an important step to ensure the achievement of the Sustainable Development Goals (Yin et al., 2022).

Assessments of erosion risks in the semi-arid steppe regions of Central Asia are rare (Borrelli et al., 2021), especially for wind erosion (Bezák et al., 2021; Field et al., 2009). However, they are necessary to develop adequate solutions. Field observations and laboratory tests from less-studied regions of the world can add to existing knowledge and provide useful benchmarks for building erosion models (Webb et al., 2020). Furthermore, empirical data are more accurate at smaller scales and can support sustainable management practices. For this purpose, we studied the wind erosion processes in the Kazakh Steppe in detail. In a recent study, we derived the potential erodibility of semi-arid steppe soils from aggregate stability tests. We could show that arable fields of northern Kazakhstan are susceptible to erosion, independent of their soil properties (Koza et al., 2022). In the present study, a mobile wind tunnel was used to assess the soil erodibility by wind under real conditions. Properly constructed and operated wind tunnels can be used to investigate the erodibility of the intact surface, with and without plant residues, as well as the disturbed soil under controlled and natural wind conditions (Zobeck and Van Pelt, 2015). In areas where continuous monitoring is difficult and reliable data are limited, data collected from mobile wind tunnel experiments offer a reasonable compromise to evaluate erosion risk, even if minor inaccuracies occur during the experimental setup (Marzen et al., 2020).

Wind erosion processes can be selective by removing the fine clay and silt-sized particles that contain disproportionately greater amounts of organic matter (Chappell et al., 2013; Zobeck and Fryrear, 1986). While the coarse sand fraction (>500 µm) is predominantly unaffected by wind erosion and stays within the field, the finer fractions are eroded and blown out (Kok et al., 2012; Shao, 2008). Fine-textured soils favor aggregation and prevent erosion, but the very fine sand fraction is the size with the lowest threshold (Shao, 2008), which can initiate suspension by abrading larger aggregates (Zobeck and Van Pelt, 2015). Overall,

wind erosion can redistribute not only soil but also organic carbon (Gregorich et al., 1998). Investigating the wind-blown sediments' composition and the soil organic carbon (SOC) content is a relevant research topic (Iturri and Buschiazzo, 2023). On a local scale, land use sustainability relies on preserving SOC (Shao et al., 2011). Globally, unknown SOC rates of aeolian sediments from semi-arid environments cause uncertainty in carbon cycle estimates (Chappell et al., 2013).

Wind tunnel experiments have been used to understand the combined effects of topsoil characteristics and agricultural management practices influencing surface characteristics and soil loss rates. Sirjani et al. (2019) and Shahabinejad et al. (2019) showed a significant relationship between soil erosion rates and the mean weight diameter in Iran's arid and semi-arid regions. Overall, various studies show the significant effect of tillage on soil structure (Bronick and Lal, 2005) and the associated increase in erosion risks (Zobeck and Popham, 1990). After studying the aerodynamic roughness of five cultivated soils, Zhang et al. (2004) concluded that roughness length is the dominant parameter in evaluating soil erodibility on arable soils in China. It is well known that the soils erodibility of fixed sandy soils can accelerate under cultivation (Li et al., 2004; López et al., 1998; Reynolds et al., 2007). However, on-farm experiments that measure soil losses caused by wind erosion after the application of mechanical stresses are limited.

We provide the first indications from in situ measurements for the control and prevention of wind erosion on arable land in Central Asia's dry steppe. A mobile wind tunnel was used to explore the erosion risk of different surface characteristics under the natural conditions of Kazakhstan's agricultural steppe soils. We examined short-term soil and SOC loss as well as changes in soil characteristics at a field scale caused by aeolian processes in response to different management practices commonly used in agriculture. Wind tunnel experiments were conducted after recent steppe conversion on a bare and cloddy surface and further cultivated and sown with barley and maize. Additional experiments were conducted after applying different mechanical stresses to evaluate the effect on soil loss. Mechanical disruptions were comparable to the forces soils experience under real conditions during field cultivation. Therefore, aggregate breakdown by a light cultivator and a disc harrow was imitated by hand with a lifting or a turning tool. The pulverizing effect of aggregates by heavy tillage implements on tractor tire tracks was simulated by crushing aggregates intensively. To verify the functionality of the mobile wind tunnel, we compared the aeolian sediments collected during the experiments inside the tunnel and aeolian deposition from natural wind erosion events.

The main objectives of this study are (i) to quantify soil losses depending on different agricultural management practices and surface characteristics, (ii) to determine the changes in particle size distribution (PSD) and aggregate size distribution (ASD) of aeolian sediments and depositions, and (iii) to quantify SOC losses due to wind erosion.

2. Materials and methods

2.1. Study area and test site

The study area is located in the Eurasian steppe in northern Kazakhstan. The test site is located east of Astana and north of Pavlodar (Fig. 1A). The area of interest has been shaped by floodplains of the Irtysh River or lacustrine-alluvial depositions from thermokarst lakes during the Quaternary (Aubekerov and Gorbunov, 1999). The soils at the test site were assigned to Haplic Kastanozem (FAO, 2014) and Chestnut in the national classification system (Stolbovoi, 2000). The nearby Irtysh River has the highest water security in Kazakhstan and can be used for irrigation (FAO, 2012). Overall, the fertile soils favor the cultivation of cereals in northern Kazakhstan, but climate conditions cause a permanent risk of wind erosion (Fig. 1B).

The climate is dry continental, with an annual mean temperature of 2.9 °C and annual precipitation of 299 mm at 2 m height (based on weighted interpolation 1991–2020) (Harris et al., 2020; Zepner et al.,

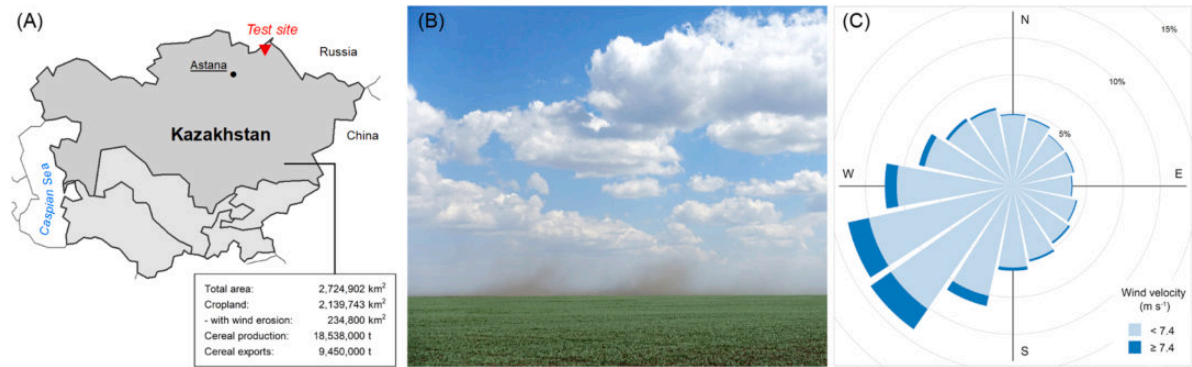


Fig. 1. Location of the test site in northern Kazakhstan (A). Typical agricultural environment in the dry steppe of Kazakhstan with aeolian sediments moved by suspension during a common wind erosion event observed on the test site in June 2022 (B). Relative frequency (%) of wind velocities, classified for 16 wind directions (average of 1991–2020). Wind speeds (at 10 m height) below (light blue) and above a threshold of 7.4 m s⁻¹ (dark blue) are shown (C).

2021). Wind is always present in the study area with the highest speed in winter and spring. The average mean wind speed in the study area at a height of 10 m is 4.1 m s⁻¹, with strong wind gusts exceeding 40 m s⁻¹. The main wind direction is southwest (Fig. 1C) (DTU, 2021; FAO, 2012; Meteoblue, 2023). The estimated threshold wind speed is 4 m s⁻¹ at 0.3 m height (Scheffer et al., 2016), corresponding to 7.4 m s⁻¹ at 10 m height derived from the logarithmic wind profile (Shao, 2008; Wieringa, 1992). The transport capacity Q (dimensionless) of the wind (Fig. 2) can be calculated based on the Eq. 1:

$$Q = u^2(u - u_t) \tag{1}$$

where u (m s⁻¹) is the wind speed and u_t (m s⁻¹) is the threshold wind speed (Fryrear et al., 1998; Funk et al., 2023).

Three adjoining agricultural fields (140 ha each) were used for the experiments. They had been abandoned for several years and were covered with typical grassland vegetation (locally called *zalesh*). One

field represents the primary situation, as the conversion from grassland steppe to arable land was carried out before by breaking the grass cover with a disc harrow and stirring the soil up to 0.25 m depth with a cultivator in the spring of 2022 (Plot 1). As usual, cultivation with a crop did not follow immediately, and the initial surface remained fallow in a rough, cloddy state. The two arable fields share the same history. They were converted from steppe in 2019 by disc harrow and cultivator. The fields were cultivated with barley in 2020, with potatoes in 2021, and seedbed preparation was carried out on both arable fields with a cultivator (depth of 0.2 m) in May 2022. Afterward, one field was sown to barley (Plot 2) and the other to maize (Plot 3). Both are common crops in the study area.

2.2. On-farm experimentation

2.2.1. Design

On-farm experiments are challenged by ensuring plot uniformity and remaining other factors equal while isolating the consequence of mechanical stress (*ceteris paribus* effect). Nevertheless, they are of unique value and of great expressiveness that comes from conducting experiments under real farm management conditions. This on-farm experiment was designed to study wind erosion processes and quantify soil losses under typical conditions in agriculture (Fig. 3). The experiments were conducted with a mobile wind tunnel, which allows repeated investigations of aeolian processes within a shorter time than in the natural environment, where these factors are highly variable in time and space (Van Pelt and Zobeck, 2013). Wind tunnel measurements were conducted in June 2022 when plants had just emerged, but soil surfaces were still susceptible to wind erosion. This allowed us to study wind erosion at the transition from bare soils to early stages of plant development. Surfaces were prepared as tilled with a cultivator, disc harrow, or pulverized by tractor tires. The timing of the experiment also ensured that they were conducted under climatic conditions where soil loss by wind erosion occurs regularly in the study area (FAO, 2012).

2.2.2. Setup: mobile wind tunnel

The mobile boundary layer wind tunnel shown in Fig. 4A (Umwelt-Geräte-Technik GmbH, Müncheberg, Germany) was extensively tested under various conditions to become familiar with its technical characteristics before conducting experiments. An axial fan of 7.7 kW powered the air stream of the push-type tunnel. In the field, the electric power was provided by an 11.5 kW diesel generator. The fan and generator are mounted on a two-axle trailer. A 5-m long flexible hose leads the air stream to a flow straightener on the ground, eliminating the fan's vortices and ensuring a laminar flow. The flow straightener consists of PVC

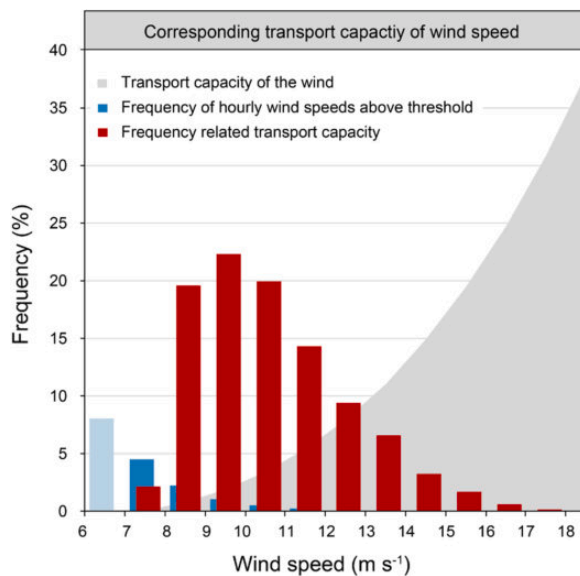


Fig. 2. The transport capacity of the wind (gray area), the frequency of hourly wind speeds above a threshold of 7.4 m s⁻¹ (blue bars), and the frequency-related transport capacity (red bars) of the test site are shown.

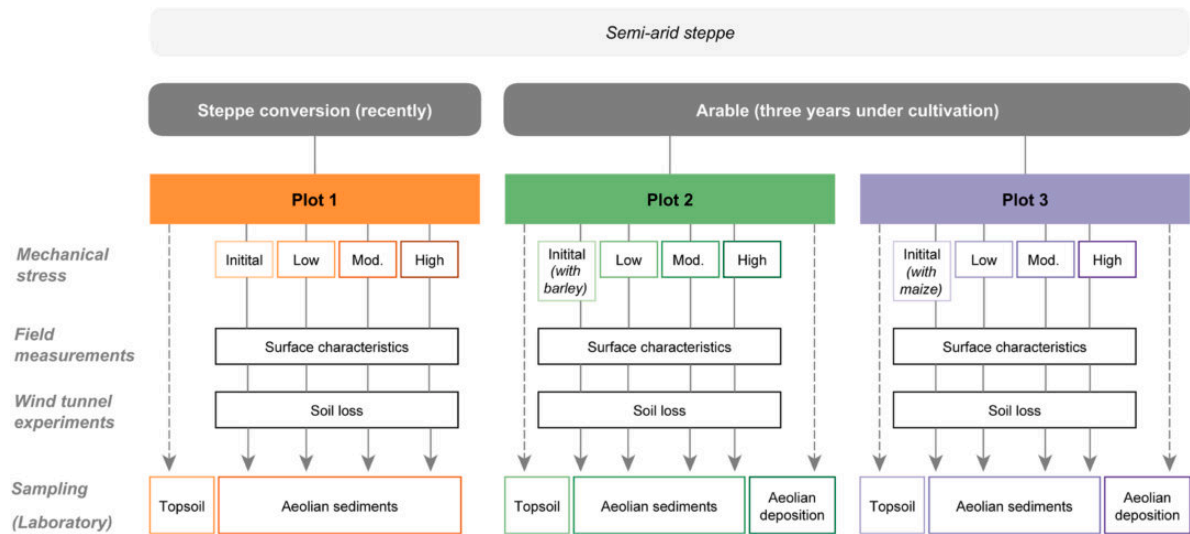


Fig. 3. Hierarchical data structure defining the study design.



Fig. 4. The mobile wind tunnel during experiments on maize (A), MWACs and SUSTRA for collecting aeolian sediments at the wind tunnel outlet (B), and aeolian depositions from natural wind erosion events on the edge of a field (C).

tubes (length = 150 mm, diameter = 12 mm, material thickness = 0.23 mm) and has the same cross section as the measurement section (height = 0.8 m, width = 0.8 m). The measurement section consists of six single segments (total length = 6 m) placed on two metal rails over an open surface area of 4.8 m². Each segment has an acrylic glass window, allowing visual observation and easy access to the inside of the tunnel between measurements. The power supply for the fan is adjustable by an attached control panel for a regulated increase in wind speed. A cup anemometer at the end of the tunnel at the height of 0.5 m was used to monitor comparability between all experiments independent of ambient conditions (temperature, air pressure, wind speed, wind direction) on the test site.

The air stream of the mobile wind tunnel showed a logarithmic wind speed profile up to 0.4 m height measured on raw concrete, comparable to sandy roughness (Appendix Fig. A1A). A maximum wind speed of 16 m s⁻¹ was measured at 50 Hz ($u^* = 0.85 \text{ m s}^{-1}$). Wind profiles of the roughness lengths of this study are presented in Appendix Fig. A1B. To ensure that the simulation of saltation in the wind tunnel is comparable to the development under natural conditions, the Froude number criterion was used (White and Mounla, 1991). The Froude number F (dimensionless) value can be calculated with Eq. 2:

$$F = \frac{u^2}{gH} \quad (2)$$

where u (m s⁻¹) is the uniform wind tunnel speed, g (m s⁻²) is the gravity constant, and H (m) is the restricted height of the wind tunnel. The saltating flow in the wind tunnel is free of facility constraints below a

value of $F = 20$ (Owen and Gillette, 1985, as cited in White and Mounla, 1991) or below the more conservative value of $F = 10$ (White and Mounla, 1991). The dimensions of this mobile wind tunnel allow a Froude number of 20 at 12.5 m s⁻¹ or 29 at 15 m s⁻¹ speed. However, the ideal Froude number can usually only be archived in large stationary wind tunnels at very low wind speeds (Maurer et al., 2006).

2.2.3. Setup: sediment traps

Two types of passive sediment traps were used at the end of the wind tunnel to collect eroded material (Fig. 4B). Modified Wilson and Cook (MWAC) samplers were used to measure the vertical distribution of the aeolian sediments. The MWAC consists of a PE bottle of 100 ml and a glass in- and outlet tube with an inner diameter of 8 mm. They were installed at the ground level and attached to a pole at 0.05 m, 0.10 m, 0.15 m, 0.20 m, 0.25 m, 0.30 m, and 0.35 m height to collect eroded material. The MWAC samplers are popular in wind erosion studies and seem less influenced by ambient wind speed (Zobeck et al., 2003). Since very low collection rates were possibly to be expected, MWACs of all heights were weighed before and after each experiment. Additionally, a SUSTRA (Suspension Sediment Trap, replica by Umwelt-Geräte-Technik GmbH, Müncheberg, Germany) with an opening diameter of 0.05 m was used to collect sediments in the height range between 0.025 and 0.075 m (Funk et al., 2004; Funk and Engel, 2015; Janssen and Tetzlaff, 1991) to catch higher amounts of aeolian sediments for further analyses. The traps were installed in the center of the tunnel with space to each other to keep the air stream's disturbance as low as possible.

The vertical distribution of the horizontal sediment loss was used to

quantify wind erosion (Funk et al., 2014). Therefore, the sediment mass collected in the MWAC was related to the MWAC's inlet surface area of $2.655 \times 10^{-4} \text{ m}^2$ and the surface area inside the mobile wind tunnel. Then, the soil loss (g m^{-2}) was derived from semi-logarithmic regression by fitting the total mass of caught sediments (q_z) at the height (z) to $\ln(z)$ (Koza et al., 2023). Quantifying soil loss with the MWACs allows good repeatability. An experiment with five repetitions on a highly erodible surface showed a standard deviation of 8.8%.

The SOC ratios were calculated as the content of SOC collected by the traps to the content of SOC in the topsoil.

2.2.4. Procedure

The weather conditions were comparable during the entire time of investigations. The mobile wind tunnel was aligned in the same direction as the crop rows, which were also aligned with the main wind direction in the study area. All experiments were conducted consistently. The wind speed was steadily increased within the first 5 min from 0 m s^{-1} to 15 m s^{-1} (at 0.5 m height) and held constant for an additional 55 min. Various experiments with running times up to 120 min were conducted before ensuring the soil loss was completely depleted during each experiment independent from plot or mechanical stress applied. Hence, the maximal soil loss was measured for each individual experiment.

The mobile wind tunnel simulated wind erosion events on three experimental plots. Plot 1 had a bare surface after steppe conversion in preparation for fallow. Small plant residues and clods were left from the land cover change (Fig. 5A). In contrast, emerging plants from the previous seeding covered the arable plots (Plot 2 and Plot 3). Barley (*Hordeum vulgare L.*) was grown on Plot 2, and maize (*Zea mays L.*) on Plot 3. Plant heights were comparable (0.15 m) but differed in densities and plant silhouettes. Barley had eight tillers (BBCH code 28) on average at the current phenological stage of development, and maize plants had four unfolded leaves (BBCH code 14) (Meier, 2018). The barley field was covered with 200 plants per m^2 and a row distance of 0.18 m. The maize field was covered with eight plants per m^2 with a row distance of 0.7 m and a distance between plants of 0.1–0.2 m. However, while Plot 2 had weak crusted soil (Fig. 5B), topsoil material on Plot 3 had already been pre-sorted (Fig. 5C) due to previous natural wind erosion events. Thus, there were already deposits in the slightly deeper seed rows, which were then easily mobilized again during the wind tunnel experiments, which were orientated along the rows.

Each plot was prepared in four ways before using the wind tunnel. The initial experiment was conducted on the original surface with the undisturbed surface structure and existing plants. The following experiment was conducted at the same position after removing the plants and refreshing and mixing the surface with a small hand-operated rake (three spikes with a length of 60 mm as a lifting tool). Hence, a low mechanical stress as made by a light cultivator was applied. We used the low mechanical stress application as a benchmark for comparing plots and applied stresses, because the initial situation differed in various

interfering factors such as soil structure and plant cover. A third experiment at the same position was prepared using a tool with three rotating spikes (radius of 70 mm as a turning tool) applying moderate stress with a disc harrow characterized by further breakdown of the aggregates. Finally, the fourth experiment was conducted at the same place after crushing all aggregates, similar to the pulverizing effect on tractor tire tracks or driving paths in the field.

2.3. Soil analyses

2.3.1. Topsoil and surface parameters

Topsoil samples for physical and chemical analyses were collected in each plot before the experiments from 0 to 25 mm depth using a flat square-cornered shovel (Larney, 2007). The topsoil's PSD was measured with a laser diffraction analyzer (Helos/KR+Quixel, Sympatec GmbH, Clausthal Zellerfeld, Germany). Before laser diffraction, 10 g soil was chemically pretreated with 30% hydrogen peroxide (H_2O_2) to oxidize organic binding material (Koza et al., 2021). In order to complete dispersion for texture analyses, 3 g of soil was pretreated with 0.05 M sodium pyrophosphate ($\text{Na}_4\text{P}_2\text{O}_7 \times 10 \text{ H}_2\text{O}$) and physically dispersed for 60 s with 60 W sonication. Particle size classes of clay (0–2 μm), silt (2–50 μm), and sand (50–2000 μm) were used to assign soil texture. Subclasses were used for further distinction (Soil Science Division Staff, 2017). Topsoils on all plots were identified as loamy sands (Soil Science Division Staff, 2017). However, while contents of sand, silt and clay were identical on Plot 1 and Plot 2 (sand: 76%, silt: 18%, clay: 6%), the sand content on Plot 3 was slightly higher (sand: 83%, silt: 13%, clay: 4%). The pH of 6.5 ± 0.2 (mean \pm standard deviation) and electrical conductivity of $137.3 \pm 57 \mu\text{S cm}^{-1}$ were measured in distilled water at a 1-to-2.5 soil-to-solution (weight-to-volume) ratio. Total carbon was analyzed by dry combustion of 1 g of soil at 1130 °C (varioMax Cube, Elementar Analysensysteme GmbH, Langenselbold, Germany). Total inorganic carbon was analyzed by dispersing 2 g of ground sample material in 50 ml 2 M HCl at 50 °C and subsequently detecting the released CO_2 (solITIC module interfaced to the varioMax Cube). The total carbon content of $15.5 \pm 1.7 \text{ g kg}^{-1}$ corresponds to the SOC because the inorganic part is negligible ($0.1 \pm 0.0 \text{ g kg}^{-1}$). The SOC content was slightly higher on the recently converted plot (Plot 1: 17.8 g kg^{-1}) compared to the arable plots (Plot 2: 14.9 g kg^{-1} , Plot 3: 13.8 g kg^{-1}). The gravimetric method determined soil water content (Gardner, 2018). Three samples were collected from each experimental plot and oven-dried at 105 °C for 24 h. The water content was calculated by the difference in sample mass before and after drying and was comparable between all runs ($2.2 \pm 0.6\%$).

Erodible fraction (EF) was determined by the dry sieving method. About 1 kg of dry topsoil was collected before each experiment. The EF can be calculated as the weight percent of aggregates < 0.84 mm after separating fragments (Chepil, 1962). In this study, a horizontal dry-sieve (López et al., 2007) with 0.85-mm openings (Koza et al., 2022) was used to calculate EF (%) with Eq. 3:

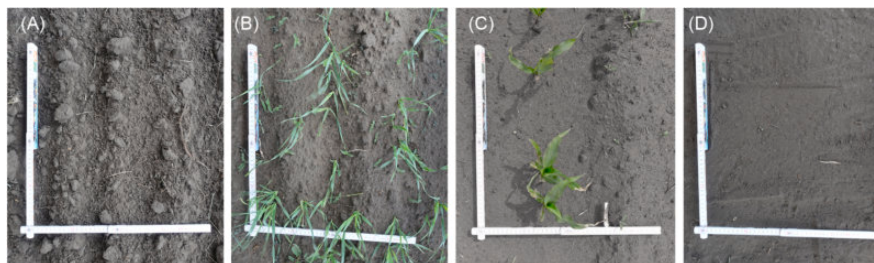


Fig. 5. The initial surface roughnesses: rough cloddy seedbed after steppe conversion on Plot 1 (A), a weak crust on Plot 2 grown with barley (B), and loose material in the rows of maize on Plot 3 (C). The surface roughness without plants and after applying high mechanical stress on Plot 3 (D). The folding ruler is 0.4 m \times 0.4 m, showing an area of 0.16 m^2 .

$$EF = \frac{W < 0.85}{TW} \times 100\% \quad (3)$$

where $W < 0.85$ is the weight (g) of < 0.85 -mm aggregates and TW is the initial weight (g) of the total sample. The risk of wind erosion is considered relatively high for soils with $EF > 60\%$ (Larney, 2007) and negligible for soils with $EF < 40\%$ (Chepil, 1953). The highest EF of the undisturbed topsoil was measured on the plot cultivated with maize (80.5%), the second highest on the plot cultivated with barley (68.4%), and the lowest after steppe conversion (54.8%). All three plots showed comparable EFs after applying high mechanical stress ($83.5 \pm 1.1\%$).

The aerodynamic roughness length (z_0) of each surface was derived as a mean from wind profile measurements with a hot-wire anemometer at three wind speeds. The roughness length of the surface can be calculated based on the logarithmic wind profile with Eq. 4:

$$u = \frac{u^*}{k} \ln\left(\frac{z-d}{z_0}\right) \quad (4)$$

where u is wind speed (m s^{-1}) at height z (m), u^* is the friction velocity (m s^{-1}), d is the displacement height, and k is the Kármán constant (~ 0.4). Soil roughness length was initially highest on the barley with 8.08 mm (Fig. 5B), second highest after steppe conversion with 7.40 mm (Fig. 5A), and lowest on maize with 5.17 mm (Fig. 5C). After high mechanical stress was applied, the roughness length was initially 0.20 mm on Plot 1, 0.19 mm on Plot 2, and 0.05 mm on Plot 3 (Fig. 5D). Topsoil and surface characteristics of laboratory and field measurements are presented in Table 1.

2.3.2. Aeolian sediments and depositions

Aeolian sediments collected during wind tunnel experiments were also analyzed with laser diffraction, but in combination with a dry dispersion unit (Helos/KR+Rodas Vibri/L, Sympatec GmbH, Clausthal Zellerfeld, Germany). This configuration determines the dry soil's ASD of 2 g in a free aerosol jet, measuring 29 physical classes up to 2 mm. The aggregate size classes microaggregates ($< 250 \mu\text{m}$) and macroaggregates ($> 250 \mu\text{m}$) were derived from the standard hierarchical aggregate order (Tisdall and Oades, 1982). Additionally, typical fractions of different modes of motion during wind erosion events were used for a better classification of aeolian sediments. These are long-term suspension ($< 20 \mu\text{m}$), short-term suspension ($20\text{--}70 \mu\text{m}$), modified saltation ($70\text{--}100 \mu\text{m}$), saltation ($70\text{--}500 \mu\text{m}$) and creep ($> 500 \mu\text{m}$) (Funk and Reuter, 2006; Kok et al., 2012; Shao, 2008).

Sediments collected by the MWACs at the ground level, 0.05 m and 0.10–0.35 m were also analyzed for SOC. Sediments collected by the SUSTRA were analyzed for pH, electrical conductivity, total carbon, total inorganic carbon, PSD, and ASD.

Aeolian depositions from natural wind erosion events in May 2022 were collected from the edges of both arable fields (Fig. 4C) by sampling the layer of buried vegetation (Larionov, 1993). They were analyzed equally to the topsoil and aeolian sediments described above for pH, electrical conductivity, total carbon, total inorganic carbon, PSD, and ASD.

2.4. Statistical analyses

RStudio (Version 4.1.2., RStudio Team) was used for statistical analyses and graphs (R Core Team, 2020). The Shapiro-Wilk test and histograms were applied to test all data for normal distribution. Consequently, the Spearman correlation (r_s) was performed between calculated sediment losses and all measured parameters. A correlation matrix was generated with "corrplot" (Taiyun and Simko, 2021), indicating the significance of correlations at a level of $p < 0.05$. The Randomized Complete Block Design was used to compare different mechanical stresses. Each level of stress was replicated on three plots. Statistically, the Kruskal-Wallis test was applied due to rank-based simulations. The Dunn's test was used to identify mean group values that are significantly different ($p \leq 0.1$).

3. Results

3.1. Relationship between soil losses and soil parameters

The results show significant correlations between soil loss, topsoil and surface characteristics. The strongest correlations occurred between soil loss, EF, and roughness length. The Spearman rank coefficient analysis showed a strong correlation between soil loss and EF ($r_s = 0.83$), sand ($r_s = 0.62$), as well as mechanical stress ($r_s = 0.60$). The strongest significant negative correlation was observed between soil loss and roughness length ($r_s = 0.73$) as well as silt ($r_s = 0.59$) and SOC ($r_s = 0.59$). Because parent material on the test site did not change between different experimental runs, there was consequently no correlation between applied mechanical stresses and topsoil texture characteristics (Fig. 6).

Table 1

Soil losses from three different plots with similar topsoil and different surface characteristics caused by different mechanical stresses similar to the disruptive forces soil experiences from a light cultivator (low), disc harrow (moderate), and tractor tires (high).

Plot	Mechanical stress	Topsoil characteristics							Surface characteristics		Soil losses		
		pH	Electrical conductivity	Soil organic carbon	Clay	Silt	Sand	Soil moisture	Erodible fraction	Roughness length	Total	Relative	
		(-)	($\mu\text{S cm}^{-1}$)	(g kg^{-1})	(%)	(%)	(%)	(%)	(%)	(mm)	(g m^{-2})	(%)	
Steppe conversion	1	Initial	6.6	72	17.8	6	18	76	1.8	55	7.40	11.7	55
		Low								56	5.21	21.4	(100)
		Moderate								67	5.29	27.1	127
		High								82	0.20	1230.3	5746
Arable	2	Initial (with barley)	6.6	129	14.9	6	18	76	3.0	68	8.08	33.8	14
		Low								71	3.80	245.6	(100)
		Moderate								61	5.36	617.1	251
		High								84	0.19	1761.0	717
	3	Initial (with maize)	6.1	211	13.8	4	13	83	1.7	80	5.17	1609.0	492
		Low								83	2.34	327.1	(100)
		Moderate								74	2.90	519.3	159
		High								85	0.05	5309.1	1623

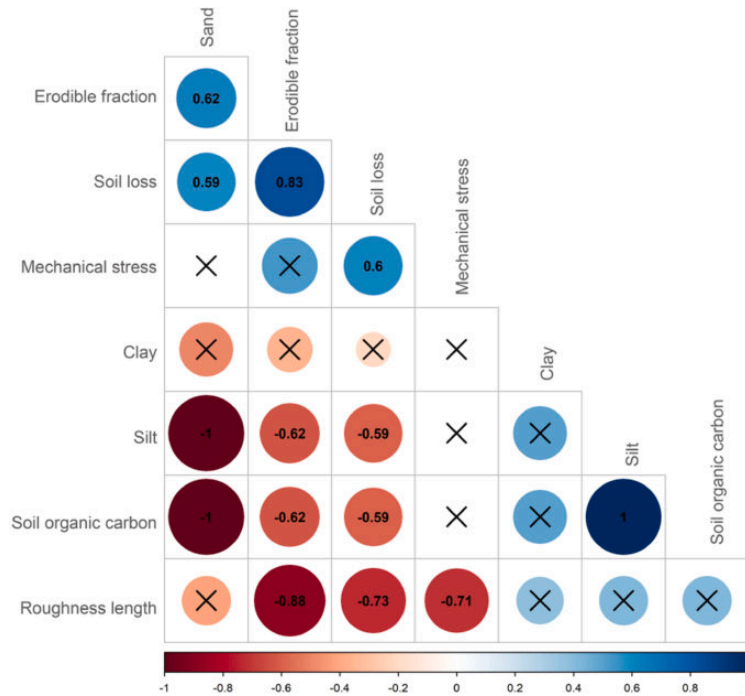


Fig. 6. Correlation matrix shows significant correlations ($p < 0.05$) between soil loss and topsoil and surface characteristics. The strongest correlations between soil loss, erodible fraction, and roughness length are revealed.

3.2. Quantity of soil losses

The wind tunnel experiments showed great differences, already under the initial situations. The lowest soil losses were measured on the rough surface after the conversion of steppe to arable land (11.7 g m^{-2})

and on the weak-crueted and well-covered surface of barley (33.8 g m^{-2}). The highest soil loss was measured on maize (1609.0 g m^{-2}), although plants were also present on the surface.

Soil losses significantly differed between the low and high mechanical stress applications. Overall, increasing mechanical stress by tillage

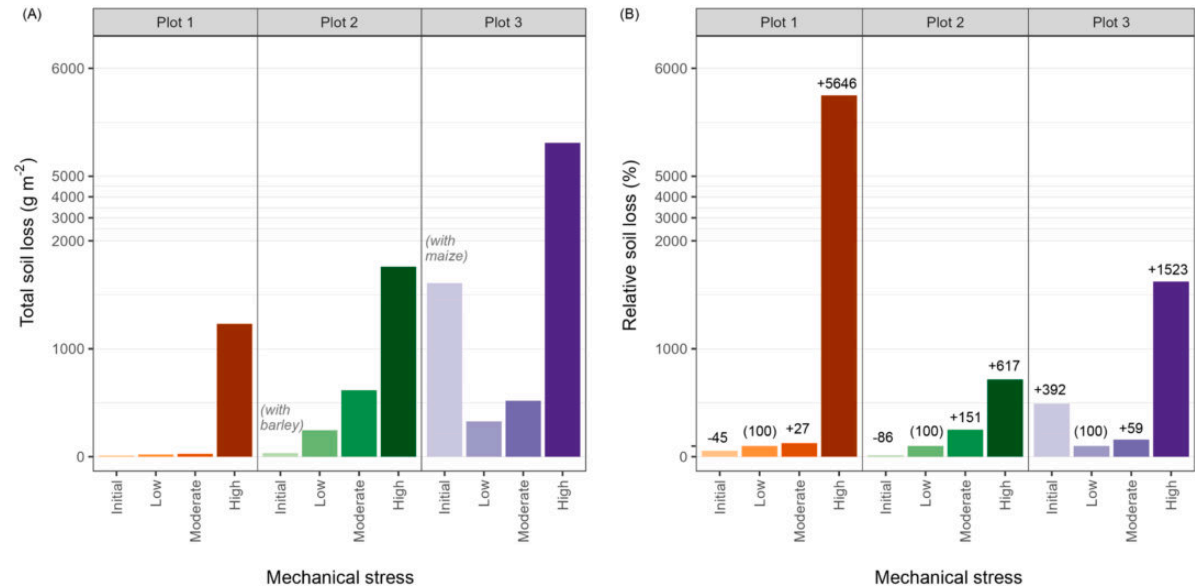


Fig. 7. Total (A) and relative (B) soil loss derived from wind tunnel experiments on three test plots with the initial situation and after different mechanical stresses were applied. During the early growth stages of maize, the soil loss is higher than on the bare surface. Please beware of the compressed scale.

or tractor tires increased total soil losses on all three plots considerably (Fig. 7A). The absolute soil losses after tractor tire crushing on Plot 1 (1230.3 g m^{-2}) and Plot 2 (1761.0 g m^{-2}) were in a similar range, which has the same texture but small differences in SOC. Soil loss on Plot 3 was several times higher (5309.1 g m^{-2}), where the highest sand content and lowest SOC are present. Regarding the cultivated area, tractor tire tracks only partially affect agricultural fields. Tillage tools for cultivating barley and maize have a working width of six meters. The tractor's two rear tires have a total width of 1.42 m. Hence, about 23% of each field is disrupted by high mechanical stress that can pulverize aggregates. From this field-size perspective, the relative changes in soil losses between low and high mechanical stress application showed that the application of tillage creates soil structures susceptible to wind erosion, but tractor tires increase soil losses by multiple (Fig. 7B).

With an estimated bulk density of 1.3 g cm^{-3} on the test site, the simulated wind erosion event would cause a loss of topsoil depth of 0.01 mm after steppe conversion and 0.03–1.24 mm after further tillage implementations. On tractor tire tracks, which account for about one-fourth of the fields, 0.95 mm of topsoil would be eroded on Plot 1, 1.35 mm on Plot 2, and 4.08 mm on Plot 3.

3.3. Changes in particle and aggregate size distributions

The PSD of topsoil and aeolian sediments from all plots showed that soils are both bimodal distributed. The two maxima were $7.5 \mu\text{m}$ and $210.0 \mu\text{m}$ in particle size. Fine silt ($2\text{--}20 \mu\text{m}$) is up to 14%, coarse silt is below 5%, and very fine sand ($50\text{--}100 \mu\text{m}$) is up to 16%. The fine to medium sand particles ($100\text{--}500 \mu\text{m}$) are the dominant particle sizes with at least 57% (Fig. 8). Comparing the particle size classes of clay, silt, and sand from the topsoil and the aeolian sediments showed a tendency to more finer particles in the sediments of the steppe conservation plot, already beginning in the clay fraction (Fig. 8A, Appendix Table A1). On Plot 2 and 3, aeolian sediments had lower silt and very fine sand content but much higher fine and medium sand fractions ($100\text{--}500 \mu\text{m}$) than the topsoil (Fig. 8B, Appendix Table A1). The fine and medium sand subclasses together showed a relative increase of 31% on Plot 2 (fine and medium sand: topsoil = 54%, aeolian sediments = 71%) and 19% on Plot 3 (fine and medium sand: topsoil = 59%, aeolian sediments = 70%). Plot 1 only showed a relative increase of 4% (fine and medium sand: topsoil = 54%, aeolian sediments = 56%) because of contrary trends within these two subclasses. However, this trend in which fine and medium sand particles' content increases during wind erosion is explicit if PSD from the depositions is considered. The depositions showed a distinct relative increase of the fine and medium

sand of 41% for barley (fine and medium sand: deposition = 76%) and 34% for maize (fine and medium sand: deposition = 79%) compared to the topsoil. This also becomes apparent by the increasing slope of the PSD curve for the aeolian sediments. On the contrary, particles below $100 \mu\text{m}$ decrease in the aeolian sediments, especially the fine silt fraction. In general, results showed no major change in clay particles. Coarse sand particles ($500\text{--}1000 \mu\text{m}$) get detached only occasionally and are less than 1% in the depositions.

Results of aggregate size analysis showed that independent of the samplers' height, aeolian sediments contained mainly (65–86%) microaggregates ($<250 \mu\text{m}$) and some (14–35%) macroaggregates ($>250 \mu\text{m}$). Non-erodible aggregates larger than $850 \mu\text{m}$ were collected only in negligible amounts (Fig. 9). Even though differences in ASD at ground level and 0.05 m height were minimal, the percentage of microaggregates decreased with increasing height. Aggregates suitable for typical long-term suspension ($<20 \mu\text{m}$) were collected on the steppe conservation plot (2–4%) but only marginally on the arable plots. Comparing aeolian sediments at the ground level with sediments from 0.10 to 0.30 m height showed that aggregates suitable for short-term suspension increased on Plot 1 with height (19–29%), but decreased on Plot 2 (13–6%) and Plot 3 (12–9%) (Appendix Table A2). At the same time, the aggregate fraction typical for saltation changed contrary. They decreased on Plot 1 (78–64%) (Fig. 9A) and increased on Plot 2 (81–88%) or remained at a high level on Plot 3 (86–85%) (Fig. 9B). While aeolian sediments collected from arable plots above 0.05 m height were larger in size than sediments collected near the ground, this applied for only for 20% of the distribution from the steppe conservation plot (crossing point between solid and dashed/dotted line in Fig. 9A).

Comparing particle and aggregate size analyses from aeolian depositions revealed that PSD is bimodal while aggregates are unimodally distributed. However, there is no major difference for about 80% of the distribution. Independent of the method, particles and aggregates above $100 \mu\text{m}$ were similarly distributed. In contrast, size distributions showed that depositions contain about 20% of particles $<50 \mu\text{m}$ and 10% of particles $<20 \mu\text{m}$ while aggregates $<50 \mu\text{m}$ are rare and aggregates $<20 \mu\text{m}$ are negligible (Fig. 10).

3.4. Quantity of soil organic carbon losses

The SOC content in the topsoil was slightly higher on the steppe conservation plot compared to arable Plots 2 and 3. Comparing the SOC contents of topsoil and aeolian sediments from all plots revealed major differences between the steppe conservation plot and the arable plots. While there was a SOC increase of 69% in the aeolian sediments

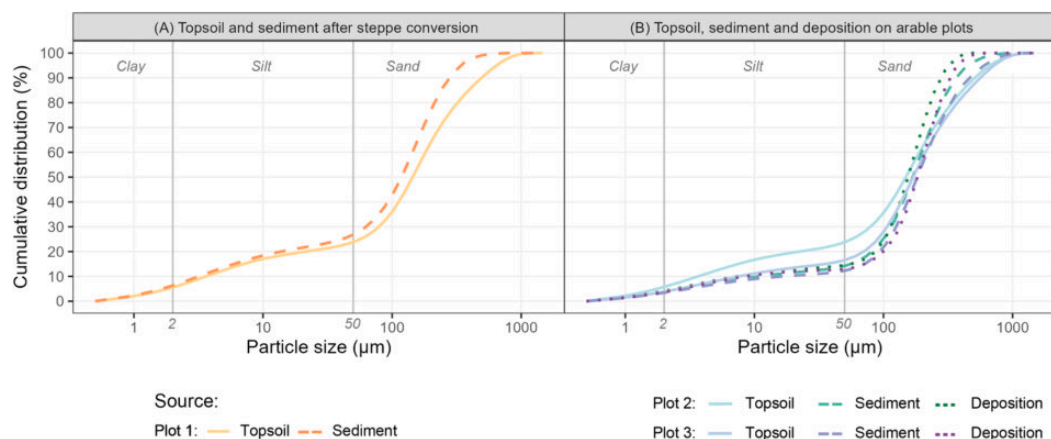


Fig. 8. Particle size distribution from topsoils (solid line), aeolian sediments collected during wind tunnel experiments (dashed line) by SUSTRA, and depositions from natural wind erosion events (dotted line).

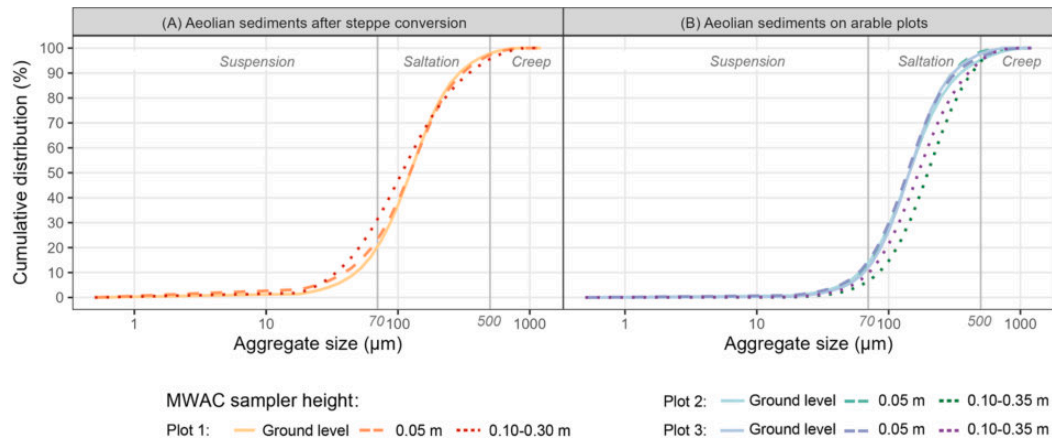


Fig. 9. Aggregate size distribution from aeolian sediments collected during wind tunnel experiments by MWAC samplers at the ground level (solid line), 0.05 m (dashed line), and 0.10–0.35 m (dotted line) during wind tunnel experiments.

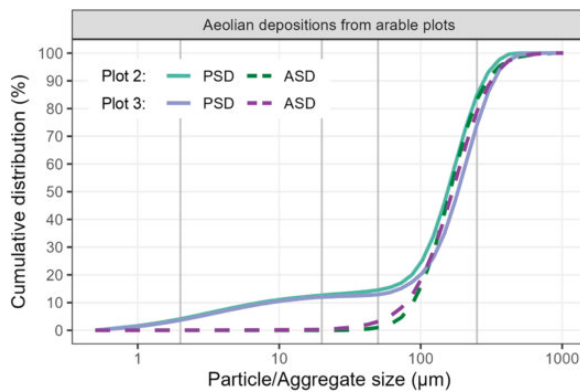


Fig. 10. Comparison of the particle (solid line) and aggregate (dashed line) size distribution of aeolian depositions from natural wind erosion events on arable plots.

compared to the topsoil on Plot 1, there was a decrease of 13% on Plot 2 and a decrease of 35% on Plot 3. The SOC decline was also apparent in the depositions, similar to the PSD results. The depositions showed a decline of SOC in the depositions of 22% on Plot 2% and 36% on Plot 3 (Fig. 11, Appendix Table A3). The calculated soil loss and the SOC content of the aeolian sediments could be used to estimate the total losses of organic carbon. The loss of SOC mass was estimated to be 0.3 g m^{-2} on the steppe conversion plot, 0.4 g m^{-2} on Plot 2, and 14.3 g m^{-2} on Plot 3. However, after high mechanical stress, the total organic carbon loss on Plot 1 with 36.9 g m^{-2} was higher than Plot 2 with 22.8 g m^{-2} , even though higher total soil loss was recorded. Similar to the total soil loss, the mass loss of organic carbon was highest on Plot 3 with 47.3 g m^{-2} .

The ratio of the SOC content collected by MWACs at different heights showed no variation between ground level and near-ground (0.05 m height). Still, the SOC ratio was enriched in aeolian sediments collected at a sampler height of 0.18 m on the steppe conversion plot and depleted on the arable plots at 0.20 m height. The contrary trends between the steppe conversion and arable plots are visualized in Fig. 12. Soil organic loss was further proven by observing depletions in the aeolian depositions of Plot 2 (SOC ratio = 0.78) and Plot 3 (SOC ratio = 0.64) (Fig. 12, Appendix Table A3).

4. Discussion

4.1. Influence of topsoil and surface on soil erodibility

Significant relationships between EF and roughness length, as well as mechanical stress and roughness length, prove that the interactions between properties affect wind soil erodibility. On the test site, EF and roughness length have the greatest effect on soil loss. This finding aligns well with previous studies by Zhang et al. (2004), Sirjani et al. (2019) and Shahabinejad et al. (2019). Altogether, our results reinforce the importance of ASD and linked roughness length to the soil's susceptibility. Recent studies showed that soil aggregation in northern Kazakhstan depends on organic binding material, favored by high amounts of silt and clay particles (Koza et al., 2022, 2021). This also applies to this study's test site, where soil loss increases with decreasing silt and SOC content. Nevertheless, the typical amount of SOC on the test site is comparable with results from sandy soils worldwide (Yost and Hartemink, 2019). Thus, the sandy soils of the Kazakh Steppe can be easily incorporated into models or evaluation schemes of erodibility.

4.2. Soil losses by wind erosion

Historical climate data (1991–2020) show that wind speeds above the threshold of 7.4 m s^{-1} occur on average about 6.5% of the year (Fig. 1C). Based on the frequency distribution of wind speeds above 7 m s^{-1} and the corresponding transport capacity of each wind speed, the weighted transport capacity was derived. Frequency-related transport capacity is highest between 8 and 11 m s^{-1} (Fig. 2), accounting for more than 60% of the total loss capacity in the study area. Wind tunnel experiments were conducted with a wind speed of 15 m s^{-1} (at 0.5 m height). Considering the logarithmic wind profile, the wind tunnel simulations are comparable to natural wind speeds above 13.2 m s^{-1} (at 10 m height) on a low roughness length of 0.05 mm. On average (1991–2020), wind speeds exceed 13.2 m s^{-1} for about 6 h per year (Meteoblue, 2023), but account for more than 10% of the frequency-related transport capacity. The overall outcome is consistent with the findings from northeast Germany (Funk et al., 2023). Please note that the mentioned weather data are hourly averages, which underestimate wind erosion because gusts are not considered, or on the contrary, wind erosion is overestimated if soil is covered.

It is well known that sandy soils, which are dominant in the study area, are more susceptible to wind erosion than fine-textured soils (Chepil, 1952). This result aligns with a previous study (Koza et al., 2022) on a test site with loamy sand about 200 km away, where the soil

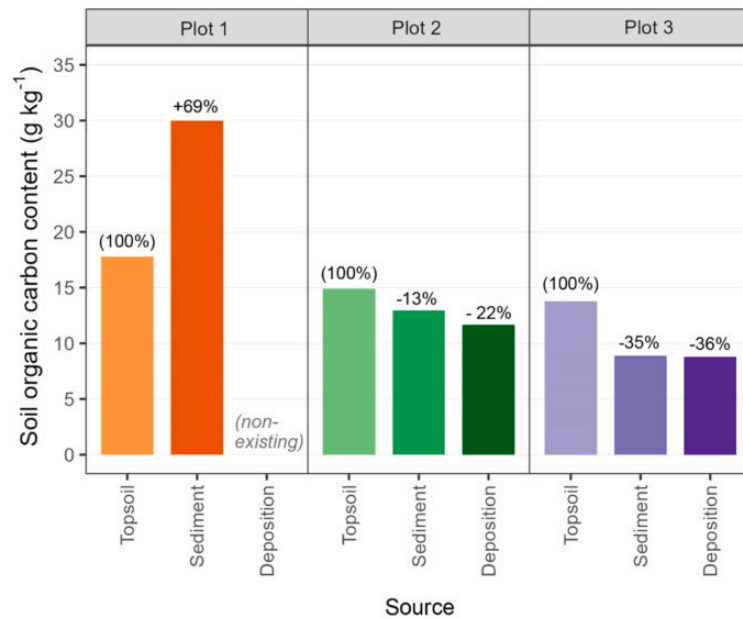


Fig. 11. Soil organic carbon content from topsoil, aeolian sediments collected during wind tunnel experiments by SUSTRA, and aeolian depositions from natural wind erosion events. Relative organic loss is shown above each bar.

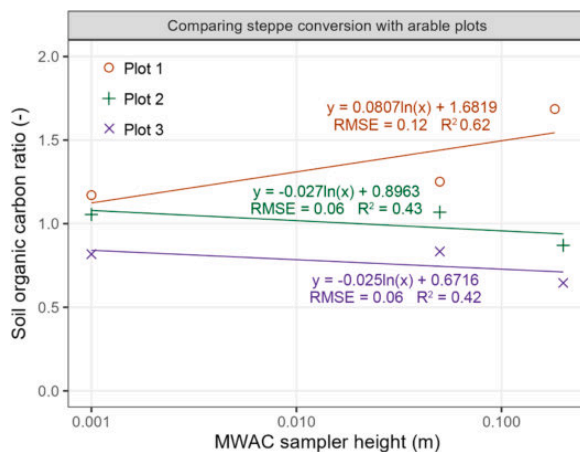


Fig. 12. Comparison of soil organic carbon ratio after steppe conversion (Plot 1) and arable plots (Plot 2 and 3) for different heights. Additionally, trend lines are shown.

erodibility was determined from aggregate stability tests. The previous and present studies underline the continuation of the degradation processes by wind erosion in the study area. The wind tunnel itself constrains saltation during simulation because the calculated Froude number is above 20. Therefore, soil losses calculated from the vertical distribution of the mass fluxes in the tunnel provide safe estimates because transport profiles of real events are assumed to increase more with height, resulting in higher transport rates. The lowest soil loss was measured after the recent steppe conversion (Plot 1) on the bare surface. Immediately after converting steppe to arable land, aggregate stability was at its best, and the SOC content was highest. Since it was the first intervention after a long period without tillage, these aggregates still

represent a part of the natural soil structure. Clods resulting from steppe conversion were decisive for the high roughness length and an effective measure against wind erosion. With further tillage, these clods are subjected to further breakdown. Similar results were obtained from cultivated fine-textured soils of the semi-arid region of Argentina (Colazo and Buschiazzo, 2010) and northwest China (Zhang et al., 2004). Comparing the effects of vegetation cover of barley and maize showed that the soil loss by wind erosion was highest on maize. Even though both arable plots had soils with EFs above 60%, indicating a high erodibility risk (Larney, 2007), the roughness length was lowest on maize. The relatively low number of plants with high row distances favored wind erosion in this early plant growth stage. With a mobile wind tunnel, Funk and Engel (2015) showed that wind can blow below the plant canopy of maize without considerable resistance throughout different growth stages. Similar results were obtained by Burri et al. (2011) for perennial ryegrass on sand. Our results for maize support the findings that soil losses during early growth stages can be higher than losses on the bare surface. It is also important to remember that soil loss on maize is different between plant rows and close to the plants themselves. Without considering the variability over the wind tunnel width, the shown results are estimations (Dong et al., 2004; Funk and Engel, 2015). For maize, the horizontal distribution of the soil loss across the wind tunnel width is highest close to the plant row and lowest between rows (Funk and Engel, 2015). Therefore, the soil loss on maize is lower if the row orientation is not parallel to the wind. In contrast, soil loss was lower with barley plants compared to the bare surface.

Farming practices can affect susceptibility considerably. The experiments showed that the mechanical disruptions in this study caused higher EFs and lower roughness lengths, accompanied by increased soil loss. Disc harrow (turning and mixing tool) caused higher soil loss than tillage with a light cultivator (lifting tool). Even though we only imitated different tillage practices, the findings agree with the study by Tanner et al. (2016), where real practices were implemented in field experiments. Our results confirm the presumption that mechanical stress by tillage weakens soil structure by breaking down aggregates, leading to increasing erodibility.

Our experiment also proved that crushing soil clods with tractor tires under dry conditions is a key contributor to soil loss from wind erosion. This worst-case scenario for aggregate breakdown is considered an important wind erosion source in the study area. Our results align with a study on Polish loamy sands, in which tractor tires were identified as a major wind erosion source (Podsiadłowski, 1988). An important step in the overall consideration of wind erosion susceptibility will be to incorporate this aspect into the design of cropping systems. Measures that prevent the destruction of dry aggregates include the consideration of soil moisture during agricultural practices, such as the timing of sowing, the temporal variation during the day, and the variability of tillage depth.

This study proves that soil degradation by management is an ongoing challenge in the study area representing semi-arid ecosystems of Central Asia (Robinson, 2016). The main objectives of erosion control are maintaining soil fertility and preventing soil loss rates from exceeding natural soil formation (Larionov, 1993). In Central Asia, conservation agriculture has developed rapidly over the past 15 years, particularly in northern Kazakhstan. Currently, 10.5 million hectares are under reduced tillage, and about 2.5 million hectares (about 15.6%) of cropland are under permanent no-till rotations (Kassam et al., 2019). No-till systems cut through the residues, leaving the soil less exposed to wind or the disruptive forces of saltating particles (Verhulst et al., 2010). In addition, no-till also improves uniform snow depositions, limits evaporation and weed growth, while yields stabilize after several years of consistent implementation (Lafond et al., 2006; Meinel et al., 2014). No-till farming practices could potentially solve the wind erosion problem in semi-arid steppe soils. It is expected that no-till is likely to expand in Asia (Lal et al., 2007) due to the increasing availability of suitable herbicides and high-quality seeding technologies (Grunwald et al., 2016). However, Central Asia's institutional, socioeconomic and agroecological contexts are diverse and require a geographically differentiated approach. In northern Kazakhstan, replacing the common bare summer fallow with cover crops such as legume forages is recommended (Suleimenov et al., 2016). However, supplies for no-till systems are sometimes too expensive for farmers and there is still a need for knowledge regarding the application under semi-arid climatic conditions (e.g., heavy rains in spring make it difficult to apply herbicides successfully). Overall, information on crop management based on conservation agriculture in Central Asia is incomplete (Kienzler et al., 2012). At the test site, strip-till was implemented in 2023 as an adaptation measure after severe soil degradation by wind occurred in 2022.

4.3. Particle and aggregate size distributions of the soil losses

The results of this study show the sorting process caused by wind erosion events on all plots. Noticeably, on the steppe conversion plot, all particles finer than medium sand (<200 μm) are enriched in the aeolian sediments except for clay. In contrast, only the fine and medium sand particles (100–500 μm) are enriched in the aeolian sediments and depositions on the arable plots. In conclusion, relatively more silt particles get eroded on the recently converted field compared to the arable fields that have been under cultivation for three years already. Lackóová et al. (2021) studied the long-term impacts of wind erosion on PSD in a dune region of Slovakia. They showed that fine particles could be eroded within a few years, changing soil texture. Our results indicate that particles below 500 μm are being carried away, causing a shift of the soil texture class into sand. This can also be detected in the results (Fig. 8), where the PSD curve follows a trend towards the typical distribution curve of dune sands with textural particles ranging from 100 μm to 1000 μm (Pye, 1994).

Furthermore, our results of aggregate size analysis from aeolian sediments are within the typical range of saltation. Most aggregates have a size of 70–500 μm , which is in the common saltation fraction (Shao, 2008). Measured aggregate sizes align with various studies showing that mainly microaggregates between 20 and 250 μm are depleted by wind

(e.g., Yan et al., 2018). This aligns with Zamani and Mahmoodabadi (2013), who suggested that macroaggregates cause the low EF of soil in arid and semi-arid environments. Creeping particles (>500 μm) were only trapped rarely. Aggregates with sizes suitable for long-term (<20 μm) and short-term suspension (20–70 μm) (Shao, 2008) were collected on the steppe conversion plot but only rarely on the arable plots. Still, the aggregate size of each transport mode may vary depending on wind speed, aggregate density, and saltation/creep load change (Hagen, 2001).

Analyzing PSD and ASD of aeolian depositions from natural wind erosion events underlines the results obtained with the wind tunnel experiments. They confirm the functionality of the mobile wind tunnel for imitating real events. The PSD and ASD from aeolian sediments collected during saltating processes are similar to the distribution of the depositions. Comparing PSD and ASD within the depositions reveals no differences for particles > 100 μm , which account for 75–81% of the soil. Hence, fine sand particles and coarser do not aggregate and can saltate several millimeters to several meters along the surface (Shao, 2008). About 19–25% of aggregates in the depositions are between 20 μm and 100 μm . Those aggregates account for all clay and silt particles bound together with organic matter. They are suitable for modified saltation and short-term suspension, typically accounting for several hours in the air while being transported hundreds of kilometers (Shao, 2008).

4.4. Soil organic carbon losses by wind erosion

The results of this study show the selective character of erosion processes, as the clay and silt fractions of the soils contain disproportionately greater amounts of SOC (Chappell et al., 2013; Zobeck and Fryrear, 1986). Comparing topsoil and aeolian sediments revealed enrichment of SOC in the eroded materials. Hence, wind erosion can be one factor responsible for the typical decline in SOC content in the topsoil caused by steppe conversion to arable land. In our recent study, we also observed this decline between grass- and cropland in northern Kazakhstan (Koza et al., 2022), similar to the nearby Kulunda steppe (Bischoff et al., 2016). Still, Gregorich et al. (1998) reviewed that carbon losses by mineralization are dominant within the first years after conversion, and erosion becomes a more important process after establishing a new equilibrium a few years later. From the recently converted plot, fine particles and aggregates suitable for suspension were removed, while on the arable plots, the dominant fractions were in the size range typical of saltation. Aeolian sediments and depositions were not enriched with SOC. The slightly enriched SOC ratio of the steppe conversion plot can be considered a reasonable value for SOC loss from topsoil by suspension and is comparable to various studies (Nerger et al., 2017). In contrast, the ratio of the arable plots is < 1. A loss of SOC is registered but somewhat unusual because SOC ratios in the saltation layer from literature are mainly > 1 (Li et al., 2020a; Nerger et al., 2017). This means that disproportional amounts of SOC do not get removed by saltation on this loamy sand test site. However, the depletion of SOC in the aeolian sediments from arable plots can be easily explained by the higher amount of fine and medium sands in aeolian sediments and depositions, unfavorable for the organic binding material. Zenchelsky et al. (1976) observed that the SOC ratio also depends on the wind speed. High wind speeds (11.4 m s^{-1}) resulted in lower SOC ratios compared to low speeds (7.3 m s^{-1}). Larger soil fractions containing more mineral than organic matter were eroded with increasing speed. This aligns with our experimental setup of 15 m s^{-1} and the archived results.

Therefore, wind erosion does not necessarily lead to a decline in primary productivity on cropland. Still, it is important to consider that the total soil loss was substantially higher on arable plots where aeolian sediments were depleted of SOC, compared to the low soil loss on the steppe conversion plot with the highly SOC-enriched sediments. Hence, estimations revealed that after applying high mechanical stress, the soil

loss on the arable plot with the same texture (Plot 2) is higher than on the steppe conversion plot, but the total SOC loss is lower.

5. Conclusions

This study assesses the risk of wind erosion in the semi-arid steppe of Kazakhstan, one of Central Asia’s most important regions for growing crops. We show first effects of wind erosion as a soil degradation process based on results obtained from field experiments:

- i. Mobile wind tunnel experiments verify that agricultural management practices severely increase the risk of wind erosion on sandy steppe soils in different ways. After the recent steppe conversion, soil loss was low. On arable plots that underwent cultivation during the past three years, soil losses increased considerably. In the early growing season, fields cultivated with barley were less affected by wind erosion than maize fields. Among common agricultural practices, a disc harrow caused higher soil losses than a light cultivator. The most severe soil losses originate from experiments simulating tractor tire tracks or driving paths in the field.
- ii. Wind erosion caused sorting processes on all plots. After recent steppe conversion, PSD and ASD of the aeolian sediments showed a composition that indicates a higher susceptibility for suspension transport. At the same time, aeolian sediments and depositions originated from arable plots were generally coarser and in the typical size range of saltation.
- iii. Associated with the sorting process of particles and aggregates on the recently converted plot, the suspension-dominated aeolian sediment was enriched in SOC and blown out from the field. In contrast, the saltation processes on the arable plots caused a depletion of SOC in the aeolian sediments and resulted in depositions on the field edges with lower SOC.

Altogether, wind erosion due to steppe conversion is a considerable

factor causing soil degradation on sandy soils. The risk of wind erosion will further increase due to climate change. Consequently, understanding the effects of wind erosion on soil and SOC losses is necessary for supporting sustainable soil management and mitigating soil degradation. Our wind tunnel experiments successfully provided first results to quantify and qualify these processes.

Funding source

This study was supported by the German Federal Ministry of Education and Research (BMBF) by funding the research project: Innovative Solutions for Sustainable Agricultural and Climate Adaptation in the Dry Steppes of Kazakhstan and Southwestern Siberia (ReKKS) – grant number 01LZ1704B.

Acknowledgements

We are particularly grateful to Lasse Pein for his contribution to the mobile wind tunnel. Thanks to Timur Kabrulov for his local expertise and support during field experiments. We express our thanks to Dorothee Kley for logistical assistance and Michael von Hoff for conducting laser diffraction analyses. We thank editor Laura Alakukku and the reviewers for their valuable feedback on this manuscript.

Declaration of competing interest

The authors declare that they have no known competing financial interests or personal relationships that could have appeared to influence the work reported in this paper.

Data availability

All data supporting the findings of this study were reviewed and are openly available at <https://doi.org/10.4228/ZALF-QQ16-T967>.

Appendix

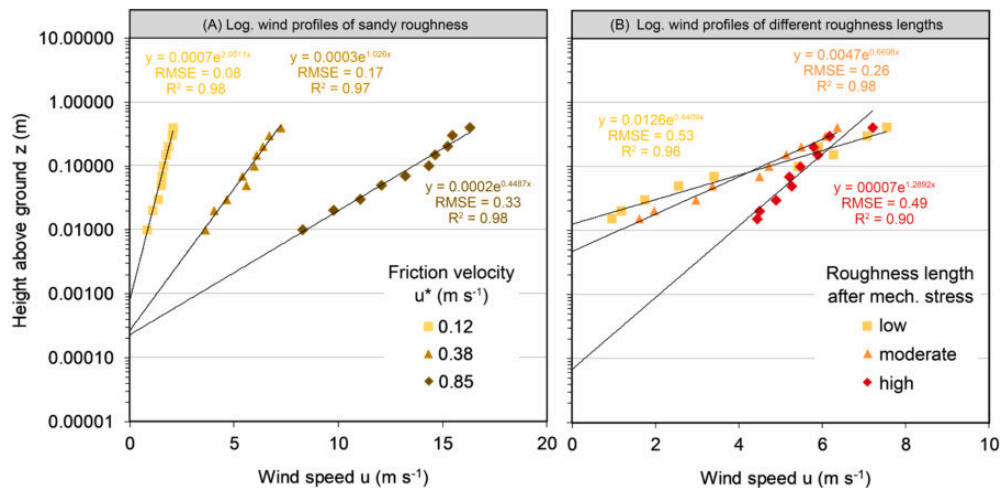


Fig. A1. Logarithmic wind profiles of sandy roughness under three different friction velocities derived from three different wind speeds (A) and logarithmic wind profiles of different roughness lengths (equal wind speed) after low (light cultivator), moderate (disc harrow), and high (tractor tires) mechanical stress application (B).

Table A1

Particle size classes and selected subclasses from topsoil, aeolian sediments, and depositions. The subclasses of fine/coarse clay and very coarse sand are not shown.

Plot	Source	Particle size classes (USDA)			Selected particle size subclasses (USDA)					
		Clay 0–2 µm (%)	Silt 2–50 µm (%)	Sand 50–2000 µm (%)	Fine silt 2–20 µm (%)	Coarse silt 20–50 µm (%)	Very fine sand 50–100 µm (%)	Fine sand 100–200 µm (%)	Medium sand 200–500 µm (%)	Coarse sand 500–1000 µm (%)
1	Topsoil	6	18	76	14	4	12	28	26	9
	Sediment	6	21	73	15	5	16	34	22	1
2	Topsoil	6	18	76	14	4	12	26	28	10
	Sediment	3	11	86	8	3	11	35	36	3
3	Deposition	4	10	85	9	2	10	45	30	0
	Topsoil	4	13	83	10	3	11	29	30	12
3	Sediment	3	9	88	7	2	9	33	37	8
	Deposition	4	9	87	8	1	7	37	43	1

Table A2

Aggregate size and modes of motion classes in aeolian sediments collected during wind tunnel experiments.

Plot	MWAC height	Aggregate size classes		Modes of motion classes				
		Micro- aggregates < 250 µm (%)	Macro- aggregates > 250 µm (%)	Long-term suspension < 20 µm (%)	Short-term suspension 20–70 µm (%)	Modified saltation 70–100 µm (%)	Saltation 70–500 µm (%)	Creep > 500 µm (%)
1	Ground level	86	14	2	19	17	78	2
	0.05 m	85	15	4	20	15	74	3
	0.10–0.30 m	83	17	3	29	16	64	4
2	Ground level	80	20	1	13	15	81	5
	0.05 m	83	17	1	12	14	86	2
	0.10–0.35 m	65	35	0	6	8	88	5
3	Ground level	83	17	1	12	15	86	2
	0.05 m	83	17	1	13	15	82	4
	0.10–0.35 m	73	27	0	9	12	85	5

Table A3

Soil organic carbon content from topsoil, aeolian sediments, and depositions, as well as soil organic carbon ratio as content from the eroded material to the content from the topsoil.

Plot	Source	Measured	Calculated	MWAC height	Measured	Calculated
		Soil organic carbon content (g kg ⁻¹)	Soil organic carbon ratio (-)		Soil organic carbon content (g kg ⁻¹)	Soil organic carbon ratio (-)
1	Topsoil	17.8	/	Ground level	20.8	1.17
	Sediment	30.0	1.69	0.05 m	22.3	1.25
2	Topsoil	14.9	/	0.10–0.30 m	30.0	1.69
	Sediment	13.0	0.87	Ground level	15.7	1.06
3	Deposition	11.7	0.78	0.05 m	15.9	1.07
	Topsoil	13.8	/	0.10–0.35 m	13.0	0.87
3	Sediment	8.9	0.65	Ground level	11.3	0.82
	Deposition	8.8	0.64	0.05 m	11.5	0.83
				0.10–0.35 m	8.9	0.65

References

- Aubekerov, B., Gorbunov, A., 1999. Quaternary permafrost and mountain glaciation in Kazakhstan 16. [https://onlinelibrary.wiley.com/doi/10.1002/\(SICI\)1099-1530\(199901/03\)10:1%3C65::AID-PPP306%3E3.0.CO;2-X](https://onlinelibrary.wiley.com/doi/10.1002/(SICI)1099-1530(199901/03)10:1%3C65::AID-PPP306%3E3.0.CO;2-X).
- Bezák, N., Mikoš, M., Borrelli, P., Alewell, C., Alvarez, P., Anache, J.A.A., Baartman, J., Ballabio, C., Biddoccu, M., Cerdà, A., Chalise, D., Chen, S., Chen, W., De Girolamo, A. M., Gessesse, G.D., Deumlich, D., Diodato, N., Efthimiou, N., Erpul, G., Fiener, P., Freppaz, M., Gentile, F., Gericke, A., Haregeweyn, N., Hu, B., Jeanneau, A., Kaffas, K., Kiani-Harchegani, M., Villuendas, I.L., Li, C., Lombardo, L., López-Vicente, M., Lucas-Borja, M.E., Maerker, M., Miao, C., Modugno, S., Möller, M., Naipal, V., Nearing, M., Owusu, S., Panday, D., Patault, E., Patriche, C.V., Poggio, L., Portes, R., Quijano, L., Rahdari, M.R., Renima, M., Ricci, G.F., Rodrigo-Comino, J., Saia, S., Samani, A.N., Schillaci, C., Syrris, V., Kim, H.S., Spinola, D.N., Oliveira, P.T., Teng, H., Thapa, R., Vantas, K., Vieira, D., Yang, J.E., Yin, S., Zema, D.A., Zhao, G., Panagos, P., 2021. Soil erosion modelling: a bibliometric analysis. *Environ. Res.* 197, 111087 <https://doi.org/10.1016/j.envres.2021.111087>.
- Bischoff, N., Mikutta, R., Shibistova, O., Puzanov, A., Reichert, E., Silanteva, M., Grebennikova, A., Schaarschmidt, F., Heinicke, S., Guggenberger, G., 2016. Land-use change under different climatic conditions: consequences for organic matter and microbial communities in Siberian steppe soils. *Agric. Ecosyst. Environ.* 235, 253–264. <https://doi.org/10.1016/j.agee.2016.10.022>.
- Borrelli, P., Alewell, C., Alvarez, P., Anache, J.A.A., Baartman, J., Ballabio, C., Bezák, N., Biddoccu, M., Cerdà, A., Chalise, D., Chen, S., Chen, W., De Girolamo, A.M., Gessesse, G.D., Deumlich, D., Diodato, N., Efthimiou, N., Erpul, G., Fiener, P., Freppaz, M., Gentile, F., Gericke, A., Haregeweyn, N., Hu, B., Jeanneau, A., Kaffas, K., Kiani-Harchegani, M., Villuendas, I.L., Li, C., Lombardo, L., López-Vicente, M., Lucas-Borja, M.E., Märker, M., Matthews, F., Miao, C., Mikoš, M., Modugno, S., Möller, M., Naipal, V., Nearing, M., Owusu, S., Panday, D., Patault, E., Patriche, C.V., Poggio, L., Portes, R., Quijano, L., Rahdari, M.R., Renima, M., Ricci, G.F., Rodrigo-Comino, J., Saia, S., Samani, A.N., Schillaci, C., Syrris, V., Kim, H.S., Spinola, D.N., Oliveira, P.T., Teng, H., Thapa, R., Vantas, K., Vieira, D., Yang, J.E., Yin, S., Zema, D.A., Zhao, G., Panagos, P., 2021. Soil erosion modelling: a

- global review and statistical analysis. *Sci. Total Environ.* 780, 146494 <https://doi.org/10.1016/j.scitotenv.2021.146494>.
- Bronick, C.J., Lal, R., 2005. Soil structure and management: a review. *Geoderma* 124, 3–22. <https://doi.org/10.1016/j.geoderma.2004.03.005>.
- Burri, K., Gromke, C., Lehning, M., Graf, F., 2011. Aeolian sediment transport over vegetation canopies: a wind tunnel study with live plants. *Aeolian Res.* 3, 205–213. <https://doi.org/10.1016/j.aeolia.2011.01.003>.
- Cerdà, A., Flanagan, D.C., le Bonis, Y., Boardman, J., 2009. Soil erosion and agriculture. *Soil Tillage Res.* 106, 107–108. <https://doi.org/10.1016/j.still.2009.10.006>.
- Chappell, A., Webb, N.P., Butler, H.J., Strong, C.L., McTainsh, G.H., Leys, J.F., Viscarra Rossel, R.A., 2013. Soil organic carbon dust emission: an omitted global source of atmospheric CO₂. *Glob. Change Biol.* 19, 3238–3244. <https://doi.org/10.1111/gcb.12305>.
- Chepil, W.S., 1952. Factors that influence Clod Structure and Erodibility of Soil by Wind: 1. Soil Texture.
- Chepil, W.S., 1953. Field structure of cultivated soils with special reference to erodibility by wind. *Soil Sci. Soc. Am. Proc.*
- Chepil, W.S., 1960. Conversion of Relative Field Erodibility to Annual Soil Loss by Wind. *Soil Science Society of America Proceedings* 143–145. <https://doi.org/doi.org/10.2136/sssaj1960.03615995002400020022x>.
- Chepil, W.S., 1962. A compact rotary sieve and importance of dry sieving in physical soil analysis. *Soil Sci. Soc. Am. J.* 26, 4–6. <https://access.onlinelibrary.wiley.com/doi/10.2136/sssaj1960.03615995002400020022x>.
- Colazo, J.C., Buschiazzi, D.E., 2010. Soil dry aggregate stability and wind erodible fraction in a semiarid environment of Argentina. *Geoderma* 159, 228–236. <https://doi.org/10.1016/j.geoderma.2010.07.016>.
- Dong, Z., Sun, H., Zhao, A., 2004. WITSEG sampler: a segmented sand sampler for wind tunnel test. *Geomorphology* 59, 119–129. <https://doi.org/10.1016/j.geomorph.2003.09.010>.
- DTU, 2021. Global Wind Atlas 3.1. Technical University of Denmark (DTU Wind Energy), Denmark. Available at: <https://globalwindatlas.info/>.
- Duulatuov, E., Chen, X., Issanova, G., Orozbaev, R., Mukanov, Y., Amanambu, A.C., 2021. Current and future trends of rainfall erosivity and soil erosion in Central Asia. *SpringerBriefs in Environmental Science*. Springer International Publishing, Cham. <https://doi.org/10.1007/978-3-030-63509-1>.
- FAO, 2012. AQUASTAT: Kazakhstan. Food and Agriculture Organization of the United Nations (FAO), Rome, Italy.
- FAO, 2014. World reference base for soil resources 2014: international soil classification system for naming soils and creating legends for soil maps. Food and Agriculture Organization of the United Nations (FAO), Rome, Italy.
- Field, J.P., Breshears, D.D., Whicker, J.J., 2009. Toward a more holistic perspective of soil erosion: Why aeolian research needs to explicitly consider fluvial processes and interactions. *Aeolian Res.* 1, 9–17. <https://doi.org/10.1016/j.aeolia.2009.04.002>.
- Frühau, M., Meinel, T., Schmidt, G., 2020. In: Frühau, M., Guggenberger, G., Meinel, T., Theesfeld, I., Lentz, S. (Eds.), *The Virgin Lands Campaign (1954–1963) Until the Breakdown of the Former Soviet Union (FSU): With Special Focus on Western Siberia*. KULUNDA: Climate Smart Agriculture, Innovations in Landscape Research. Springer International Publishing, Cham, pp. 101–118. https://doi.org/10.1007/978-3-030-15927-6_8.
- Fryrear, D.W., Saleh, A., Bilbro, J.D., Schomberg, H.M., Stout, J.E., Zobeck, T.M., 1998. Revised Wind Erosion Equation (RWEQ). Wind Erosion and Water Conservation Research Unit, Technical Bulletin No. 1. USDA-ARS, Texas, USA.
- Funk, R., Reuter, H.L., 2006. Wind erosion. In: Boardman, J., Poesen, J. (Eds.), *Soil Erosion in Europe*. John Wiley & Sons, Ltd, Chichester, pp. 563–582. <https://doi.org/10.1002/0470859202.ch41>.
- Funk, R., Engel, W., 2015. Investigations with a field wind tunnel to estimate the wind erosion risk of row crops. *Soil Tillage Res.* 145, 224–232. <https://doi.org/10.1016/j.still.2014.09.005>.
- Funk, R., Skidmore, E., Hagen, L., 2004. Comparison of wind erosion measurements in Germany with simulated soil losses by WEPS. *Environ. Model. Softw.* 19, 177–183. [https://doi.org/10.1016/S1364-8152\(03\)00120-8](https://doi.org/10.1016/S1364-8152(03)00120-8).
- Funk, R., Hoffmann, C., Reiche, M., 2014. Methods for quantifying wind erosion in steppe regions. In: Mueller, L., Saparov, A., Lischeid, G. (Eds.), *Novel Measurement and Assessment Tools for Monitoring and Management of Land and Water Resources in Agricultural Landscapes of Central Asia*. Environmental Science and Engineering. Springer International Publishing, Cham, pp. 315–327. https://doi.org/10.1007/978-3-319-01017-5_18.
- Funk, R., Völker, L., Deumlich, D., 2023. Landscape structure model based estimation of the wind erosion risk in Brandenburg, Germany. *Aeolian Res.* 62, 100878. <https://doi.org/10.1016/j.aeolia.2023.100878>.
- Gardner, W.H., 2018. Water Content. In: Klute, A. (Ed.), *SSSA Book Series*. Soil Science Society of America, American Society of Agronomy, Madison, WI, USA, pp. 493–544. <https://doi.org/10.2136/sssabookser5.1.2ed.c21>.
- Gregorich, E.G., Greer, K.J., Anderson, D.W., Liang, B.C., 1998. Carbon distribution and losses: erosion and deposition effects. *Soil Tillage Res.* 47, 291–302. [https://doi.org/10.1016/S0167-1987\(98\)00117-2](https://doi.org/10.1016/S0167-1987(98)00117-2).
- Grunwald, L.-C., Belyaev, V.I., Hamann, M., Illiger, P., Stephan, E., Bischoff, N., Rudev, N.V., Kozhanov, N.A., Schmidt, G., Frühau, M., Meinel, T., 2016. Modern cropping systems and technologies for soil conservation in siberian agriculture. In: Mueller, L., Sheudshen, A.K., Eulenstein, F. (Eds.), *Novel Methods for Monitoring and Managing Land and Water Resources in Siberia*. Springer Water. Springer International Publishing, Cham, pp. 681–715. https://doi.org/10.1007/978-3-319-24409-9_31.
- Hagen, L.J., 2001. Assessment of wind erosion parameters using wind tunnels. In: Stott, D.E., Mohtar, R.H., Steinhardt, G.C. (Eds.), *Sustaining the Global Farm*, pp. 742–746.
- Harris, I.C., Jones, P.D., Osborn, T., 2020. CRU TS4.04: Climatic Research Unit (CRU) Time-Series (TS) version 4.04 of high-resolution gridded data of month-by-month variation in climate (Jan. 1901–Dec. 2019). *Sci Data* 7.
- Hornbeck, R., 2012. The enduring impact of the american dust bowl: short- and long-run adjustments to environmental catastrophe. *Am. Econ. Rev.* 102, 1477–1507. <https://doi.org/10.1257/aer.102.4.1477>.
- Iturri, L.A., Buschiazzi, D.E., 2023. Interactions between wind erosion and soil organic carbon. In: *Agricultural Soil Sustainability and Carbon Management*. Elsevier, pp. 163–179. <https://doi.org/10.1016/B978-0-323-95911-7.00005-0>.
- Janssen, W., Tetzlaff, G., 1991. Construction and calibration of a recording sand trap. (in German: Entwicklung und Eichung einer registrierenden Suspensionsfalle). *Z. Kult. Landentwicklung* 32, 167–179.
- Kassam, A., Friedrich, T., Depsch, R., 2019. Global spread of conservation agriculture. *Int. J. Environ. Stud.* 76, 29–51. <https://doi.org/10.1080/00207233.2018.1494927>.
- Keesstra, S.D., Bouma, J., Wallinga, J., Tittonell, P., Smith, P., Cerdà, A., Montanarella, L., Quinton, J.N., Pachepsky, Y., van der Putten, W.H., Bardgett, R.D., Moolenaar, S., Mol, G., Jansen, B., Fresco, L.O., 2016. The significance of soils and soil science towards realization of the United Nations Sustainable Development Goals. *SOIL* 2, 111–128. <https://doi.org/10.5194/soil-2-111-2016>.
- Kienzler, K.M., Lamers, J.P.A., McDonald, A., Mirzabaev, A., Ibragimov, N., Egamberdiev, O., Ruzibaev, E., Akramkhanov, A., 2012. Conservation agriculture in Central Asia—what do we know and where do we go from here? *Field Crops Res.* 132, 95–105. <https://doi.org/10.1016/j.fcr.2011.12.008>.
- Kok, J.F., Parteli, E.J.R., Michaels, T.I., Karam, D.B., 2012. The physics of wind-blown sand and dust. *Rep. Prog. Phys.* 75, 106901. <https://doi.org/10.1088/0034-4885/75/10/106901>.
- Koza, M., Funk, R., Schmidt, G., 2023. Wind erosion after steppe conversion in Kazakhstan: Data from mobile wind tunnel experiments [Dataset]. Leibniz Centre for Agricultural Landscape Research (ZALF). <https://doi.org/10.4228/ZALF-QQ16-1967>.
- Koza, M., Schmidt, G., Bondarovich, A., Akshalov, K., Conrad, C., Pöhlitz, J., 2021. Consequences of chemical pretreatments in particle size analysis for modelling wind erosion. *Geoderma* 396, 115073. <https://doi.org/10.1016/j.geoderma.2021.115073>.
- Koza, M., Pöhlitz, J., Prays, A., Kaiser, K., Mikutta, R., Conrad, C., Vogel, C., Meinel, T., Akshalov, K., Schmidt, G., 2022. Potential erodibility of semi-arid steppe soils derived from aggregate stability tests. *Eur. J. Soil Sci.* 73 (5), e13304. <https://doi.org/10.1111/ejss.13304>.
- Kraemer, R., Prishchepov, A.V., Müller, D., Kuemmerle, T., Radeloff, V.C., Dara, A., Terekhov, A., Frühau, M., 2015. Long-term agricultural land-cover change and potential for cropland expansion in the former Virgin Lands area of Kazakhstan. *Environ. Res. Lett.* 10, 054012. <https://doi.org/10.1088/1748-9326/10/5/054012>.
- Lackóová, L., Pokrývková, J., Kozlovsky Dufková, J., Policht-Latawiec, A., Michałowska, K., Dąbrowska, J., 2021. Long-term impact of wind erosion on the particle size distribution of soils in the eastern part of the European Union. *Entropy* 23, 935. <https://doi.org/10.3390/e23080935>.
- Lafond, G.P., May, W.E., Stevenson, F.C., Derksen, D.A., 2006. Effects of tillage systems and rotations on crop production for a thin Black Chernozem in the Canadian Prairies. *Soil Tillage Res.* 89, 232–245. <https://doi.org/10.1016/j.still.2005.07.014>.
- Lal, R., 2001. Soil degradation by erosion. *Land Degrad. Dev.* 12, 519–539. <https://doi.org/10.1002/ldr.472>.
- Lal, R., Reicosky, D.C., Hanson, J.D., 2007. Evolution of the plow over 10,000 years and the rationale for no-till farming. *Soil Tillage Res.* 93, 1–12. <https://doi.org/10.1016/j.still.2006.11.004>.
- Larionov, G.A., 1993. *Erosion and deflation of soils: General regularities and quantitative assessment (in Russian: Эрозия и дефляция почв: основные закономерности и количественные оценки)*. Moscow State University, Moscow.
- Larney, F., 2007. *Dry-Aggregate Size Distribution*. In: Carter, M., Gregorich, E. (Eds.), *Soil Sampling and Methods of Analysis*, Second Edition. CRC Press, pp. 821–831. <https://doi.org/10.1201/9781420005271.ch63>.
- Lee, J.A., Gill, T.E., 2015. Multiple causes of wind erosion in the Dust Bowl. *Aeolian Res.* 19, 15–36. <https://doi.org/10.1016/j.aeolia.2015.09.002>.
- Li, J., Chen, H., Zhang, C., 2020a. Impacts of climate change on key soil ecosystem services and interactions in Central Asia. *Ecol. Indic.* 116, 106490. <https://doi.org/10.1016/j.ecolind.2020.106490>.
- Li, J., Ma, X., Zhang, C., 2020b. Predicting the spatiotemporal variation in soil wind erosion across Central Asia in response to climate change in the 21st century. *Sci. Total Environ.* 709, 136060. <https://doi.org/10.1016/j.scitotenv.2019.136060>.
- Li, X.-Y., Liu, L.-Y., Wang, J.-H., 2004. Wind tunnel simulation of aeolian sandy soil erodibility under human disturbance. *Geomorphology* 59, 3–11. <https://doi.org/10.1016/j.geomorph.2003.09.001>.
- López, M.V., Sabre, M., Gracia, R., Arráe, J.L., Gomes, L., 1998. Tillage effects on soil surface conditions and dust emission by wind erosion in semiarid Aragón (NE Spain). *Soil and Tillage Research* 45, 91–105. [https://doi.org/10.1016/S0167-1987\(97\)00066-4](https://doi.org/10.1016/S0167-1987(97)00066-4).
- López, M.V., de Dios Herrero, J.M., Hevia, G.G., Gracia, R., Buschiazzi, D.E., 2007. Determination of the wind-erodible fraction of soils using different methodologies. *Geoderma* 139, 407–411. <https://doi.org/10.1016/j.geoderma.2007.03.006>.
- Marzen, M., Kirchhoff, M., Marzolf, I., Ait Hssaine, A., Ries, J.B., 2020. Relative quantification of wind erosion in argan woodlands in the Souss Basin, Morocco. *Earth Surf. Process. Landf.* 45, 3808–3823. <https://doi.org/10.1002/esp.5002>.

- Maurer, T., Herrmann, L., Gaiser, T., Mounkaila, M., Stahr, K., 2006. A mobile wind tunnel for wind erosion field measurements. *J. Arid Environ.* 66, 257–271. <https://doi.org/10.1016/j.jaridenv.2005.11.002>.
- McLeman, R.A., Dupre, J., Berrang Ford, L., Ford, J., Gajewski, K., Marchildon, G., 2014. What we learned from the Dust Bowl: lessons in science, policy, and adaptation. *Popul. Environ.* 35, 417–440. <https://doi.org/10.1007/s11111-013-0190-z>.
- Meier, U., 2018. Growth stages of mono- and dicotyledonous plants: BBCH Monograph. Open Agrar Repository, Quedlinburg. <https://doi.org/10.5073/20180906-074619>.
- Meinel, T., Akshalov, K., 2015. Development of land use management in the Eurasian steppe area: from moldboard to direct seeding (in Russian: Стратегия Северная Евразия: Материалы VII Международного симпозиума). In: Chibilev, A.A. (Ed.), *Steppes of Northern Eurasia: Materials of VII International Symposium*. Publishing House “Dimur”, Orenburg, pp. 64–66.
- Meinel, T., Grunwald, L.-C., Akshalov, K., 2014. Modern technologies for soil management and conservation in Northern Kazakhstan. In: Mueller, L., Saparov, A., Lischeid, G. (Eds.), *Novel Measurement and Assessment Tools for Monitoring and Management of Land and Water Resources in Agricultural Landscapes of Central Asia*, Environmental Science and Engineering. Springer International Publishing, Cham, pp. 455–464. https://doi.org/10.1007/978-3-319-01017-5_27.
- Meteoblue, 2023. Simulated historical climate and weather data. Basel. Available at: <https://www.meteoblue.com/en/weather/historyclimate/climatemodelled/>.
- Montgomery, D.R., 2007. Soil erosion and agricultural sustainability. *Proc. Natl. Acad. Sci. U. S. A.* 104, 13268–13272. <https://doi.org/10.1073/pnas.0611508104>.
- Nerger, R., Funk, R., Cordsen, E., Fohrer, N., 2017. Application of a modeling approach to designate soil and soil organic carbon loss to wind erosion on long-term monitoring sites (BDF) in Northern Germany. *Aeolian Res.* 25, 135–147. <https://doi.org/10.1016/j.aeolia.2017.03.006>.
- Peters, D.P., Goffman, P.M., Nadelhoffer, K.J., Grimm, N.B., Collins, S.L., Michener, W.K., Huston, M.A., 2008. Living in an increasingly connected world: a framework for continental-scale environmental science. *Front. Ecol. Environ.* 6, 229–237. <https://doi.org/10.1890/070098>.
- Podsiadlowski, S.T., 1988. Wind erosion of light soil in the wheel tracks of a farm tractor. *J. Agric. Eng. Res.* 39, 231–243. [https://doi.org/10.1016/0021-8634\(88\)90145-X](https://doi.org/10.1016/0021-8634(88)90145-X).
- Prishchepov, A.V., Schierhorn, F., Dronin, N., Ponkina, E.V., Müller, D., 2020. 800 Years of Agricultural Land-use Change in Asian (Eastern) Russia. In: Frühauf, M., Guggenberger, G., Meinel, T., Theesfeld, I., Lentz, S. (Eds.), *KULUNDA: Climate Smart Agriculture, Innovations in Landscape Research*. Springer International Publishing, Cham, pp. 67–87. https://doi.org/10.1007/978-3-030-15927-6_6.
- Pye, K., 1994. *Sediment transport and depositional processes*. Blackwell Scientific Publications, Oxford; Boston.
- R. Core Team, 2020. A language and environment for statistical computing. R Foundation for Statistical Computing, Vienna. Available at: <https://www.r-project.org/>.
- Reyer, C.P.O., Otto, I.M., Adams, S., Albrecht, T., Baarsch, F., Carlsburg, M., Coumou, D., Eden, A., Ludi, E., Marcus, R., Mengel, M., Mosello, B., Robinson, A., Schleussner, C.-F., Serdeczny, O., Stagl, J., 2017. Climate change impacts in Central Asia and their implications for development. *Reg. Environ. Change* 17, 1639–1650. <https://doi.org/10.1007/s10113-015-0893-z>.
- Reynolds, J.F., Smith, D.M.S., Lambin, E.F., Turner, B.L., Mortimore, M., Batterbury, S.P. J., Downing, T.E., Dowlatabadi, H., Fernández, R.J., Herrick, J.E., Huber-Sannwald, E., Jiang, H., Leemans, R., Lynam, T., Maestre, F.T., Ayarza, M., Walker, B., 2007. Global desertification: building a science for dryland development. *Science* 316, 847–851. <https://doi.org/10.1126/science.1131634>.
- Robinson, S., 2016. Land degradation in central asia: evidence, perception and policy. In: Behnke, R., Mortimore, M. (Eds.), *Springer Earth System Sciences, The End of Desertification?*. Springer Berlin Heidelberg, Berlin, Heidelberg, pp. 451–490. https://doi.org/10.1007/978-3-642-16014-1_17.
- Scheffer, F., Schachtschabel, P., Blume, H.-P., 2016. *Soil science, first ed.* Springer, Berlin.
- Shahabinejad, N., Mahmoodabadi, M., Jalalian, A., Chavoshi, E., 2019. In situ field measurement of wind erosion and threshold velocity in relation to soil properties in arid and semiarid environments. *Environ. Earth Sci.* 78, 501. <https://doi.org/10.1007/s12665-019-8508-5>.
- Shao, Y. (Ed.), 2008. *Physics and modelling of wind erosion, Atmospheric and oceanographic sciences library*. Springer, Cambridge.
- Shao, Y., Wyrwoll, K.-H., Chappell, A., Huang, J., Lin, Z., McTainsh, G.H., Mikami, M., Tanaka, T.Y., Wang, X., Yoon, S., 2011. Dust cycle: an emerging core theme in Earth system science. *Aeolian Res.* 2, 181–204. <https://doi.org/10.1016/j.aeolia.2011.02.001>.
- Sirjani, E., Sameni, A., Moosavi, A.A., Mahmoodabadi, M., Laurent, B., 2019. Portable wind tunnel experiments to study soil erosion by wind and its link to soil properties in the Fars province, Iran. *Geoderma* 333, 69–80. <https://doi.org/10.1016/j.geoderma.2018.07.012>.
- Soil Science Division Staff, 2017. *Soil survey manual, eighteenth ed.* Government Printing Office, Washington, D.C. USA.
- Stolbovoi, V., 2000. *Soils of Russia: Correlated with the Revised Legend of the FAO Soil Map of the World and World Reference Base for Soil Resources*. International Institute for Applied Systems Analysis, Laxenburg, Austria.
- Suleimenov, M., Kaskarbayev, Z., Akshalov, K., Tulegenov, A., 2016. Principles of conservation agriculture in continental steppe regions. In: Mueller, L., Sheudshen, A. K., Eulenstein, F. (Eds.), *Novel Methods for Monitoring and Managing Land and Water Resources in Siberia*. Springer Water. Springer International Publishing, Cham, pp. 667–679. https://doi.org/10.1007/978-3-319-24409-9_30.
- Taiyun, W., Simko, V., 2021. R package “corrplot”: Visualization of a correlation matrix (version 0.92).
- Tanner, S., Katra, I., Haim, A., Zaady, E., 2016. Short-term soil loss by eolian erosion in response to different rain-fed agricultural practices. *Soil Tillage Res.* 155, 149–156. <https://doi.org/10.1016/j.still.2015.08.008>.
- Tisdall, J.M., Oades, J.M., 1982. Organic matter and water-stable aggregates in soils. *Eur. J. Soil Sci.* 33, 141–163. <https://doi.org/10.1111/j.1365-2389.1982.tb01755.x>.
- Van Pelt, R.S., Zobeck, T.M., 2013. Portable wind tunnels for field testing of soils and natural surfaces. In: Ahmed, N. (Ed.), *Wind tunnel designs and their diverse engineering applications*. InTech. <https://doi.org/10.5772/54141>.
- Verhulst, N., Govaerts, B., Verachtert, E., Castellanos-Navarrete, A., Mezzalama, M., Wall, P.C., Chocobar, A., Deckers, J., Sayre, K.D., 2010. Conservation agriculture, improving soil quality for sustainable production systems? In: Lal, R., Stewart, B.A. (Eds.), *Food Security and Soil Quality*. CRC Press, pp. 137–208. <https://doi.org/10.1201/EBK1439800577-7>.
- Webb, N.P., Kachergis, E., Miller, S.W., McCord, S.E., Bestelmeyer, B.T., Brown, J.R., Chappell, A., Edwards, B.L., Herrick, J.E., Karl, J.W., Leys, J.F., Metz, L.J., Smarik, S., Tatarko, J., Van Zee, J.W., Zwicke, G., 2020. Indicators and benchmarks for wind erosion monitoring, assessment and management. *Ecol. Indic.* 110, 105881. <https://doi.org/10.1016/j.ecolind.2019.105881>.
- White, B.R., Mounla, H., 1991. An experimental study of Froude number effect on wind-tunnel saltation. In: Barndorff-Nielsen, O.E., Willetts, B.B. (Eds.), *Aeolian Grain Transport 1*, Acta Mechanica Supplementum. Springer, Vienna, pp. 145–157. https://doi.org/10.1007/978-3-7091-6706-9_9.
- Wieringa, J., 1992. Updating the Davenport roughness classification. *J. Wind Eng. Ind. Aerodyn.* 41, 357–368. [https://doi.org/10.1016/0167-6105\(92\)90434-C](https://doi.org/10.1016/0167-6105(92)90434-C).
- Yan, Y., Wang, X., Guo, Z., Chen, J., Xin, X., Xu, D., Yan, R., Chen, B., Xu, L., 2018. Influence of wind erosion on dry aggregate size distribution and nutrients in three steppe soils in northern China. *CATENA* 170, 159–168. <https://doi.org/10.1016/j.catena.2018.06.013>.
- Yin, C., Zhao, W., Pereira, P., 2022. Soil conservation service underpins sustainable development goals. *Glob. Ecol. Conserv.* 33, e01974. <https://doi.org/10.1016/j.gecco.2021.e01974>.
- Yost, J.L., Hartemink, A.E., 2019. Soil organic carbon in sandy soils: a review. In: *Advances in Agronomy*. Elsevier, pp. 217–310. <https://doi.org/10.1016/bs.agron.2019.07.004>.
- Zamani, S., Mahmoodabadi, M., 2013. Effect of particle-size distribution on wind erosion rate and soil erodibility. *Arch. Agron. Soil Sci.* 59, 1743–1753. <https://doi.org/10.1080/03650340.2012.748984>.
- Zenchelsky, S.T., Delany, A.C., Pickett, R.A.L., 1976. The organic component of wind-blown soil aerosol as a function of wind velocity. *Soil Sci.* 122, 129–132.
- Zepner, L., Karrasch, P., Wiemann, F., Bernard, L., 2021. ClimateCharts.net – an interactive climate analysis web platform. *Int. J. Digit. Earth* 14, 338–356. <https://doi.org/10.1080/17538947.2020.1829112>.
- Zhang, C.-L., Zou, X.-Y., Gong, J.-R., Liu, L.-Y., Liu, Y.-Z., 2004. Aerodynamic roughness of cultivated soil and its influences on soil erosion by wind in a wind tunnel. *Soil Tillage Res.* 75, 53–59. [https://doi.org/10.1016/S0167-1987\(03\)00159-4](https://doi.org/10.1016/S0167-1987(03)00159-4).
- Zobeck, T.M., Fryrear, D.W., 1986. Chemical and physical characteristics of windblown sediment II. chemical characteristics and total soil and nutrient discharge. *Trans. ASAE* 29, 1037–1041. <https://doi.org/10.13031/2013.30266>.
- Zobeck, T.M., Popham, T.W., 1990. Dry aggregate size distribution of sandy soils as influenced by tillage and precipitation. *Soil Sci. Soc. Am. J.* 54, 198–204. <https://doi.org/10.2136/sssaj1990.03615995005400010031x>.
- Zobeck, T.M., Van Pelt, R.S., 2015. Wind erosion. In: Hatfield, J.L., Sauer, T.J. (Eds.), *Soil Management: Building a Stable Base for Agriculture*. Soil Science Society of America, Madison, WI, USA, pp. 209–227. <https://doi.org/10.2136/2011.soilmanagement.c14>.
- Zobeck, T.M., Baddock, M., Scott Van Pelt, R., Tatarko, J., Acosta-Martinez, V., 2013. Soil property effects on wind erosion of organic soils. *Aeolian Res.* 10, 43–51. <https://doi.org/10.1016/j.aeolia.2012.10.005>.
- Zobeck, T.M., Sterk, G., Funk, R., Rajot, J.L., Stout, J.E., Van Pelt, R.S., 2003. Measurement and data analysis methods for field-scale wind erosion studies and model validation. *Earth Surf. Process. Landf.* 28, 1163–1188. <https://doi.org/10.1002/esp.1033>.

6. Discussion

Various research questions were addressed and discussed in the published journal contributions, all focusing on the main drivers of erosion under the influence of parent soil, land use, and climate. The following discussion is structured according to the research questions developed at the beginning of the dissertation.

Which chemical pretreatment efficiently removes the binding agents to successfully measure PSD by laser diffraction?

Results indicate that chemical pretreatments seem unnecessary if LDA include standard dispersion and sonication for particle size analyses of Chernozem and Kastanozem silty soils containing low and medium amounts of organic binding material and medium to high amounts of secondary carbonates. Steppe soils show incomplete dispersion or even aggregation when HCl is used to dissolve carbonates. Therefore, HCl is not advised as a pretreatment, and carbonates do not support aggregation in the topsoil layer. However, the results show that organic matter is the most important binding agent in steppe soils and H₂O₂ removes organic efficiently (Koza et al., 2021).

What are the effects of different pretreatments for measuring particle sizes with laser diffraction for modeling soil loss estimates?

Different pretreatments did not affect texture class for silty soils in the study area. Modeling soil loss by wind erosion using SWEEP shows that pretreatments did not influence soil loss estimates if texture-based parameters were measured. Pretreatments affect aggregates mainly built of silt, clay, and binding agents. Therefore, sand is less affected by pretreatments and stays low in silty soils (Koza et al., 2021). However, the very fine sand fraction is also an erosion driver, because it has the lowest threshold friction velocity at which wind erosion begins, and the ability to increase the detachment of particles by abrasion (Shao, 2008). On the contrary, if texture-based parameters, such as the GMD, are derived by pedotransfer functions from PSD and binding agents, the modeled results show a high variation of soil loss estimates. Hence, using input data from measured values are recommended. New pedotransfer functions are

required to derive soil parameters based on PSD data obtained by laser diffraction for steppe soils. Neglecting the pretreatments to remove binding agents is recommended because standard dispersion for LDA is sufficient (Koza et al., 2021). Additionally, the measured mean wind speeds with a temporal resolution of 15 minutes are rarely high enough for modeling soil loss in the study area. A higher resolution of wind speeds will likely improve the accuracy of estimated soil losses. Furthermore, the complex interactions between soil erodibility and climate erosivity must be considered in semi-arid regions and are challenging erosion models. Measuring soil loss rates under field conditions with in-situ experiments is required to validate erosion models for steppe soils of Central Asia (Koza et al., 2021).

Which physical and chemical soil properties of the topsoil enhance aggregation and counteract erosion in dry steppe soils?

Analyzing texture and its binding agents to model wind erosion (Koza et al., 2021) points out the importance of the structural unit the soil exist in the field. Therefore, aggregates were investigated to assess the soil's potential erodibility by Koza et al. (2022). The number of test sites was increased to cover a large range of physical and chemical soil properties (sand: 2–76%, silt: 18–80%, clay: 6–30%, SOC: 7.3–64.2 g kg⁻¹, TIC: 0.0–8.5 g kg⁻¹, pH: 4.8–9.5, EC: 32–946 μS cm⁻¹) that follow a regional approach. Results show that texture and aligned organic matter content determine the aggregate stability in a given soil. Therefore, sandy soils with low SOC content have the highest risk of erosion in the study area (Koza et al., 2022).

How does land use affect aggregate stability and how erodible are steppe soils by wind and water?

Results from the two most dominant land use types in the semi-arid steppe of northern Kazakhstan, crop- and grassland, show that tillage decreases aggregate stability severely, even without organic carbon changes. All soils under cultivation are susceptible to the erosive forces of wind and water, independent of their soil properties. Tillage serves as an additional modifier, enhancing the overall risk of soil degradation (Koza et al., 2022). The results are consistent with previous studies (e.g., Amézketa, 1999; Six et al., 1998) and demonstrate that soil structure is severely degraded due to the repeated application of mechanical stress by tillage. Despite semi-

arid climate conditions, soil's potential erodibility seems higher for the disruptive forces caused by water than by wind. During an observed period of one year (2019–2020), precipitation occurred on 154 days. Predominantly light rain, repetitive snowmelt in spring, and rare heavy rainfall were recorded (Koza et al., 2022). However, future model projections indicate a change in precipitation duration, magnitude, and intensity, causing an increase in rainfall erosivity in the study area (Duulatov et al., 2021). Disrupting aggregates by water may promote subsequent soil loss by wind erosion. Aggregate stability tests indicated that overall soil erodibility by wind is moderate, and the erosivity by wind implied a limited risk due to low wind speed conditions in the study area (Koza et al., 2022). Still, wind speed increased significantly in Central Asia from 2011 to 2019, and moderate and heterogeneous changes are expected (Li et al., 2020; Wang et al., 2020). Climate models also indicate extreme temperatures causing draughts (WHO, 2012). The interplay of climatic factors will result in complex spatiotemporal patterns of soil erosion in Central Asia in the future.

What are the short-term effects of various agricultural management practices on surface characteristics and soil loss rates by wind erosion?

Various field experiments on loamy sands were carried out by Koza et al. (2024) on initial soil surfaces to quantify the soil loss by wind erosion under real soil conditions. Wind tunnel experiments on bare surfaces after plowing and arable plots under cultivation with common crops showed that soil loss after recent steppe conversion was low but considerable on arable plots that underwent cultivation during the past three years. In-situ measurements also demonstrated that wind erosion affects maize fields more than plots cultivated with barley. Maize plants show a reduced roughness length, which favors wind erosion during the early growth stadium. After simulating common agricultural practices (light cultivator, disc harrow, tractor tires), results show that tillage tools determine soil susceptibility to wind erosion. The effect of tractor tires was most severe causing the highest soil loss rates (Koza et al., 2024).

What particle and aggregate sizes are detached and deposited during aeolian processes?

All investigated loamy sand plots experienced a sorting process due to wind erosion. After the recent steppe conversion, aeolian sediments contained more clay, silt, and very fine sand

particles. In contrast, clay and silt content decreased while fine and medium sand particles increased in the aeolian sediments and depositions originating from arable topsoils (Koza et al., 2024). Measured aggregate sizes of aeolian sediments correspond to findings from several studies indicating that predominantly microaggregates between 20–260 μm are depleted by wind (Yan et al., 2018). The PSD and ASD of aeolian sediments collected during wind tunnel experiments and from natural wind erosion deposition were similar and underline the functionality of the mobile wind tunnel for imitating real events (Koza et al., 2024).

How much organic carbon is lost by aeolian processes?

Associated with the sorting process of particles (Koza et al., 2024), the blown-out material after recent steppe conversion was enriched in SOC (ratio of content collected by the traps to the topsoil = 1.7), while aeolian sediments and depositions from the arable plots were depleted (SOC ratio = < 0.9). Hence, on sandy soils, more SOC is lost directly after steppe conversion compared to the plots that have been under cultivation for three years already. The decrease in SOC aligns with the decrease in clay content caused by wind erosion (Koza et al., 2024).

7. Future research

This dissertation's scientific contributions and sequential discussions underpin the progress achieved in the addressed research questions. In the course of numerous sampling campaigns and field experiments, several observations were scientifically investigated, for example, the high risk of water erosion after snowmelt (Koza et al., 2022) or tractor tire tracks as a major source of soil loss by wind erosion (Koza et al., 2024). However, research must continue to investigate further interactions of factors that cause erosion to support and develop sustainable management practices in cultivated steppes. During the course of this dissertation, new research ideas and gaps were identified. Research approaches that could be of serious value include:

Area-based estimation of soil loss:

After assessing key parameters for wind erosion events in Koza et al. (2021) and monitoring the vegetation and landscape structure throughout the study area during a field campaign in 2019, the next step is to use remote sensing to model wind erosion on a larger scale in order to derive area-based estimations of wind erosion hotspots and their origin.

Transferability of methods and knowledge to other regions of interest:

It is conceivable that the tools and methods developed in Kazakhstan are of potential interest for arid and semi-arid regions in Central Asia. Field experiments are lacking along the Eurasian Steppe Belt (e.g., southern Russia, Mongolia). However, they do not have to be limited to Central Asia. For example, one of the driest regions in Germany ("Mitteldeutsches Trockengebiet") is located leeward of the Harz Mountains. This area has a similar latitude as the study area in northern Kazakhstan, and pedogenesis developed similar soils. Currently, different climatic conditions with higher mean temperatures and precipitation sums are present (Zepner et al., 2021). Dry periods have increased over the last century, indicating regional climate change and the risk of wind and water erosion have been present in the past, and adaptation measures are needed (Fabig, 2007). The know-how established in Kazakhstan could also be applied in this vulnerable but fertile region of Germany to support adaptation measures and prevent soil degradation.

Wind tunnel experiments on Chernozems:

The sandy Kastanozem soils investigated by Koza et al. (2024) showed that blown-out material was enriched in SOC only after steppe conversion but depleted on cropland. Based on the findings of Koza et al. (2024), it is necessary to measure the carbon loss from Chernozems due to their high organic carbon content and role in climate change mitigation (Krasilnikov et al., 2018). Chernozems are present at the northern end of the study area. Field observations from April 2018 and severe deposition at the luv side of the fields in June 2022 confirm the presence of wind erosion events on Chernozems.

Extension of field observations with a focus on dust and SOC:

Dust significantly impacts the Earth's system by transporting organic matter that contributes to the carbon cycle. However, knowledge of the role of wind erosion in the redistribution of fine and carbon-rich materials is limited (Shao et al., 2011). The MWAC samplers collected aeolian sediments during wind tunnel experiments by Koza et al. (2024). These samples can be used for dust emissions but lack efficiency (Mendez et al., 2016). Subsequently, a portable aerosol spectrometer can obtain further information on the temporal variation, size distributions, and fractions of dust particles. Further studies would help to understand how agriculture influences the interaction between dust and the carbon cycle that affects climate via feedback loops.

Quantifying soil loss from dirt roads and agricultural driving paths

Koza et al. (2024) showed that tillage creates soil structures susceptible to wind erosion. Still, tractor tires increase soil losses by a multiple. Accounting for about 20% of each field, the disruption caused by tractors and resulting soil losses must be investigated in more detail (e.g., temporal and spatial scale) to prevent this major dust emission source.

Controlling specific adaptation measures:

The results of Koza et al. (2024) have prompted the local farmer of the test site to implement strip-till as an adaptation measure to prevent the particularly high soil loss from wind erosion on corn. Crop residues are known to prevent wind erosion (Meinel et al., 2014), but empirical data showing the difference between conventional tillage and strip-till in terms of soil loss quantities are of interest for the cultivated steppe soils of Central Asia.

8. Conclusion and synthesis

Concerning the overall research questions:

What are the main drivers of erosion under the influence of parent material, land use, and climate in the cultivated steppe of Kazakhstan?

With its sequential publications, findings, and considerations, this dissertation is to my knowledge the first comprehensive and up-to-date study investigating the drivers and processes of soil degradation processes based on field measurements in northern Kazakhstan. Parent material with high sand contents is particularly erodible. The risk of erosion is limited under grassland but all cropland soils are prone to erosion by wind and water. Furthermore, cultivated steppe soils seem much more susceptible to water than wind erosion. Therefore, sustainable land use strategies must consider the interplay between the disruptive forces of wind and water. During snowmelt, slaking breaks down aggregates and potentially paves the way for extensive wind erosion events in spring. Soil organic matter is the most important binding agent counteracting soil erosion in the cultivated steppe of Kazakhstan. Management strategies must increase soil organic content to favor aggregation but also decrease tillage intensities because mechanical stress from seedbed preparation determines soil susceptibility to wind erosion. A wider approach to sustainable land use also requires considering the consequences of tractor tire tracks to prevent further soil degradation. Overall, agriculture on steppe soils requires best-adapted measures of erosion prevention from the very beginning. This synthesis introduces a unique perspective that adds to the current understanding of erosion drivers and processes under semi-arid climate.

References

- Alewell, C., Borrelli, P., Meusburger, K., Panagos, P., 2019. Using the USLE: Chances, challenges and limitations of soil erosion modelling. *International Soil and Water Conservation Research* 7, 203–225. <https://doi.org/10.1016/j.iswcr.2019.05.004>
- Almaganbetov, N., Grigoruk, V., 2008. Degradation of soil in Kazakhstan: Problems and challenges, in: Simeonov, L., Sargsyan, V. (Eds.), *Soil chemical pollution, risk assessment, remediation and security*. Springer Netherlands, Dordrecht, pp. 309–320. https://doi.org/10.1007/978-1-4020-8257-3_27
- Amézketa, E., 1999. Soil aggregate stability: A review. *Journal of Sustainable Agriculture* 14, 83–151. https://doi.org/10.1300/J064v14n02_08
- Bagnold, R.A., 1941. *The physics of blown sand and desert dunes*. London: Methuen.
- Barthès, B., Roose, E., 2002. Aggregate stability as an indicator of soil susceptibility to runoff and erosion; validation at several levels. *CATENA* 47, 133–149. [https://doi.org/10.1016/S0341-8162\(01\)00180-1](https://doi.org/10.1016/S0341-8162(01)00180-1)
- Bezák, N., Mikoš, M., Borrelli, P., Alewell, C., Alvarez, P., Anache, J.A.A., Baartman, J., Ballabio, C., Biddoccu, M., Cerdà, A., Chalise, D., Chen, S., Chen, W., De Girolamo, A.M., Gessesse, G.D., Deumlich, D., Diodato, N., Efthimiou, N., Erpul, G., Fiener, P., Freppaz, M., Gentile, F., Gericke, A., Haregeweyn, N., Hu, B., Jeanneau, A., Kaffas, K., Kiani-Harchegani, M., Villuendas, I.L., Li, C., Lombardo, L., López-Vicente, M., Lucas-Borja, M.E., Maerker, M., Miao, C., Modugno, S., Möller, M., Naipal, V., Nearing, M., Owusu, S., Panday, D., Patault, E., Patriche, C.V., Poggio, L., Portes, R., Quijano, L., Rahdari, M.R., Renima, M., Ricci, G.F., Rodrigo-Comino, J., Saia, S., Samani, A.N., Schillaci, C., Syrris, V., Kim, H.S., Spinola, D.N., Oliveira, P.T., Teng, H., Thapa, R., Vantas, K., Vieira, D., Yang, J.E., Yin, S., Zema, D.A., Zhao, G., Panagos, P., 2021. Soil erosion modelling: A bibliometric analysis. *Environmental Research* 197, 111087. <https://doi.org/10.1016/j.envres.2021.111087>
- Bittelli, M., Andrenelli, M.C., Simonetti, G., Pellegrini, S., Artioli, G., Piccoli, I., Morari, F., 2019. Shall we abandon sedimentation methods for particle size analysis in soils? *Soil and Tillage Research* 185, 36–46. <https://doi.org/10.1016/j.still.2018.08.018>
- Borrelli, P., Alewell, C., Alvarez, P., Anache, J.A.A., Baartman, J., Ballabio, C., Bezák, N., Biddoccu, M., Cerdà, A., Chalise, D., Chen, S., Chen, W., De Girolamo, A.M., Gessesse, G.D., Deumlich, D., Diodato, N., Efthimiou, N., Erpul, G., Fiener, P., Freppaz, M., Gentile, F., Gericke, A., Haregeweyn, N., Hu, B., Jeanneau, A., Kaffas, K., Kiani-Harchegani, M., Villuendas, I.L., Li, C., Lombardo, L., López-Vicente, M., Lucas-Borja, M.E., Märker, M., Matthews, F., Miao, C., Mikoš, M., Modugno, S., Möller, M., Naipal, V., Nearing, M., Owusu, S., Panday, D., Patault, E., Patriche, C.V., Poggio, L., Portes, R., Quijano, L., Rahdari, M.R., Renima, M., Ricci, G.F., Rodrigo-Comino, J., Saia, S., Samani, A.N., Schillaci, C., Syrris, V., Kim, H.S., Spinola, D.N., Oliveira, P.T., Teng, H., Thapa, R., Vantas, K., Vieira, D., Yang, J.E., Yin, S., Zema, D.A., Zhao, G., Panagos, P., 2021. Soil erosion modelling: A global review and statistical analysis. *Science of The Total Environment* 780, 146494. <https://doi.org/10.1016/j.scitotenv.2021.146494>

- Breshears, D.D., Whicker, J.J., Johansen, M.P., Pinder, J.E., 2003. Wind and water erosion and transport in semi-arid shrubland, grassland and forest ecosystems: quantifying dominance of horizontal wind-driven transport. *Earth Surf. Process. Landforms* 28, 1189–1209. <https://doi.org/10.1002/esp.1034>
- Brevik, E.C., Hartemink, A.E., 2010. Early soil knowledge and the birth and development of soil science. *CATENA* 83, 23–33. <https://doi.org/10.1016/j.catena.2010.06.011>
- Bullard, J.E., Livingstone, I., 2002. Interactions between aeolian and fluvial systems in dryland environments. *Area* 34, 8–16. <https://doi.org/10.1111/1475-4762.00052>
- Cerdà, A., Flanagan, D.C., le Bissonnais, Y., Boardman, J., 2009. Soil erosion and agriculture. *Soil and Tillage Research* 106, 107–108. <https://doi.org/10.1016/j.still.2009.10.006>
- Chappell, A., Webb, N.P., Butler, H.J., Strong, C.L., McTainsh, G.H., Leys, J.F., Viscarra Rossel, R.A., 2013. Soil organic carbon dust emission: an omitted global source of atmospheric CO₂. *Glob Change Biol* 19, 3238–3244. <https://doi.org/10.1111/gcb.12305>
- Chendev, Y., Sauer, T., Ramirez, G., Burras, C., 2015. History of East European Chernozem soil degradation; protection and restoration by tree windbreaks in the Russian Steppe. *Sustainability* 7, 705–724. <https://doi.org/10.3390/su7010705>
- Chepil, W.S., 1960. Conversion of relative field erodibility to annual soil loss by wind. *Soil Science Society of America Proceedings* 143–145. <https://doi.org/doi.org/10.2136/sssaj1960.03615995002400020022x>
- Chepil, W.S., 1952. Factors that influence clod structure and erodibility of soil by wind: I. Soil texture. *Soil Science Society of America Journal* 75, 473–483.
- Chepil, W.S., 1950a. Properties of soil which influence wind erosion: I. The governing principle of surface roughness. *Soil Science Society of America Proceedings* 69, 149–162.
- Chepil, W.S., 1950b. Properties of soil which influence wind erosion: II. Dry aggregate structure as index of erodibility. *Soil Science Society of America Journal* 69, 10.
- Chepil, W.S., Woodruff, N.P., 1963. The physics of wind erosion and its control, in: *Advances in Agronomy*. Elsevier, pp. 211–302. [https://doi.org/10.1016/S0065-2113\(08\)60400-9](https://doi.org/10.1016/S0065-2113(08)60400-9)
- Cox, P.M., Betts, R.A., Jones, C.D., Spall, S.A., Totterdell, I.J., 2000. Acceleration of global warming due to carbon-cycle feedbacks in a coupled climate model. *Nature* 408, 184–187. <https://doi.org/10.1038/35041539>
- Diaz-Zorita, M., Perfect, E., Grove, J.H., 2002. Disruptive methods for assessing soil structure. *Soil and Tillage Research* 64, 3–22. [https://doi.org/10.1016/S0167-1987\(01\)00254-9](https://doi.org/10.1016/S0167-1987(01)00254-9)

- Dou, X., Ma, X., Zhao, C., Li, J., Yan, Y., Zhu, J., 2022. Risk assessment of soil erosion in Central Asia under global warming. *CATENA* 212, 106056. <https://doi.org/10.1016/j.catena.2022.106056>
- Duulatov, E., Chen, X., Issanova, G., Orozbaev, R., Mukanov, Y., Amanambu, A.C., 2021. Current and future trends of rainfall erosivity and soil erosion in Central Asia, *SpringerBriefs in Environmental Science*. Springer International Publishing, Cham. <https://doi.org/10.1007/978-3-030-63509-1>
- Fabig, I., 2007. Changing precipitation leeward of the Harz Mts. - Indicators of a regional climate change (in German: Wandel der Niederschlagsverhältnisse im Lee des Harzes - Indikatoren eines regionalen Klimawandels?). *Hercynia* 40, 1.
- FAO, 2012. *AQUASTAT: Kazakhstan*. Food and Agriculture Organization of the United Nations (FAO), Rome, Italy.
- FAO/UNESCO, 2007. *The digital soil map of the world, 1:5.000.000; Version 3.6*.
- Farsang, A., Szatmári, J., Bartus, M., Tiszlavicz, Á., Barta, K., 2022. Quantification of deflation-induced soil loss on chernozems: Field protocol and sediment trap development based on wind tunnel experiments. *zfg* 63, 329–341. <https://doi.org/10.1127/zfg/2021/0709>
- Field, J.P., Breshears, D.D., Whicker, J.J., 2009. Toward a more holistic perspective of soil erosion: Why aeolian research needs to explicitly consider fluvial processes and interactions. *Aeolian Research* 1, 9–17. <https://doi.org/10.1016/j.aeolia.2009.04.002>
- Foley, J.A., Ramankutty, N., Brauman, K.A., Cassidy, E.S., Gerber, J.S., Johnston, M., Mueller, N.D., O’Connell, C., Ray, D.K., West, P.C., Balzer, C., Bennett, E.M., Carpenter, S.R., Hill, J., Monfreda, C., Polasky, S., Rockström, J., Sheehan, J., Siebert, S., Tilman, D., Zaks, D.P.M., 2011. Solutions for a cultivated planet. *Nature* 478, 337–342. <https://doi.org/10.1038/nature10452>
- Free, E.E., 1911. *The movement of soil material by the wind*. Government Printing Office, Washington, D.C, USA.
- Frühauf, M., Meinel, T., Schmidt, G., 2020. The Virgin Lands Campaign (1954–1963) until the breakdown of the former Soviet Union (FSU): With special focus on Western Siberia, in: Frühauf, Manfred, Guggenberger, G., Meinel, Tobias, Theesfeld, I., Lentz, S. (Eds.), *KULUNDA: Climate smart agriculture, innovations in landscape research*. Springer International Publishing, Cham, pp. 101–118. https://doi.org/10.1007/978-3-030-15927-6_8
- Funk, R., 2016. Assessment and measurement of wind erosion, in: Mueller, L., Sheudshen, A.K., Eulenstein, F. (Eds.), *Novel methods for monitoring and managing land and water resources in Siberia*, Springer Water. Springer International Publishing, Cham, pp. 425–449. https://doi.org/10.1007/978-3-319-24409-9_18
- Funk, R., Hoffmann, C., Reiche, M., 2014. Methods for quantifying wind erosion in Steppe Regions, in: Mueller, L., Saparov, A., Lischeid, G. (Eds.), *Novel measurement and assessment tools for monitoring and management of land and water resources in agricultural landscapes of Central Asia*, *Environmental Science and Engineering*.

Springer International Publishing, Cham, pp. 315–327. https://doi.org/10.1007/978-3-319-01017-5_18

- Funk, R., Reuter, H.I., 2006. Wind erosion, in: Boardman, J., Poesen, J. (Eds.), *Soil erosion in Europe*. John Wiley & Sons, Ltd, Chichester, UK, pp. 563–582. <https://doi.org/10.1002/0470859202.ch41>
- Funk, R., Skidmore, E., Hagen, L., 2004. Comparison of wind erosion measurements in Germany with simulated soil losses by WEPS. *Environmental Modelling & Software* 19, 177–183. [https://doi.org/10.1016/S1364-8152\(03\)00120-8](https://doi.org/10.1016/S1364-8152(03)00120-8)
- Gleditsch, J.G., 1767. III. Consideration of the sand floes in Brandenburg according to their origin, differences, harmfulness and necessary reductions (in German: III. Betrachtung der Sandschollen in der Mark Brandenburg nach ihren Ursprunge, Unterschiede, Schädlichkeit und nöthigen Verminderungen), in: *Vermischte Physicalisch-Botanisch-Oeconomische Abhandlungen*. Halle, pp. 45–143.
- Gregorich, E.G., Greer, K.J., Anderson, D.W., Liang, B.C., 1998. Carbon distribution and losses: erosion and deposition effects. *Soil and Tillage Research* 47, 291–302. [https://doi.org/10.1016/S0167-1987\(98\)00117-2](https://doi.org/10.1016/S0167-1987(98)00117-2)
- Gyssels, G., Poesen, J., Bochet, E., Li, Y., 2005. Impact of plant roots on the resistance of soils to erosion by water: A review. *Progress in Physical Geography: Earth and Environment* 29, 189–217. <https://doi.org/10.1191/0309133305pp443ra>
- Harris, I.C., Jones, P.D., Osborn, T., 2020. CRU TS4.04: Climatic Research Unit (CRU) Time-Series (TS) version 4.04 of high-resolution gridded data of month-by-month variation in climate (Jan. 1901- Dec. 2019). *Sci Data* 7.
- Höök, M., Tang, X., 2013. Depletion of fossil fuels and anthropogenic climate change—A review. *Energy Policy* 52, 797–809. <https://doi.org/10.1016/j.enpol.2012.10.046>
- Horn, R., Fleige, H., Rattan, L., Zimmermann, I., 2018. Soil health and functions as a basic requirement for advancing the SDGs, in: Lal, R., Horn, R., Kosaki, T. (Eds.), *Soil and Sustainable Development Goals, GeoEcology Essays*. Catena Soil Sciences, Stuttgart, pp. 52–60.
- Iturri, L.A., Buschiazzi, D.E., 2023. Interactions between wind erosion and soil organic carbon, in: *Agricultural Soil Sustainability and Carbon Management*. Elsevier, pp. 163–179. <https://doi.org/10.1016/B978-0-323-95911-7.00005-0>
- Jarrah, M., Mayel, S., Tatarko, J., Funk, R., Kuka, K., 2020. A review of wind erosion models: Data requirements, processes, and validity. *CATENA* 187, 104388. <https://doi.org/10.1016/j.catena.2019.104388>
- Kemper, W.D., Rosenau, R.C., 2018. Aggregate stability and size distribution, in: Klute, A. (Ed.), *SSSA Book Series*. Soil Science Society of America, American Society of Agronomy, Madison, WI, USA, pp. 425–442. <https://doi.org/10.2136/sssabookser5.1.2ed.c17>

- Koza, M., Funk, R., Pöhlitz, J., Conrad, C., Shibistova, O., Meinel, T., Akshalov, K., Schmidt, G., 2024. Wind erosion after steppe conversion in Kazakhstan. *Soil and Tillage Research* 236, 105941. <https://doi.org/10.1016/j.still.2023.105941>
- Koza, M., Funk, R., Schmidt, G., 2023. Wind erosion after steppe conversion in Kazakhstan: Data from mobile wind tunnel experiments [Dataset]. Leibniz centre for Agricultural Landscape Research (ZALF). <https://doi.org/10.4228/ZALF-QQ16-T967>
- Koza, M., Pöhlitz, J., Prays, A., Kaiser, K., Mikutta, R., Conrad, C., Vogel, C., Meinel, T., Akshalov, K., Schmidt, G., 2022. Potential erodibility of semi-arid steppe soils derived from aggregate stability tests. *European J Soil Science* 73, e13304. <https://doi.org/10.1111/ejss.13304>
- Koza, M., Schmidt, G., Bondarovich, A., Akshalov, K., Conrad, C., Pöhlitz, J., 2021. Consequences of chemical pretreatments in particle size analysis for modelling wind erosion. *Geoderma* 396, 115073. <https://doi.org/10.1016/j.geoderma.2021.115073>
- Krasilnikov, P., Sorokin, A., Golozubov, O., Bezuglova, O., 2018. Managing Chernozems for advancing SDGs, in: Lal, R., Horn, R., Kosaki, T. (Eds.), *Soil and Sustainable Development Goals, GeoEcology Essays*. Catena Soil Sciences, Stuttgart, pp. 175–188.
- Lal, R., 2021. Managing Chernozem for reducing global warming, in: Dent, D., Boincean, B. (Eds.), *Regenerative agriculture*. Springer International Publishing, Cham, pp. 81–93. https://doi.org/10.1007/978-3-030-72224-1_7
- Lal, R. (Ed.), 2017. *Encyclopedia of soil science*, Third edition. ed. CRC Press, Taylor & Francis Group, Boca Raton, FL.
- Lal, R., 2001. Soil degradation by erosion. *Land Degrad. Dev.* 12, 519–539. <https://doi.org/10.1002/ldr.472>
- Le Bissonnais, Y., 1996. Aggregate stability and assessment of soil crustability and erodibility: I. Theory and methodology. *European Journal of Soil Science* 47, 425–437. <https://doi.org/10.1111/j.1365-2389.1996.tb01843.x>
- Lev-Yadun, S., Gopher, A., Abbo, S., 2000. The cradle of agriculture. *Science* 288, 1602–1603. <https://doi.org/10.1126/science.288.5471.1602>
- Li, J., Ma, X., Zhang, C., 2020. Predicting the spatiotemporal variation in soil wind erosion across Central Asia in response to climate change in the 21st century. *Science of The Total Environment* 709. <https://doi.org/10.1016/j.scitotenv.2019.136060>
- Marzen, M., Kirchhoff, M., Marzloff, I., Aït Hssaine, A., Ries, J.B., 2020. Relative quantification of wind erosion in argan woodlands in the Souss Basin, Morocco. *Earth Surf. Process. Landforms* 45, 3808–3823. <https://doi.org/10.1002/esp.5002>
- Meinel, T., Grunwald, L.-C., Akshalov, K., 2014. Modern technologies for soil management and Conservation in Northern Kazakhstan, in: Mueller, L., Saporov, A., Lischeid, G. (Eds.), *Novel measurement and assessment tools for monitoring and management of land and water resources in agricultural landscapes of Central Asia*, Environmental

- Science and Engineering. Springer International Publishing, Cham, pp. 455–464.
https://doi.org/10.1007/978-3-319-01017-5_27
- Mendez, M.J., Funk, R., Buschiazzo, D.E., 2016. Efficiency of Big Spring Number Eight (BSNE) and Modified Wilson and Cook (MWAC) samplers to collect PM10, PM2.5 and PM1. *Aeolian Research* 21, 37–44. <https://doi.org/10.1016/j.aeolia.2016.02.003>
- Mirzabaev, A., Goedecke, J., Dubovyk, O., Djanibekov, U., Le, Q.B., Aw-Hassan, A., 2016. Economics of land degradation in Central Asia, in: Nkonya, E., Mirzabaev, A., von Braun, J. (Eds.), *Economics of Land Degradation and Improvement – A Global Assessment for Sustainable Development*. Springer International Publishing, Cham, pp. 261–290. https://doi.org/10.1007/978-3-319-19168-3_10
- Monger, H.C., Martinez-Rios, J.J., Khresat, S.A., 2005. Tropical soils: Arid and semiarid, in: *Encyclopedia of Soils in the Environment*. Elsevier, pp. 182–187.
<https://doi.org/10.1016/B0-12-348530-4/00021-7>
- Montgomery, D.R., 2007. Soil erosion and agricultural sustainability. *Proc. Natl. Acad. Sci. U.S.A.* 104, 13268–13272. <https://doi.org/10.1073/pnas.0611508104>
- Morgan, R.P.C., 2005. *Soil erosion and conservation*, 3rd ed. ed. Blackwell Pub, Malden, MA.
- Morgan, R.P.C., Quinton, J.N., 2001. Erosion modeling, in: Harmon, R.S., Doe, W.W. (Eds.), *Landscape erosion and evolution modeling*. Springer US, Boston, MA, pp. 117–143.
https://doi.org/10.1007/978-1-4615-0575-4_6
- Mutchler, C.K., Murphree, C.E., McGregor, K.C., 2017. Laboratory and field plots for erosion research, in: Lal, R. (Ed.), *Soil erosion research methods*. Routledge, pp. 11–38. <https://doi.org/10.1201/9780203739358-2>
- Pi, H., Sharratt, B., 2017. Evaluation of the RWEQ and SWEEP in simulating soil and PM10 loss from a portable wind tunnel. *Soil and Tillage Research* 170, 94–103.
<https://doi.org/10.1016/j.still.2017.03.007>
- Pimentel, D., Kounang, N., 1998. Ecology of soil erosion in ecosystems. *Ecosystems* 1, 416–426. <https://doi.org/10.1007/s100219900035>
- Prishchepov, A.V., Schierhorn, F., Dronin, N., Ponkina, E.V., Müller, D., 2020. 800 years of agricultural land-use change in Asian (Eastern) Russia, in: Frühauf, M., Guggenberger, G., Meinel, T., Theesfeld, I., Lentz, S. (Eds.), *KULUNDA: Climate smart agriculture, innovations in landscape research*. Springer International Publishing, Cham, pp. 67–87. https://doi.org/10.1007/978-3-030-15927-6_6
- Reyer, C.P.O., Otto, I.M., Adams, S., Albrecht, T., Baarsch, F., Carlsburg, M., Coumou, D., Eden, A., Ludi, E., Marcus, R., Mengel, M., Mosello, B., Robinson, A., Schleussner, C.-F., Serdeczny, O., Stagl, J., 2017. Climate change impacts in Central Asia and their implications for development. *Reg Environ Change* 17, 1639–1650.
<https://doi.org/10.1007/s10113-015-0893-z>

- Ritchie, P.D.L., Clarke, J.J., Cox, P.M., Huntingford, C., 2021. Overshooting tipping point thresholds in a changing climate. *Nature* 592, 517–523.
<https://doi.org/10.1038/s41586-021-03263-2>
- Robinson, S., 2016. Land degradation in Central Asia: Evidence, perception and policy, in: Behnke, R., Mortimore, M. (Eds.), *The end of desertification?*, Springer Earth System Sciences. Springer Berlin Heidelberg, Berlin, Heidelberg, pp. 451–490.
https://doi.org/10.1007/978-3-642-16014-1_17
- Rotnicka, J., 2013. Aeolian vertical mass flux profiles above dry and moist sandy beach surfaces. *Geomorphology* 187, 27–37.
<https://doi.org/10.1016/j.geomorph.2012.12.032>
- Scheffer, F., Schachtschabel, P., Blume, H.-P., 2016. *Soil science*, 1st ed. Springer, Berlin.
- Schultz, J., 2005. *The ecozones of the world: the ecological divisions of the geosphere*, 2nd ed. Springer, Aachen.
- Shao, Y., 2008. *Physics and modelling of wind erosion*, Atmospheric and oceanographic sciences library. Springer, Cambridge.
- Shao, Y., Wyrwoll, K.-H., Chappell, A., Huang, J., Lin, Z., McTainsh, G.H., Mikami, M., Tanaka, T.Y., Wang, X., Yoon, S., 2011. Dust cycle: An emerging core theme in Earth system science. *Aeolian Research* 2, 181–204.
<https://doi.org/10.1016/j.aeolia.2011.02.001>
- Sirjani, E., Sameni, A., Moosavi, A.A., Mahmoodabadi, M., Laurent, B., 2019. Portable wind tunnel experiments to study soil erosion by wind and its link to soil properties in the Fars province, Iran. *Geoderma* 333, 69–80.
<https://doi.org/10.1016/j.geoderma.2018.07.012>
- Six, J., Bossuyt, H., Degryze, S., Deneff, K., 2004. A history of research on the link between (micro)aggregates, soil biota, and soil organic matter dynamics. *Soil and Tillage Research* 79, 7–31. <https://doi.org/10.1016/j.still.2004.03.008>
- Six, J., Elliott, E.T., Paustian, K., Doran, J.W., 1998. Aggregation and soil organic matter accumulation in cultivated and native grassland soils. *Soil Science Society of America Journal* 62, 1367–1377. <https://doi.org/10.2136/sssaj1998.03615995006200050032x>
- Skidmore, E.L., Hagen, L.J., Armbrust, D.V., Durar, A.A., Fryrear, D.W., Potter, K.N., Wagner, L.E., Zobeck, T.M., 1994. Methods for investigating basic processes and conditions affecting wind erosion, in: Lal, R. (Ed.), *Soil erosion, research methods*. St. Lucie Press, Delray Beach, pp. 295–330.
- Song, X.-P., Hansen, M.C., Stehman, S.V., Potapov, P.V., Tyukavina, A., Vermote, E.F., Townshend, J.R., 2018. Global land change from 1982 to 2016. *Nature* 560, 639–643.
<https://doi.org/10.1038/s41586-018-0411-9>
- Steffen, W.L. (Ed.), 2005. *Global change and the Earth system: a planet under pressure*, Global change--the IGBP series. Springer, Berlin ; New York.

- Tanner, S., Katra, I., Haim, A., Zaady, E., 2016. Short-term soil loss by eolian erosion in response to different rain-fed agricultural practices. *Soil and Tillage Research* 155, 149–156. <https://doi.org/10.1016/j.still.2015.08.008>
- Tatarko, J., 2008. Single-event Wind Erosion Evaluation program: SWEEP user manual draft. United States Department of Agriculture, Agricultural Research Service, Manhattan/Kansas, USA.
- Tatarko, J., Sporcic, M.A., Skidmore, E.L., 2013. A history of wind erosion prediction models in the United States Department of Agriculture prior to the Wind Erosion Prediction System. *Aeolian Research* 10, 3–8. <https://doi.org/10.1016/j.aeolia.2012.08.004>
- Tatarko, J., van Donk, S.J., Ascough, J.C., Walker, D.G., 2016. Application of the WEPS and SWEEP models to non-agricultural disturbed lands. *Heliyon* 2, e00215. <https://doi.org/10.1016/j.heliyon.2016.e00215>
- Tatarko, J., Wagner, L., Fox, F., 2019. The wind Erosion prediction system and its use in conservation planning, in: Wendroth, O., Lascano, R.J., Ma, L. (Eds.), *Advances in Agricultural Systems Modeling*. American Society of Agronomy and Soil Science Society of America, Madison, WI, USA, pp. 71–101. <https://doi.org/10.2134/advagricsystmodel8.2017.0021>
- Tisdall, J.M., Oades, J.M., 1982. Organic matter and water-stable aggregates in soils. *European Journal of Soil Science* 33, 141–163. <https://doi.org/10.1111/j.1365-2389.1982.tb01755.x>
- Tsoar, H., 1994. Bagnold, R.A. 1941: *The physics of blown sand and desert dunes*. London: Methuen. *Progress in Physical Geography: Earth and Environment* 18, 91–96. <https://doi.org/10.1177/030913339401800105>
- Tubiello, F.N., Salvatore, M., Rossi, S., Ferrara, A., Fitton, N., Smith, P., 2013. The FAOSTAT database of greenhouse gas emissions from agriculture. *Environ. Res. Lett.* 8, 015009. <https://doi.org/10.1088/1748-9326/8/1/015009>
- Turner, B.L., Lambin, E.F., Reenberg, A., 2007. The emergence of land change science for global environmental change and sustainability. *Proc. Natl. Acad. Sci. U.S.A.* 104, 20666–20671. <https://doi.org/10.1073/pnas.0704119104>
- United Nations, 2022. *The Sustainable Development Goals: Report 2022*. United Nations, New York.
- Uspanov, U.U., Yevstifeyev, U.G., Storozhenko, D.M., Lobova, E.V., 1975. Soil map of the kazakh SSR 1:2.500.000.
- Van Pelt, R.S., Zobeck, T.M., 2013. Portable wind tunnels for field testing of soils and natural surfaces, in: Ahmed, N. (Ed.), *Wind tunnel designs and their diverse engineering applications*. InTech. <https://doi.org/10.5772/54141>
- Van Pelt, R.S., Zobeck, T.M., Baddock, M.C., Cox, J.J., 2010. Design, construction, and calibration of a portable boundary layer wind tunnel for field use. *Transactions of the ASABE* 53, 1413–1422. <https://doi.org/10.13031/2013.34911>

- Visser, S.M., Sterk, G., Ribolzi, O., 2004. Techniques for simultaneous quantification of wind and water erosion in semi-arid regions. *Journal of Arid Environments* 59, 699–717. <https://doi.org/10.1016/j.jaridenv.2004.02.005>
- Wagner, L.E., 2013. A history of wind erosion prediction models in the United States Department of Agriculture: The Wind Erosion Prediction System (WEPS). *Aeolian Research* 10, 9–24. <https://doi.org/10.1016/j.aeolia.2012.10.001>
- Wang, W., Samat, A., Ge, Y., Ma, L., Tuheti, A., Zou, S., Abuduwaili, J., 2020. Quantitative soil wind erosion potential mapping for Central Asia using the Google Earth Engine platform. *Remote Sensing* 12, 3430. <https://doi.org/10.3390/rs12203430>
- Webb, N.P., Kachergis, E., Miller, S.W., McCord, S.E., Bestelmeyer, B.T., Brown, J.R., Chappell, A., Edwards, B.L., Herrick, J.E., Karl, J.W., Leys, J.F., Metz, L.J., Smarik, S., Tatarko, J., Van Zee, J.W., Zwicke, G., 2020. Indicators and benchmarks for wind erosion monitoring, assessment and management. *Ecological Indicators* 110, 105881. <https://doi.org/10.1016/j.ecolind.2019.105881>
- WHO, 2012. Capacity of the health system in Kazakhstan for crisis management: Kazakhstan, 2010. World Health Organization, Regional Office for Europe, Copenhagen, Denmark.
- Wilkinson, B.H., McElroy, B.J., 2007. The impact of humans on continental erosion and sedimentation. *Geological Society of America Bulletin* 119, 140–156. <https://doi.org/10.1130/B25899.1>
- Woodruff, N.P., Siddoway, F.H., 1965. A wind erosion equation. *Soil Science Society of America Journal* 29, 602. <https://doi.org/10.2136/sssaj1965.03615995002900050035x>
- Yan, Y., Wang, X., Guo, Z., Chen, J., Xin, X., Xu, D., Yan, R., Chen, B., Xu, L., 2018. Influence of wind erosion on dry aggregate size distribution and nutrients in three steppe soils in northern China. *CATENA* 170, 159–168. <https://doi.org/10.1016/j.catena.2018.06.013>
- Zepner, L., Karrasch, P., Wiemann, F., Bernard, L., 2021. ClimateCharts.net – an interactive climate analysis web platform. *International Journal of Digital Earth* 14, 338–356. <https://doi.org/10.1080/17538947.2020.1829112>
- Zhang, W., Tan, L., Zhang, G., Qiu, F., Zhan, H., 2014. Aeolian processes over gravel beds: Field wind tunnel simulation and its application atop the Mogao Grottoes, China. *Aeolian Research* 15, 335–344. <https://doi.org/10.1016/j.aeolia.2014.07.001>
- Zhuang, Y., Du, C., Zhang, L., Du, Y., Li, S., 2015. Research trends and hotspots in soil erosion from 1932 to 2013: A literature review. *Scientometrics* 105, 743–758. <https://doi.org/10.1007/s11192-015-1706-3>
- Zomer, R.J., Xu, J., Trabucco, A., 2022. Version 3 of the Global Aridity Index and potential evapotranspiration database. *Sci Data* 9, 409. <https://doi.org/10.1038/s41597-022-01493-1>

Appendix



(A)

Fig. A1.

Typical signs of soil erosion observed in the study area:

(A) dust devil,



(B)

(B) dust emission by tractor tires on dirt road,



(C)

(C) soil depositions along shelterbelts, and



(D)

(D) rill erosion and missing plant emergence.



Fig. A2.

Soil sampling and determination of soil type in the study area.

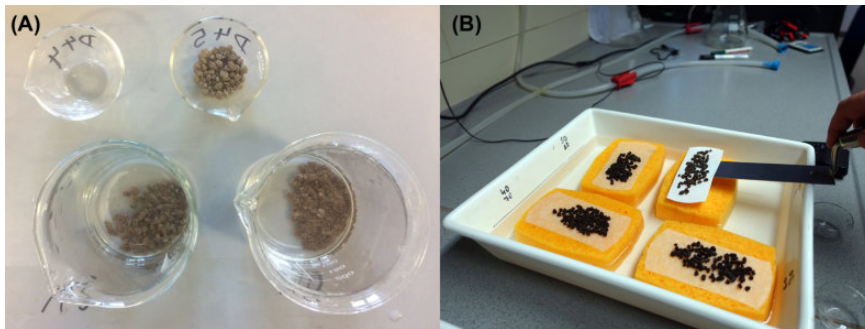


Fig. A3.

Fast (A) and slow (B) wetting tests to determine the resistance of the soil to heavy or light rain events.



Fig. A4.

The installation of the wind tunnel on a trailer to be mobile throughout the study area.

Curriculum vitae

Persönliche Daten:

Moritz Koza

Fachgebiet der Promotion:

Geoökologie

Werdegang:

Seit 2018	Projektmitarbeiter Martin-Luther-Universität Halle-Wittenberg, Halle (Saale)
2015	Master of Science Geographie Martin-Luther-Universität Halle-Wittenberg, Halle (Saale)
2014	DAAD Stipendiat
2014	ERASMUS Stipendiat
2012	Bachelor of Science Geographie Martin-Luther-Universität Halle-Wittenberg, Halle (Saale)
2011	PROMOS Stipendiat
2009	Freiwilliges Soziales Jahr
2008	Abitur

Declaration on oath (Eidesstattliche Erklärung)

I declare under penalty of perjury that this dissertation is my own work entirely and has been written without any help from other people. I used only the sources mentioned and included all the citations correctly, both in words and content.

(Ich erkläre an Eides statt, dass ich die Arbeit selbstständig und ohne fremde Hilfe verfasst, keine anderen als die von mir angegebenen Quellen und Hilfsmittel benutzt und die den benutzten Werken wörtlich oder inhaltlich entnommenen Stellen als solche kenntlich gemacht habe.)

Halle (Saale), 20.12.2023

Moritz Koza